Topics in Mining, Metallurgy and Materials Engineering
Series Editor: Carlos P. Bergmann

Abdul Majid
Maryam Bibi

Cadmium based II-VI Semiconducting Nanomaterials

Synthesis Routes and Strategies

Springer

Topics in Mining, Metallurgy and Materials Engineering

Series editor

Carlos P. Bergmann, Porto Alegre, Brazil

"Topics in Mining, Metallurgy and Materials Engineering" welcomes manuscripts in these three main focus areas: Extractive Metallurgy/Mineral Technology; Manufacturing Processes, and Materials Science and Technology. Manuscripts should present scientific solutions for technological problems. The three focus areas have a vertically lined multidisciplinarity, starting from mineral assets, their extraction and processing, their transformation into materials useful for the society, and their interaction with the environment.

More information about this series at http://www.springer.com/series/11054

Abdul Majid · Maryam Bibi

Cadmium based II-VI Semiconducting Nanomaterials

Synthesis Routes and Strategies

Springer

Abdul Majid
Department of Physics
University of Gujrat
Gujrat
Pakistan

Maryam Bibi
Department of Physics
University of Gujrat
Gujrat
Pakistan

ISSN 2364-3293 ISSN 2364-3307 (electronic)
Topics in Mining, Metallurgy and Materials Engineering
ISBN 978-3-319-68752-0 ISBN 978-3-319-68753-7 (eBook)
https://doi.org/10.1007/978-3-319-68753-7

Library of Congress Control Number: 2017955239

Printed on acid-free paper

This Springer imprint is published by Springer Nature
The registered company is Springer International Publishing AG
The registered company address is: Gewerbestrasse 11, 6330 Cham, Switzerland

How to Cite this Book

American Psychological Association (APA)	Majid, A., & Maryam, B. (2018). *Cadmium based II-VI semiconducting nanomaterials: Synthesis routes and strategies*. Cham: Springer.
American Physical Society (APS)	A. Majid, B. Maryam, *Cadmium based II-VI Semiconducting Nanomaterials: Synthesis Routes and Strategies* (Springer, Cham, 2018)
Basic Springer Nature	Majid A, Maryam B (2018) Cadmium based II-VI semiconducting nanomaterials: synthesis routes and strategies. Springer, Cham
Chemistry	Majid A, Maryam B (2018) Cadmium based II-VI semiconducting nanomaterials: synthesis routes and strategies. Springer, Cham
Chicago	Majid, A., and B. Maryam. 2018. *Cadmium based II-VI Semiconducting Nanomaterials: Synthesis Routes and Strategies*. Cham: Springer.
Math and Physical Sciences	Majid, A., Maryam, B.: Cadmium based II-VI Semiconducting Nanomaterials: Synthesis Routes and Strategies. Springer, Cham (2018)
Vancouver	Majid A, Maryam B. Cadmium based II-VI semiconducting nanomaterials: synthesis routes and strategies. Cham: Springer; 2018.

Foreword

Nanotechnology has been the hype word ever since the legendary lecture by Prof. Richard Feynman, where he famously declared, “there’s plenty of room at the bottom”. It is the promise of delivering enhanced novel properties by these materials with restricted growth in the nanometer regime, that has made nanoscience and technology survive through decades and centuries. Nowadays, applications for nanomaterials can be found almost everywhere from food and drug formulations to cosmetics and athletic gear; information technology to the energy sector. Among these, the fusion of semiconductor science with nanotechnology has created a plethora of widely variable applications, enriching both the fields. This book focuses on Cd-based II-VI semiconducting nanomaterials and covers various aspects of this important class of compounds including their different morphologies, characterization techniques, and different classes of Cd-based semiconductors. The book specifically focuses on the different synthesis methods and covers a range of nanomaterial synthesis techniques including solution-based, plasma-based as well as gas phase methods. Cd-based II-VI semiconductors have been at the center of materials science and engineering largely due to their potential application in alternative energy research. Cadmium telluride has been touted as one of the most promising materials for thin film solar cells, with efficiencies close to that of Si-based solar cell, but with half the cost of fabrication. Thus, the more economically feasible CdTe solar cell module has led to the birth of several companies that are trying to market the technology. The other cadmium-based chalcogenides such as CdS and CdSe also show promising photovoltaic activities, and hence they are being hot topics for research activities. Nanostructured morphologies of these solids are attracting the same attention owing to their promise of delivering higher efficiency lightweight solar cell modules. Making nanostructured morphology in bulk quantities and predicted dimensions is a challenge researchers are still trying to comprehend. A proper understanding of the different synthesis techniques, their

difficulties, experimental design, and outcome will lead us toward gaining more know-how on morphology-controlled nanomaterials synthesis. This book will equip the reader with such understanding that will help them create the nanostructured morphology as desired for any particular application.

In Chap. 1, the authors have introduced the concept of nanotechnology, the benefits, contradictions, and scope. Then after a brief introduction of Cd-chalcogenide-based nanomaterials, the readers will be drifted through to Chap. 2, where the authors have described the Cd-based nanomaterials in great detail. It includes the known classes of Cd-based nanomaterials, their different morphologies, properties, and applications. Rest of the chapters in the book deals with various synthesis techniques of Cd-based semiconducting nanomaterials, ranging from methods close to equilibrium, like solution-based methods to far-from-equilibrium processes such as vapor-phase synthesis and plasma-based synthesis. The authors have also discussed methods to grow ordered arrays of Cd-chalcogenide nanostructures, which owing to their promising photovoltaic efficiency, are becoming increasingly important in energy conversion devices. These chapters will give the readers a comprehensive view of the widely different synthesis methods that are normally adapted to produce these nanostructures.

The view of the book points to hard work of the authors. The primary author of the book, Abdul Majid Sandhu, is currently an Associate Professor in the Department of Physics, University of Gujrat, Gujrat, Pakistan. Professor Majid is an active researcher on semiconducting nanomaterials with interest in materials science within the broad area of alternative energy research. His research encompasses different classes of semiconductors, diluted magnetic semiconductors and semiconductor surface devices including Li-ion batteries. His excellent contributions in the area of semiconductor nanomaterial research have earned him several awards and accolades. He has been awarded the very competitive and prestigious fellowship from Japan Society for Promotion of Sciences (2015–2016) to carry out postdoctoral research in Osaka University. Dr. Majid has also fulfilled his duties as head of the department as well as director research and has acquired academic as well as administrative expertise.

I, personally have had the opportunity to work on nanoscience and nanotechnology for more than a decade throughout my academic career. Major chunk of my research activities covers designing materials for energy-related research, where nanomaterials synthesis occupies a significant portion. Being an active researcher in the field, I understand how precisely a go-to synthesis book explaining the concepts, design, and outcome can become very useful and even indispensable. Hence, I believe the readers of this book will thoroughly enjoy reading it from cover-to-cover to build up their knowledge, as well as use it as a guide to learn more about any particular topic.

I believe, nanotechnology as promised will show us ways to change the world. When it does, equipped with knowledge gained from books such as these, we will be right there to use its potential to the fullest.

Manashi Nath, PhD
Associate Professor
Department of Chemistry
Missouri University of Science and Technology
Rolla, USA

Preface

The various scientific fields, depending upon worth and applications, have earned due attention and contributed toward human development and technological progress. In this context, the science of materials has undoubtedly played a vital role in the realization of current technological status of mankind. The recent scientific progress has increased the awareness as well as the demands and expectations of the society which has raised the obligations of the researchers to meet the future necessities. The leading fraction of the community believes that the renaissance of science has taken place in the form of nanotechnology which is considered as a proud intervention of current generation of scientists. The material researchers and scientists are supposed not only to replicate every known material into its nanoscale counterpart but also to prepare new materials to meet the future technological requirements.

In my view, the evolution of any new science discipline involves four stages: discovery of relevant phenomenon, establishing the theoretical/conceptual background, developing a research methodology, and finally utilization of the attained knowledge for applications or improvement in basic understanding of the relevant fields. Unlike majority of the scientific areas, despite extensive activities, the research related to nanotechnology is simultaneously continued at fronts related to last three stages which points to an inefficient and undirectional progress in the field. Besides several other issues, the problems related to reproducibility, quality control, yield, aging, and availability of reliable characterization tools for nanomaterials need to be addressed without any further delay. In order to accomplish the logical and desired climax in the field of nanotechnology, the community should exclusively work on producing consensus in production and processing of nanomaterials to make them usable in device grade applications. A worldwide narrative and globally accepted protocol on nanotechnology need to be established. For this purpose, a widespread overview of the global research activities and a dialogue is needed to revisit the preparation strategies, material's handling and processing, characterization techniques, and potential of the materials for commercial grade devices. The current book is aimed at providing an exhaustive analysis of the research activities carried out to prepare cadmium chalcogenides II-VI

semiconducting nanomaterials. The synthesis of CdS, CdTe, CdSe, and CdO using more than 25 experimental techniques carried out over the years and reported in the scientific literature has been described in this book to provide a comprehensive review for analysts, critics, researchers, and general readers.

The compound semiconductors especially II-VI semiconductors are potential candidates for a variety of technological applications in addition to their conventional use in electronic, electro-optic, and piezoelectric devices. At present, these materials have fascinated the investigators for their remarkable properties which are due to three-dimensional confinement of carriers and rise in the number of surface atoms. These semiconductors, when downsized to nanometer, have become the center of attention because of their tunable band structure, high extinction coefficient, possible multiple exciton generation, electronic and transport properties. These materials are extremely valuable to cover the extensive range of expositions in optoelectronic devices, solar energy conversions, etc. Out of II-VI family, cadmium-based semiconductors are prominent members due to their excellent physical, chemical, and device grade properties. A lot of work related to these materials in bulk has been done, reported, and reviewed at almost every possible forum. However, in case of nanoscale counterpart of these materials, although significant work has appeared in the form of research articles, review papers, and internet sources, a comprehensive source in the form of book is not available so far. This book is aimed at providing comprehensive information on synthesis of cadmium-based semiconducting nanomaterials in one source with wide target readership comprising of students, researchers, scientists, technicians, academicians, industrialists, etc. The write-up was planned to provide one-stop-solution on research activities in the field. A section of Chap. 2 is dedicated to provide guidelines to junior researchers and students to interpret the experimental results, obtained from traditional characterization tools, on nanomaterials. The rest of the chapters of the book provide an all-inclusive and updated overview of the global research efforts made by researchers and scientists to produce nanomaterials of cadmium chalcogenide semiconductors by using nearly every reported synthesis technique. It is hoped that the readers having different expertise, disciplines, backgrounds, and knowledge will find stuff of their interest. Moreover, this book will not only be helpful for people working in the field of chalcogenide nanomaterials but also in exploring the synthesis strategies for other metallic and insulating/semiconducting compound materials. The researchers, technicians, and industrialists related to coating technology will be highly benefited from this document. I am confident to say that, the current book has significant material of interest for beginners, experts, technologists, and policy makers related to the fields of nanoscience and nanotechnology.

Abdul Majid, PhD
Department of Physics
University of Gujrat
Gujrat, Pakistan

Contents

Abbreviations

AAO	Anodic aluminum oxide
AFM	Atomic force microscopy
CR	Congo Red
CV	Crystal Violet
DRS	Diffused reflectance spectroscopy
DSSCs	Dye-sensitized solar cells
EDTA	Ethylenediaminetetraacetic acid
FTIR	Fourier transform infrared spectroscopy
FWHM	Full width at half maximum
GAEPE	Glycolic acid ethoxylate 4-non-phenyl ether
HMTA	Hexamethylene tetramine
LDPE	Modified low density polyethylene
MG	Malachite Green
MPA	3-mercaptopropionic acid
MSA	Mercaptosuccinic acid
NCs	Nanocrystals
NPs	Nanoparticles
NRs	Nanorods
NWs	Nanowires
NTs	Nanotubes
PES	Polyethersulfone
PET	Polyethylene terephthalate
PL	Photoluminescence
PMMA	Polymethyl methacrylate
PSH	Parkia speciosa Hassk
PVC	Poly(vinyl chloride)
PVP	Polyvinylepyrrolidone
QDs	Quantum dots
QY	Quantum yield
RT	Room temperature

SEM	Scanning electron microscope
SPM	Scanning probe microscopy
STM	Scanning tunneling microscopy
TCOs	Transparent conductive oxides
TED	Thermal evaporation deposition
TEM	Transmission electron microscopy
USP	Ultrasonic spray pyrolysis
UV	Ultraviolet
VFE	Vacuum flash evaporation
XPS	X-ray photoelectron spectroscopy
XRD	X-ray diffraction

Chapter 1
Introduction

A casual look into list of newly appeared words and terminologies during last two decades indicates that the term "nanotechnology" has just crossed its teenage. It is a recently emerged interdisciplinary field of science offering materials on nanoscale for novel applications in devices and daily life. The materials scaled down to about one billionth of one meter present entirely different characteristics which are not available from their bulk counterparts. The experimental realization of nanomaterials and the explanation of scientific behaviors related to them is mostly a challenging task and requires out-of-the-box approach. Quantum physics is fully involved in the business; to understand the behavior of these materials and analyze their chemical and physics properties, since they exhibit unusual features related to energetics, structural evolution, interaction with light and the external world, conduction, magnetism, etc. (Band and Avishai 2013). Though a lot of work has been carried out to explore functional nanomaterials which are being utilized in different applications, a major part of research is still due. Owing to huge potential of nanotechnology to solve the global problems, the humankind is looking towards the researchers and scientist with hopes to put their best efforts to tackle energy crises, drinking water issues, health problems, environmental threats, security concerns, and improve the quality of living. Keeping this into account and explore more natural mysteries in the best interest of humanity, an ever-increasing research and industrialist focus towards nanotechnology is being observed. The appearance of a number of high-class research journals, societies, research funding and carrier opportunities, academic disciplines, business and investment opportunities, conferences and workshops, research institutes, and organizations related to nanotechnology in recent decade points towards future global trends (Ghosh and Krishnan 2014). Moreover, a remarkable increase in number of research articles and patents containing the word "nanomaterials" revealed a major scientific interest in the field of nanotechnology. As per BBC's report on nanotechnology research, the global market related to nanotechnology will grow at annual rate of 18.2% to cause an increase in investment from $39.2 billion noted in 2016 to approximately $90.5 billion by 2021.

Abdul Majid and Maryam Bibi, *Cadmium based II-VI Semiconducting Nanomaterials*, Topics in Mining, Metallurgy and Materials Engineering,
https://doi.org/10.1007/978-3-319-68753-7_1

1.1 New Areas, Applications, and Future of Nanotechnology

Nanomaterials have vast areas of applications in diverse fields like medicine, biotechnology, electronics, communications, electronic systems, batteries, sensors and solar cells, etc. The diagnosis, drug delivery, and cure of complicated medical problems through nanotechnology are under operation and will be expected to become more trustworthy and available in near future. For drug delivery, the nanoparticles (NPs) are directed towards the damaged cells without injury to the healthy cells and QDs are utilized in antibiotic resistant infections. It has been tested to distroy the tumers without harming the healthy tissues using the intense sound waves produced through lenses coated with carbon nanotubes. The composites of NPs and polymers with a layer of red blood cells can be utilized to absorb the poison from the bloodstream. Nanomaterials in electronics have been utilized to enhance the capacity, functionality, cost-effectiveness, life and efficiency of devices. In lightening and display screens, the usage of nanotechnology has been found helpful not only to reduce thickness, weight, and input power but also to add into value, display quality, and human friendliness. The applications of nanotechnology in solar cells have given a new life to this field by lowering the manufacturing costs, usage of less toxic materials, improved performance and efficiency as well as lifetime. In rechargeable batteries, the usage of nanotechnology can increase the output as well as efficiency and decrease the recharging time. These advantages can be achieved by applying the layers of NPs on the surface of electrodes. Carbon NTs and metal oxide nanowires (NWs) can be applied to the nanotechnology detectors. Due to smaller size, the electrical characteristics of nanomaterials are significantly different when compared with bulk counterparts. Clean energy, genetics, robots, artificial intelligence, agriculture, health care, and automobile are future priority areas of nanotechnology.

1.2 Interdisciplinary Nature of Nanotechnology

Different disciplines of science have been conventionally supposed to be confined within certain boundaries until the birth of nanoscience and nanotechnology. The individuals working in different areas of nanotechnology have realized in very beginning that they are working on same problem for same cause. Nanotechnology research is highly integrative and multidisciplinary area of knowledge which is based on integration of information from different sources and fields to draw meaningful scientific conclusions (Porter and Youtie 2009). It has provided platform for convergence of different technologies and scientific disciplines to accelerate the level of knowledge and streamline the cognitive and social sciences for achieving collective human goals. The identification of current and future needs, synthesis and characterization of materials, manufacturing the devices based on the

prepared materials, financial and academic investments, entrepreneurial and social management, etc., related to nanotechnology have included basic and natural sciences, engineering and applied sciences, management and social sciences in the mainstream of future technologies. This convergence along with provision of global online access to knowledge has given an exponential uplift to the quantity and quality of research products. The emerging field of nanotechnology has brought the researchers and scientists closer and they are working in collaborations and have more access to resources. The workers belonging to different disciplines are now collectively publishing their results in interdisciplinary research journals under the umbrella of nanotechnology.

1.3 Scientific Disagreements in Nanotechnology

Despite the growing efforts carried out in collaborations by renowned research groups to prepare and utilize nanomaterials, the consensus on scientific conclusions and technological application of the products are lacking. The availability and emergence of more synthesis techniques, precursors materials and choice of growth conditions, widespread options to select materials to synthesize, handling and post-growth processing of nanomaterials, the diversity in characterization techniques, etc., are important aspects which contribute to diversity in findings. Furthermore, the careless human handling and taking records of synthesis conditions along with poor documentation and proper revelation of experimental details and scientific history of prepared nanomaterials add into the confusions and scientific disagreements.

The usage of characterization tools having different specifications, equipment's calibrations and scan rates, environmental conditions, sample handling and choice of sample's regions to probe, etc., are some unavoidable but crucial issues which cause errors in results even after careful fabrication of the materials. The changes in laboratory temperature, synthesis temperature, storage conditions, aging factors related to the products often found to hinder the reproducibility of nanomaterials prepared under identical growth conditions (Karakoti et al. 2012). Neglecting diverse interpretation of results made by individuals having different academic and research backgrounds, the above-mentioned factors are putting serious limits on scientific agreements and obtaining meaningful results in field of nanotechnology. After the preparation and growth of nanomaterials, the fabrication of devices based on the prepared samples also involves similar concerns and contribute significantly in the confusions and technological disagreements. In our opinion, the negligence of these factors is diverging the human efforts from arriving at logical conclusion and wasting the resources even though number of publications and patents related to nanomaterials are increasing.

This book is aimed at providing a collective view on fabrication and characterization of same materials carried out by using variety of synthesis conditions and investigation tools to shed light on scientific and technological disagreements. This

collection of up-to-date exhaustive overview of the planned contents is expected to provide a scientific consensus for utilization of cadmium chalcogenide nanomaterials in the best interest of humankind.

1.4 Nanomaterials Classes

Naturally existing nanomaterials and human-made materials can be categorized to understand their resemblances and distinctions. There is an extensive range and classes of nanomaterials like carbon-based materials, ceramic, dendrimers, biomaterials, composites and metallic nanomaterials. Dimensionality is very important to categorize the semiconducting nanomaterials. Typically, nanomaterials categorized in 3D structures, 2D structures, 1D structures, and 0D structures. The description of the structures and their implications on properties of cadmium chalcogenides are given in Chap. 2.

1.5 Cadmium Chalcogenide Nanomaterials

The II–VI semiconducting nanomaterials comprising of cadmium as cation and chalcogens from 16th group (oxygen, sulfur, selenium, tellurium) as anions are known as cadmium chalcogenides. The nanocrystals (NCs) of these materials CdO, CdS, CdSe, CdTe have earned extensive research interest among family of other nanomaterials. Unlike other compound semiconductors, the nanomaterials of cadmium chalcogenides are such optically active materials which have shown unprecedented potential for optoelectronic and photovoltaic devices. They have exhibited quantum size dependence of exciton energy and shown opportunities of tailoring of electronic and optical properties in wide range. Their nanomaterials have been grown in variety of morphologies showing possibility to tune the grain size, shape, orientation, and structural arrangements. The materials are naturally rich to offer variety of properties on the basis of their diverse morphologies, since the literature review indicates availability of reports on almost every known shape of nanomaterials involving cadmium chalcogenides.

Unlike III–V nanomaterials, comparatively less work is done on doping of these materials which points to availability of research gap for curious minds, especially young researchers. The establishment of diluted magnetic materials based on doping of transition metals or rare earth metals into cadmium chalcogenides for future magneto-optic and sprintronic applications is another unexplored area. The potential of nanomaterials especially NWs for realization of quantum computers urges the researchers to utilize the chalcogenides for spin-manipulation to prepare future computers (Frolov et al. 2013).

1.6 Motivation, Justifications, and Recipe of the Book

The synthesis conditions of nanomaterials are significantly important in determining the optical, electronic, and structural properties of the materials and their potentials for applications. Cadmium chalcogenide nanomaterials prepared by different techniques are the main focus of this book. A closer look into the literature indicates scientific disparity in structure, quality and hence properties of same materials prepared by different routes and in some cases even by same technique. We have identified lack of utilization of several resourceful techniques to prepare one or more materials out of cadmium chalcogenides. It may have restricted the preparation of quality nanomaterials and their utilization for applications in devices and daily life. This book is written with motivation to shed light on such research gaps and provide recommendations to researchers and investigators of research projects related to cadmium chalcogenide nanomaterials. Despite availability of an abundant data in form of research publications, review articles, perspectives, Internet sources, patents, and partially in some books, etc., no comprehensive source is yet available which is solely dedicated to cadmium chalcogenide nanomaterials. This book covers an exhaustive overview of worldwide research efforts related to CdO, CdS, CdSe, and CdTe nanomaterials. The description of bulk materials related to the chalcogenides is out of scope of this book which is exclusively dedicated only to their nanometer counterparts. This is the starting chapter of the book written in order to provide a brief introduction about nanomaterials and nanotechnology, the relevant issues, and concerns. The second chapter discusses the structure, morphology properties, and applications of nanomaterials, specifically related to cadmium chalcogenide nanomaterials. A glimpse on routine characterization methods to study the nanomaterials has also been given in this chapter. The next chapters involve a description on synthesis techniques and conditions used to prepare cadmium chalcogenide nanomaterials. The characterization results and reported properties along with applications have also been given in detail. This book is providing an exhaustive review of nearly all reported efforts that have mentioned utilization of every established technique which have been used to prepare these nanomaterials. The description of every technique involves an introduction of the technique with schematic diagram to explain the working mechanism, advantages, and disadvantages followed by extensive literature review of synthesis of nanomaterials in order CdS, CdSe, CdTe, and CdO by using this technique. The third chapter deals with the chemical synthesis methods, fourth chapter describes the vapor deposition methods, while fifth chapter covers the mechanical plasma assisted, radiation-assisted and green synthesis methods to to prepare these nanomaterials.

This book is expected to provide a thorough understanding of the mentioned field to the physicists, chemists, material scientists, and engineers of any level and background. More specifically, the beginners, undergraduate and graduate students, doctoral and postdoctoral researchers working in the field of nanoscience will find the sufficient information of their interest in this book. The references are given in American Psychological Association (APA) format to provide complete information of the cited articles.

References

Band, Y. B., & Avishai, Y. (2013). *Quantum mechanics with applications to nanotechnology and information science*. Cambridge: Academic Press.

Frolov, S. M., Plissard, S. R., Nadj-Perge, S., Kouwenhoven, L. P., & Bakkers, E. P. (2013). Quantum computing based on semiconductor NWs. *MRS Bulletin, 38*(10), 809–815.

Ghosh, A., & Krishnan, Y. (2014). At a long-awaited turning point. *Nature Nanotechnology, 9*(7), 491–494.

Karakoti, A. S., Munusamy, P., Hostetler, K., Kodali, V., Kuchibhatla, S., Orr, G., et al. (2012). Preparation and characterization challenges to understanding environmental and biological impacts of ceria NPs. *Surface and Interface Analysis, 44*(8), 882–889.

Porter, A. L., & Youtie, J. (2009). How interdisciplinary is nanotechnology? *Journal of Nanoparticle Research, 11*(5), 1023–1041.

Chapter 2
Cadmium-Based Nanomaterials

Nanotechnology is unquestionably a greatest discovery of current human generation. It is a complicated science involving unique strategies, synthesis procedures, characterization techniques, and applications of materials at scale of one billionth of a meter. At this very scale, quantum physics comes into action to explain the behavior of materials where the individual atoms, molecules and their interconnecting assemblies possess novel phenomenon due to quantum confinement and energetics. Moreover, the increased surface-to-volume ratio associated with this business causes an enhancement of interactions with the external world. These considerations and exciting properties related to nanomaterials have led the scientific world to an engrossment which has resulted into the current progress in the fields of nanostructures, their fabrication, and implementation.

2.1 Introduction to the Nanotechnology and Nanomaterials

The technological development and the related glamor have fascinated the experts as well as beginners towards the cosmos of this novel class of materials. These materials with astonishing structural, optical, and electronics properties provide great evolution in applications related to different fields of life at domestic as well as industrial levels. Nanomaterials are the starting stone of nanotechnology having at least one dimension within scale of 100 nm. This length scale has provided a driving force to renovate the existing technology with unprecedented technological benefits in applications related to information, communication, energy, optoelectronics, photovoltaics and facilities related to daily life. The structure of materials at this scale allows the control of important properties without shifting the basic chemical properties. These materials are important due to their entirely exceptional physical properties based on their unique structure, shape, and morphological features. The downscaling of bulk materials to the nanoregime causes changes in energetics involving electronic energy

Abdul Majid and Maryam Bibi, *Cadmium based II-VI Semiconducting Nanomaterials*, Topics in Mining, Metallurgy and Materials Engineering,
https://doi.org/10.1007/978-3-319-68753-7_2

levels. The packing of elementary atomic or molecular species to produce nanomaterials produces almost an infinite number of structural arrangements of molecules leading to abundant possibilities of lattices and energy levels. These energy levels introduce principal bands separated by band gap which is a key finger print of the electronic materials. The materials are normally considered as semiconductors when they exhibit band gaps up to about 3.8 eV. The electronic properties based on density of states, energy levels diagram, and band structure are significantly altered when an electronic material is thinned down to nanoscale. The energy levels are very close and hence they can be described as continuum to produce conduction and valance bands whose gap is usually higher for nanomaterials as compared to the bulk counterparts. The transfer from indirect to direct band gap has also been observed when bulk materials are converted to nanoscale. It points to engineering of electronic properties which opens up a large number of opportunities for the material scientists to utilize such materials for ongoing and future applications.

In recent years, this engineered technology has led the workers to tailor the properties of conventional materials into desired functionalities by realizing novel nanomaterials having extraordinary properties. For example, carbon atoms are structured in a bit loose interlayer pattern to produce graphite used in refractories, batteries, and pencils. The strong bonding of these carbon atoms in three-dimensional covalent network throughout the lattice produces very hard structure of diamond. Another allotropic form of carbon is known as graphene in which carbon atoms are bonded in two-dimensional sheet-like structures to produce hardest ever-known material. The graphene is a monolayered nanomaterial which has exhibited exceptional properties for variety of applications. Carbon nanotube is another allotropic form of carbon which has presented largest length-to-diameter ratio and offers excellent thermal, electrical, and optical properties. Fullerene in the form of buckyballs is another allotropic form of carbon in the form of nanomaterial. Several other examples may be quoted which shed light on provision of new properties upon structural evolution as well as thinning of bulk materials to their nanoscale counterparts. For example, nanocrystalline form of copper is harder as compared to the micro-sized crystalline copper.

The nanostructured materials are obtained in form of thin films, clusters, multilayers, and in the form of nanocrystalline structures having 0, 1, 2, and 3 dimensions. These materials may categorize in the form of metals, alloys, compounds, semiconductors, etc., in various crystal structures, shapes, and morphologies. Following sections shed some light on relevant features of nanomaterials.

2.2 Structure of Nanomaterials

Crystal structure and crystallography are key features of nanomaterials which put direct influence on their properties. The crystallinity directly affects the surface chemistry as well as physical properties of the nanomaterials. The crystal structure can be changed as per elemental composition, elemental ratio, and packing geometry

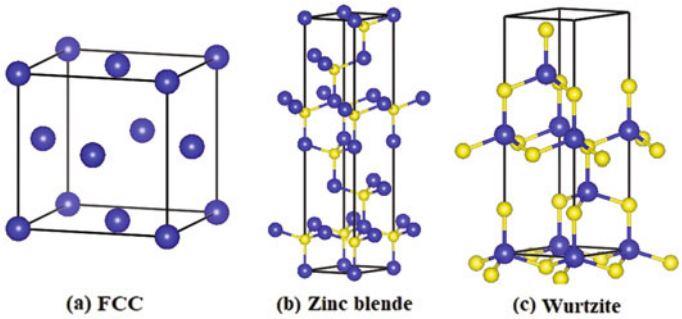

Fig. 2.1 Illustration of typical crystal structures, **a** face centered cubic, **b** cubic zinc blende and **c** hexagonal wurtzite

and nature of bonding of constituents (Guo and Tan 2009). The nanomaterials of cadmium containing II–VI semiconducting materials are usually crystallized into face-centered cubic (FCC), cubic zinc blende (ZB) and hexagonal wurtzite (WZ) crystal structures (Fig. 2.1).

2.3 Properties of Nanomaterials

The robustness of nanostructures is simply due to their exceptional properties which appear upon downscaling the materials from bulk to their nanoscale. The extraordinary response of nanostructured materials depends basically upon the following two features (Mews et al. 1994).

1. The quantum size effect: The electronic structure of the materials is strongly size dependent.
2. The surface/interface effect: The surface-to-volume ratio of nanomaterials is significantly higher.

The physical qualities of the nanomaterials are mostly explained by considering the quantum size effect and the investigation of this effect has become a primary criterion to characterize the materials. Due to the diverse degrees of confinement of particles (with different dimensions), the band gap energies of the nanostructure changes significantly (Yu et al. 2003a, b). Correspondingly, the size and dimensionality determines electronic and electrical properties of the materials. In nanostructured materials, the band edge states are closely packed because of the dimensionality and quantization. It points to tailoring the band diagram of nanomaterials and availability of diverse optical transitions. The II–VI semiconducting nanomaterials exhibits unique optical properties, particularly the semiconductors which have direct band gaps (Djurišić and Leung 2006; Arora and Sundar 2007). The particles scattering at the boundaries of the nanostructures have an effect on the

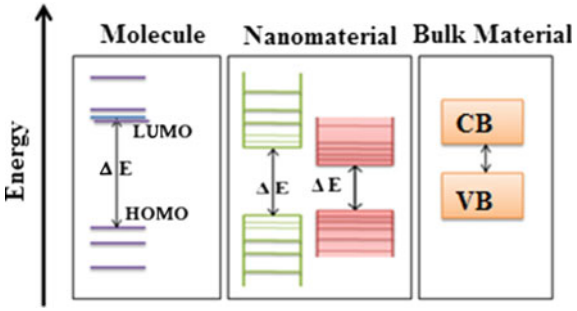

Fig. 2.2 Evolution of band diagram of bulk material from molecular structures to exhibit a link to nanomaterials

electronic properties, showing an increase in resistivity because of large surface scattering. In nanomaterials, the energy of surface atoms plays very significant role in determining their characteristics (Aqra and Ayyad 2014). An illustration showing the comparison of energy levels and band gaps of nanomaterials with the bulk material and molecular structures is given in Fig. 2.2.

The enhanced surface-to-volume ratio sheds light onto the surface free energy and availability of abundant place in nanomaterials to interact with the external world. For nanostructured materials, the surface energy is higher than bulk atoms which causes enhancement in chemical reactivity of nanosized materials (Li et al. 2015). On the same lines, the biological cells operate in a different way with the nanomaterials than bulk (Wong et al. 2013). The interface effect is also an important function to describe the chemical properties which are of prime importance in case of catalysis. This effect has got prime importance to explain exceptional characteristics of nanomaterials; e.g., specific heat, thermal conductivity, optical response, etc. In comparison with the bulk, the nanomaterials usually have low melting points, reduced lattice constants, higher band gaps, varied thermal stability, and enhanced surface interactions (Cao 2004).

2.4 Morphology of Nanomaterials

One important aspect of nanomaterials is surface morphology which is highly dependent upon synthesis strategies and leaves strong impact on properties of the materials for utilization in different applications. To investigate the morphology of NCs is of prime importance just after synthesis of the nanomaterials since it gives information about size, shape, structural arrangement, and surface of species of the obtained material. The nanomaterials have properties different from their bulk counterparts. The dimensional features of a solid play important role to determine its properties and it has been established that upon sufficient reduction in the dimensions the characteristics of the materials become remarkably different from those of the starting bulk solid. As the size of the solid material is reduced, the considerable modifications in the optical, electrical, chemical, and magnetic properties can be

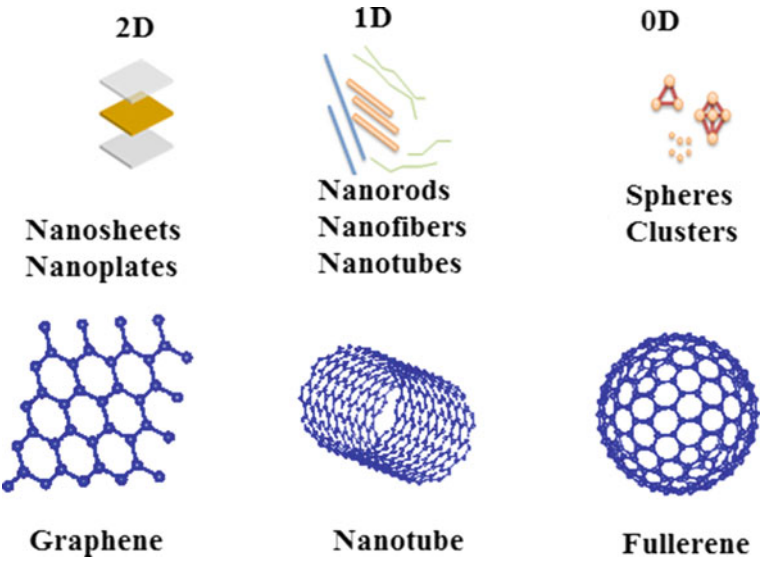

Fig. 2.3 Types of nanomaterials based on size, shape, morphology, and dimensionality of structural units. The examples from carbon allotropes are also given

introduced. The electrons and holes confined in a low-dimensional system behave significantly different and leave strong impact on performance of the devices based on such quantum size effects. The materials are classified according to the format given by Pokropivny and Skorokhod (2007) into several categories; (i) Three-dimensional (3D) structures (nanocups), (ii) Two-dimensional (2D) structures including nanofilms, nanosheets, nanolayers nanoslabs, etc. (iii) One-dimensional (1D) structures like NWs, nanorods(NRs), nanobelts (NBs), etc. (iv) Zero-dimensional (0D) structures as NPs, nanospheres, nanodots, etc. (Fig. 2.3).

2.4.1 Three-Dimensional (3D) Structure

In such materials, the particle motion is not quantized in any direction and they can freely move in the material. These materials have large surface area and offer several distinctive properties on the basis of enhanced surface-to-volume ratio and quantum confinement effects (Khalily et al. 2016). There is a great research attention in realization of these materials for several applications (Hu et al. 2009). 3D nanocups as Second Harmonic Generators (SHG) have been used for generation of second harmonic light with rising strength (Zhang et al. 2011). SHG gives a capability to devise and manufacture well-established second-order nonlinear nanomaterials. The performance of 3D nanomaterials can be increased by controlling the structure, size, and morphology in its broad range of applications as

Table 2.1 The classification of nanomaterials and their sizes on the basis of dimensionality

Nanostructures	Characteristic nanoscale dimensions
2D structures (nanosheets, nanoslabs)	1–1000 nm (thickness)
1D structures (NWs, NTs)	1–100 nm (radius)
0D structures (QDs)	1–10 nm (radius)
Porous material	1–50 nm (pore size)

batteries (Kamarudin et al. 2009), electrodes (Kargar et al. 2013) and catalysis (Sun et al. 2011; Shi et al. 2016).

Unlike for the case of bulk solids, there are several novel physicochemical characteristics which can be exploited for applications by suitable control of size, shape, morphology, and structural arrangement in case of nanomaterials. The conversion from a three-dimensional material to a low-dimensional nanostructure usually enhances the band gap value of that material (Moras et al. 1996). The number of reductions in dimensions frequently categorizes the different low-dimensional nanostructures. The number of degrees of freedom in case of particle momentum is controlled by the dimensionality of the material. The classification of nanostructures on the basis of dimensionality and granular size is given in Table 2.1.

2.4.2 Two-Dimensional (2D) Structure

Thin films, nanoplates, nanosheets, nanodisks, and nanoslabs are few examples of the two-dimensional nanomaterials (Fox 2002). Recently, 2D nanomaterials have attained great attention in research due to exceptional reactivity and shape-dependent properties and consequent use in nanotechnology (Buhro and Colvin 2003). Graphene is a well-known 2D nanomaterial having atomic thickness and its every atom is available to react with the external world. These materials are very attractive for understanding the nanostructure synthesis as well as for exploring advanced applications in many fields like sensors, electrocatalysis (Yu et al. 2015), and photocatalysis etc. (Luo et al. 2016).

Nanosheets of alloyed CdS and ZnS have been prepared with different Cd and Zn concentrations and it was observed that $Zn_{0.7}Cd_{0.3}S$ and $Zn_{0.88}Cd_{0.12}S$ nanosheets showed higher emission intensity (Fig. 2.4b). Exclusive MoS_2/CdS heterostructure showed striking properties used in solar energy conversion process with quantum yield of 41.37% at 420 nm and hydrogen evolution reaction 49.80 $mmolg^{-1}$ h^{-1}. These MoS_2/CdS nanosheets on nanorod revealed their applications for inexpensive photocatalysts for water splitting (Yin et al. 2016). CdS NPs decorated Cd nanosheets (CdS NP/Cd NSs) confirmed a notable improvement in visible-light activated photocatalytic performance for hydrogen production (Shang et al. 2016).

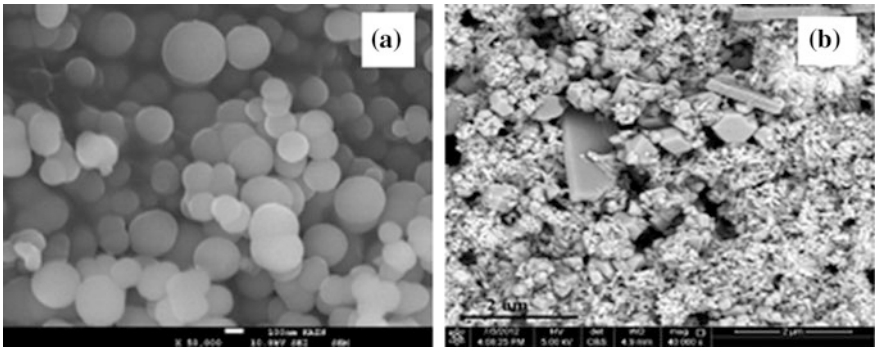

Fig. 2.4 **a** SEM image of CdO NPs with size ranging from 40 to 100 nm (Aldwayyan et al. 2013). © Open access **b** FESEM image of $Zn_{0.88}Cd_{0.12}S$ nanosheets (Mahdi et al. 2013). © Open access

2.4.3 One-Dimensional (1D) Structure

In 1D material, the motion of electrons and holes is confined in two directions. These materials have diverse optical and electronic properties because of their 2D confinement. NWs, nanofibers, NTs, NBs, quantum wires, NRs, nanoribbons and nanospindles are renowned 1D structures which have been synthesized.

NTs is an interesting class of 1D nanomaterials. Metal NTs showed more exciting catalytic properties than that of their respective NPs (Tang et al. 2013; Ge et al. 2016). Due to special surface plasmon effect, NBs can be adjusted in order to absorb or emit light in particular direction. As the gas atoms are adsorbed on the surface, they act like flow of current which allows the utilization of the respective material as analogous to FETs. NBs have properties analogous to the NWs; displaying FET-like performance and functional surface. NBs have desirable and exclusive qualities due to their surface area which makes them attractive for applications in nerve gas sensors, ethanol detectors, and hydrogen gas sensors. These structures have also been considered as suitable candidates to fabricate novel optoelectronic devices, like in LEDs, laser diodes, detectors, and optical sensors (Huang et al. 2015). NRs are promising materials for use as multifunctional material due to its high sensitivity, uniform morphology, and light detection ability. These nanomaterials can be created using different materials like metals, metal oxides, and organic materials. The size-dependent properties of NRs were studied in range 1–10 nm. ZnO/CdS and ZnO/CdO NRs showed great potential for use in gas sensing mechanism (Kim et al. 2016). A list of some famous nanomaterials having different morphologies with their properties and applications is shown in Table 2.2.

Owing to the ability to confine the electromagnetic waves into one particular direction, 1D nanomaterials are found potential candidates to function as waveguides. 1D nanomaterials offer important features for technological applications due to their extraordinary optical, magnetic, electrical, and chemical characteristics

Table 2.2 Some famous nanomaterial types, their morphology, synthesis strategies and applications

Types of nanostructures	Typical size	Mostly used synthesis methods	Properties	Applications
QDs	2–3 nm and 5–6 nm	Solvothermal, hydrothermal, aqueous synthesis	Tunable absorption spectrum, high extinction coefficient, high quantum yield, water splitting, hydrogen production	Quantum computation, solar cells, LEDs, biology, photocatalysis, photodetectors
Clusters	Less than 2 nm	Pulsed laser deposition, wet chemical methods, arc discharge method, ion sputtring	Large surface-to-volume ratio	Catalysis, solar cells, fluorescence bio-imaging, bio-labeling, detectors, photoluminescence, biosensor
NRs	1–100 nm Standard aspect (l/w) ratio 3–5	All wet chemical synthesis methods, condensation evaporation, pulsed laser deposition	linearly polarized emission, large absorption cross-sections, amplifying stimulated emission and lasing	Displays, cancer therapeutics, LEDs, sensor, photovoltaic
NWs	10^{-9} m l/w ratio is 1000	CBD, SILAR, electrodeposition, polyol synthesis	Uniform morphology, huge surface area, high conductivity, high chemical reactivity	Thermoelectric cooling system, energy conversion devices, junction diode, memory cells and switches, lasers
NTs	Less than 100 nm diameter, and ½ nm thick wall	CVD, CBD, microemulsion, microwave synthesis, polyol synthesis	High length-to-diameter ratio	Energy storage, fuel emission, biomedical applications
Nanosheets	1–100 nm thick (graphene nanosheet 0.34 nm thin)	Co-precipitation, hydrothermal, solvothermal	Crystalline surface, anisotropic confinement of nanospaces, layered thinness, colloidal properties	Photovoltaic, meta-materials, chem/biosensors, photochemistry

(Tang et al. 2002; Zhao et al. 2008; Qi et al. 2012). Until now, numerous synthesis methods have been employed to prepare the 1D nanostructures like electrochemical synthesis (Wu et al. 2010), microwave-assisted synthesis (Liu et al. 2010; Lu et al. 2004), inert gas condensation, spark discharge method, spray pyrolysis, thermal plasma, solvothermal (Ghoshal et al. 2009), sono-chemical, template method (Cao

and Liu 2008), and polyol process (Mayers and Xia 2002a, b; Ma et al. 2011; Yang et al. 2010; Zhu et al. 2011). Despite establishment of a number of these and other methods, achieving an easy, straightforward, inexpensive, and convenient method to provide high yield of 1D nanomaterial is still a challenge.

2.4.4 Zero-Dimensional (0D) Structure

The reduction of the size of bulk material near the value of its Bohr radius gives us the system with zero dimensions (Alivisatos 1996). These materials belong to an extraordinary class of semiconducting materials and offer quantization in three directions. Their quantized energy levels relate them more strongly to the molecules rather than the bulk materials.

QDs (QDs), spheres, and clusters are examples of 0D materials in which the motion of particle is fully confined. QDs are small crystals of semiconducting materials with radius of 1–5 nm and exhibit exclusive electronic characteristics in-between bulk and molecules. QDs are also known as "fluorescent NPs" and can exhibit any color of light by simply altering their size (Hu et al. 2011). Their emission color can also be varied by changing their composition through doping process. They can be categorized as core, core/shell, and alloyed QDs. Core-type QDs are single constituent materials with homogeneous compositions like CdS, CdSe, ZnS, etc. Core/shell QDs have small section of one material enclosed in a different material like CdSe in core and ZnS is shell (Wei et al. 2015). The knowledge of the physical and chemical characteristics of the core/shell QDs provides information on their use in light emission technology. Pan et al. synthesized the CdSe/CdS QDs at 180/140 °C in an autoclave with core size varying between 1.2 and 1.5 nm. These nanostructures showed dominant peaks in emission spectra ranging from 445 to 517 nm with quantum yield (QY) of 60–90%. Spherical CdO NPs with uniform size of 50 nm and some particles have joined with size of 100 nm were obtained, as shown in Fig. 2.4a.

Alloyed QDs structured obtained after alloying two semiconductors with dissimilar band gap values have revealed unique and fascinating characteristics. The alloyed QDs have not exhibited only quantum confinement effect but also presented composition-tunable characteristics. Highly emissive alloyed $CdSe_xS_{1-x}$ QDs showed the photoluminescence (PL) peak at 490 nm with absolute QY of 79% (Zhang et al. 2016). At present, QDs are utilized for numerous biological, biomedical (Plaza et al. 2016), optical and optoelectronic applications, varying from biosensors to solar cells (He and Ma 2014). The electronic properties of these materials are directly linked to the size and shape of the nanostructures.

A variety of techniques is available to prepare the 0D nanomaterials, like mechanochemical ball milling, ion sputtering, molecular beam epitaxy (MBE), inert gas condensation, pulsed laser ablation, sono-chemical, electrodeposition, microwave-assisted, sol-gel, solvothermal, CVD and laser pyrolysis etc. Each

method has its own benefits. Thermal plasma is also used for preparation of 0D materials due to its high reactivity, high enthalpy, rapid quenching and also exceptional characteristic of plasma to provide proficient solution.

2.5 Cadmium Chalcogenide Nanomaterials

The nanomaterials comprising of compounds of elements II and VI groups of periodic table are termed as II–VI semiconducting nanomaterials. At absolute zero temperature, they behave like the insulator but at finite temperature they present temperature-dependent properties of conductors and insulators. In case of these compounds, if cation is cadmium (Cd) and anions is taken from list of chalcogens (oxygen, sulfur, selenium, tellurium) in group 16 of periodic table, the resulting group of materials (CdO, CdS, CdSe, CdTe) will be referred as cadmium chalcogenides. Generally, these materials are synthesized as zinc blende (cubic) structure (Majid et al. 2015; Ranjithkumar et al. 2016) and represent the semiconducting properties. There is inversion symmetry present in these materials and some important bulk parameters of cadmium chalcogenides are shown in Table 2.3. The materials with such properties can be used for optoelectronic and piezoelectric applications (Willardson and Beer 1977). At present, the II–VI semiconductor materials have fascinated many investigators for their remarkable physical properties which are due to their three-dimensional confinement of carriers and increase in the number of surface atoms (Zhang et al. 2007). These semiconductors in analogous nanocrystalline form have become center of attention because of their tunable band structure (Kamat 2008), high extinction coefficient (Yu et al. 2003a, b) and possible multiple exciton generation (Nozik 2002). These materials have shown unparalleled potential to cover the extensive range of expositions in optoelectronic devices and photovoltaics (Zhu et al. 2015; Xu et al. 2014).

This class of II–VI semiconductors materials has got prime research and industrial attention because of their innovative characteristics along with size- and shape dependence of these properties. The nanomaterials display functional characteristics not available in their bulk correspondents. A subclass of these nanomateials with size of 2 nm or less exhibite some additional properties to be utilized in advanced technology (Harrell et al. 2013). The synthesis strategies and characterization of the materials CdO, CdS, CdSe, and CdTe in nanoscale, whose cationic and anionic

Table 2.3 Important parameters of bulk CdO, CdS, CdSe, and CdTe semiconducting materials at 300 K (Jefferson et al. 2008; Thirsk 1989)

Nanomaterial	Structure	E_{gap} (eV)	Lattice parameters (Å)	Density (kgm^{-3})
CdO	FCC	2.16	4.69	8150
CdS	Wurtzite	2.49	4.13/6.71	4820
CdSe	Wurtzite	1.74	4.3/7.01	5810
CdTe	Zinc blende	1.43	6.48	5870

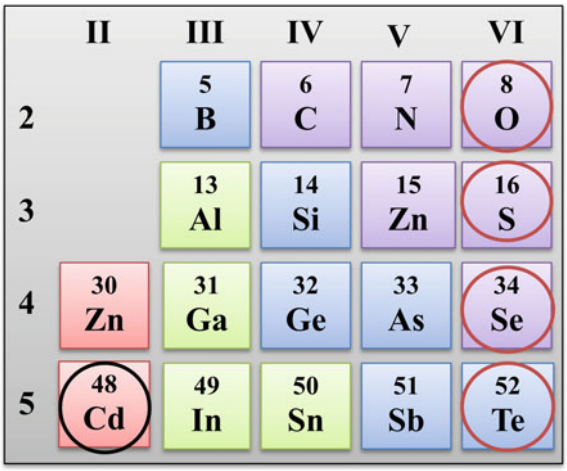

Fig. 2.5 Part of periodic table showing the cationic and anionic components of cadmium containing II–VI semiconducting materials described in this book

composition are shown Fig. 2.5 is primary theme of this book. The QDs based on these materials revealed extraordinary size-dependent optical characteristics with narrow band-gap. These materials have shown exceptional potential for device grade applications due to their size-tunable electronic and optical properties (Murugadoss et al. 2015; Salem et al. 2017; Zhu et al. 2013; Wageh et al. 2011).

The remaining sections of this chapter are dedicated to describe the structural, thermal, mechanical, vibrational, electronic, optical, and transport characteristics of these materials.

2.6 Properties and Applications of Cadmium Chalcogenide Nanomaterials

The cadmium chalcogenides (CdO, CdS, CdSe, CdTe) have been extensively investigated both in bulk and nanoscale. However, there is a huge interest in nanostructures of these materials due to their potential in existing and future applications. These materials are recognized with great promise for photovoltaics due to their high light sensitivity and quantum efficiency. Furthermore, the range of their direct band gap indicates the opportunity to manufacture optoelectronic devices with response to different electromagnetic radiations. However, the flexibility of these devices is restricted by the dissimilar band gap for individual material. The structural arrangement of their heterostructures can make these semiconductors to present good performance since they offer "band engineering" opportunities. Currently, utilizing the QDs for solar energy yield has become a striking field for research. In such systems, the photoexcited electrons are transferred to the large band gap of TiO_2 and ZnO semiconductors. In contrast with other sensitizers the semiconductor QDs exhibit superior properties due to their sizes.

Their band gap can be varied by changing the size of QDs and they can form many excited charged particles with the impulse of a single photon (Gao et al. 2009; Nozik 2002). Nanoscale hetero-, core/shell, and hierarchical structures are formed by combining the two materials with same chemistry-, size-, and material-dependent properties show more efficiency and multifunctionality than their single structures. CdTe-sensitized TiO_2 NTs have been synthesized and studied with enhanced photo-electro-chemical activity (Gao et al. 2009). A summary of these materials with their applications is given in Fig. 2.9.

2.6.1 Cadmium Oxide

Cadmium oxide (CdO) exhibits distinctive properties when compared to other cadmium chalcogenides. Translucent conductive oxides (TCOs) have been studied with superb photoelectronic behavior because of low specific resistance and high transmittance. Among all TCOs, the study of CdO nanomaterials is highly attractive and exciting field. CdO is a binary compound of cadmium and oxygen which is normally obtained in NaCl-like cubic structure (Brock 2004). It is n-type semiconductor, insoluble in water and soluble in mineral acids. It has direct and indirect band gap with values of energy as 2.28 and 0.55 eV respectively. There is a worthwhile research consideration for CdO because of its fascinating features such as its low electrical resistivity and concurrently high transparency in the visible region (Afify et al. 2014).

CdO nanomaterials synthesized with different morphologies show excellent properties. Cadmium interstitials are shallow donors and oxygen vacancies produce deep levels in band gap of CdO NPs, therefore their study is worthwhile to explore the luminescence process (Goswami and Choudhury 2015). High density and ordered CdO NW array with diameter $\sim$50 nm and length $\sim$2.5 μm showed high transmittance over 80% in visible region (Chaure 2016). These homogeneous and vertically aligned NW arrays exhibited direct band conversion at 440 nm and exciton emission at 510 nm.

In the biomedical field, CdO nanopowders play a vital role due to their antibacterial properties. These microstructures proved their significant antibacterial and antifungal capabilities against pathogenic bacteria and fungi strains because of (i) formation of reactive oxygen species (ii) discharge of Cd^{2+} ions (iii) the size and morphology of the product nanopowders (Balamurugan et al. 2016). CdO nanopowders can be applied as efficient antimicrobial agent against the pathogenic microorganisms. Unique rhombus-like structure of CdO showed the photocatalytic performance for the degradation of different pollutants like CR, MG, and CV (Tadjarodi et al. 2014).

Recently, highly capable flower-like CdO-SiO_2 nanomaterial was prepared and studied. It has shown good photodegradation performance under UV light irradiation for Rhodamine B dye and maximum degradation was observed at pH value 7 (Senthilvelan 2017). The current–voltage characteristics of CdO/Si devices have been studied in light and darkness which revealed high sensitive reactivity in the

visible and the near IR regions of electromagnetic spectrum (Ortega et al. 2000). A needle-shaped CdO NC shown in Fig. 2.6b, exhibited single crystalline and uniform structure. These nanostructures showed excellent response to infrared light and diluted NO_2 gas, and they have ability to absorb IR light due to their indirect band gap. This indicated the potential of the material to be applied as infrared photo-sensors and poisonous gas detectors. Due to high surface area, CdO NTs (Fig. 2.6a) showed potential to be applicable in fields of nanooptics, catalysis, and nanosensors. NBs of CdO mostly have length below the 100 μm scales and characteristic width ranging between 100 and 500 nm.

Like bulk materials, the process of doping also greatly affects the properties of nanomaterials. The nanostructures of CdO doped with different metals have been studied, e.g., including light metals Li (Dakhel 2011b), B (Yakuphanoglu 2011), transition metals like Ti (Gupta et al. 2008), Zn (Dakhel 2012) and some rare earth metals like Gd (Alemi et al. 2013), Ce (Dakhel 2011a). Doping of Cu in CdO improved its optical transmittance in visible range. The prepared NWs showed good activity to be applied in optoelectronic devices (Benhaliliba et al. 2012). CdO nanofilms showed an increase in band gap energy after doping with Bi, due to quantum size effect (Dagdelen et al. 2012). The current–voltage results and other electrical measurements showed CdO nanofilms acts as electron transport layer (Soylu and Kader 2016). These nanofilms layered on *p*-Si (a photodetector) CdO/*p*-Si heterojunction revealed the properties of a rectifier diode and a well-built photoreactive response.

An appropriate thermal treatment and accordingly the variations in morphology and electrical behavior of CdO based nanostructures have exposed a wire-to-rod conversion and reduction of electrical resistance (Krishnakumar et al. 2011). These CdO nanofilms proved to be appropriate candidate as CO_2 sensors for useful applications. Highly crystalline CdO nanostructures have been studied as detecting layer in resistive detectors and exhibited high reactivity to NO_2 at low working temperature of 100 °C and high selectivity against CO (Rajesh et al. 2014).

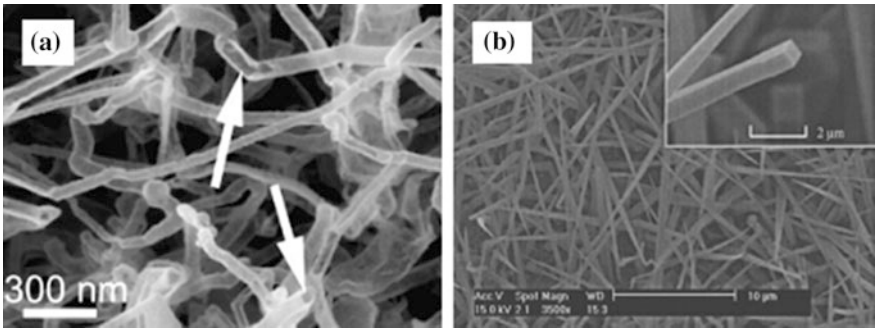

Fig. 2.6 **a** SEM image of thermally synthesized CdO NTs. White arrows indicate the hatches of NTs (Lu et al. 2008). © 2008 Elsevier **b** SEM image CdO nanoneedles with a square cross section (Liu et al. 2003). © 2003 American Institute of Physics

The exclusive properties of CdO makes it a potential candidate for photodiodes (Soylu and Kader 2016), phototransistors, photovoltaic cells (Usharani et al. 2015), transparent electrodes (Tang et al. 2015), solar cells (Radi et al. 2006), liquid crystal displays (Baranov et al. 1997), photodetectors (Ortega et al. 2000), gas sensors (Rajesh et al. 2014) and spintronics etc. (Thovhogi et al. 2016; Thema et al. 2015; Jimenez-Perez et al. 2015). It has attraction for use as a gas sensing material due to its liquid petroleum gas sensing properties (Waghulade et al. 2007). Such extraordinary properties and multifunctionality of CdO has given it a valuable place in the family of nanomaterials.

2.6.2 Cadmium Sulfide

Cadmium sulfide (CdS) is a binary compound of cadmium and sulfur. Its bulk structure has a hexagonal wurtzite structure with melting point 1600 °C (Goldstein et al. 1992) and is insoluble in water, but soluble in dilute mineral acids. It is an n-type semiconductor. It has a deep acceptor level and shows conductivity due to sulfur vacancies. At room temperature, the bulk structure of CdS has the value of band gap energy 2.42 eV, (Rajeshwar et al. 2001) and this value of energy shows that it is one of the most capable applicant for sensing visible light (Singh and Chauhan 2009). With the modifications in reaction conditions, CdS shows the corresponding changes in its 1D morphology. Band gap of CdS straightforwardly can be tuned through preparing the ternary alloys with CdSe to be applied in tunable photodetectors (Takahashi et al. 2012). Though CdS has a number of applications in bulk form but its conversion into nanoscale provide exceptional physical, chemical, electrical, optical, and transport properties. Due to size-dependent characteristics of the II–VI semiconductor nanostructures, 2.5 nm CdS reveal its very low melting point as ∼400 °C (Goldstein et al. 1992). A change in the band gap was observed for CdS nanocrystallites with its band gap energy 3.85 eV (Banerjee et al. 2000). At high pressure a difference in its phase from hexagonal wurtzite type to rock salt cubic phase was also observed (Chen et al. 1997).

Different structures of CdS shows different properties, wurtzite CdS nanostructures have been prepared with complex morphologies (Yao et al. 2006). CdS NRs (shaped as very structured hierarchical nanoflowers), NWs (branched), and nanotrees (construct via branched nanopines) showed good photocatalytic properties. Their photocatalytic performance for the degradation of acid fuchsine has been studied and branched NWs proved to be good photocatalyst. Nanostructures of CdS can easily be tuned for emitting the visible light through variations in the initial ratios of Cd and S (Lopes et al. 2014). NBs are chemically pure and structurally homogeneous and create a class of nanostructures with 30–300 nm width, 10–30 thickness and length in millimeters (Fig. 2.7). Dielectric properties of CdS NPs have been investigated in frequency range between 50 Hz and 5 MHz (Suresh 2013). There was an increase in these properties observed at low-frequency range at diverse temperatures.

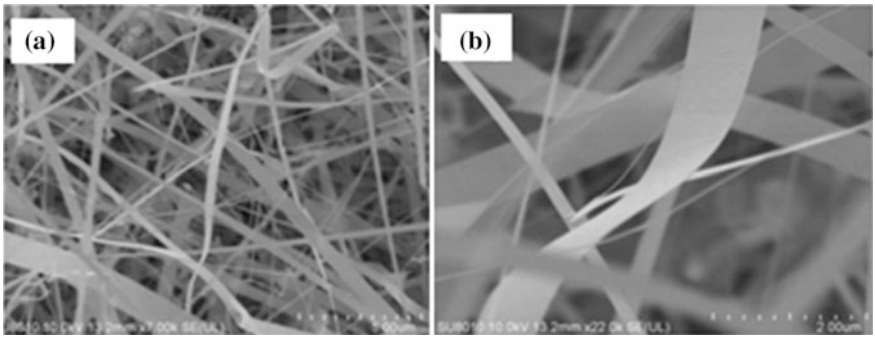

Fig. 2.7 SEM images of sythesized CdS NBs (Li et al. 2014). © Open access

At present, nanostructured mosquito larvicides have an important role for controlling the malaria vectors Anopheles stephensi and A. sundaicus (Sujitha et al. 2017). CdS NPs have been proved to be very toxic for young instars of the malaria vectors populations and also against the chloroquine-resistant (CQ-r) plasmodium falciparum parasites. This nanoproduct showed considerable affects on the enzymatic activity of non-target aquatic organisms, with unique reference to mud crabs. CdS is one of the most proficient nanomaterial for solar cells (El-Baz et al. 2016) and there are numerous applications of this material in the field of optoelectronics, photonics, photovoltaic, and photocatalysis (Rathinamala et al. 2014). CdS is also used as a pigment in paints and in engineered plastic for good thermal stability (Acharya 2009). In photonics, CdS is employed to make NCs (Dai et al. 2010). A little modification in size and morphology of CdS NPs leads to its increased photocatalytic activity (Khan et al. 2016). High-sensitivity photodetector material have been observed from CdS NTs and NWs, proving their potential as photodetectors in technological applications with high capability at low-cost (An and Meng 2016). Due to high value of surface to volume ratio, CdS nanomaterials can be used to design photocells (Samarasekara and Madushan 2016), light-emitting diodes (LEDs) (Lin et al. 2002; Murai et al. 2005), lasers (Duan et al. 2003), address decoders (Zhong et al. 2003), sensors (Travas-Sajdic et al. 2006), optical biosensors (Lin et al. 2013), optical switches (Li et al. 2010), hydrogen production (Zyoud et al. 2010), and water purification (Zhu et al. 2009). All of these striking properties points to potentials of CdS nanomaterials for ongoing and future applications.

2.6.3 Cadmium Selenide

Cadmium selenide (CdSe) is a binary compound of cadmium and selenium which shows n-type conductivity and has a band gap of 1.74 eV at room temperature. The molecular mass of CdSe is 191.37 g/mol, and appears as a dark red material (Amiri et al. 2013), it can have structures of hexagonal as well as cubic. In research, CdSe

nanomaterials have been one of the most attractive semiconducting materials unlike bulk counterparts of other members of cadmium chalcogenides. Due to their unique characteristics and applications, CdSe nanomaterials are of great interest in different fields of science and technology. The electrical and optical properties of the CdSe nanomaterials are size-dependent. These nanomaterials are extensively studied because of their adjustable band gap and reducing their size plays an important role in devices covering the whole spectrum of visible light (Qu and Peng 2002).

The coating of hydrophilic polymers enables them to be soluble in water, protect the photophysical properties of CdSe core, and secure the relatively compact dimensions (Fig. 2.8a). The shell additionally offers the surface trap states, increasing the fluorescence QY and making the nanostructures to be applied in fields of biological labeling and light-emitting devices. CdSe NPs prepared by Kalhori et al., showed the increased photoconductivity as compared to the preceding research work and photosensitivity of 110, which is also better than the earlier work (Kalhori et al. 2015). In the Fig. 2.8b, different-sized ZnS-capped CdSe QDs are shown; every test tube emits a light of diverse color, displaying the variation in size of the particles.

CdSe and CDSe/CdS NPs have been prepared by Suganthi et al. and their optical properties were studied. TEM and HR-TEM images revealed a narrow size distribution for CdSe NPs and for both of structures "quantum confinement effect" was observed (Suganthi et al. 2012). The size of CdSe and CdSe/CdS NPs were 2.5 and 5 nm respectively.

There is a focused progress towards the development of controlled synthesis of CdSe nanomaterials of different sizes, shapes, and morphologies. These nanostructures have a number of captivating applications in the field of optoelectronics (Chaudhari et al. 2016), photodetectors (An and Meng 2016), nanosensing (Hooshmand and Es' haghi 2017), biomedical imaging (Li et al. 2016), and high-efficiency solar cells (McElroy et al. 2014). CdSe NPs can be synthesized by different techniques like co-precipitation, electrodepotion (Soundararajan et al. 2009), pulsed sonoelectrochemical (Mastai et al. 1999), solvothermal (Singh et al. 2011) and hot injection method (Williams et al. 2009).

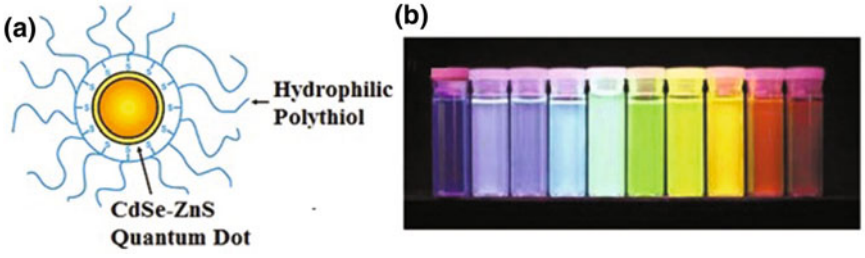

Fig. 2.8 **a** Schematic diagram of hydrophilic polythiol coated CdSe-ZnS QD (Yildiz et al. 2009). © 2009 American Chemical Society **b** The emission of fluorescence colors in ZnS-capped CdSe QDs different-sized CdSe QDs (Han et al. 2001). © 2011 Nature Publishing Group

2.6.4 Cadmium Telluride

Cadmium selenide (CdTe) is a binary compound of cadmium and tellurium. It is a direct band gap semiconductor with a band gap of 1.56 eV, and its nanomaterial has a band gap ranging from 1.5 to 2.1 eV. The thermal conductivity of these nanomaterials makes them suitable for use in thermoelectric applications.

This is comparatively a narrow band gap semiconductor and achieved huge consideration because it covers unique portion of solar spectrum and have a high absorption coefficient which make it an appropriate material for use in photovoltaic devices (Li et al. 2013), light-emitting diodes (Chin et al. 2008), and drug nanocarriers (Wang et al. 2014). CdTe is used as window material for heterojunction solar cells to avoid the recombination of photo-generated carriers which consequently improves the solar cells efficiency (Morales-Acevedo 2006). CdTe NWs were self-assembled by eliminate the shielding of organic stabilizer

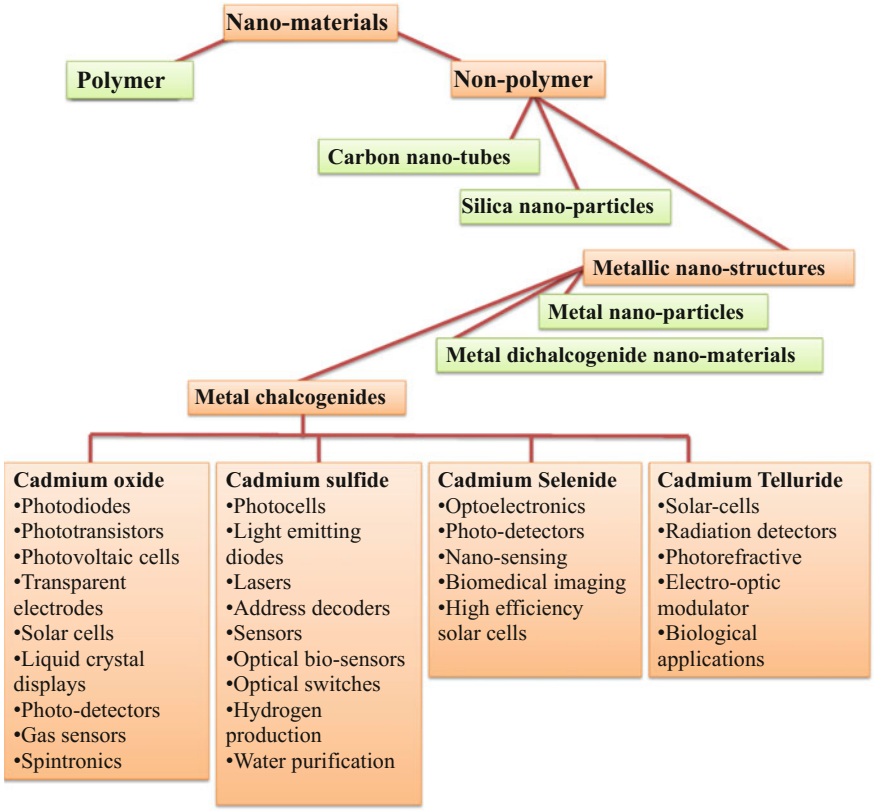

Fig. 2.9 Classification of nanomaterials and applications-tree of cadmium chalcogenide nanomaterials

(Tang et al. 2006). The synthesized NWs have a high aspect ratio, homogeneity, and optical performance (Tang et al. 2002). CdTe nanostructures have been stabilized by the thioglycolic acid. Exclusion of stabilizer is one of the main features to obtain NWs from NPs. CdTe in the form of NWs showed suitable properties to be used in optoelectronic applications (Yang et al. 2010).

In photovoltaics, it has been exploited to fabricate CdTe and copper indium diselenide solar cells to act as a window layer that separates charge carriers produced due to photon absorption and photo detectors (Wang et al. 2006) and in the fabrication of thin film solar cells (Romeo et al. 2007). Crisp et al. has prepared a monolithic CdTe–PbS tandem solar cell structural design with 40% power conversion efficiency (Crisp et al. 2017). CdTe and PbS absorber layers are properly merged in sequence through a ZnTe-ZnO tunnel junction. In medical field, molecular analysis is very significant in determining the progress in health. CdTe QDs immobilized on paper-based sensing device are very potential materials to analyze the beginning and development of disease conditions (Lin et al. 2017). CdTe nanostructures have potential for application in solar cells (Singh et al. 2004), radiation detectors (Toyama et al. 2006), photorefractive (Shcherbin et al. 2002), electro-optic modulator (Taki 2013), and biological (Wang et al. 2005) applications. The classification of nanomaterials and applications of cadmium chalcogenide nanomaterials is sketeched in Fig. 2.9.

2.7 Characterization Methods

In order to study the properties of synthesized nanomaterials, a number of characterization techniques are used. A brief description on major experimental techniques used to characterize the nanomaterials is given in the following.

2.7.1 Structural Characterization via X-ray Diffraction

XRD (X-ray diffraction) is a basic and necessary tool for study of structural properties of nanomaterials. It is the most widely used method to investigate the crystal structure, lattice parameters, grain size, and phase of nanomaterials. In order to establish the formation of structural phase of synthesized nanomaterials, it is a primary and non-destructive tool which provides quick and reliable information.

The Bragg positions of the lines on the XRD patron gives information on crystal structure unit cell parameters and related data. The grain size of the nanomaterials is usually obtained from the width of peak and computed by using the Scherrer equation given below;

$$D = \frac{k\lambda}{\beta \cos\theta},$$

where λ = wavelength of X-rays, β = width at half maximum of peaks. D is mean crystalline dimension perpendicular to the reflecting parts. The value of Scherrer constant k depends upon the shape of nanomaterial; for spherical shaped particles, its value is 0.9.

The XRD graph with 2θ (degrees) versus intensity is commonly used to collect basic crystallographic information about the samples. The position, height, width, and shape of the obtained peak are finger prints of the material and can be used to access its structural properties. In order to find these parameters, Gaussian and Lorentz functions are commonly used to analyze single peaks as well as overlapping peaks via multiple curve fitting procedure. For crystallographic analysis of XRD data, several software are available, e.g., X'Pert Highscore, JADE, Match, GSAS, TOPAS, XLENS, DQUANT, etc. Following sections may help in interpretation of XRD results.

Peak position: 2θ values given on x-axis are related to miller indices (hkl) of planes and provide information related to interplanar spacing, lattice constants, etc. The phases identification can be made using peak position. From the obtained XRD patron, chose a peak and find the corresponding Bragg angle θ (by halving the position of the peak) of your sample. Using this angle θ, wavelength of X-rays and order of diffraction, one can easily find d-value of the corresponding phase using Bragg's law $2d\sin\theta = n\lambda$. Similarly, d-values corresponding to all notable peaks can be found which help to index and hence identification of probable phases after comparison with standard phases (using JCPDS for instance).

Peak height: The intensity of peaks given along y-axis shed light on crystallinity, atomic positions, thickness of structural phases etc.

Peak width: Full width of peak at half of maximum intensity (FWHM) gives its width measured usually in degrees. It can be used to find crystallite size, size distribution, micro-strain analysis, etc. The broadening of peak (excluding the chances of instrumental broadening) is inversely proportional to crystallite size and can be used to find the size as per Scherrer equation. For a particular material, if we keep on gradually dividing the crystallite into smaller and smaller grains, the broadening of peak will increase accompanied with decrease in peak height but *in-principle* area under the curve remains constant.

It is worth mentioning that broadening due to grain size, micro-strain, and instrument greatly increase for the higher Bragg angles. At lower Bragg angles, peak symmetry whereas at higher Bragg angles peak height are considered to obtain meaningful results. For comparison purposes, and getting reliable results, it is recommended that data related to intermediate 2θ scale (30–60°) should be preferred.

Peak Shape: The shape of XRD peak is usually ignored but it contains important structural information. The changes in shape of peak at its top and bottom should be considered to shed light on grain size, lattice strain, etc. Sometimes, peak

is found asymmetric (at lower or higher angle sides) which contains important information and should be carefully analyzed.

Determination of Strain: The structural variations (due to issues related to chemical compositions, lattice relaxation, etc.) observed for materials when compared with the bulk point to the presence of strain in the synthesized nanomaterials or thin films. It should be carefully analyzed because the presence of strain in local regions of microstructure changes the material's behavior. The strain may be present in two different modes; (i) The shift in peak position without any change in its broadening points to the presence of homogenous strain in the sample. In this case, every crystallite is strained in same amount which uniformly changes the interplaner spacing throughout. The peak is shifted to higher (lower) angles exhibiting compressive (tensile) strain. (ii) The shift in peak position associated with change in its broadening points to the presence of inhomogeneous strain. The crystallites are non-uniformly strained so every crystallite causes different change in 2θ and hence produces different shift in peak position. The inhomogeneous strain associated with structural defects (point, line, areal, volume, etc.) is calculated via ratio of change in interplanar spacing to the unstrained spacing. The strain evaluation should be carefully monitored because the broadening may also be caused by simultaneous effects of inhomogeneous strain and size which demands more rigorous treatment (e.g., Williamson Hall method).

2.7.2 Surface Morphological Characterization

The investigation of morphology of prepared nanomaterials is very important, since the resulting properties of the product are highly dependent on its size, shape, and structural arrangement. The techniques involving microscopy giving high-resolution images of local areas of samples are used to be employed for this purpose.

2.7.2.1 Scanning Probe Microscopy (SPM)

SPM consists of scheme closely related to STM and AFM. Piezoelectric transducer is used with a pointed probe scanned transversely on the surface; the probes can be placed upon the surface with Angstrom precisions. This provides the capability to investigate the spectroscopic information related even to a single atom.

2.7.2.2 Scanning Tunneling Microscopy (STM)

This method works on the basis of quantum mechanical tunneling phenomenon. Real-space images of the surfaces can be generated with atomic resolution. The

tunneling happens between the atomically pointed metallic tip and the conductive surface of the sample. This characterization method has started the advancement in novel classes of materials.

2.7.2.3 Atomic Force Microscopy (AFM)

AFM is an inexpensive method and is a modification appeared after development of STM (Binnig et al. 1986). In this method, van der Waals forces are mechanically determined between atomically pointed metallic tip and the surface using a flexible cantilever. STM can study the electronic behavior around the surface as well as can manipulate the individual atoms. This method can also be used for several forces like magnetic and electrostatic forces and for the study of chemical interactions. This double ability to investigate the currents and forces at nanometer and atomic scale has initiated a range of scanning probe microscopy (SPM) methods like magnetic force microscopy, electrostatic force microscopy, scanning capacitance microscopy, near-field scanning optical microscopy. These methods offered the potential for study of local, mechanical, optical, electrical, magnetic, thermal, and chemical properties of nanomaterials.

2.7.2.4 Scanning Electron Microscope (SEM)

SEM characterization technique was first time introduced in 1938. This method can offer the extremely magnified images of the surface and near-surface composition of the nanomaterials. Size, shape, microstructure, composition, and grain orientation can be calculated using this technique. The resolution and magnification of SEM can be simply controlled to a small number of nanometers and 10–300,000 times respectively. The working mechanism of this technique involves incidence of a focused electron beam on the surface of material ranging from 50 nm to 1 cm as a result of which electrons hit the surface to produce several signals which are recorded by detectors. These signals obtained from the specimen are then processed and showed on screen of CRO in the form of images. Secondary electron and backscattered electrons produce the images in SEM. The properties of these images are shown in Table 2.4.

2.7.2.5 Transmission Electron Microscopy (TEM)

TEM is the study of ultra-thin specimen through transmission of electrons from it, typical thickness 50–100 nm for beam of 100 keV. It is very costly method with beam of electrons having energy 100,000–400,000 eV. The obtained information is detected and displayed in the form of images onto an imaging device with range 50 nm–500 μm. A TEM consists of a vacuum system, chain of electromagnetic

Table 2.4 Image profiles of SEM

Properties/ SEM images	Scattering type	Energy	Resolution	Image type	Occurred
Secondary electron images	Inelastic scattering with atomic electrons	Less than 50 eV	High	3D appearance	Area near the beam impact zone
Backscattered electron images	Elastic scattering with atomic nucleus	Greater than 50 eV	–	–	In material with high atomic number

lenses, additional electrostatic plates, and imaging devices. An electron gun is included for thermionic emission of electrons.

TEM has appeared in diverse forms as high-resolution transmission microscopy (HRTEM), scanning transmission electron microscopy (STEM), etc. Variations in the phases of scattered electron beam show the contrast in TEM images, which provides basis for HRTEM. STEM offers a diverse number of modes to find the electronic structure and elemental composition of atoms. This is similar to SEM, only the specimen used is very thin for providing the transmission modes of imaging. Resolution of TEM depends upon the volume of the specimen, smaller volume shows the higher resolution, and so limitation of volume is a disadvantage of this method. Dimensionality is another problem using TEM, because it displays 2D images of 3D objects.

2.7.2.6 X-ray Photoelectron Spectroscopy (XPS)

This method was initially developed for investigation of composition and stoichiometry of the materials. XPS is a surface-sensitive technique for chemical analysis in which X-rays (high energy photons) are used to eject the core electrons from surface atoms. Study of the kinetic energy of these X-ray photoelectrons is used to determine the properties of the nanomaterials ranging from 1 to 10 nm.

The spectra obtained after XPS of samples gives binding energy (BE) of core shell electrons which can be used to explain the physical process (splitting of multiplets, chemical interactions, etc.) and measurement of material's parameters (chemical environment, ionic charge states, chemical composition, bonding, etc.). This technique is useful for characterization of top 1–10 nm of materials so it is highly sensitive to provide important information in case of nanomaterials.

Careful sample handling (including cleaning), choice of experimental conditions, and correct operation of the spectrometer are prerequisites to obtain reliable spectroscopic results. After conducting XPS of your samples, or upon receiving XPS data from your laboratory staff, the identification of peaks is the step of prime importance. The entire peaks obtained in XPS spectra are not photoelectron signatures of the material but also contain Auger lines, satellite peaks, background

signal, and noise. A careful analysis is required to assign peaks purely related to photoelectrons for measurement of corresponding BE.

Two most important parameters reflected from XPS spectra obtained after ionization of a particular core shell are BE on *x*-axis and intensity on *y*-axis. The XPS data processing includes background subtraction (and smoothing, if needed) and peak fitting analysis (using XPSPEAK, CasaXPS, etc.) to perform elemental identification by using NIST data or published literature by considering position of the peaks. The multiple peak fitting helps to deconvolute the overlapping peaks which are sometimes obtained in XPS spectra. It is an important step in which you should anticipate the spectrum by considering the recipe of your sample and the substrate (if any) into account. The interpretation of the spectrum should be carried out by focusing on different aspects of the peaks including position, height, width, shape, etc. The primary information on these features is given below.

Peak position: The peak position gives BE and acts as finger print to obtain information on chemical state of the material. It is at heart of XPS spectroscopy and provides elemental identification based on analysis of orbital's peaks. It should be noted that peaks related to **s** orbital are in the form of singlets whereas the peaks representing **p**, **d**, **f** orbitals are doublets due to spin-splitting.

Peak height: The intensity points out the amount of material in the scanning region (sample's surface), because number of emitting electrons is proportional to number of atoms therein. If multiple peaks, instead of a single peak, are obtained then relative intensity provide useful information and can be used to estimate the elemental or chemical composition in the surface region. The atomic percentage depends upon relative intensity and is equal to ratio of intensity of relevant peak to cumulative intensity of all peaks by taking sensitivity factor into account.

Peak width: The peak width (FWHM) and change in its value upon sample's processing contains information about chemical environment and change of chemical state of the material. It may help in shedding light on number and nature of chemical bonds. The reasons of broadening include presence of charge, inhomogeneity, vibrational states, etc., of the samples.

Peak shape: The changes in peak shape points to surface modification of samples and appearance of charge upon processing or X-ray irradiation. The asymmetry in the form of tailing of BE curves on higher energy side is often found in case of metals, metallic compounds, or metals doped semiconductor/insulators. It contains important information and should be carefully analyzed by suitable choice of fitting function.

2.7.2.7 Auger Electron Spectroscopy (AES)

AES method was proposed in 1925 when Auger observed that due to the X-rays or high energy irradiation, the ionized atom can eject one more electron. The first emitted electron must be from inner shells to eject another electron from surface known as auger electron. This second emitted electron is used to investigate the

material properties by calculating its kinetic energy. As in XPS, AES can also determine the 10 nm of the material`s surface and used to recognize the elements in the material. The value of resolution of AES is 10 nm with sensitivity of about 0.3% higher than XPS.

2.7.3 Optical Characterization Techniques

There are a number of techniques used for optical characterization of prepared nanomaterials. These techniques are mostly quick, reliable, and non-destructive. These are available in several configurations and several research groups used home built equipment for the purpose.

2.7.3.1 UV–Vis Spectroscopy

This is a comparatively simple and efficient method to observe the characteristic absorption edges and band gap of the materials. It is also used to find the concentration of components of organic and inorganic nanomaterials and recognize the functional groups in the substances. Ultra-violet and visible range electromagnetic radiations are used to quantitatively study the materials ranging from 400 nm to 1 nm and analyze through their absorption spectra. The broadening of the absorption peak tells about the composition, quality, and size distribution of the nanomaterials. Electronic properties like band gap and size-dependent properties like peak broadening and shifts in absorption spectra at nanoscales can also be measured.

UV–Vis spectroscopy can be used to characterize the nanomaterials for determination of concentration, size, distribution, band gap, and several optical properties. It is employed to measure the sample's response (in terms of absorbance, reflectance, transmittance) by shining light in UV and visible regions of electromagnetic spectrum. Generally, it is used in absorbance mode to provide information on the extent of absorption of light (intensity along *y*-axis) as a function of wavelength or energy (along *x*-axis) of incident photons.

Not every wavelength will be absorbed by the sample but the absorption will only happen when energy of incident photon matches with energy difference (band gap) of accessible electronic states. When incident energy matches the band gap, an electron in highest occupied energy level (HOMO in case of molecular and VB in case of solids) jumps to lowest unoccupied energy level (LUMO in case of molecular and CB in case of solids) to produce a peak or band in absorption spectrum. The graph gives broad peaks or bands giving spectrum of absorbed radiations and often displays maximum absorbance at certain wavelength.

Band gap determination: In case of insulating or semiconducting samples, HOMO-LUMO gap (for molecular) or band gap (VB-CB difference for solids) can

be straightforwardly measured by observing major absorption peak or absorption edge in the spectrum. Sometimes the peak or the edge shifts to higher energies (blue shift) or lower energies (red shift) due to band gap modifications upon processing of the as-grown sample (alloying, doping, annealing, etc.) which can be easily determined using this technique.

The calculation of band gap of thin films, using data from UV–Vis spectroscopy, involves calculation of absorption coefficient and drawing Tauc plot. However, surface and size effects dominating in case of nanoparticles and film thickness usually does not matter due to which modified procedures are needed to measure the band gap. The fitting of absorption spectrum (Ghobadi 2013) can be used to evaluate the optical band gap of nanomaterials as per following equation;

$$\text{Abs.}(\lambda) = B_1 \lambda \left(\frac{1}{\lambda} - \frac{1}{\lambda_g} \right)^m + B_2,$$

where B_1 and B_2 are constants. Plot a graph of $\left[\frac{Abs.(\lambda)}{\lambda}\right]^{1/m}$ as a function of $\frac{1}{\lambda}$ and extrapolate the linear portion of the curve (or drop a tangent) to intersect x-axis which will be the value of λ_g after which value of optical band gap can be found by using $E_g = \left(\frac{1240}{\lambda(\text{nm})}\right)\text{eV}$. The value of fitting parameter m points towards direct (with m = 1/2) and indirect (with m = 2) nature of the optical band gap.

Intensity or Absorbance: The absorbance plotted along y-axis gives ratio of transmitted to incident light and reveals relative number of photons absorbed by the structure which depends upon the concentration of structural units of the material. The comparison of peak intensities in a spectrum helps finding the transition probability for the electronic transitions involved in the process. The absorbance can be translated to the dimensions of the samples by measuring *optical density* which is ratio of absorbance to film thickness (in case of thin films).

Quantum confinement effects: In case of semiconducting nanomaterials, absorption spectrum changes with size of nanomaterial when the size becomes smaller than exciton Bohr radius of the material. Therefore, as the size of nanomaterial decreases the absorption peak shifts to higher energies and this size dependence is known as quantum confinement effect.

2.7.3.2 Photoluminescence (PL) Spectroscopy

It is contactless, non-destructive method which utilizes the electromagnetic radiations usually from laser source to study the luminescent properties of the materials. Many material properties like band gap, impurity levels and recombination mechanism can be determined from intensity, wavelength, peak's width, and stability.

2.7.4 Vibrational Characterization Techniques

The study of vibrational properties is often carried out to study lattice vibrational and bonding details of the materials. This class of investigation gives key information of materials to provide reliable information.

2.7.4.1 Vibrational Spectroscopy

Vibrational spectroscopy is the study of radiation-mater interaction through vibrational excitation and de-excitation. Vibrational spectroscopy is used for structural study, chemical bonds in the detecting materials, multicomponent qualitative, and quantitative analysis. Vibrational properties of molecules can be studied using the Infrared and Fourier transform infrared spectroscopy technique. **IR and Raman** spectroscopy are examples of vibrational spectroscopy.

2.7.4.2 Raman Spectroscopy

This method is used in materials characterization to investigate the vibrational, rotational, and other low-frequency modes.

2.7.4.3 IR Spectroscopy

IR spectroscopy is the analysis of interaction of IR radiations with the materials. It is a popular and versatile characterization method based on the vibrations of the atoms and molecules. It is used to study the attachment of organic ligands to organic/inorganic NPs. IR spectrum is determined by examining the sample through a continuous series of IR wavelength as from 400 to 4000 cm^{-1}. IR photons are irradiated to the molecules each have its exclusive nature and their bond type is recognized. Chemical bonds can be turned to many ways: stretching, scissoring, rocking, wagging, and twisting. Almost all organic materials absorb the IR radiations, but inorganic materials are not usually investigated as their peak intensities possibly too weak to be determined. In this method, almost any sample in almost any condition can be characterized. From their results in absorption spectra, the values of energy showing the peaks indicate the vibrational frequencies of that part of the sample.

In IR spectra, peak position, intensity, and width tells about the structure of molecules, concentration of the molecules, and sensitivity for chemical medium (hydrogen bonding and pH) of samples respectively (Suart 2004). This method is comparatively fast, easy, low-cost and almost a universal characterization method. However, there are some disadvantages like it cannot detect some molecules. If the sample is more complicated, then the spectral peaks are so mixed that they cannot be distinguished from each other.

2.7.4.4 Fourier Transform Infrared (FTIR) Spectroscopy

FTIR spectroscopy is the specific form of IR spectrometry with advanced qualities of IR characterization method. It is used to study the molecular vibrations and resonance study (Smith 2011). IR photons are produced from a blackbody source. The interferometer is used to encode these photons resulting in the form of signals. These signals are transmitted to or reflected off the surface of the sample. Then these signals are perceived by specially designed detector for further processing. Analog to digital conversion is performed and the digital signals are sent to computer. Fourier transform carried out in computer and the FTIR spectrum is obtained.

This method is very fast and the measurements are made in seconds. There are many frequencies which can be measured at the same time using this method. Signal-to-noise ratio (SNR = signal/noise) determines the quality of the peak. Signal is the measure of size of the peak, while noise is the error. In comparison to IR, FTIR provides an advantage of measuring a high value of SNR and 10–100 times better than IR spectrometers.

References

Acharya, K. P. (2009). *Photocurrent spectroscopy of CdS/plastic, CdS/glass, and ZnTe/GaAs hetero-pairs formed with pulsed-laser deposition* (Doctoral dissertation, Bowling Green State University).

Acharya, A., Sahu, S., Balamurgan, S., & Roy, G. S. (2011). Effect of doping on nano cadmium-selenide (CdSe)-assessment through UV-VIS spectroscopy. *Latin American Journal of Physics Education, 5*(1), 134.

Afify, H. H., Ahmed, N. M., Tadros, M. Y., & Ibrahim, F. M. (2014). Temperature dependence growth of CdO thin film prepared by spray pyrolysis. *Journal of Electrical Systems and Information Technology, 1*(2), 119–128.

Aldwayyan, A. S., Al-Jekhedab, F., Al-Noaimi, M., Hammouti, B., Hadda, T. B., Suleiman, M., et al. (2013). Synthesis and characterization of CdO NPs starting from organometalic dmphen-CdI_2 complex. *International Journal of Electrochemical Science, 8*(10506), e10514.

Alemi, A., Joo, S. W., Khademinia, S., Dolatyari, M., Bakhtiari, A., Moradi, H., et al. (2013). Sol-gel synthesis, characterization, and optical properties of Gd^{3+}-doped CdO sub-micron materials. *International Nano Letters, 3*(1), 1.

Alivisatos, A. P. (1996). Perspectives on the physical chemistry of semiconductor NCs. *The Journal of Physical Chemistry, 100*(31), 13226–13239.

Amiri, G. R., Fatahian, S., & Mahmoudi, S. (2013). Preparation and optical properties assessment of cdse QDs. *Materials Sciences and Applications, 4*(02), 134.

An, Q., & Meng, X. (2016). Aligned arrays of CdS NTs for high-performance fully nanostructured photodetector with higher photosensitivity. *Journal of Materials Science: Materials in Electronics, 27*(11), 11952–11960.

Aqra, F., & Ayyad, A. (2014). Surface free energy of alkali and transition metal NPs. *Applied Surface Science, 314,* 308–313.

Arora, S., & Manoharan, S. S. (2007). Size-dependent photoluminescent properties of uncapped CdS particles prepared by acoustic wave and microwave method. *Journal of Physics and Chemistry of Solids, 68*(10), 1897–1901.

Balamurugan, S., Balu, A. R., Usharani, K., Suganya, M., Anitha, S., Prabha, D., et al. (2016). Synthesis of CdO nanopowders by a simple soft chemical method and evaluation of their antimicrobial activities. *Pacific Science Review A: Natural Science and Engineering, 18*(3), 228–232.

Banerjee, R., Jayakrishnan, R., & Ayyub, P. (2000). Effect of the size-induced structural transformation on the band gap in CdS NPs. *Journal of Physics: Condensed Matter, 12*(50), 10647.

Baranov, A. M., Malov, Y. A., Teryoshin, S. A., & Val'dner, V. O. (1997). Investigation of the properties of CdO films. *Technical Physics Letters, 23*(10), 805–806.

Benhaliliba, M., Benouis, C. E., Tiburcio-Silver, A., Yakuphanoglu, F., Avila-Garcia, A., Tavira, A., et al. (2012). Luminescence and physical properties of copper doped CdO derived nanostructures. *Journal of Luminescence, 132*(10), 2653–2658.

Binnig, G., Quate, C. F., & Gerber, C. (1986). Atomic force microscope. *Physical Review Letters, 56*(9), 930.

Brock, S. L. (2004). *Nanostructures and nano-materials: Synthesis, properties and applications By Guozhang Cao (University of Washington)* (434 pp.). London: Imperial College Press (distributed by World Scientific). ISBN 1-86094-415-9.

Buhro, W. E., & Colvin, V. L. (2003). Semiconductor NCs: Shape matters. *Nature Materials, 2* (3), 138–139.

Cao, G. (2004). *Nanostructures and nanomaterials: Synthesis, properties and applications*. World Scientific.

Cao, G., & Liu, D. (2008). Template-based synthesis of nanorod, nanowire, and nanotube arrays. *Advances in Colloid and Interface Science, 136*(1), 45–64.

Chaudhari, K. B., Gosavi, N. M., Deshpande, N. G., & Gosavi, S. R. (2016). Chemical synthesis and characterization of CdSe thin films deposited by SILAR technique for optoelectronic applications. *Journal of Science: Advanced Materials and Devices, 1*(4), 476–481.

Chaure, S. (2016). Synthesis and characterization of vertically aligned cadmium oxide nanowire array. *Journal of Materials Science: Materials in Electronics, 2*(28), 1832–1836.

Chen, C. C., Herhold, A. B., Johnson, C. S., & Alivisatos, A. P. (1997). Size dependence of structural metastability in semiconductor NCs. *Science, 276*(5311), 398–401.

Chin, P. T., Stouwdam, J. W., van Bavel, S. S., & Janssen, R. A. (2008). Cluster synthesis of branched CdTe NCs for use in light-emitting diodes. *Nanotechnology, 19*(20), 205602.

Crisp, R. W., Pach, G. F., Kurley, J. M., France, R. M., Reese, M. O., Nanayakkara, S. U., et al. (2017). Tandem solar cells from solution-processed CdTe and PbS QDs using a ZnTe–ZnO tunnel junction. *Nano Letters, 17*(2), 1020–1027.

Dagdelen, F., Serbetci, Z., Gupta, R. K., & Yakuphanoglu, F. (2012). Preparation of nanostructured Bi-doped CdO thin films by sol–gel spin coating method. *Materials Letters, 80,* 127–130.

Dai, G., Zou, B., & Wang, Z. (2010). Preparation and periodic emission of superlattice CdS/CdS: SnS_2 microwires. *Journal of the American Chemical Society, 132*(35), 12174–12175.

Dakhel, A. A. (2011a). Effect of cerium doping on the structural and optoelectrical properties of CdO nanocrystallite thin films. *Materials Chemistry and Physics, 130*(1), 398–402.

Dakhel, A. A. (2011b). Effect of thermal annealing in different gas atmospheres on the structural, optical, and electrical properties of Li-doped CdO nanocrystalline films. *Solid State Sciences, 13*(5), 1000–1005.

Dakhel, A. A. (2012). Structural and optoelectronic properties of Zn-incorporated CdO films prepared by sol–gel method. *Journal of Alloys and Compounds, 539,* 26–31.

Djurišić, A. B., & Leung, Y. H. (2006). Optical properties of ZnO nanostructures. *Small, 2*(8–9), 944–961.

Duan, X., Huang, Y., Agarwal, R., & Lieber, C. M. (2003). Single-nanowire electrically driven lasers. *Nature, 421*(6920), 241–245.

El-Baz, A. F., Sorour, N. M., & Shetaia, Y. M. (2016). Trichosporon jirovecii–mediated synthesis of cadmium sulfide NPs. *Journal of Basic Microbiology, 56*(5), 520–530.

Fox, M. (2002). *Optical properties of solids. Oxford Master Series in Condensed Matter Physics*. New York: Oxford University Press.

Gao, X. F., Li, H. B., Sun, W. T., Chen, Q., Tang, F. Q., & Peng, L. M. (2009). CdTe QDs-sensitized TiO_2 nanotube array photoelectrodes. *The Journal of Physical Chemistry C, 113*(18), 7531–7535.

Ge, M., Li, Q., Cao, C., Huang, J., Li, S., Zhang, S., … & Lai, Y. (2016). One-dimensional TiO_2 nanotube photocatalysts for solar water splitting. *Advanced science.*

Ghobadi, N. (2013). Band gap determination using absorption spectrum fitting procedure. *International Nano Letters, 3*(1), 2.

Ghoshal, T., Biswas, S., Nambissan, P. M. G., Majumdar, G., & De, S. K. (2009). Cadmium oxide octahedrons and NWs on the micro-octahedrons: A simple solvothermal synthesis. *Crystal Growth & Design, 9*(3), 1287–1292.

Goldstein, A. N., Echer, C. M., & Alivisatos, A. P. (1992). Melting in semiconductor NCs. *Science, 256*(5062), 1425–1427.

Goswami, B., & Choudhury, A. (2015). Enhanced visible luminescence and modification in morphological properties of cadmium oxide NPs induced by annealing. *Journal of Experimental Nanoscience, 10*(12), 900–910.

Guo, Z., & Tan, L. (2009). *Fundamentals and applications of nanomaterials*. Norwood: Artech House.

Gupta, R. K., Ghosh, K., Patel, R., & Kahol, P. K. (2008). Effect of oxygen partial pressure on structural, optical and electrical properties of titanium-doped CdO thin films. *Applied Surface Science, 255*(5), 2414–2418.

Han, M., Gao, X., Su, J. Z., & Nie, S. (2001). Quantum-dot-tagged microbeads for multiplexed optical coding of biomolecules. *Nature Biotechnology, 19*(7), 631.

Harrell, S. M., McBride, J. R., & Rosenthal, S. J. (2013). Synthesis of ultrasmall and magic-sized CdSe NCs. *Chemistry of Materials, 25*(8), 1199–1210.

He, X., & Ma, N. (2014). An overview of recent advances in QDs for biomedical applications. *Colloids and Surfaces B: Biointerfaces, 124,* 118–131.

Hooshmand, S., & Es' haghi, Z. (2017). Microfabricated disposable nanosensor based on CdSe quantum dot/ionic liquid-mediated hollow fiber-pencil graphite electrode for simultaneous electrochemical quantification of uric acid and creatinine in human samples. *Analytica Chimica Acta, 972,* 28–37.

Hu, D., Zhang, P., Gong, P., Lian, S., Lu, Y., Gao, D., et al. (2011). A fast synthesis of near-infrared emitting CdTe/CdSe QDs with small hydrodynamic diameter for in vivo imaging probes. *Nanoscale, 3*(11), 4724–4732.

Hu, L., Choi, J. W., Yang, Y., Jeong, S., La Mantia, F., Cui, L. F., et al. (2009). Highly conductive paper for energy-storage devices. *Proceedings of the National Academy of Sciences, 106*(51), 21490–21494.

Huang, L., Lin, C. C., Riediger, M., Röder, R., Tse, P. L., Ronning, C., et al. (2015). Nature of AX Centers in Antimony-Doped Cadmium Telluride NBs. *Nano Letters, 15*(2), 974–980.

Jefferson, P. H., Hatfield, S. A., Veal, T. D., King, P. D. C., McConville, C. F., Zúñiga-Pérez, J., et al. (2008). Bandgap and effective mass of epitaxial cadmium oxide. *Applied Physics Letters, 92*(2), 022101.

Jimenez-Perez, J. L., Fuentes, R. G., Sánchez-Sosa, R., Torres, M. Z., Correa-Pacheco, Z. N., & Ramírez, J. S. (2015). Thermal diffusivity study of NPs and NRs of titanium dioxide (TiO 2) and titanium dioxide coated with cadmium sulfide (TiO 2 CdS). *Materials Science in Semiconductor Processing, 37,* 62–67.

Kalhori, H., Irajizad, A., Azarian, A., & Ashiri, R. (2015). Synthesis and characterization of electrochemically grown CdSe NWs with enhanced photoconductivity. *Journal of Materials Science: Materials in Electronics, 26*(3), 1395–1402.

Kamarudin, S. K., Achmad, F., & Daud, W. R. W. (2009). Overview on the application of direct methanol fuel cell (DMFC) for portable electronic devices. *International Journal of Hydrogen Energy, 34*(16), 6902–6916.

Kamat, P. V. (2008). Quantum dot solar cells. Semiconductor NCs as light harvesters. *The Journal of Physical Chemistry C, 112*(48), 18737–18753.

Kargar, A., Sun, K., Jing, Y., Choi, C., Jeong, H., Jung, G. Y., et al. (2013). 3D branched nanowire photoelectrochemical electrodes for efficient solar water splitting. *ACS Nano, 7*(10), 9407–9415.

Khalily, M. A., Eren, H., Akbayrak, S., Susapto, H. H., Biyikli, N., Özkar, S., et al. (2016). Facile synthesis of three-dimensional Pt-TiO_2 nano-networks: A highly active catalyst for the hydrolytic dehydrogenation of ammonia-borane. *Angewandte Chemie, 128*(40), 12445–12449.

Khan, A., Khan, R., Waseem, A., Iqbal, A., & Shah, Z. H. (2016). CdS nanocapsules and nanospheres as efficient solar light-driven photocatalysts for degradation of Congo red dye. *Inorganic Chemistry Communications, 72,* 33–41.

Kim, W., Baek, M., & Yong, K. (2016). Fabrication of ZnO/CdS, ZnO/CdO core/shell nanorod arrays and investigation of their ethanol gas sensing properties. *Sensors and Actuators B: Chemical, 223,* 599–605.

Krishnakumar, T., Jayaprakash, R., Prakash, T., Sathyaraj, D., Donato, N., Licoccia, S., et al. (2011). CdO-based nanostructures as novel CO_2 gas sensors. *Nanotechnology, 22*(32), 325501.

Li, D., Wang, S., Wang, J., Zhang, X., & Liu, S. (2013). Synthesis of CdTe/TiO 2 NPs and their photocatalytic activity. *Materials Research Bulletin, 48*(10), 4283–4286.

Li, L., Abild-Pedersen, F., Greeley, J., & Nørskov, J. K. (2015). Surface tension effects on the reactivity of metal NPs. *The Journal of Physical Chemistry letters, 6*(19), 3797–3801.

Li, L., Yang, S., Han, F., Wang, L., Zhang, X., Jiang, Z., et al. (2014). Optical sensor based on a single CdS nanobelt. *Sensors, 14*(4), 7332–7341.

Li, X., Jia, Y., Wei, J., Zhu, H., Wang, K., Wu, D., et al. (2010). Solar cells and light sensors based on nanoparticle-grafted carbon nanotube films. *ACS Nano, 4*(4), 2142–2148.

Li, Y., Zhang, J., Guo, Y., Chen, M., Wang, L., Sun, R., et al. (2016). Cellulosic micelles as nanocapsules of liposoluble CdSe/ZnS QDs for bioimaging. *Journal of Materials Chemistry B, 4*(39), 6454–6461.

Lin, C. F., Liang, E. Z., Shih, S. M., & Su, W. F. (2002, June). CdS nanoparticle light-emitting diode on Si. In *Symposium on Integrated Optoelectronic Devices* (pp. 102–110). International Society for Optics and Photonics.

Lin, S. X., Wong, M. M. K., Pat, P. K., Wong, C. Y., Chiu, S. K., & Pun, E. Y. B. (2013, May). Optical biosensor based on cadmium sulfide-silver nanoplate hybrid structure. In *Proc. of SPIE Vol* (Vol. 8774, pp. 877413–1).

Lin, Z., Lv, S., Zhang, K., & Tang, D. (2017). Optical transformation of a CdTe quantum dot-based paper sensor for a visual fluorescence immunoassay induced by dissolved silver ions. *Journal of Materials Chemistry B, 5*(4), 826–833.

Liu, J. W., Chen, F., Zhang, M., Qi, H., Zhang, C. L., & Yu, S. H. (2010). Rapid microwave-assisted synthesis of uniform ultralong Te NWs, optical property, and chemical stability. *Langmuir, 26*(13), 11372–11377.

Liu, X., Li, C., Han, S., Han, J., & Zhou, C. (2003). Synthesis and electronic transport studies of CdO nanoneedles. *Applied Physics Letters, 82*(12), 1950–1952.

Lopes, P. A., Santos, M. B., Mascarenhas, A. J. S., & Silva, L. A. (2014). Synthesis of CdS nano-spheres by a simple and fast sonochemical method at room temperature. *Materials Letters, 136,* 111–113.

Lu, H. B., Liao, L., Li, H., Tian, Y., Wang, D. F., Li, J. C., et al. (2008). Fabrication of CdO NTs via simple thermal evaporation. *Materials Letters, 62*(24), 3928–3930.

Lu, Q., Gao, F., & Komarneni, S. (2004). Microwave-assisted synthesis of one-dimensional nanostructures. *Journal of Materials Research, 19*(6), 1649–1655.

Luo, B., Liu, G., & Wang, L. (2016). Recent advances in 2D materials for photocatalysis. *Nanoscale, 8*(13), 6904–6920.

Ma, J., Lian, J., Duan, X., Liu, Z., Peng, P., Liu, X., et al. (2011). Growth of tellurium nanowire bundles from an ionic liquid precursor. *CrystEngComm, 13*(7), 2774–2778.

Mahdi, M. A., Hassan, J. J., Ng, S. S., & Hassan, Z. (2013). High-quality ZnCdS nanosheets prepared using solvothermal synthesis. *Journal of Nanoscience*, *2013*.

Majid, A., Arshad, H., & Murtaza, S. (2015). Synthesis and characterization of Cr doped CdSe NPs. *Superlattices and Microstructures, 85,* 620–623.

Mastai, Y., Polsky, R., Koltypin, Y., Gedanken, A., & Hodes, G. (1999). Pulsed sonoelectrochemical synthesis of cadmium selenide NPs. *Journal of the American Chemical Society, 121* (43), 10047–10052.

Mayers, B., & Xia, Y. (2002a). Formation of tellurium NTs through concentration depletion at the surfaces of seeds. *Advanced Materials, 14*(4), 279–282.

Mayers, B., & Xia, Y. (2002b). One-dimensional nanostructures of trigonal tellurium with various morphologies can be synthesized using a solution-phase approach. *Journal of Materials Chemistry, 12*(6), 1875–1881.

McElroy, N., Page, R. C., Espinbarro-Valazquez, D., Lewis, E., Haigh, S., O'Brien, P., et al. (2014). Comparison of solar cells sensitised by CdTe/CdSe and CdSe/CdTe core/shell colloidal QDs with and without a CdS outer layer. *Thin Solid Films, 560,* 65–70.

Mews, A., Eychmüller, A., Giersig, M., Schooss, D., & Weller, H. (1994). Preparation, characterization, and photophysics of the quantum dot quantum well system cadmium sulfide/mercury sulfide/cadmium sulfide. *The Journal of Physical Chemistry, 98*(3), 934–941.

Morales-Acevedo, A. (2006). Can we improve the record efficiency of CdS/CdTe solar cells? *Solar Energy Materials and Solar Cells, 90*(15), 2213–2220.

Moras, J. D., Strandberg, B., Suc, D., & Wilson, K. (1996). Semiconductor clusters, NCs, and QDs. *Science, 271,* 933.

Murai, H., Abe, T., Matsuda, J., Sato, H., Chiba, S., & Kashiwaba, Y. (2005). Improvement in the light emission characteristics of CdS: Cu/CdS diodes. *Applied Surface Science, 244*(1), 351–354.

Murugadoss, G., Thangamuthu, R., Jayavel, R., & Kumar, M. R. (2015). Narrow with tunable optical band gap of CdS based core shell NPs: applications in pollutant degradation and solar cells. *Journal of Luminescence, 165,* 30–39.

Nozik, A. J. (2002). Quantum dot solar cells. *Physica E: Low-dimensional Systems and Nanostructures, 14*(1), 115–120.

Ortega, M., Santana, G., & Morales-Acevedo, A. (2000). Optoelectronic properties of CdO/Si photodetectors. *Solid-State Electronics, 44*(10), 1765–1769.

Plaza, D. O., Gallardo, C., Straub, Y. D., Bravo, D., & Pérez-Donoso, J. M. (2016). Biological synthesis of fluorescent NPs by cadmium and tellurite resistant Antarctic bacteria: exploring novel natural nanofactories. *Microbial Cell Factories, 15*(1), 76.

Pokropivny, V. V., & Skorokhod, V. V. (2007). Classification of nanostructures by dimensionality and concept of surface forms engineering in nanomaterial science. *Materials Science and Engineering C, 27*(5), 990–993.

Qi, H., Glembocki, O. J., & Prokes, S. M. (2012). Plasmonic properties of vertically aligned nanowire arrays. *Journal of Nanomaterials, 2012,* 1.

Qu, L., & Peng, X. (2002). Control of photoluminescence properties of CdSe NCs in growth. *Journal of the American Chemical Society, 124*(9), 2049–2055.

Radi, P. A., Brito-Madurro, A. G., Madurro, J. M., & Dantas, N. O. (2006). Characterization and properties of CdO NCs incorporated in polyacrylamide. *Brazilian Journal of Physics, 36*(2A), 412–414.

Rajesh, N., Kannan, J. C., Leonardi, S. G., Neri, G., & Krishnakumar, T. (2014). Investigation of CdO nanostructures synthesized by microwave assisted irradiation technique for NO 2 gas detection. *Journal of Alloys and Compounds, 607,* 54–60.

Rajeshwar, K., de Tacconi, N. R., & Chenthamarakshan, C. R. (2001). Semiconductor-based composite materials: Preparation, properties, and performance. *Chemistry of Materials, 13*(9), 2765–2782.

Ranjithkumar, R., Irudayaraj, A. A., Jayakumar, G., Raj, A. D., Karthick, S., & Vinayagamoorthy, R. (2016). Synthesis and properties of CdO and Fe doped CdO NPs. *Materials Today: Proceedings, 3*(6), 1378–1382.

Rathinamala, I., Pandiarajan, J., Jeyakumaran, N., & Prithivikumaran, N. (2014). Synthesis and physical properties of nanocrystalline CdS thin films-influence of sol aging time & annealing temperature. *International Journal of Thin Films Science and Technology, 3*(3), 113–120.

Romeo, N., Bosio, A., Mazzamuto, S., Romeo, A., & Vaillant-Roca, L. (2007, September). High efficiency CdTe/CdS thin film solar cells with a novel back contact. In *Proceedings of 22nd European Photovoltaic Solar Energy Conference, Milan, Italy* (pp. 3–7).

Salem, A., Saion, E., Al-Hada, N. M., Kamari, H. M., Shaari, A. H., Abdullah, C. A. C., et al. (2017). Synthesis and characterization of CdSe NPs via thermal treatment technique. *Results in Physics, 7,* 1556–1562.

Samarasekara, P., & Madushan, P. A. S. (2016). Structural and electrical properties of CdS thin films spin coated on glass substrates. *arXiv preprint* arXiv:1606.02435.

Senthilvelan, S. (2017). Morphology convenient flower like nanostructures of CdO-SiO2 nanomaterial and its photocatalytic application. *World Scientific News, 62,* 46–63.

Shang, L., Tong, B., Yu, H., Waterhouse, G. I., Zhou, C., Zhao, Y., … & Zhang, T. (2016). CdS nanoparticle-decorated Cd nanosheets for efficient visible light-driven photocatalytic hydrogen evolution. *Advanced Energy Materials, 6*(3).

Shcherbin, K., Shumelyuk, O., Odoulov, S., & Kratzig, E. (2002, May). Spectrum of the photorefractive CdTe: Ge response in the near infrared. In *Lasers and Electro-Optics, 2002. CLEO'02. Technical Digest. Summaries of Papers Presented at the* (pp. 208–209). IEEE.

Shi, Q., Cha, Y., Song, Y., Lee, J. I., Zhu, C., Li, X., et al. (2016). 3D graphene-based hybrid materials: Synthesis and applications in energy storage and conversion. *Nanoscale, 8*(34), 15414–15447.

Singh, J., Lotey, G. S., & Verma, N. K. (2011). Structural, optical and magnetic properties of Cr-doped CdSe NPs. *Digest J Nanomaterd Biostruct, 6,* 1733–1740.

Singh, R. S., Rangari, V. K., Sanagapalli, S., Jayaraman, V., Mahendra, S., & Singh, V. P. (2004). Nano-structured CdTe, CdS and TiO 2 for thin film solar cell applications. *Solar Energy Materials and Solar Cells, 82*(1), 315–330.

Singh, V., & Chauhan, P. (2009). Synthesis and structural properties of wurtzite type CdS NPs. *Chalcogenide Letters, 6*(8), 421–426.

Smith, B. C. (2011). *Fundamentals of fourier transform infrared spectroscopy*. Boca Raton: CRC press.

Soundararajan, D., Yoon, J. K., Kim, Y. I., Kwon, J. S., Park, C. W., Kim, S. H., et al. (2009). Vertically aligned CdSe and Zn-doped CdSe nanorod arrays grown directly on FTO coated glass: synthesis and characterization. *International Journal of Electrochemical Science, 4*(6), 1628–1637.

Soylu, M., & Kader, H. S. (2016). Photodiode based on CdO thin films as electron transport layer. *Journal of Electronic Materials, 11*(45), 5756–5763.

Suart, B. (2004). Infrared spectroscopy: Fundamental and applications.

Suganthi, A. B., Joshi, A. G., & Sagayaraj, P. (2012). A novel two-phase thermal approach for synthesizing CdSe/CdS core/shell nanostructure. *Journal of Nanoparticle Research, 14*(2), 691.

Sujitha, V., Murugan, K., Dinesh, D., Pandiyan, A., Aruliah, R., Hwang, J. S., et al. (2017). Green-synthesized CdS nano-pesticides: Toxicity on young instars of malaria vectors and impact on enzymatic activities of the non-target mud crab Scylla serrata. *Aquatic Toxicology, 188,* 100–108.

Sun, Z., Kim, J. H., Zhao, Y., Bijarbooneh, F., Malgras, V., Lee, Y., et al. (2011). Rational design of 3D dendritic TiO_2 nanostructures with favorable architectures. *Journal of the American Chemical Society, 133*(48), 19314–19317.

Suresh, S. (2013). Studies on the dielectric properties of CdS NPs. *Applied Nanoscience, 4*(3), 325.

Tadjarodi, A., Imani, M., Kerdari, H., Bijanzad, K., Khaledi, D., & Rad, M. (2014). Preparation of CdO rhombus-like nanostructure and its photocatalytic degradation of azo dyes from aqueous solution. *Nanomaterials and Nanotechnology, 4,* 16.

Takahashi, T., Nichols, P., Takei, K., Ford, A. C., Jamshidi, A., Wu, M. C., et al. (2012). Contact printing of compositionally graded CdS_xSe_{1-x} nanowire parallel arrays for tunable photodetectors. *Nanotechnology, 23*(4), 045201.

Taki, M. (2013). Structural and optical properties of cadmium telluride Cd_XTe_{1-X}thin film by evaporate. *International Journal of Application or Innovation in Engineering & Management, 2*(5), 413–417.

Tang, X., Hseih, C., Ou, F., & Ho, S. T. (2015). Ohmic contact of indium oxide as transparent electrode to n-type indium phosphide. *RSC Advances, 5*(29), 22685–22691.

Tang, Z. R., Yin, X., Zhang, Y., & Xu, Y. J. (2013). Synthesis of titanate nanotube–CdS nanocomposites with enhanced visible light photocatalytic activity. *Inorganic Chemistry, 52* (20), 11758–11766.

Tang, Z., Kotov, N. A., & Giersig, M. (2002). Spontaneous organization of single CdTe NPs into luminescent NWs. *Science, 297*(5579), 237–240.

Tang, Z., Zhang, Z., Wang, Y., Glotzer, S. C., & Kotov, N. A. (2006). Self-assembly of CdTe NCs into free-floating sheets. *Science, 314*(5797), 274–278.

Thema, F. T., Beukes, P., Gurib-Fakim, A., & Maaza, M. (2015). Green synthesis of Monteponite CdO NPs by Agathosma betulina natural extract. *Journal of Alloys and Compounds, 646,* 1043–1048.

Thirsk, H. R. (1989). Electrochemistry. In *Royal Society of Chemistry* (Vol. 7).

Thovhogi, N., Park, E., Manikandan, E., Maaza, M., & Gurib-Fakim, A. (2016). Physical properties of CdO NPs synthesized by green chemistry via Hibiscus Sabdariffa flower extract. *Journal of Alloys and Compounds, 655,* 314–320.

Toyama, H., Higa, A., Yamazato, M., Maehama, T., Ohno, R., & Toguchi, M. (2006). Quantitative analysis of polarization phenomena in CdTe radiation detectors. *Japanese Journal of Applied Physics, 45*(11R), 8842.

Travas-Sejdic, J., Peng, H., Cooney, R. P., Bowmaker, G. A., Cannell, M. B., & Soeller, C. (2006). Amplification of a conducting polymer-based DNA sensor signal by CdS NPs. *Current Applied Physics, 6*(3), 562–566.

Usharani, K., Balu, A. R., Nagarethinam, V. S., & Suganya, M. (2015). Characteristic analysis on the physical properties of nanostructured Mg-doped CdO thin films—Doping concentration effect. *Progress in Natural Science: Materials International, 25*(3), 251–257.

Wageh, S., Higazy, A. A., & Algradee, M. A. (2011). optical properties and activation energy of a novel system of CdTe NPs embedded in phosphate glass matrix. *Journal of Modern Physics, 2* (08), 913.

Waghulade, R. B., Patil, P. P., & Pasricha, R. (2007). Synthesis and LPG sensing properties of nano-sized cadmium oxide. *Talanta, 72*(2), 594–599.

Wang, G., Jin, L., Dong, Y., Niu, L., Liu, Y., Ren, F., et al. (2014). Multifunctional Fe 3 O 4–CdTe@ SiO 2–carboxymethyl chitosan drug nanocarriers: Synergistic effect towards magnetic targeted drug delivery and cell imaging. *New Journal of Chemistry, 38*(2), 700–708.

Wang, Y., Ramanathan, S., Fan, Q., Yun, F., Morkoc, H., & Bandyopadhyay, S. (2006). Electric field modulation of infrared absorption at room temperature in electrochemically self assembled QDs. *Journal of Nanoscience and Nanotechnology, 6*(7), 2077–2080.

Wang, Y., Tang, Z., Tan, S., & Kotov, N. A. (2005). Biological assembly of nanocircuit prototypes from protein-modified CdTe NWs. *Nano Letters, 5*(2), 243–248.

Wei, H., Zhou, J., Zhang, L., Wang, F., Wang, J., & Jin, C. (2015). The core/shell structure of CdSe/ZnS QDs characterized by X-ray absorption fine spectroscopy. *Journal of Nanomaterials, 2015,* 3.

Willardson, R. K., & Beer, A. C. (1977). *Semiconductors and semimetals* (Vol. 12). Cambridge: Academic Press.

Williams, J. V., Kotov, N. A., & Savage, P. E. (2009). A rapid hot-injection method for the improved hydrothermal synthesis of CdSe NPs. *Industrial and Engineering Chemistry Research, 48*(9), 4316–4321.

Wong, I. Y., Bhatia, S. N., & Toner, M. (2013). Nanotechnology: Emerging tools for biology and medicine. *Genes & Development, 27*(22), 2397–2408.

Wu, X. J., Zhu, F., Mu, C., Liang, Y., Xu, L., Chen, Q., et al. (2010). Electrochemical synthesis and applications of oriented and hierarchically quasi-1D semiconducting nanostructures. *Coordination Chemistry Reviews, 254*(9), 1135–1150.

Xu, H., Mo, R., Cheng, C., Ai, G., Chen, Q., Yang, S., et al. (2014). ZnSe/CdS/CdSe triple-sensitized ZnO nanowire arrays for multi-bandgap photoelectrochemical hydrogen generation. *RSC Advances, 4*(88), 47429–47435.

Yakuphanoglu, F. (2011). Synthesis and electro-optic properties of nanosized-boron doped cadmium oxide thin films for solar cell applications. *Solar Energy, 85*(11), 2704–2709.

Yang, J., Gao, Y., Kim, J. W., He, Y., Song, R., Ahn, C. W., et al. (2010). Self-reorganization of CdTe NPs into two-dimensional Bi_2Te_3/CdTe nanosheets and their thermoelectrical properties. *Physical Chemistry Chemical Physics, 12*(38), 11900–11904.

Yao, W. T., Yu, S. H., Liu, S. J., Chen, J. P., Liu, X. M., & Li, F. Q. (2006). Architectural control syntheses of CdS and CdSe nanoflowers, branched NWs, and nanotrees via a solvothermal approach in a mixed solution and their photocatalytic property. *The Journal of Physical Chemistry B, 110*(24), 11704–11710.

Yildiz, I., McCaughan, B., Cruickshank, S. F., Callan, J. F., & Raymo, F. M. (2009). Biocompatible CdSe-ZnS core-shell QDs coated with hydrophilic polythiols. *Langmuir, 25*(12), 7090–7096.

Yin, X. L., Li, L. L., Jiang, W. J., Zhang, Y., Zhang, X., Wan, L. J., et al. (2016). MoS2/CdS nanosheets-on-nanorod heterostructure for highly efficient photocatalytic H_2 generation under visible light irradiation. *ACS Applied Materials & Interfaces, 8*(24), 15258–15266.

Yu, H., Li, J., Loomis, R. A., Lin-Wang, W., & Buhro, W. E. (2003a). Two-versus three-dimensional quantum confinement in indium phosphide wires and dots. *Nature Materials, 2*(8), 517.

Yu, W. W., Qu, L., Guo, W., & Peng, X. (2003b). Experimental determination of the extinction coefficient of CdTe, CdSe, and CdS NCs. *Chemistry of Materials, 15*(14), 2854–2860.

Yu, Z., Tetard, L., Zhai, L., & Thomas, J. (2015). Supercapacitor electrode materials: nanostructures from 0 to 3 dimensions. *Energy & Environmental Science, 8*(3), 702–730.

Zhang, J., Yang, Q., Cao, H., Ratcliffe, C. I., Kingston, D., Chen, Q. Y., et al. (2016). Bright gradient-alloyed $CdSe_xS_{1-x}$ QDs exhibiting cyan-blue emission. *Chemistry of Materials, 28*(2), 618–625.

Zhang, Y., Grady, N. K., Ayala-Orozco, C., & Halas, N. J. (2011). Three-dimensional nanostructures as highly efficient generators of second harmonic light. *Nano Letters, 11*(12), 5519–5523.

Zhang, Y., Wang, L. W., & Mascarenhas, A. (2007). "Quantum coaxial cables" for solar energy harvesting. *Nano Letters, 7*(5), 1264–1269.

Zhao, Y. S., Fu, H. B., Hu, F. Q., Peng, A. D., Yang, W. S., & Yao, J. N. (2008). Tunable emission from binary organic one-dimensional nanomaterials: An alternative approach to white-light emission. *Advanced Materials, 20*(1), 79–83.

Zhong, Z., Qian, F., Wang, D., & Lieber, C. M. (2003). Synthesis of p-type gallium nitride NWs for electronic and photonic nanodevices. *Nano Letters, 3*(3), 343–346.

Zhu, H., Jiang, R., Xiao, L., Chang, Y., Guan, Y., Li, X., et al. (2009). Photocatalytic decolorization and degradation of Congo Red on innovative crosslinked chitosan/nano-CdS composite catalyst under visible light irradiation. *Journal of Hazardous Materials, 169*(1), 933–940.

Zhu, L., Li, C., Li, Y., Feng, C., Li, F., Zhang, D., et al. (2015). Visible-light photodetector with enhanced performance based on a ZnO@ CdS heterostructure. *Journal of Materials Chemistry C, 3*(10), 2231–2236.

Zhu, Y., Mei, T., Wang, Y., & Qian, Y. (2011). Formation and morphology control of NPs via solution routes in an autoclave. *Journal of Materials Chemistry, 21*(31), 11457–11463.

Zhu, Y., Mendelsberg, R. J., Zhu, J., Han, J., & Anders, A. (2013). Dopant-induced band filling and bandgap renormalization in CdO: In films. *Journal of Physics. D. Applied Physics, 46*(19), 195102.

Zyoud, A. H., Zaatar, N., Saadeddin, I., Ali, C., Park, D., Campet, G., et al. (2010). CdS-sensitized TiO 2 in phenazopyridine photo-degradation: Catalyst efficiency, stability and feasibility assessment. *Journal of Hazardous Materials, 173*(1), 318–325.

Chapter 3
Wet Chemical Synthesis Methods

The growth of nanomaterials can be carried out by either bottom-up or top-down methods and the growth strategy should be selected by considering the requisite properties of the product NPs. The nanomaterials of cadmium-based II–VI semiconducting materials can be prepared by a variety of ways out of which vapor–liquid–solid (VLS) has been found popular approach which can be implemented in a number of experimental routs. A comprehensive description of VLS mechanism and reported efforts for preparation of the nanomaterials through different routes is given in the following sections. This chapter covers the chemical synthesis techniques including Co-Precipitation method, Chemical bath deposition, SILAR deposition, Electroplating and electrophoretic deposition, Hydrothermal method, Solvothermal Synthesis, Microemulsion Synthesis, Polyol Method, Sol-Gel Synthesis methods for growth of the nanomaterials.

Chemical synthesis using liquid-phase precursors is a popular class of techniques to prepare nanomaterials. It involves chemical reaction of the precursor species to produce nucleation followed by formation of nanomaterials having a broad particle size distribution and morphology. In order to achieve a narrow size distribution, good crystal quality, desired morphology of the product nanomaterials, the provision of sufficient supersaturation, careful selection of precursors and concentration of species, synthesis parameters and dynamics of chemical reaction play a key role. This category of synthesis is performed at low temperatures, ambient conditions and operationally requires simple equipment which makes it cost-effective and a popular choice. The methods based on this route offer good control of stoichiometry to mix the precursors at atomic scale. The materials of good stoichiometry and size ranging from 1 nm to a few microns can be prepared and easily be stabilized through the use of capping agents. Reactant concentration, precursor pH, heating temperature, and reaction time are the basic parameters that affect the properties of the product nanomaterials. This class of synthesis mechanism has been implemented in a number of ways including chemical precipitation, chemical bath, SILAR, electrochemical, microemulsion, hydrothermal, solvothermal, polyol and sol-gel methods.

Abdul Majid and Maryam Bibi, *Cadmium based II-VI Semiconducting Nanomaterials*, Topics in Mining, Metallurgy and Materials Engineering,
https://doi.org/10.1007/978-3-319-68753-7_3

The nanomaterials in various shapes like particles, spheres, rods, diks, tubes etc., can be prepared by changing the reaction conditions and synthesis technique. The molar ratio of Cd:S, Cd:Se, Cd:Te, and Cd:O is a key factor to define the properties of the prepared respective CdS, CdSe, CdTe, and CdO nanomaterials. The inappropriate value of pH causes the agglomeration resulting in decrease of fluorescence properties of QDs; therefore, pH value of precursor solution has been maintained within 8–9 for preparation of CdTe/CdS QDs (Zhao et al. 2008). The higher temperature is advantageous in the synthesis as it reduces the surface defects and increases the growth rate of nanomaterials. The time of heating is usually found proportional to the size of nanomaterials. The description of wet chemical techniques, principles involved, mechanism of growth, merits, and demerits along with an overview of the reported literature on preparation of Cd containing II–VI semiconducting nanomaterials is given in the following sections.

3.1 Chemical Bath Deposition Synthesis

The controlled precipitation and condensation of a compound on a substrate dipped into the precursor solution is known as the chemical bath deposition (CBD) method (Mugle and Jadhav 2016). In this method, precipitation in solid phase takes place due to supersaturation as a result of chemical reaction in a bath. The control of chemical reaction to deposit films on the substrate by precipitation is a basic principle of this technique. A schematic diagram showing CBD process is given in Fig. 3.1a.

In a CBD procedure for all metal chalcogenides, the substrate is dipped into a solution which is prepared from chalcogenide source, metal ion and additional base. A complex agent (e.g., CN^-, NH_3, $C_6H_5O_7^{3-}$, $C_6H_5O_6^{2-}$, EDTA, etc., in case of Cd) is added to manage the hydrolysis of the metal ion (Chopra et al. 1982). When a metal complex in the solution is dissociated (like Cd^{2+} metal ion) as per reaction

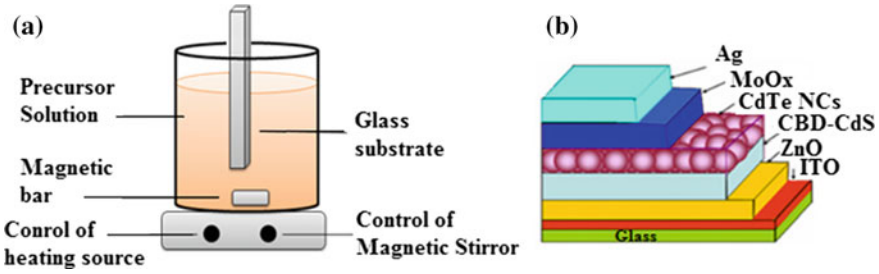

Fig. 3.1 **a** Schematic diagram for synthesis of CdS films using chemical bath deposition technique (Kumar et al. 2015). **b** Schematic of layer-by-layer CdTe NCs-CdS heterojunctions solar cell device (Tian et al. 2013). © 2013 Springer

$M(A)^{2+} \rightleftharpoons M^{2+} + A$, the stability of complex ion in solution can be calculated using stability constant (K_i);

$$K_i = \frac{[M^{2+}][A]}{\left[M(A)^{2+}\right]}$$

Higher value of K causes reduction in the stability and the concentration of metal ions in the solution. The reduction in the temperature and increase in pH of the solution result in the better stability of the metal complexes (Chopra et al. 1982). Solution chemistry (precursors, temperature, pH, and concentration), nature and geometry of substrate and practical characteristics of deposition route (experimental design) control the deposition process. The film thickness, uniformity, and composition can be monitored by changing the solution pH, temperature, reagent concentration, and kinetics of chemical reaction. CBD of thin film related to chalcogenides of cadmium involves (i) ion by ion growth and (ii) cluster by cluster growth mechanisms (Gorer and Hodes 1994). The growth process can be divided into four different mechanisms by combining these two steps. The illustration of mechanism of CBD deposition of CdS is given in Table 3.1 (Hodes 2002). These steps involve formation of free sulfide ions (or other anions), nucleation, and finally the complete conversion of $Cd(OH)_2$ into CdS. The last two steps are based on the process of breaking the bond between carbon–chalcogen and to avoid the creation of free chalcogenides.

One of the major benefits of the CBD method is the facility to use a wide range of substrates (in terms of material and geometry). The deposition of layers on substrate is usually carried out without risk of dissolution of substrate in chemical bath. Glass substrates are mostly utilized in such a way that two glass substrates are vertically dipped into the solution filled between them. The substrates are applied in

Table 3.1 The stages of chemical reaction in CBD synthesis of CdS films (Hodes 2002)

Simple ion by ion mechanism	
• Dissociation of complex to free Cd ions • Formation of sulfide ions • Ionic reaction to form CdS	$Cd(NH_3)_4^{2+} \rightleftharpoons Cd^{2+} + 4NH_3$ $(NH_2)_3CS + 2OH^- \rightarrow S^{2-} + CN_2H_2 + 2H_2O$ $Cd^{2+} + S^{2-} \rightarrow CdS$
Simple cluster (hydrooxide) mechanism	
• Formation of solid $Cd(OH)_2$ cluster • Exchange reaction	$nCd^{2+} + 2nOH^- \rightleftharpoons \left[Cd(OH)_2\right]_n$ $\left[Cd(OH)_2\right]_n + nS^{2-} \rightarrow nCdS + 2nOH^-$
Complex decomposition and ion by ion mechanism	
$(NH_2)_3CS + Cd^{2+} \rightleftharpoons \left[(NH_2)_2CS - Cd\right]^{2+}$ $\left[(NH_2)_2CS - Cd\right]^{2+} + 2OH^- \rightarrow CdS + CN_2H_2 + 2H_2O$	
Complex decomposition and cluster mechanism	
$\left[Cd(OH)_2\right]_n + (NH_2)_2CS \rightleftharpoons \left[Cd(OH)_2\right]_{n-1}(OH)_2Cd - S - C(NH_2)_2$ $\left[Cd(OH)_2\right]_{n-1}(OH)_2Cd - S - C(NH_2)_2 \rightarrow \left[Cd(OH)_2\right]_{n-1}CdS + CN_2H_2 + 2H_2O$	

the form of microscopic slides or glass sheets. A variety of other substrates are less commonly used like Kapton polymide (Cardoso et al. 2001), transparent polyster sheets (Grozdanov et al. 1994), LDPE (Kunita et al. 2002), PMMA (Hu and Nair 1996), PET (Yamamoto et al. 1993) and PES (Nair et al. 2001). The spacing between the substrates, the solution composition, and temperature defines the deposition rate. The characteristics of complexing agents and reagents affect the composition of the final product. Increase in concentration of reagents increases the thickness and deposition rate, but at high values the deposition rate may show anamoloies. The variation in concentration of complexing agents changes the deposition rate and film thickness. An increase in temperature increases the reaction rate. However, film thickness may increase or decrease as per extent of supersaturation of the solution. Increase in pH value of the solution increases the stability of complexing agent which results in lower reaction rate and thus higher film thickness. The growth of high-quality nanofilms takes place at a slow reaction rate. These factors show collective dependence instead of individual influence on the reaction and growth mechanism.

CBD is a simple and low-cost method for large-area growth of nanofilms at low temperature. Multi component nanofilms can be synthesized by this method. A short review on the synthesis process with different experimental conditions has been given in Table 3.2. This technique also offers possibility of in-situ n-type or p-type doping into semiconducting materials. Bath parameters are standardized providing high reproducibility with minimum wastage. There are also some demerits of the method like external doping and adjustment of stoichiometry in multicomponent nanomaterials. The control over order of deposition of multilayer and growth of very thick layer of film are restrictions of this technique.

CdS nanofilms have been prepared using CBD and spray pyrolysis techniques (Hiie et al. 2006). The value of optical band gap for CBD prepared CdS films has been observed to decrease from bulk value 2.51 to 2.42 eV, while there has not been any change observed in band gap of sprayed films. All the films have high transparency over 80% in the visible spectrum (520–850 nm). Uniform and dense CdS nanofilms have been prepared using CBD method (Zhou et al. 2008). The chemical reaction of CBD synthesis process for CdS is described in the following:

$$NH_3 + H_2O \rightarrow NH_4^+ + OH^- \quad \text{and} \quad Cd^{2+} + 4NH_3 \rightarrow Cd(NH_3)_4^{2+}$$

$$(NH_2)_2CS + OH^- \rightarrow CN_2H_2 + H_2O + HS^- \quad \text{and} \quad HS^- + OH^- \rightarrow S^{2-} + H_2O$$

$$\text{And finally, } Cd(NH_3)_4^{2+} + S^{2-} \rightarrow \mathbf{CdS} \downarrow + 4NH_3 \uparrow$$

It was concluded that deposition temperature has played a significant role in the growth process of CdS nanofilms and determining their band gap. The nanocrystalline CdS thin films of polycrystalline nature have been prepared by CBD method with SEM image given in Fig. 3.2b (Saikia et al. 2010). Photoluminescence (PL) measurements revealed emission at 476 nm/468 nm in case of deposition heat

Table 3.2 Cd containing II–VI semiconductor nanomaterials prepared through CBD method using different synthesis conditions

Material	Substrate	Reagents/complexing agent	Deposition temp./dep.time After heat treatment/time	pH	References
CdS nanofilms	Indium tin oxide (ITO)	$Cd(NO_3)_2$ $(NH_2)_2CS$, KOH	356 K/20, 40, 50 min 573 K	10	Zhou et al. (2008)
CdO NWs	Microslides glass substrate	Cadmium chloride, ammonium hydroxide	RT/48 h 623 K for 3 h	–	Dhawale et al. (2008)
CdO nanostructured films	Commercial glass slide	Cadmium sulfate and thiourea/ammonia	70 ± 2 °C/1 h 400–75 °C/10 h	9.5–10	Kawar (2012)
CdO nanostructured films	Glass substrate	Cadmium chloride ($CdCl_2 \cdot 2H_2O$)/ Ammonium hydroxide	60 °C/7 h 573 K/3 h	10.2 and 12.4	Ismail et al. (2014)
CdO nanostructured films	Glass substrate	$(NO_3)_2 \cdot 4H_2$/ONH_4OH	RT/48 h 373, 473, 573 and 673 K/10 min	11–12	Ahmed (2017)
CdO nanostructured films	Glass substrate	Cadmium nitrate salt	673 K for 90 min	–	Asmial et al. (2012)
CdS nanostructured films	Commercial glass slide	Cadmium chloride, thiourea and ammonium chloride/ammonia	80 °C for 6 h	9	Al-Hussam and Jassim (2012)
CdS nanostructured films	Glass and ITO-covered glass	$CdCl_2$ and thiocarbamide	450 °C for 5 min	–	Hiie et al. (2006)
CdS nanostructured films	Glass substrate	Cadmium chloride and cadmium acetate	90 °C/6 h	–	Zia et al. (2016)
CdS nanostructured films	Glass substrate	Cadmium acetate and thiourea	60 °C/8 h	5.6–9.5	Saikia et al. (2010)
	Glass substrate		85 °C/6 h	9.5	

(continued)

Table 3.2 (continued)

Material	Substrate	Reagents/complexing agent	Deposition temp./dep.time After heat treatment/time	pH	References
CdSe nanostructured films		Cadmium acetate, tartaric acid, ammonia and sodium selenosulphate			Hone et al. (2015)
CdS, CdSe and CdSSe nanostructures	Glass substrate	Cadmium acetate and sodium selenosulfate/thiourea/Aqueous ammonia	RT/–	–	VanderHyde et al. (2015)
CdSe NW thin films	Glass substrates	Cadmium sulfate and sodium selenosulphate	70 °C/ – 273K/1h	–	Gubur et al. (2015)
CdSe nanostructured films	Glass substrates	Cadmium nitrite tetrahydrate, selenourea/glycine	A series of different temp. and time	10	Olmos et al. (2015)
CdSe nanostructured films	Glass substrates	Cadmium acetate, sodium selenosulphate triethanolamine (TEA)	60 °C/1 h	–	Singh et al. (2011b)

treatment/without heat, respectively. In another effort, highly adhesive and smooth CdS nanocrystalline thin films have been prepared through CBD method (Al-Hussam and Jassim 2012). These nanofilms have been deposited on glass substrates with two different concentrations of thiourea. The synthesized films showed nanocrystalline nature having cubic structures with sizes of NPs between 3.8 and 8 nm. A blue shift of absorption edge was studied showing the quantum size effects of the NPs.

Nanocrystalline CdS films with two different Cd sources have been prepared using CBD method (Zia et al. 2016). The effects of changing thiourea concentration were studied in two different Cd sources as cadmium chloride and cadmium acetate. The nanostructured films synthesized using cadmium chloride showed cubic structure whereas the films prepared with cadmium acetate were found in the mixed phase of hexagonal and cubic structures. A blue shift in the absorption edge was observed with the increase in thiourea concentration. The value of band gap was found increased from 2.45 to 2.71 eV and 2.65 to 2.74 eV for the films grown using cadmium chloride and cadmium acetate, respectively. PbS/ZnO, CdS/ZnO, and CdSe/ZnO hierarchical heterostructures have been prepared on indium-doped tin oxide substrate (Gao et al. 2017). These heterostructures were organized by the joining the water bath and CBD techniques. ZnO nano rods (NRs) and nano tubes (NTs) have been sensitized by the QDs and their photocatalytic performance was studied through degradation of methyl orange under irradiation. QDs sensitized ZnO heterostructured nanomaterials showed better photocatalytic activity and considerable potential to resolve environmental and energy problem.

CdSe and CdS NCs with a tunable size in range 4–20 nm diameters have been obtained with CBD route (Němec et al. 2008). These two nanostructures facilitated to cover the whole visible spectrum in such a way that CdS and CdSe covered 430–500 nm and 490–710 nm respectively. In another attempt, CdSe nanocrystalline thin films with hexagonal structure have been prepared using CBD (Singh et al. 2011a). These films had grains in the form of balls with sizes 8 nm and 4 nm and band gap values of 1.77 and 1.89 eV respectively. CdSe films showed uniformity and excellent surface quality along with high transmittance >80% in the visible

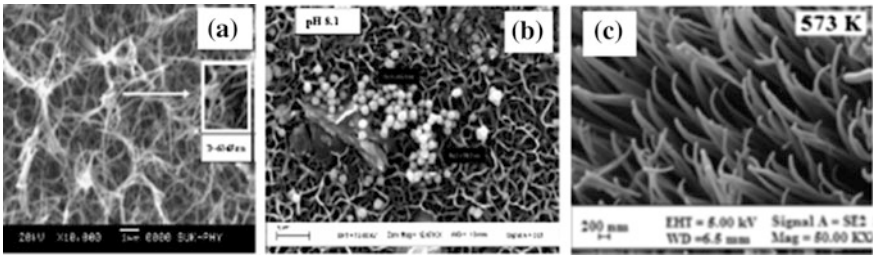

Fig. 3.2 SEM images of CBD prepared (**a**) CdO nanostructured thin film with inset showing a typical NW with diameter 6–65 nm (Dhawale et al. 2008). © 2008 Elsevier. **b** CdS nanocrystalline films with pH 8.1 (Saikia et al. 2010). © 2010 Open access. **c** Cross sectional view of CdSe NWs annealed at 573 K (Gubur et al. 2015). © 2015 Springer Publishing

region. Such features like high crystallinity, appropriate band gap, and high transmittance prove their potential for use in photovoltaic cells. CdSe QDs have been synthesized by restraining the synthesis amorphous SeO_2 film on the surface of CdSe QDs (Choi et al. 2014). These nanostructures showed good efficiency for quantum dot-sensitized solar cell (QDSSC) applications.

An easy, straightforward and inexpensive growth method has been developed for the deposition of nanostructured CdS, CdSe, and CdSSe (VanderHyde et al. 2015). The process for growth of CdS was explained in the form of chemical reactions (Zhou et al. 2008). The reactions showing the process of formation CdSe and CdSSe nanofilms is given below:

$$Na_2SeSO_3 + OH^- \rightarrow Na_2SO_4 + HSe^- \quad Cd^{2+} + 4NH_3 \rightarrow Cd(NH_3)_4^{2+}$$

$$HSe^- + OH^- \rightarrow Se^{2-} + H_2O \quad \text{And finally,} \quad Cd(NH_3)_4^{2+} + Se^{2-} \rightarrow \mathbf{CdSe} \downarrow + 4NH_3 \uparrow$$

$$\text{And} \quad Cd(NH_3)_4^{2+} + Se^{2-} + S^{2-} \rightarrow \mathbf{CdSSe} \downarrow + 4NH_3 \uparrow$$

The homogeneous material having suitability to the glass substrate have been obtained at room temperature. Selenium and sulfur composition played a significant role in the color of the nanomaterial. CdSe, CdS, and CdSSe films were nanocrystalline having a structure in the form of cubic, hexagonal, and a mixed phase of cubic and hexagonal, respectively. In another work, CdSe thin films in the form of NWs have been synthesized on glass substrates using CBD technique at 70 °C (Gubur et al. 2015). These NWs shown in Fig. 3.2c were found in mixed cubic and hexagonal phase with lengths 642 nm–2.5 μm and diameters 46–211 nm. Nanostructures showed low activation energy, better thermal conduction, good electrical conductivity and good optical and crystal features which showed their potential for electronics and photovoltaic applications. CdSe nanocrystalline films with a band gap of 1.86 eV have been prepared using CBD technique (Hone et al. 2015). The chemical reactions happened in anionic and cationic precursors for the formation processes as of these CdSe films are given below:

$$Na_2SeSO_3 + OH^- \leftrightarrow Na_2SO_3 + HSe^- \quad \text{and} \quad HSe^- + OH^- \leftrightarrow H_2O + Se^-$$

$$[Cd(\text{tartaric acid})]^{2+} \rightarrow Cd^{2+} + \text{tartaric acid} \quad \text{and} \quad Cd^{2+} + Se^- \rightarrow CdSe + \text{tartaric acid}$$

The spherical grains with a preferred orientation along (111) were observed in the films deposited on glass substrate. CdSe nanostructured thin films have been prepared using CBD (Olmos et al. 2015). The band gap value was found increased from 1.23 to 1.97 eV as per PL spectra recorded in range 600–800 nm. The material showed its potential for application in opto-electronics. CdTe nanocrystal (NC)/CdS p–n heterojunction solar cells have been prepared with a layer-by-layer solution route (Fig. 3.1b). These NCs have been fabricated with ITO/ZnO-In/CdS/CdTe/MoO_x/Ag-inverted structure by CBD method on top of ITO/ZnO-In. High-quality CdTe NCs showed improved values of power conversion efficiency with different annealing temperatures for a solution-based CdTe/CdS NC-inverted

solar cells. CdTe–CdS nanotube arrays configured using electrodeposition of CdTe on lithographically decorated nanoelectrodes on the conducting substrates coated with CdS layer deposited through CBD (Liyanage and Nath 2016). An illustration of synthesis process is given in Fig. 3.3 which shows different steps involved in the synthesis process. CdTe NTs showed band gap of 1.52 eV whereas the band gap of CdS was found 2.31 eV. The interface between CdS and CdTe showed homogeneity and continuity in rod-like structures. These nanomaterials showed better photocurrent efficiency (50% increased performance) as compared to the bulk counterparts.

This technique has been found inexpensive and convenient for CdO nanomaterials as well. CdO NWs have been grown at room temperature on a glass substrate using CBD method (Dhawale et al. 2008). The NWs were cubic in structure with n-type electrical conductivity and lattice parameter 4.68 Å. Direct/indirect band gap with value 2.42/2.04 eV was observed for the NWs having a diameter of 60–65 nm and length of 2.5–3 μm (Fig. 3.2a). Asmial et al. reported preparation of nanostructured CdO films through CBD method (Asmial et al. 2012). The film was

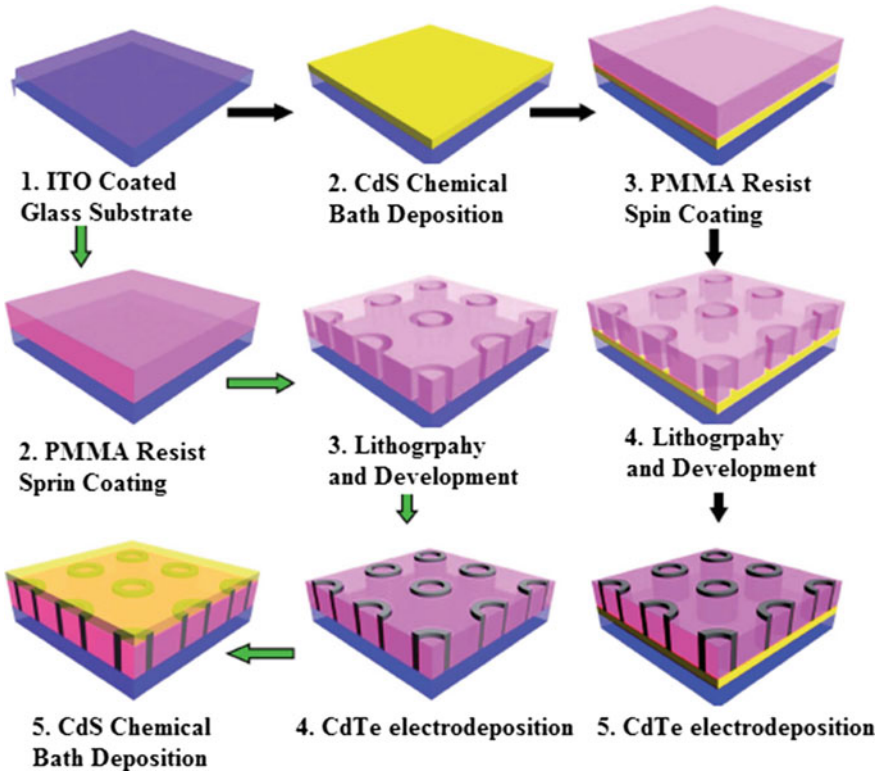

Fig. 3.3 Design for fabrication of CdS–CdTe heterojunction through chemical bath deposition method (Liyanage and Nath 2016). © 2016 Royal Society of Chemistry

polycrystalline showed different grain sizes with corresponding to different molar ratios used. For the molar ratio of 0.03 M, the nanostructures exhibited an average size and root mean square (rms) value of about 87 and 13 nm, respectively. Similarly, for the molar ratio of 0.1 M, the nanostructures exhibited an average size and rms value of about 98 nm and 17 nm, respectively. The transmittance of CdO nanofilms has been observed in the visible range with value 70–80%. Direct optical band gap with value in range 2.41–2.5 eV was recorded.

CdO nanostructured films with average grain size of 16–29 nm have been prepared using low-cost CBD method (Kawar 2012). The value of band gap for this nanostructured film was found 2.31 eV. The study revealed these nanostructured films with small grain size and large surface area have potential to be applied in the field of opto-electronics. In another study, CdO nanocrystalline thin films have been synthesized using the CBD method (Ismail et al. 2014). The grown films were of cubic crystal structure having grains composed of NWs with a diameter of less than 100 nm. The band gap of the films deposited using solutions having pH value of 10.2 and 12.2 was recorded as 2.38 and 2.57 eV, respectively. In another effort, cubic structured CdO nanocrystalline films have been prepared at temperature 573 ° C using CBD technique (Ahmed 2017). These smooth and uniform nanofilms with the size of 100 nm showed a high transparency of 85% in visible range. The grown nanostructures showed polycrystalline nature with a band gap of about 2.42 to 2.7 eV. An improvement in properties caused by thermal annealing and reduction in electrical resistivity with an increase in the value of growth temperature was observed.

3.2 Successive Ion Layer Adsorption and Reaction Deposition

Successive ion layer adsorption and reaction (SILAR) is a chemical deposition process carried out in the liquid phase. It is a simpler technique which offers a number of advantages in comparison to other deposition methods. It can be used to deposit uniform films on any substrate at controlled deposition rate, composition, and thickness. Since no vacuum is required and the process is operated at low temperature, this technique does not require any expensive and technologically complicated equipment. SILAR is a solution-based technique that has emerged after modification in traditional chemical bath deposition (CBD) in which deposition is controlled by monitoring the adsorption and reaction kinetics (Nicolau and Menard 1988). The precursors in CBD are simultaneously placed in a vessel which causes the production of precipitates leaving to loss of materials besides the deposition on the surface of the immersed substrate. This drawback is tackled in SILAR where the formation of precipitation is avoided by alternately immersing the substrate in cationic and anionic precursors.

In a SILAR process, as a result of reaction at solid/solution interface, the adsorbed cation C^{n+} (e.g., Cd^{2+}) and anion A^{m-} (e.g., S^{2-}) interact with each other to produce a compound C_mA_n (e.g., CdS). Adsorption and chemical reaction are key components in SILAR deposition of films. Though adsorption takes place via gas/solid, liquid/solid or gas/liquid type interactions but in SILAR process the adsorption is of liquid/solid interaction. When selected solid substrate and liquid precursors are allowed to interact, the cations from cationic solution are adsorbed on the substrate. Similarly, anions from anionic solution adsorb on the surface of the substrate and react with preadsorbed cations to electrically bind with each other to produce a solid phase on the substrate in the form of thin film. The growth parameters include nature of solution and substrate, pH of the solution, ionic concentration in solution, adsorption and reaction times, temperature etc. The deposition rate can be enhanced by using a complexing agent which facilitates dissociation/ionization of the solution and adsorption of ions on the substrate.

The SILAR deposition is carried out in cycles and a cycle comprises of four steps; (i) the properly cleaned substrate is dipped into cationic precursor which results into adsorption of cations on the substrate surface. (ii) The substrate containing adsorbed cations is then rinsed to remove the loosely bonded cations. (iii) The substrate containing pre-deposited cations is then immersed into anionic precursor where anions are get adsorbed and make the chemical reaction to form the required compound (iv). The substrate containing thin film is rinsed (Sankapal et al. 2000). The process of SILAR deposition is sketched in Fig. 3.4.

The SILAR has been initially employed to deposit II–VI compound semiconductors including CdS, ZnS and CdZnS (Nicolau and Menard 1988). This technique has been found reliable, cheap and quick to deposit compound

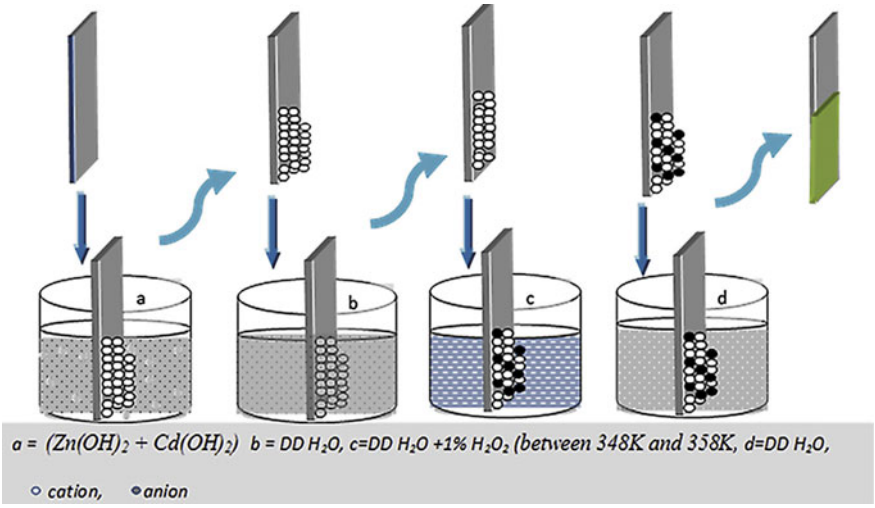

Fig. 3.4 Schematic diagram showing stages of SILAR deposition (Nwanya et al. 2015). © 2015 Elsevier Publishing

semiconductors, chalcogenides, oxides, polymers etc. for a variety of applications. SILAR has been applied to prepare CdSe/CdS epitaxial core/shell nanostructures (Li et al. 2003). During SILAR cycles, shell and core monolayers were deposited on the substrate by alternately dipping into respective precursors. For the shells, CdO and S precursors were used and the reaction was carried out at 220–240 °C. It was observed that size of core/shell NCs does not change with an increase in thickness of monolayer shells of CdS and volume of CdSe core. On the basis of an investigation of structural and optical properties, the quality of prepared core/shell NCs was reported to be higher than individual CdSe NCs. With the motivation to promote SILAR deposition, Chandra et al. have prepared CdS NPs by using cadmium acetate and ammonium sulfide precursor solutions (Chandra et al. 2014). The prepared nanomaterial has grain size 21–24 nm and band gap value of 2.44 eV. On the basis of the observations, the authors recommended SILAR as a useful technique to grow other Cd containing NCs. SILAR has also been employed to deposit CdS NPs on TiO_2 NRs (Xie et al. 2014). In the starting step TiO_2 NRs were prepared on silicon using oblique angle deposition after which these substrates were immersed into precursor solutions of $Cd(Ac)_2$ and Na_2S for coating with CdS NPs. On the basis of XRD measurements, the formation of CdS in cubic phase was confirmed after executing 25 SILAR cycles. The photocurrent measurements revealed the higher value of photocurrent and thus higher efficiency to separate electron/holes for samples prepared with more SILAR cycles. The photoluminescence intensity was found proportional to a number of SILAR cycles and can be used to monitor photocatalytic performance. The prepared nanocrystalline films CdS/TiO_2/Silicon were found to have superior photocatalytic and photoelectrochemical features in comparison to that of individual components of the structure. The authors have described the mechanism of photoelectrochemical process in the deposited structure in detail.

SILAR technique has also been tested for doping into nanocrystalline materials. The pure and Ag-doped CdS nanocrystalline films have been deposited on silicon using this technique (Dariani and Emami 2015). The solutions of cadmium nitrate and silver nitrate were used as cationic precursors whereas sodium sulfide solution was taken as an anionic precursor. The stoichiometric changes in CdS NCs were observed which indicated that the sample with Cd:S ratio of 1:3 presented most intense XRD peaks. The pure NCs have cubic whereas the doped NCs have hexagonal structures. The doping appeared to reduce band gap of the host and introduce dopant related gap levels. In another SILAR deposition, the solutions of cadmium nitrate and sodium sulfide were used as cationic and anionic precursors to deposit CdS films on a glass substrate (Manikandan et al. 2015). Triethanolamine was added as a complexing agent in order to achieve uniformity and stoichiometry thereby reducing the unbonded metallic ions in the films. The complexing agent appeared to reduce the grain size and the films were found suitable for photovoltaic applications on the basis of observed optical properties. The SILAR preparation of CdS NWs has also been reported (Dariani and Salehi 2016). The deposition of stoichiometric NWs on glass was carried out at S:Cd ratios of 1:1, 3:1, 5:1, and 7:1 after 15 SILAR cycles. The study was carried out using increasing concentration of

anionic precursor with the objective to achieve CdS NWs having improved stoichiometry. The authors expected stoichiometric improvement on increasing the anionic concentration due to increase in temperature resulting from the higher entropy of the system. It was observed that grain size and length of NWs increased whereas S:Cd ratio remains 1:1 with the increase in anionic concentration. In another report, SILAR preparation of nanocrystalline CdS thin films is found (Ashith and Rao 2016). It was observed that film thickness increases with increase in SILAR cycles and increase in Cd and S concentrations in precursors. However, with an increase in the cycles beyond 100, thickness did not further increase and "peeling effect" is triggered due to development of cracks on the film surface.

CdS NPs have also been prepared using SILAR technique to decorate an array of α-Fe_2O_3 nanopillar (Shuang et al. 2017). The materials were deposited with motivation to check photodegradation of methylene blue. The results indicated that the heterojunctions prepared at 10 SILAR cycles presented maximum degradation efficiency which is significantly higher than that measured for pure CdS nanomaterials. The photocatalytic performance of heterojunctions was also higher which points toward the potential of these materials for applications in photovoltaics.

Owing to the feasibility of SILAR for deposition of Cd containing II–VI nanomaterials, research efforts have also been carried out to prepare CdSe NCs. CdSe nanocrystalline films have been deposited on glass using this method (Kale et al. 2004). After 150 immersion cycles, the film was 0.18 μm thick and this thickness was found decreased with further increase in the cycles. The prepared films were found under compressive strain with a grain size of 6–8 nm. The optical band gap of the deposited film was 2.1 eV which was higher than bulk value of band gap for CdSe. Keeping in view the importance of SILAR cycles on characteristics of deposited films, Chaudhari et al. carried out a study to correlate the physical properties of CdSe films with a number of the immersion cycles. They reported SILAR deposition of nanocrystalline CdSe thin films on a glass substrate at a different number of immersion cycles (Chaudhari et al. 2016). It was observed that the intensity of XRD peak related to the hexagonal phase of CdSe increases with increase in number of the cycles. Moreover, as per optical measurements, absorbance and optical band gap increase with an increase in number of the cycles. In order to find the influence of synthesis route on physical properties of quantum dot-sensitized solar cells, a comparative study of SILAR and CBD prepared CdSe QDs has been carried out (Zhou et al. 2015). The CdS seeded QDs of CdSe prepared via CBD exhibited complete conformal coverage of QDs whereas SILAR prepared QDs presented partial coverage.

CdTe films have been deposited on the ZnO NWs for fabrication of core/shell heterostructures using the SILAR method (Salazar et al. 2014). The SILAR-deposited CdTe film was not of good quality due which thermal annealing and chemical treatment were carried out which appeared to improve the quality of the films. The thickness of CdTe shells was dependent on a number of SILAR cycles. In another report, SILAR deposition of nanoporous CdTe films on TiO_2 and conducting oxide electrode at a different number of immersion cycles have been demonstrated (Haydous and Halaoui 2014). It was found that the electrolyte

solution of Se^{2-} can be used for stabilization of CdTe films. The authors assigned the observed stability to the growth of $CdTe_{1-x}Se_x$ layers and suppression of anodic dissolution.

Unlike other Cd compounds, fewer numbers of reports on SILAR preparation of nanocrystalline CdO films are found in the literature. The deposition of nanocrystalline CdO on glass using dextrin as surfactant by utilizing SILAR route has been reported (Sahin et al. 2015). The XRD measurements revealed improvement in crystallinity of the films upon addition of dextrin which is found to

Table 3.3 Cd containing II–VI semiconductor nanomaterials prepared through SILAR method using different synthesis conditions

Material prepared	Cationic precursor	Anionic precursor	References
CdS NPs	Cadmium acetate	Ammonium sulfide	Chandra et al. (2014)
CdS NPs decorated TiO_2 NRs	$Cd(Ac)_2$	Na_2S	Xie et al. (2014)
Ag:CdS NCs	Cadmium nitrate ($Cd(NO_3)_2$) and $AgNO_3$	Sodium sulfide (Na_2S)	Dariani and Emami (2015)
CdS NCs	$CdCl_2$	Sodium Sulfide (Na_2S)	Ashith and Rao (2016)
CdS NCs	Cadmium nitrate ($Cd(NO_3)_2 \cdot 9H_2O$)	Sodium Sulfide (Na_2S)	Manikandan et al. (2015)
CdS NWs	Cadmium nitrate	Sodium sulfide	Dariani and Salehi (2016)
CdS NPs decorated α-Fe_2O_3 nanopillars	$Cd(Ac)_2$	Na_2S	Shuang et al. (2017)
CdSe NCs	tartaric acid and triethanolamine [$Cd(CH_3COO)_2$]	Sodium selenosulfate	Kale et al. (2004)
CdSe NCs	$CdCl_2 \cdot H_2O$	Sodium selenosulphite (Na_2SeSO_3)	Chaudhari et al. (2016)
CdSe QDs	$Cd(CH_3COO)_2 \cdot 2H_2O$	$Na_2S \cdot 9H_2O$	Zhou et al. (2015)
ZnO/CdTe core/shell heterostructure	$Cd(NO_3)_2 \cdot 4H_2O$	$NaBH_4$ and TeO_2	Salazar et al. (2014)
Nanoporous CdTe	$Cd(ClO_4)_2 \cdot H_2O$	Te powder and $NaBH_4$	Haydous and Halaoui (2014)
ZnO–CdO nanocomposite	NH_4OH and $CdSO_4$	H_2O_2	Nwanya et al. (2015)
Nanoporous CdO	$Cd[CH_3COO]_2 \cdot 2H_2O$	Hydrogen peroxide (H_2O_2)	Nwanya et al. (2016)
CdO NPs	$Cd(CH3COO)_2 \cdot H_2O$	Water	Sahin et al. (2015)
Mn:CdO NCs	Cadmium acetate	Water	Sahin et al. (2014)

assist diffusion of Cd and O and facilitate the deposition. Furthermore, the presence of dextrin appeared to decrease the grain size and increase the transmittance as well as band gap of deposited films. In another work, SILAR deposition of composite ZnO–CdO nanocrystalline thin films on steel and glass substrates prepared for the purpose of gas sensing have been reported (Nwanya et al. 2015). The band gap was measured as 3.8 eV which was reduced to 2.9 eV upon annealing treatment of the films. The gas sensing potential of the deposited film was checked to detect LPG which indicated the response of 50% recorded at 623 K when exposed to 780 ppm of the gas. Recently, nanoporous CdO film deposited on glass using SILAR technique has been reported (Shameem et al. 2017). The films prepared at three different molar concentrations exhibited a consistent change in band gap values of 2.8, 2.72 and 2.60 eV. The deposited films were found to have excellent photocatalytic performance under the UV-visible light. SILAR technique has also been utilized to dope CdO nanocrystalline films. Sahin et al. have prepared pure and Mn-doped nanocrystalline CdO films deposited on glass using SILAR (Sahin et al. 2014). The measurements revealed doping and annealing dependent modifications in physical properties of the films. A consistent and Mn concentration-dependent increase in grain size and band gap was observed. A short review of the synthesis process with different experimental conditions has been given in Table 3.3.

The workers have found SILAR a reliable synthesis strategy to prepare Cd containing nanomaterials. On the basis of their reported experience, this technique is found operative at low temperature, inexpensive, quick, and offers deposition virtually any material on any substrate with controlled thickness and deposition rate.

3.3 Chemical Co-precipitation Method

Chemical precipitation is one of the most popular and simple chemical synthesis techniques and it is found efficient to prepare the metal–chalcogenides with good control over composition. In this method, inorganic salts are dissolved into some appropriate medium to form a uniform solution containing clusters of ions. The salts (sulfates, nitrates etc.) are used as starting agents and the product consists of two or more unsolvable types; solvents comprise of de-ionized water, ethanol, methanol and acidic solutions. In this method, a basic solution of the precursors is made through drop-wise mixing in solvents for a better pH value control (Zhong 2012). Then, at room temperature, these prepared solutions are mixed and stirred for hours to fully react. In chemical precipitation, the reacting materials precipitate in basic solvents after the reaction is finished due to their low solubility. In co-precipitation, reaction materials precipitate in basic solvents as precursors and the solubility depends upon pH value. Metal salts frequently need a basic/weak acidic environment for this process, so a well-organized pH value is necessary for the reaction.

Chemical precipitation involves two basic steps: (i) synthesis in a liquid state (ii) thermal treatment. Chemical composition is an essential feature influencing the structures and properties of nanomaterials. Therefore, it is necessary to organize the stoichiometric ratio of precursors accurately. The concentration of precursors in the solution is also an essential part in synthesis, so it is needed to mix the precursors with preset molar ratios. The properties of product NPs are dependent upon temperature, salt concentration, and pH modifications. Different stages involved in the synthesis of nanomaterials using co-precipitation are sketched in Fig. 3.5.

There are many advantages of this method, like (i) low-cost, (ii) comparatively low temperature and high yield of products, (iii) convenient operation, (vi) a uniform distribution of constituents, (v) simple equipment (vi) a direct method for fine particle synthesis, and (vii) consistent particle size. However, this method is not suitable for the reactants which have dissimilar solubility and precipitate rate.

Many researchers widely employed this method to prepare the Cd–chalcogenide nanomaterials. Cadmium sulfide NPs have been prepared using the colloidal chemical precipitation technique (Rao et al. 2011). XRD and SEM studies confirmed the formation of identical and very well-structured particles with single phase hexagonal structure. The size of the aggregated NCs was found to be 13 nm. The electronic properties of the sample were studied in detail and exhibited a shift of band edge towards the higher energy with a decrease in the particle size. CdS NPs have also been prepared through chemical precipitation process using $CdCl_2$, Na_2S, tetrabutylammonium bromide and water as a solvent (Devi et al. 2015). During the process temperature was varied in range 20–80 °C. All of the prepared NPs showed the cubic structure with their size varying in the range of 15–80 nm. The prepared nanomaterial was found stoichiometric with Cd to S ratio of 1:1. The optical properties of spherical-shaped CdS NPs exhibited the absorption in range of

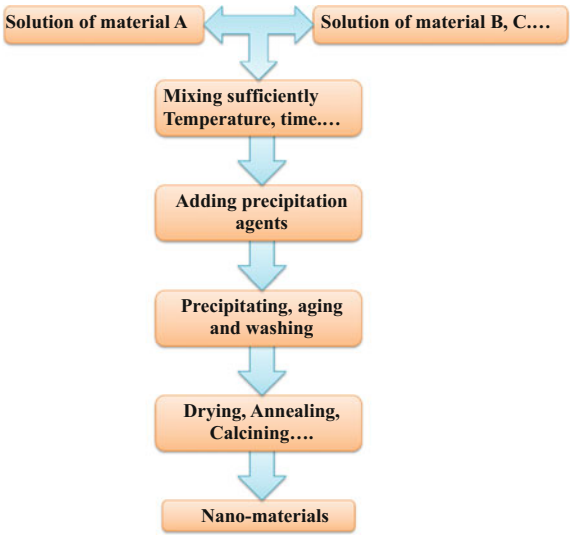

Fig. 3.5 Schematic diagram showing synthesis strategy using chemical precipitation method (Zhong 2012)

460–480 nm and the band gap was found to be 3.2–3.5 eV; larger than bulk due to quantum effects.

In another work by Raj and Rajendran, CdS NPs have been prepared in an aqueous environment by reaction of cadmium acetate and sodium sulfide (Raj and Rajendran 2015). The pH value of the solution was observed 9–10 and the chemical reaction for this process is given below;

$$Cd(CH_3COO)_2 + Na_2S \rightarrow \mathbf{CdS} + 2CH_3COONa$$

As-synthesized NPs showed polycrystalline characteristic with average particle size of 7 nm and specific surface area 74.26 m^2/g. The study revealed that CdS particles are suitable candidates to be used in DSSCs. CdS NPs have been prepared through co-precipitation technique and their structures and morphologies were investigated in detail (Reddy et al. 2016). In contrast to their bulk counterparts, a considerable shift in the band gap of CdS NPs have been observed due to quantum effects. These NPs (Fig. 3.7a) exhibited high photocatalytic activity under UV-irradiation for the degradation of methyl orange. It was observed that CdS nanoparticles prepared with 0.3 wt% showed highest photocatalytic behavior. The morphology, structure and optical performance of stable CdS nanostructures prepared by the same method showed a wurtzite structure (Kumar and Sharma 2016). The lattice parameters were observed smaller as compared to the bulk due to lattice contractions. A quantum size effect was also observed by examining the absorption spectra of the synthesized nanomaterials.

The process of doping has great effects on the properties of the nanomaterials. Cerium-doped CdS NPs have been prepared by using co-precipitation technique (Saravanan et al. 2012). The doping of Ce atom was carried out at concentrations of 1, 2 and 3 mol% and the prepared samples were characterized in detail. Both the doped and undoped NPs were found having wurtzite structure with particle size 3 nm. The measured absorption and emission spectra showed a blue shift with the decrease in the Ce concentration. The co-precipitation synthesis and characterization of Mn-doped CdS NPs have been reported by Gupta et al. (Gupta and Kripal 2012). The grown material was wurtzite in structure and having 2–4 nm crystallite size. The optical properties revealed a blue shift in absorption edge with a decrease in particle size due to quantum confinement effects. Furthermore, a consistent doping-dependent decrease in band gap was observed. There was also a consistent blue shift observed in the phonon modes whereas an enhancement in their intensity ratio with decreasing the Mn doping concentration was found.

The straightforward chemical precipitation method has also been applied to prepare doped nanomaterials. The preparation of pure and Cr-doped CdS NPs using chemical co-precipitation process has been reported (Elavarthi et al. 2016). The doping at 3–5% Cr concentration appeared to change the structure of the NPs. Quantum confinement effect was observed in both undoped and Cr-doped CdS NPs when other optical properties were compared with that of bulk CdS. For Cr-doped CdS the cubic structure was converted to the mixed phase of cubic and hexagonal structures. Due to the appearance of defects in the doped material a broad emission

band was observed. The ferromagnetic properties of the doped samples were found strongly dependent on doping concentration. The chemical precipitation method has been applied to synthesize CdS NCs doped with diverse metals (Ertis and Boz 2016). The analysis revealed the NCs showed the cubic structures with crystal size 4.0–4.5 nm. Degradation of methylene blue was improved with metal-doped CdS as compared to that of undoped CdS. As per UV-Vis measurements, the band gap of these NPs was found in range 2.25–2.55 eV. Co:CdS showed the highest photocatalytic behavior about 87%. The preparation of PVP-capped CdS NPs and doping with Cu and Mn was carried out using chemical precipitation technique (Muruganandam et al. 2017). The band gap value was observed to be increased showing quantum confinement. Many properties of these NPs like the number of spins, covalency, and electrode application properties were investigated from cyclic voltammetry and EPR methods.

Co-precipitation technique has also been utilized to synthesize the Cr-doped CdSe NPs (Majid et al. 2015). The study revealed the zinc blend cubic structure of the prepared NPs. With increasing the chromium doping concentration, the lattice parameters showed a consistent decrease in such a way that for 4, 5, and 6% doping concentration the size of NPs was observed to be 3.02, 2.48 and 2.11 nm, respectively. Fe:CdSe NPs have been synthesized through Chemical Co-precipitation technique (Fig. 3.7c). The quantum confinement effects were observed in the hexagonal structure of the pure and doped samples having 5 and 10% doping concentration. Raising the doping concentration of Fe resulted decrease in size from 18 to 12 nm and increase in band gap value from 1.88 to 2.20 eV. These NPs were found to be appropriate materials for spintronic devices. Another effort was carried out to prepare Fe-doped CdSe NPs using this technique (Dangi and Dhar 2016). In the absorption spectra of doped and undoped CdSe, a blue shift was observed in contrast to bulk CdSe which points to quantum confinement effect. An increase in the band gap was observed with increase in Fe doping concentration. In contrast to the pure CdSe NPs, Fe-doped CdSe QDs revealed a clear nonlinear optical response. The preparation of pure and Mn-doped CdTe NPs by using co-precipitation method has also been reported in the literature (Majid et al. 2016). The effects of Mn doping on structural, morphological, and magnetic characteristics of CdTe NPs were studied in detail and the SEM image of these nanoparticles is shown in Fig. 3.7b. The doped NPs exhibited clear room temperature hysteresis with doping-dependent decrease in saturation magnetization pointing to antiferromagnetic ordering in the material.

The co-precipitation technique has also been used to prepare CdO nanomaterials. Nanosized particles of CdO were prepared using the co-precipitation technique by using cadmium acetate and the ammonium hydroxide precursors (Waghulade et al. 2007). The grown nanomaterial was investigated in detail and tested for sensing of liquid petroleum gas (LPG). In another effort, co-precipitation technique was applied to prepare Ag-doped CdO nanomaterials with varying doping concentration between 0.1 and 10% (Kumar et al. 2016). The size of nanocomposites has been observed to be homogeneous and decrease with increase in doping concentration. The results showed that the pure CdO is polycrystalline while the structure of

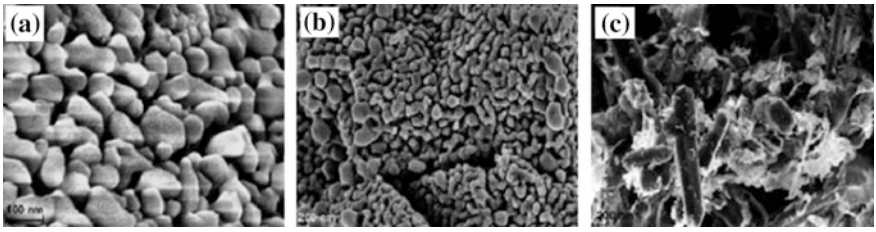

Fig. 3.6 FE-SEM images of **a** CdO, **b** Ag-CdO **c** Ag–ZnO–CdO (Balachandran et al. 2014). © 2014 Royal Society of Chemistry

nanomaterial with 10% doping is cubic. An increased photocatalytic response was observed for this silver-doped-coupled semiconductor oxide Ag–ZnO–CdO. It shows the potential of the material for photocatalytic applications with self-cleaning properties. FESEM images indicated the plate-like structure of pure CdO (Fig. 3.6a). Figure 3.6 shows Ag NPs scattering on CdO (Fig. 3.6b), Ag–ZnO–CdO heterostructures (Fig. 3.6c) as a combination of hexagonal nanosheets, nanoclusters and NPs with a huge number of cavities (Fig. 3.7).

Pure and zinc-doped CdO NPs have also been prepared by chemical precipitation process (Ravichandran et al. 2016). The effect of zinc doping concentration (0, 2 and 5%) was studied using XRD, FESEM, UV-Vis, and PL spectroscopy techniques. The doped material showed a polycrystalline character with an increase in size and also exhibited the variations in band gap values according to the doping concentration. Recently, chemical precipitation method has been applied to prepare CdO NPs as a chemically adjusted electrode (Ahmadzadeh et al. 2017). The grown material showed a good performance to oxidize chlorpromazine (CPZ). The oxidation peak potential of chlorpromazine at CdO surface was shown at 695 mV and linear calibration curves were investigated. These reported nanomaterials showed potential as a highly responsive and advanced detector to investigate the chlorpromazine in pharmaceutical samples.

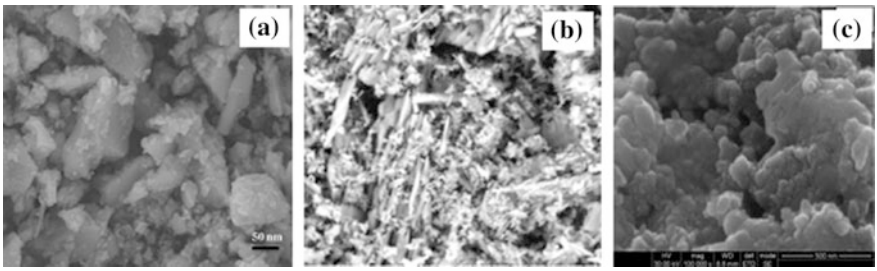

Fig. 3.7 Microscopy of co-precipitation produced nanomaterials (**a**) SEM image of CdS NPs (Reddy et al. 2016). © 2016 Springer Publishing. (**b**) SEM image of CdTe NPs (Majid et al. 2016). © 2016 Springer Publishing. (**c**) FESEM image of CdSe NPs (Chalapathi et al. 2015). © 2015 Open access

3.4 Electrochemical Synthesis

The deposition using electrochemical process is one of the extensively adopted methods to grow nanomaterials. It has been found an efficient and straightforward synthesis technique which provides high-quality nanomaterials and links top-down and bottom-up approaches (Kalska-Szostko 2012). This method employs electric current as driving force to deposit a nanocrystalline thin film onto a suitable substrate for different applications. The synthesis of nanomaterials using this technique involves a substrate, two or three electrodes, the electrolyte solution in a container and source of electric current. The factors that affect the growth of nanostructures are electric current, deposition potential, nature of the substrate, deposition time, temperature, nature, and pH of solution etc. The electrolyte is an anionic solution comprising of solutes of metal salts. The nature, type, and concentration of the electrolyte solution along with a quantity of oxygen dissolved determine the crystal quality, size and distribution of nanomaterials.

The electrodes used in electrodeposition are working electrodes; cathode made up of metal/metal oxides, an anode made up of inert metals, i.e., platinum (counter electrode) and a reference electrode (Zhong 2012). The deposition can be made on the electrode using current either as an alternating current or direct current. The solid–liquid interface supports the synthesis of nanofilms on substrates with diverse morphologies. General apparatus used for electrochemical deposition method is shown in Fig. 3.8a. In Fig. 3.8b, the synthesis of CdSe nanomaterials using this method have been schematically shown.

The electrochemical synthesis process offers several features which cannot be attained by other chemical methods. There is no need of elevated temperatures since the deposition process can be controlled thermodynamically and kinetically by monitoring electrical current. The control over the oxidation reduction potential can

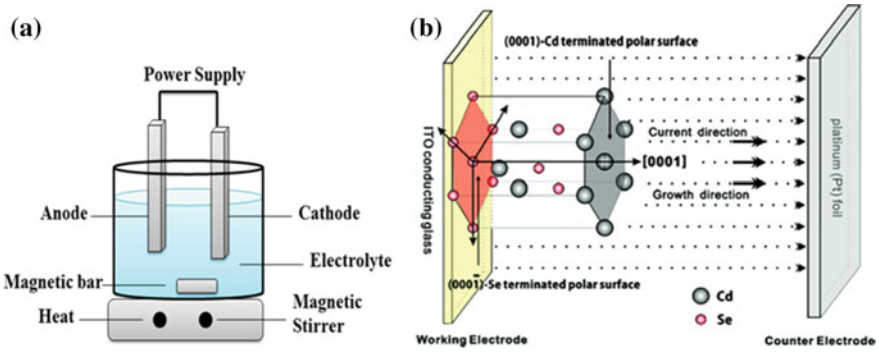

Fig. 3.8 **a** Apparatus for electrochemical synthesis. **b** Schematic diagram of electrodeposition process of CdSe NWs showing one of three fastest growth directions (Feng et al. 2010). © 2010 American Chemical Society

also be managed by changing the applied potential (Bensebaa 2012). A number of factors like solvent polarity, current density, electrode separation, and temperature can control the deposition process and yield of nanomaterials. The growth parameters using the electrosynthesis process include several choices; (i) choice of reactive electrodes (ii) selection of electrolyte and its constituents (iii) appropriate values of pH and temperature (iv) choice of electrolyte concentration (v) galvanostatic/potentiostatic electrolysis type (Ramimoghadam et al. 2014). A short review for the synthesis of Cd-based nanomaterials with different experimental conditions has been given in Table 3.4.

This is a low-cost process and offers growth of nanocomposites with improved thermomechanical properties (Bensebaa 2012). When this technique is merged with self-assisted templates, there is a possibility to synthesize the nanomaterials with more stimulating properties and control over morphology, size distribution, and crystal quality. The growth of nanomaterials can be optimized by changing the deposition potential, substrate and deposition time. Furthermore, this technique is eco-friendly, inexpensive and produced high yield at low expense of energy.

Cd-based II–VI semiconducting nanocrystalline structures can be efficiently synthesized by using the electrochemical method. The epitaxially orientated CdS nanocrystallites have been prepared on graphite by electrochemical method (Anderson et al. 1997). The synthesis involved three steps; (i) Deposition of NCs, (ii) Oxidization of NCs at high pH value, (iii) Formation of wurzite phase NCs. The characterization of the materials revealed the orientation of the nanocrystals along the *c*-axis of crystallite has been found in a direction perpendicular to the base plane. The identical azimuthal orientation possessed by the NCs was positioned within the single grain boundaries on the graphite basal plane. The semiconductor/metals NWs arrays similar to cadmium sulfide have been prepared following the electrochemical deposition of semiconductor into the pores of anodic aluminum oxide films. These homogeneous CdS NWs with lengths of 1 μm and diameters 9 nm have been processed with an electrolyte having Cd^{2+} and S^{2-} ions in dimethyl sulfoxide. The work reported growth of hexagonal CdS. It was also observed that by changing the conditions of preparation, the dimensional properties of the material can also be adjusted.

In ethylene glycol, CdS nanoparticles have been synthesized by one-step electrochemical method (Yang et al. 2006b). The electrode used in the experiment was made of gold and the reaction was free of capping agent and carried out at temperature 70 °C. The magnetic stirrer was used to avoid the deposition of CdS on the electrode. Electrosynthesis of the CdS nanostructures has also been performed using the pulsed current of 100 $mAcm^{-2}$ (Karami and Kaboli 2010). In pulsed current synthesis, the prepared CdS nanofibers were not attached to the electrode surface, leaving the electrode surface not fully covered with NPs. In electrochemical synthesis, this method is more capable than the constant current method. During the electrochemical growth of CdS NPs following chemical reactions take place:

Table 3.4 Cd containing II–VI semiconductor nanomaterials prepared through electrochemical method using different synthesis conditions

Material	Anode	Cathode	Solution	Sweep potential/ current density	pH	Temperature (°C)	References
CdSe NPs	Graphite	Ti	$CdCl_2$ and H_2SeO_3	200 mA/cm^2		95 °C	Fomanyuk et al. (2016)
CdSe NCs	Ag/ AgCl	Graphite	$CdCl_2$ and SeO_2	–	–	400 °C	Peng et al. (2001)
CdSe NWs	Ag/ AgCl	Pt	$CdCl_2$ and SeO_2	400–800 mV		RT	Shpaisman et al. (2010)
CdSe NWs	Ag/ AAO	Pt	$CdCl_2$ and Se	0.85 mA/cm^2 (dc density)		185 °C	Xu et al. (2000)
CdSe NWs	Calomel	–	$CdSO_4$ and SeO_2	−0.55 V	2.5	RT	Kalhori et al. (2015)
MPA-capped CdTe QDs	–	–	NaOH, Te and $Cd(Cl\ O_4)_2$/ MPA/NaOH	−1.3 V	13/ 10.5	90 °C	Ribeiro et al. (2013)
CdO nanofilms	Ag/ AgCl	Pt	$CdCl_2$, KOH and MPA	–	–	–	Wang et al. (2008)
CdS nanofibers	Pt	Pt	$CdCl_2$ and $Na_2S_2O_3$	100 mA/cm^2 (dc density)	2	150 °C	Karami and Kaboli (2010)
Sn:CdO NCs	Calomel	Pt	$CdSO_4$ and H_2O_2	–	8	80 °C	Ganjiani et al. (2016)

$$S_2O_3^{2-} + 6H^+ + 8e \rightarrow 2S^{2-} + 3H_2O \quad \text{and,} \quad Cd^{2+} + 2e \rightarrow Cd$$
$$S^{2-} + Cd^{2+} \rightarrow \mathbf{CdS}$$

First, two chemical reactions happened on cathode surface and depend on several parameters including pulse amplitude and frequency, temperature, concentrations, and pH of the solution. The last chemical reaction is completed in the solution and depends on the Cd^{2+} concentration, formation of S^{2-} ions and solution temperature. The process has been done at a frequency of 8 Hz and a solution temperature of 50 °C. The Cd content is decreased with increasing the temperature and the nanomaterial was formed at 150 °C. The work described the synthesis of nanostructured CdS at optimum conditions. The results obtained on characterizing the nanomaterials showed the homogeneous CdS nanofibers having a diameter between 80 and 100 nm and length 5–7 μm. In another report, the formation of nanostructured CdS thin films using pulsed current via electrochemical method (Wang et al. 2012). The utilized electrode was made from gold and modified by self-assembled p-aminothiophenol monolayer (PATP/Au). A structured array of CdS NRs with a comparatively higher *c*-axis orientation have been deposited on PATP/Au. The analysis demonstrated that pulse width and current should be monitored to obtain the required size and morphology of the NRs. The size and coverage of the NRs were found directly proportional whereas the structural uniformity was inversely proportional to the pulse width. A review written on the electrochemical synthesis of CdS in different media including aqueous, non-aqueous and the ionic liquid has been reported by Mammadov et al. (2012). The conditions like pH values, temperature of reaction, composition of the solution, and the sources for the sulfur were discussed in detail.

CdSe NW arrays have been synthesized by DC electrodeposition method (Xu et al. 2000). Precursors comprising of dimethyl sulfoxide solution of cadmium chloride and elemental selenium were used. The process has been performed in permeable anodic aluminum oxide templates as a result of which stoichiometric CdSe NWs with hexagonal crystal structure having homogeneous morphology were obtained. The same method has been used to fabricate the polycrystalline CdSe NW arrays (Peng et al. 2001). Ammonia alkaline solution in anodic alumina membrane (AAM) was used to fabricate these highly structured NWs with homogeneous radius of about 30 nm, length of 5 μm and pore spacing 100 nm. DC electrodeposited CdSe NWs exhibited a wurtzite structure with good stoichiometry.

The growth of CdSe NWs by employing different sweeping rates in electrodeposition process has been reported (Shpaisman et al. 2010). The computer controlled process at three sweep rates was carried out to produce the NWs of controlled morphology. The morphology and dimensions of the NWs were monitored by the degree of co-deposition of cadmium along with the deposition of CdSe. The dense CdSe segment lengths of 380, 200, and 50 nm were managed through inverse adjustment of the scan rates at 10, 30, 90 mV/s, respectively. The images of the grown NWs are given in Fig. 3.9b, c, d. The authors recommended this method as extremely quick and straightforward to grow high-quality NWs with control over

structure and morphology. A thin film of CdSe with fine crystallinity has been electrochemically deposited on the substrate by photoresist templates (Erenturk et al. 2011). These as-synthesized arrays of hexagonal structured CdSe NWs showed uniform crystallinity after excluding the photoresist templates. The obtained NWs were 100 nm in thickness, 300–500 nm in width, and several centimeters in length.

The template-free electrochemical method has been found to be appropriate for growth of NWs (Feng et al. 2010). CdSe NWs with single-crystal wurtzite structure have been prepared using template-free electrochemical deposition process. These CdSe NWs have been synthesized along the [0001] as schematically shown in Fig. 3.9a. NWs prepared by this method have been found longer than those prepared by CVD. An improved photovoltaic performance has been observed with these CdSe NWs signifying their striking potential in photovoltaics. This method is suggested to be easily applicable to the growth of other nanostructures related to II–VI semiconductors. CdSe NPs have been prepared using the electrochemical method with DC electrolysis process (Fomanyuk et al. 2016). The chemical reaction involved during the growth process is given below:

$$H_2SeO_3 + 4H^+ + 6e \rightarrow Se^{2-} + 3H_2O \quad \text{and} \quad Cd^{2+} + 2e \rightarrow Cd$$
$$Se^{2-} + Cd^{2+} \rightarrow \mathbf{CdSe}$$

Smaller sized particles (2–5 nm) have been obtained from cathode extractable in xylene whereas larger size NPs (20–100 nm) stayed in the electrolyte and mixed with nitric–hydrochloric acids. These NPs revealed hexagonal as well as cubic structure. Electrochemical deposition technique has also been used for the synthesis of CdSe NWs in polycarbonate and the growth mechanism was examined during the potentiostatic deposition (Kalhori et al. 2015). Many properties like structure, morphology, binding of fragments and band gap energy of the prepared nanomaterial were characterized using a variety of techniques. The results showed that these CdSe NWs exhibited increased photoconductive reaction and photosensitivity contrary to the earlier reports.

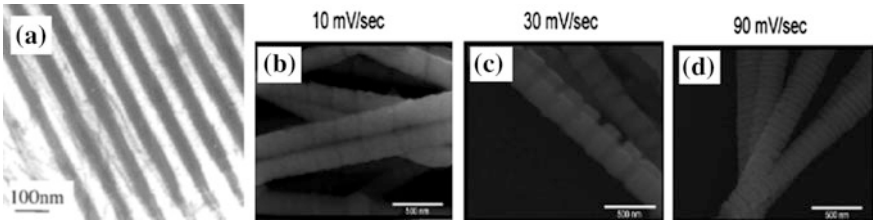

Fig. 3.9 **a** TEM image of a row of electrochemically prepared CdTe NWs (Zhao et al. 2003). © 2003 Spring Publishing. SEM images of sweep electrochemically deposited segmented CdSe NWs with **b** 10 mV/s, **c** 30 mV/s and **d** 90 mV/s scan rates (Shpaisman et al. 2010). © 2010 American Chemical Society

In nanostructure films deposition, the electrochemical method plays a leading role. The physical deposition method and the electrochemical method have been compared and led to a conclusion that the electrochemical method is comparatively better to cover the inner surface of the porous silicon (Montes et al. 1997). CdTe nanocomposites have been synthesized using this method in order to provide the charge injection in the structure. The samples were characterized using auger electron microscopy, X-ray diffraction method and X-ray photoelectron spectroscopy. The growth direction of CdTe was found as (111). The photoluminescence characteristics of the porous silicon were strongly affected after deposition and drying. There has been a comprehensive study of different telluride compounds under the optimized electrolyte method (Miles and McEwan 1972).

Cadmium telluride NPs have been prepared and the electric field directed layer-by-layer assembly method have been reported which combined the electrophoretic deposition and the layer-by-layer self-assembly method (Sun and Feldmann 2001). This method has been used to understand the special deposition of cadmium telluride nanoparticles on indium tin oxide electrode. The material after the evaluation by measuring the florescence described that the selection of the deposition of the film increased by the applied voltage and went to 99% when the applied voltage reached to 1.4 V. However, the further increase in the applied voltage caused the decrease in a deposition. Increase in the voltage has been adjusted toward the degradation of CdTe NPs and reduced the intensity of the fluorescence. It describes the protection of CdTe film at the high voltage. The NPs manufactured by layer-by-layer assembly of poly (p-phenylenevinylene) exhibited strong electroluminescence for use in a light-emitting diode. The electroluminescence has been observed at a voltage of 4 V (Chen et al. 2002). The photoluminescence measurements revealed the presence of trap centers and de-trapping of surface states.

The electrochemical method for the preparation of adherent nanostructured CdTe films has been reported by employing the direct templating of material with lyotropic liquid crystalline mesophases (Gabriel et al. 2002). The obtained materials were characterized by transmission electron microscopy and low angle X-ray scattering which indicated that the material was in the form of uniform cylindrical pores arranged in the hexagonal array. The potentiostatic electrochemical deposition method has been used to prepare CdTe NW arrays entrenched in the nanochannels of the porous anodic alumina (PAA) template (Zhao et al. 2003). The electrolyte solution was a mixture of $CdSO_4$ and $HTeO_2^+$, and the electrochemical growth of CdTe nanostructures taken place via chemical reactions given below:

$$HTeO_2^+ + 3H^+ + 4e \rightarrow Te + 2H_2O \quad \text{and} \quad Cd^{2+} + 2e \rightarrow Cd$$
$$Te + 2e + Cd^{2+} \rightarrow \mathbf{CdSe}$$

The obtained CdTe NWs were single crystalline with a cubic phase having an average diameter of 60 nm. The NWs were stoichiometric and found as homogeneously implanted in the nanochannels of the PAA template (Fig. 3.10a). The electrochemical method has also been used to prepared CdTe QDs in an aqueous solution of telluride ions and $Cd(ClO_4)_2$ (Ribeiro et al. 2013). The obtained CdTe

QDs have been stabilized by negatively or positively charged ligands from mercaptopropionic acid (MPA) or cysteamine (Cys). The process has been observed to be eco-friendly due to the absence of chemical reducing agent and simply managed the reduced species production. The reported work showed that the obtained material possessed good stability and high luminescence with a particle size of 3.1 nm.

This technique has also been employed to prepare CdO nanostructures. CdO nanofilms on glassy carbon surfaces have been synthesized by controlled-potential electrodeposition of Cd (Wang et al. 2008). The electrolyte solution containing $CdCl_2$ and 3-mercaptopropionic acid formed the Cd layer which reacted with oxygen from air and resulted in production of dendritic CdO nanostructure. These nanostructured films revealed a stable and well-built ECL emission in aqueous solution. Highly transparent CdO nanostructures have also been deposited on Indium-doped tin oxide (ITO) substrate (Singh et al. 2011b). CdO nanostructures prepared at low temperatures 70, 80 and 90 °C, showed FCC structure with good crystallinity. Large-area polycrystalline CdO and $Cd_{1-x}Co_xO$ NWs have also been synthesized by this method (Liu et al. 2012). The process was carried out in oxygen-rich solution of $CdCl_2$ + citric acid at a temperature of 90 °C. Electrochemical process for the NWs fabrication can be referred to nucleation-coalescence method. The synthesis process of these CdO NWs by electrochemical deposition is described by following reactions:

$$O_2 + 2H_2O + 4e \rightarrow 4OH^- \quad \text{and,} \quad Cd^{2+} + 2e \rightarrow Cd$$
$$2OH^- + Cd^{2+} \rightarrow \mathbf{CdO} + H_2O$$

During the synthesis process carried out in different time intervals 15, 25, and 90 min, different morphologies of CdO structures were observed (Fig. 3.10). The deposition at intervals 15, 25 and 90 min produced the NWs composed of NPs, short NWs with coarse surfaces and curved NWs with smooth surfaces, respectively. Electrochemical synthesis method provides good control of structure and morphology by adjusting the concentration of the solution and provides a significant development in process of formation of NWs. Undoped and Sn-doped CdO

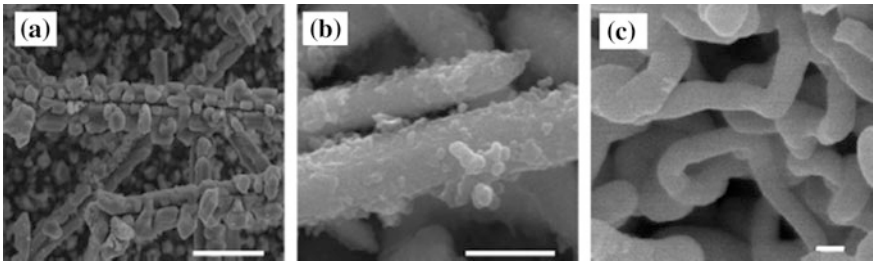

Fig. 3.10 Electrochemically synthesized CdO **a** nuclei, **b** NPs, **c** curved NWs (Liu et al. 2012). © 2012 Elsevier Publishing

thin films have also been prepared using same method and analysis showed their cubic nanostructures with flower- and rod-like morphologies (Ganjiani et al. 2016).

3.5 Solvothermal Synthesis

A solvothermal synthesis method comprises of the chemical reaction of precursors, in the presence of solvents, carried out at a temperature which is higher than boiling point of the solvent (Byrappa and Yoshimura 2012). The solvothermal process involves organic solvents under specific conditions which refers this technique toward green chemistry. Early precursor concentrations play important role in controlling the structure and shape of synthesized nanomaterials. The choice of solvent, appropriate temperature, and pressure conditions are important parameters involved in solvothermal process.

In this technique, physiochemical reactions are performed at high pressure and temperature. The growth process is carried out in a closed chamber known as autoclave (usually Teflon/stainless steel). This process allows the integration of species available in precursor during the nanostructure formation. Precursors and solvents are mixed and kept at a specific temperature for different time periods.

Solvthermal synthesis methods are typically performed in two steps; crystal nucleation and development. The structure, morphology, and properties of the product nanostructures can be controlled via parameters including starting agent type and concentration, pH value, temperature conditions and processing time etc. The processes involved in solvothermal mechanism can be approximately classified as; transport of entities via solution, their development on the surface and connection to the growth sites. There is a broad range of non-aqueous organic solvents used in solvothermal technique like methanol (Yin et al. 2003), 1,4-butanediol (Kang 2003), and amine (Zhu et al. 2011) etc. Different morphologies can be obtained with different solutions (Yang et al. 2010). Chemical composition and concentration of precursors is a very significant factor in the solvothermal process which affect the nature of reagents and solvents (Demazeau 2008). In the solvothermal method, reactions take place at comparatively low temperatures than hydrothermal (discussed later). The benefits of the environment-friendly solvothermal process include obtaining very small grain size without any impurity.

Plenty of research works for the preparation of metals, metal oxides, silicates, carbonates, sulfides, tellurides, nitrides, and selenides have been obtained using solvothermal/hydrothermal methods. These methods have been widely utilized for a variety of nanostructures like NTs, NWs, NPs, and NRs, etc. (Aliofkhazraei 2016). The recent work demonstrated that the solvothermal/hydrothermal process become necessary for controlled size synthesis of II–VI semiconductors nanomaterials. CdS NPs have been prepared by means of solvothermal process to study the optical properties of the material (Li et al. 2000). These NPs showed potential for a large number of applications in the field of optics. The characterization results showed the spherical shape and cubic structure of the NPs. UV-vis spectrum demonstrated

the effect of amount and molar ratio of reactants. CdS NRs with changing dimensions prepared via solvothermal process have also been reported explaining the importance of cadmium anion in calculating the dimension of NRs (Datta et al. 2007). The dimensions, shape, and size of the NRs can be controlled by monitoring the parameters of the reaction like sulfur source, precursors, solvent, and temperature. By varying the temperature from 100 to 250 °C, the size of the NRs showed variation between 7 and 100 nm.

A report on colloidal QDs of CdS prepared via solvothermal technique has been presented (Arellano et al. 2010). The synthesis system having three components possessed the ability of formation of particles with various sizes at diameter ranging from 3.36 to 8.41 nm. The effects of time and temperature on the optical properties and band gap characteristics have been studied. Novel optical properties and high photocatalytic activity were observed in another study on 3D CdS nanomaterials (Guo et al. 2011). Synthesis of these 3D assemblies of flower shaped cadmium sulfide has been conducted by using the additive-free solvothermal method. The reported work revealed the importance of ethanol in the formation of CdS assemblies. The time-dependent experiments have also been performed and the effects of variable solvothermal time on the morphology of nanomaterials were studied. Different values of synthesis time exhibited different morphologies and size of CdS nanomaterials as shown in Fig. 3.12. In first half hour NPs with size 20 nm was obtained, whereas after 1 and 3 h, bowl-like structures were found. The evolution process for these flower-like nanostructures showed completeness at 6 h after which no effect was observed on the morphology. The solvothermal method with ethanol as solvent has been observed very appropriate for the synthesis of flower-like nanostructures.

The synthesis of one-dimensional CdS NRs at the moderate temperature of about 200 °C has been conducted at 12–24 h reaction time (Phuruangrat et al. 2012). The results explained the hexagonal single phase crystalline CdS NRs with 20 nm diameter and 100–200 μm length showing the absorption peak at 482 nm and band at 403 nm. Copper-doped CdS nanomaterials synthesized by the same method have been reported mentioning the diameters about 30–50 nm and the length about 0.5–10 μm (Arbuj et al. 2013). The properties of the hexagonal wurtzite structure-doped NRs have been studied by varying the molar ratio of reactance from 0.1 to 5 mol%. The photocatalytic activities of the doped NRs were discussed for the blue degradation of methylene which revealed the higher degradation rate for the sample $Cu_{0.01}Cd_{0.99}S$.

The solvothermal method has the ability to grow 2D nanosheets. Nanosheets of the CdS alloyed with ZnS have been prepared via aqueous phase solvothermal process employing the different concentration of cadmium and zinc at the temperature of 200 °C for 4 and 24 h (Mahdi et al. 2013). The analysis of the nanosheets demonstrated the wurtzite crystalline structure and optical band gap variation with the change of concentration. The increase in Zinc concentration showed an increase in the band gap of the material. The PL spectra showed the higher intensities for 24 h than at 4 h. Exclusive MoS_2/CdS nanosheets-on-nanorod heterostructure has been prepared using both hydrothermal and solvothermal

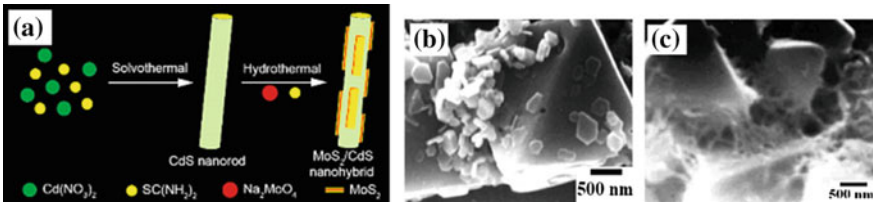

Fig. 3.11 **a** Schematic diagram of synthesis process of MoS_2/CdS nanosheets-on-NRs (Yin et al. 2016). © 2016 American Chemical Society. SEM images of CdO octahedrons (**b**) prepared at 493 K with hexagonal nanosheets formed on their surface, (**c**) prepared at 453 K with NWs formed from their surfaces (Ghoshal et al. 2009). © 2009 American Chemical Society

process (Yin et al. 2016). These CdS NRs have been prepared through thiourea and $Cd(NO_3)_2$ in ethylenediamine and MoS_2 nanosheets have been developed on the CdS NRs using hydrothermal method (Fig. 3.11a). The prepared samples showed striking properties for solar energy conversion process with a quantum yield of 41.37% at 420 nm and hydrogen evolution reaction 49.80 mmol g^{-1} h^{-1}. These MoS_2/CdS nanosheets-on-nanorod revealed their applications as inexpensive well-organized photocatalysts for water splitting.

Morphology-controlled CdSe and CdTe NCs with zinc blende structure have been prepared using solvothermal method (Wang et al. 2006b). These nanostructures clearly showed quantum confinement effect and this method have been found to be suitable for synthesis of II-IV nanomaterials. Well-dispersed and homogeneous CdSe NRs have been prepared using solvothermal method (Wang et al. 2006a). The influence of diethanolamine (DEA), ethanolamine (MEA), and triethanolamine (TBA) on prepared CdSe NRs having length 10 μm has been discussed in detail. CdSe NRs with a diameter of 25 nm and length of 82 nm have been again synthesized by this method with hydrazine hydrate ($N_2H_4 \cdot H_2O$) as the reducing agent (Ramalingam et al. 2009). The synthesis of CdSe NRs, along with agglomeration of NPs and the existence of a small number of spherical NPs have been confirmed. A blue shift has been observed for these CdSe NRs in contrast to their bulk counterpart.

WZ CdSe NPs have been prepared via solvothermal method (Yang et al. 2010). Ball-like ZB CdSe as starting agents was converted into wurtzite structure of CdSe NPs. This method has been found suitable to prepare the metal chalcogenides. In another study, ZB CdSe hollow nanospheres and WZ CdSe solid NPs have been prepared using solvothermal process (Wang et al. 2010). Time-dependent synthesis process proposed the development of CdSe hollow nanospheres. The effects of reaction time, temperature and solution concentration on the morphology and size of these nanospheres have also been studied. Zinc blende CdSe hollow nanospheres exhibited a noticeable blue shift when compared to the bulk.

CdSe NRs have also been synthesized using solvothermal method (Zuala and Agarwal 2016). These CdSe NRs with wurtzite structure showed better stoichiometry, less dislocation density and crystallite morphological variations dependent on reaction time. For short reaction time, spherical and oval-shaped NPs

are frequently observed. For longer reaction time, extended rod-shape particles have been obtained. The growth process of these thermally stable nanostructures happened quickly on the surface of the cylindrical NPs. Water-soluble monodisperse CdSe NCs have also been prepared using solvothermal method (Shahi et al. 2016). Wurtzite phase of hexagonal CdSe NCs has been observed with predictable sizes about 13–29 nm. Some well-built and fine peaks were studied and a blue shift in the absorption band was observed because of quantum confinement effect. These prepared CdSe nanostructures showed their potential for applications in biology labeling/imaging, photocatalytic activities, photovoltaics and LEDs.

An easy solvothermal method has been carried out to form CdTe needle-like nanostructures (Selvakumar et al. 2007). In this process, a new single source molecular precursor has been applied. These NPs showed FCC structure with the size of 29.5 nm. The surfactant-assisted solvothermal method has been used to prepare CoTe, Ag_2Te/Ag, and CdTe nanostructures (Jiang et al. 2010). A range of different surfactants like PVP and CTAB has been used and it showed remarkable variations in morphology of synthesized nanomaterials. The surfactant-assisted solvothermal method has again been used to prepare a range of metal telluride nanostructures including PbTe, CdTe, $CoTe_2$, Bi_2Te_3, and Cu_7Te_4 (Jiang et al. 2010). The nanostructures with different morphologies were obtained.

In order to enhance the properties of the materials, the doped nanomaterials can be easily synthesized by means of the solvothermal method. CdTe NPs doped with mercury have been prepared by means of the solvothermal process (Arnepalli and Dutta 2005). The analysis of the product showed the cubic structure of the mercury-doped CdTe nanoparticles with (111) dominate plane and the average size of the particles was found in range from 10 to 15 nm with a narrow size distribution. Mercury-doped CdTe NRs with the size of about 20–50 nm have also been prepared using the solvothermal method by means of stable Na_2TeO_3 (Khatei and Koteswara 2012). The reported work demonstrated the temperature dependence of the photoluminescence showing the three dominant photoluminescence bands in the temperature range 10–300 K. The photoluminescence bands with activation energies 50–100 meV were observed in the range from 0.5 to 0.7 eV related to the defect centers. CdTe nanorods with an average length of 1.23 and 0.15 μm have been prepared with solvothermal method (Tiwari et al. 2013). The arrays of carbon-coated CdTe NRs have been synthesized via solvothermal process (Yuan et al. 2012). This reported work revealed the good fluorescence and demonstrated the significant importance of KOH in the arrays of CdTe NRs.

CdO NWs and micro-octahedrons have been prepared using solvothermal method (Ghoshal et al. 2009). Sodium hydroxide and temperature were the main factors to organize the phase and morphology of the synthesized nanomaterials. CdO octahedrons have been observed made up from two reversed pyramids joined from the square base with varied length from 1.5 to 3.5 μm. The usage of different amounts of NaOH showed different morphologies of CdO nanostructures, like nanoparticle and NRs attached to these octahedrons (Fig. 3.11b, c). The synthesis process carried out at 453 °C produced nanosheets like structures with homogeneous size and clear

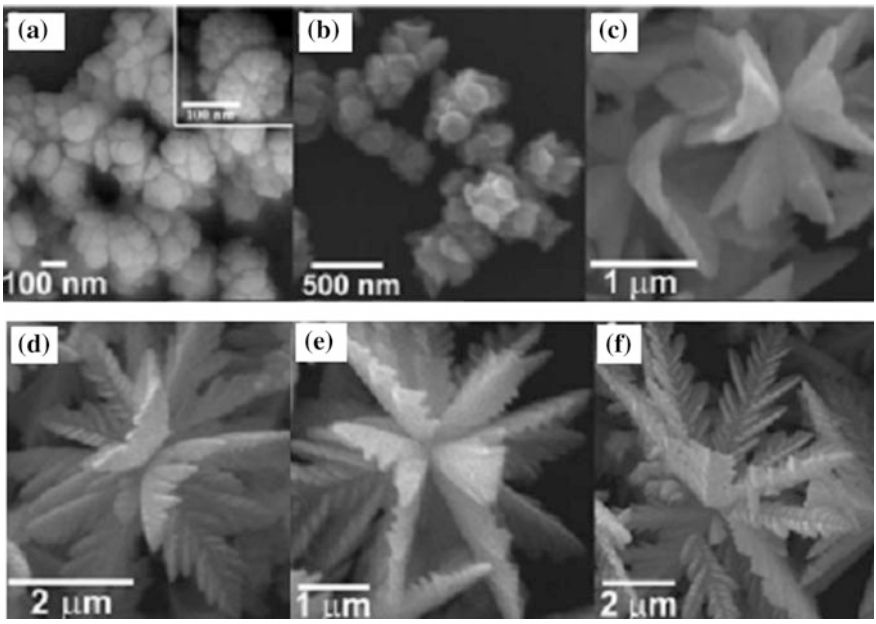

Fig. 3.12 Morphology-evolution process of flower-like CdS nanostructures at different solvothermal time **a** 0.5 h, **b** 1 h, **c** 3 h, **d** 6 h, **e** 9 h and **f** 18 h (Guo et al. 2011). © 2016 Royal Society of Chemistry

hexagonal shape on the surface of octahedrons. By changing the temperature of the system to 493 °C, the nanomaterials in the form of NWs were obtained.

3.6 Hydrothermal Synthesis

The hydrothermal process is similar to the solvothermal process, with a little difference that water is used as the solvent (Aliofkhazraei 2016). In the case of hydrothermal reactions, the precursor is provided with water in an autoclave to perform synthesis process. Since, water is an exceptional solvent it is possible to dissolve even nonionic compounds at high pressure and temperature conditions involved in the hydrothermal process. There are two classes of this synthesis method; (i) batch hydrothermal system performs the process with required ratio phases and (ii) continuous hydrothermal system which offers a better rate of reaction at shorter time period (Hayashi and Hakuta 2010). In the hydrothermal method, the particle morphology and structure can be controlled by utilizing diverse precursors and hydrothermal conditions (Mustafa et al. 2017).

The hydrothermal technique works at low energy without wasting materials which makes it a preferred choice. It is an inexpensive, controllable, reproducible

deposition strategy with better nucleation control so it is considered as an attractive technique to prepare the nanostructures (Aliofkhazraei 2016). There are also some difficulties linked with hydrothermal synthesis like (i) requirement of costly autoclaves, (ii) necessity for high-quality seeds, (iii) high temperature, and (iv) Unfeasibility to observe the process during growth.

Hydrothermally prepared $CdCO_3$ NWs have been converted into porous CdO NWs through thermal decomposition (Jia et al. 2008). These CdO NWs have been found made up of individual NPs joined with each other. Spherical ring structured CdO NPs with crystalline phase and size of 65 nm were prepared using inexpensive, easy and convenient hydrothermal method (Barve et al. 2014). During the study of photocatalytic properties, degradation percentage of CdO nanomaterials was observed to decrease with increase in the concentration of methyl red. Degradation of azo dyes has also been studied with rhombus-like structures of CdO NPs (Fig. 3.13) prepared through hydrothermal method (Tadjarodi et al. 2014). The size of the NPs was observed 29 nm with band gap energy of 1.9 eV. CdO NPs showed good efficiency for effective degradation of azo dyes like congo red, malachite green and crystal violet. These hydrothermally synthesized nanomaterials have been found to be compatible for photoactivity in the visible region with 100% potential to decolorize these pollutants. For the study of gas sensing properties, CdS films have been deposited on hydrothermally prepared ZnS NRs by SILAR. The subsequent annealing at 400 °C for 2 h changed the ZnO/CdS core/shell NRs into ZnO/CdO nanostructures (Kim et al. 2016). Regarding ethanol gas sensing mechanism, ZnO/CdO nanostructures showed excellent responses in contrast to that of ZnO/CdS core/shell NRs.

CdS NPs have been prepared by hydrothermal method and their properties were studied in detail (Zang et al. 2007). The quality of these hexagonally structured NPs revealed that hydrothermal synthesis technique is very efficient to synthesize these nanomaterials at low temperature. The prepared particles with size of about 10 nm, showed a blue shift in UV-Vis spectra as compared to the bulk. The formation of

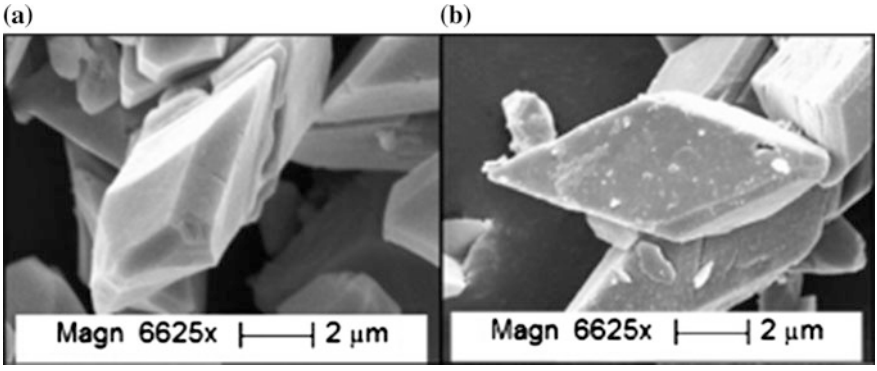

Fig. 3.13 SEM images of CdO nanostructures synthesized through hydrothermal reaction (Tadjarodi et al. 2014). © 2014 Open Access

flower-like CdS nanocluster using hydrothermal technique has been studied (Xu et al. 2007). The NRs are very important nanomaterials and have abundant technological applications. CdS having flower-like nanostructure have been prepared using thioglycolic acid as capping agent via hydrothermal (Salavati-Niasaria et al. 2009). In optical absorption spectra, a clear peak observed at 500 nm revealed a blue shift as compared to the bulk counterpart due to quantum confinement effect. The result evaluated the importance of thioglycolic acid which plays the considerable role in the formation of the nanostructure.

CdS nanostructures have been prepared through ethylenediamine assisted hydrothermal method (Li et al. 2009). The morphology, size, and phases of nanocrystalline CdS NPs have been observed to be significantly changed due to reactant concentration and temperature. Higher photoreactivity has been observed for rod-like structures which was found smaller in case of granular shapes. Pt deposited CdS exhibited the highest efficiency in photoactivity for hydrogen evolution under the visible light irradiation. CdS NPs have been synthesized at room temperature along with Cd complexes and thioacetamide have been used as precursors (Dumbrava et al. 2010). The smaller diameter NPs have been formed showing emission at smaller wavelength via UV-Vis spectra, in comparison to that of bulk material, due to quantum confinement. Their size and morphology were studied using TEM and uniform CdS NPs have been found with a diameter in the range of 3.55–10.70 nm. CdS nanostructures capped with thiol group have been synthesized by means of the hydrothermal process (Salavati-Niasaria 2011). The synthesis involved the cadmium (II) phthalate as a precursor and thioglycolic acid. On the basis of detailed characterization, it was concluded that a variety of parameters like the reactant concentration effect, the molar ratio of the stabilizer to cadmium ion, reaction time and temperature strongly affect the properties including particle size, morphology, and nanocrystalline phase. The precursor cadmium (II) phthalate has been again used with TGA to prepare CdS nanostructures through thioglycolic acid assisted hydrothermal method (Salavati-Niasari et al. 2013). The morphology, size and structural properties of the prepared CdS NPs were studied in detail. The properties of as-synthesized materials were significantly affected by the reactant concentration, mole ratio of TGA, temperature, and reaction time.

Pure CdS and HMTA-capped CdS nanostructures of respective sizes of 4.5 and 3 nm have been prepared using hydrothermal method (Chinnu et al. 2011). The results showed the structures of CdS nanomaterial as cubic faced spherical-shaped NPs. The HMTA-capped CdS NPs showed flower-like structures. The optical properties and photocatalytic characteristics of the nanomaterials were investigated. The capped CdS nanostructures showed good photodegradation activity for the methylene blue (MB). It showed an increase in decolorization of MB with the passage of time in such a way that photodegradation activity raised to 95% after 90 min. CdS NPs capped with polyvinlypyrrolidone have been prepared by hydrothermal process (Jothi et al. 2012). Recombination of holes in VB of CdS and electrons trapped in the sulfur vacancies played a significant role in determining the surface trap fluorescence. In this study, the hydrothermal method has been found appropriate for synthesizing the capped CdS nanostructures. PVP-capped CdS

nanomaterials have been again prepared with iron (Fe) containing CdS NPs using the hydrothermal technique (Kumar et al. 2014). A reduction in the band gap value as 2.84, 2.75 and 2.55 eV and a decrease in emission intensity was noted with an increase in Fe content. The average size of the product NPs has been observed about 12 nm, and increase in Fe concentration caused a redshift in emission as per photoluminescence spectra. The wurtzite-type hexagonal structured particles showed a ferromagnetic behavior and also revealed Fe dependent change in electrical conductivity.

CdS NCs have been synthesized at room temperature using the hydrothermal technique with synthesis time varying from 0 to 1440 min at a temperature of 180 °C (Kumar et al. 2015). The results showed the zinc blende structure of particles with average crystallite size about 10 nm. These nanostructures prepared in nontoxic and easy reaction medium showed an attractive homogeneity and better emission properties. CdS in the hexagonal crystal structure with rod- and flower-like crystallites have been grown using the hydrothermal technique (Liang and Lung 2016). The analysis indicated that the hexagonal structure of CdS led the efficient growth process and the flower-like crystallites showed the higher photoactivity. The thermal annealing in the air appeared to oxidize the flower-like CdS crystal structured NPs to develop CdO. The interface between CdS and CdO was found supportive to improve the photoactivity of flower-like nanomaterials.

A number of research efforts have also been carried out to prepare CdTe nanomaterials by using hydrothermal approach. Water-soluble CdTe NCs have been prepared via hydrothermal route (Zhang et al. 2003). High PL quantum yield (QY) and narrow fluorescence emission spectra were observed due to low precursor concentration and moderate temperature synthesis process. These NCs exhibited 30% QY for the green-yellow emitting samples. The grown nanomaterials showed great potential for use in many biological applications for the bioimaging purpose. The water-soluble CdTe NCs have been synthesized by the same hydrothermal route (Yang et al. 2006a). The growth process was carried out in aqueous media at 100 °C with tripeptide thiol glutathione as a stabilizing agent. The obtained CdTe nanocrystal capped with tripeptide thiol glutathione possessed the narrower FWHM of photoluminescence and high quantum yield. Their emission peaks have been observed more symmetrical compared to nanocrystal of CdTe capped with thiohydracrylic acid. CdTe NCs have been prepared using the facile hydrothermal route under optimum conditions (Jain et al. 2009). The as-prepared NCs showed strong photoluminescence intensity with narrow lines. High-quality CdTe NCs have been reported by employing this simple and suitable two-step hydrothermal method (Zhu et al. 2010). SEM and TEM results showed the shapes of the crystals in the form of the spindle and rod-like. The effects of reaction temperature were also studied.

The hydrothermal method has also been employed to prepare the nanomaterials of different types and morphologies for technological applications (Yong et al. 2010). This method has been utilized to use ascorbic acid as reducing agent and the carbonization source for growth of CdTe NWs. The observed diameter of NWs and the width of the obtained carbon sheath were found 20 and 10 nm, respectively.

Nanogenerators supported by Micro/NWs of CdTe with zinc blende structure have been prepared using a facile one-step hydrothermal process (Hou et al. 2013). The single microwire generator could produce voltage up to 0.3 V and current 40 nA by applying strain. The hydrothermal method allows a quick synthesis of CdTe QDs exhibiting adjustable emission spectra with high QY nearly 45% (Li et al. 2013). The average size of the spherical, high-quality water-soluble NAC-capped QDs has been found approximately 2.7 nm. Higher temperature resulted in rapid growth mechanism, consequently larger size QDs were formed, whereas lower temperature synthesis provided the poor quantum yield. The optimum temperature for hydrothermal synthesis has been found to be in-between 170 and 210 °C. In another study, CdTe–TiO_2–graphene nanocomposites have been prepared via hydrothermal method (Liu and Li 2014). During the process, CdTe QDs have been *in-situ* fabricated on the carbon basal planes. CdTe QDs have been prepared in aqueous solution through hydrothermal synthesis technique and characterized using a variety of techniques (Borse et al. 2016). These QDs stored at 4 °C exhibited exceptional luminescence and fluorescence properties with diverse physicochemical states. The fluorescent properties make these QDs highly applicable for use as biosensors.

3.7 Microemulsion Technique (Synthesis in Structured Media)

Microemulsion synthesis is carried out by using a uniform solution containing water, oil, surfactant, and amine-based or alcohol co-surfactant (Hirai et al. 1994). This technique comprises of a collection of processes in the thermodynamically established colloidal system and involves an isotropic mixture of hydrophilic liquid (water), lipophilic liquid (oil), and an amphiphilic surfactant (hydrophilic and hydrophobic groups). The oil may be a mixture of hydrocarbons and olefins; surfactant can also be merged with a co-surfactant. The surfactants play an important role in microemulsion reactions by lowering the tension among microemulsion and excess phases and to prepare the smaller NPs with narrow size distribution (Zhong 2012). They facilitate the synthesis of NPs in limited space by acting as a reagent to make the system stable and it can also merge with a co-surfactant.

Microemulsion consists of conventional micelles and reverses/inverted micelles to serve as nanoreactor locations in which limited growth of NPs occur. A reverse micelle is a system of monodispersed spherical droplets of water-in-oil (w/o) phase, in which the water phase is swollen by a continuous oily phase. Water to surfactant ratio plays a significant role in determining the particle size; smaller ratio gives the smaller particles. The hydrophilic groups on the surface of surfactant make the water core and organic tails of their molecules turn toward outside. Commonly, two types of microemulsion schemes are employed for the synthesis process (Fig. 3.14a, b), (i) one microemulsion scheme and (ii) two microemulsion scheme (Dhand et al. 2015). The single microemulsion procedure involves; one reactant is in the walls of microemulsion, reducing agent, oxidants and/or the second reactant

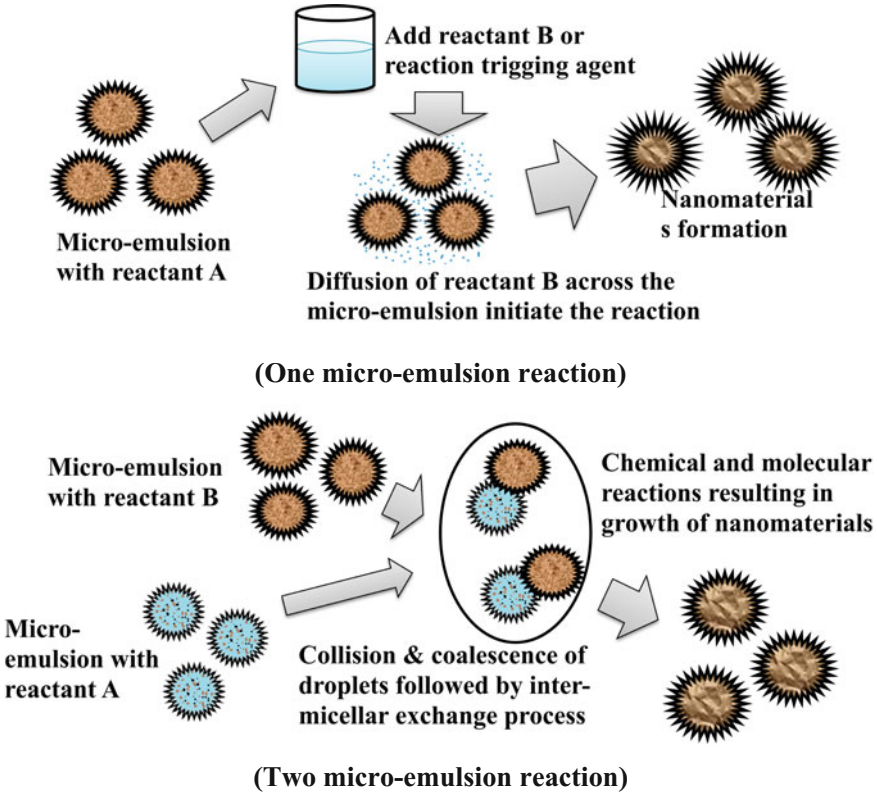

Fig. 3.14 Synthesis diagram of (**a**) One microemulsion and (**b**) Two microemulsion synthesis scheme (Dhand et al. 2015)

has to diffuse through the wall to complete the growth process. This process is diffusion controlled where an energy/pulse triggering (reactant) agent is required to start the growth process. Two microemulsion processes, two microemulsions with divided reactants are merged in suitable ratios along with surfactant, oil and water. Brownian motion offers the chance to mix the micellar constituents in two different micelles or reverse micelles and to initiate the chemical reaction.

Microemulsion reaction can easily be carried out at room temperature and no aggregation occurs between the NPs due to the presence of surfactant material. Water to surfactant molar fraction is an important factor where the nature of surfactant must be controlled to efficiently synthesize the nanomaterials. Well-organized confinement of NPs synthesis is the most striking feature of this method which gives the accurate control of particle size, crystal quality, size distribution, and shape. Therefore, this method allows the preparation of various morphologies and intricate nanostructures including pyramidal, core-shell, hollow and belts/rods etc. Microemulsion synthesis process with different experimental conditions has been given in Table 3.5.

Table 3.5 Cd containing II–VI semiconductor nanomaterials prepared through microemulsion method using different synthesis conditions

Materials	Surfactants	Co-surfactant	Oil	One or two Microemulsion Scheme	Mechanical Agitation time	References
CdO NPs	Cetyl tri-methyl ammonium bromide (CTAB)	n-butyl	Cyclohexane	One microemulsion scheme with w/o system	5 days	Shukla et al. (2012)
ZnO–CdO nanocomposites	–	–	–	w/o system	–	Khalili and Hassanzadeh (2017)
CdS/PMMA nanocomposites	Sodium bis(2-ethylhexyl) sulfosuccinate (AOT)	No	methyl methacrylate (MMA)	Two microemulsion scheme with w/o system	–	Li et al. (2004)
(PANI)/CdS nanocomposites	Poly (oxyethylene)$_5$ nonyl phenol ether (NP5) and poly (oxyethylene)$_{10}$ nonyl phenol ether (NP10)	–	Cyclohexane	Two microemulsion scheme with w/o system nonionic system	–	Khiew et al. (2004)
CdS NRs	TX-100 (polyoxyethylene Tert-octylphenyl ether)	Hexanol	Cyclohexane	Two microemulsion scheme with w/o system	4 days	Zhang et al. (2005)
CdS QDs	IGEPAL	–	Cyclohexane	Two microemulsion scheme with w/o system	–	Veeranarayanan et al. (2012)
CdTe@SiO_2 Nanospheres	Triton X-100 (t-octylphenoxypolyethoxyethanol, Sigma)	n-hexanol	Cyclohexane	One microemulsion scheme with w/o system	3 days	Yang and Gao (2005)
CdSe NRs	sodium bis(2-ethylhexyl) sulfosuccinate (AOT)	n-heptane	Hydrazine hydrate	One microemulsion scheme with w/o system	–	Xi and Lam (2007)
CdSe Nanospheres	CTAB	Isobutanol	Cyclohexane	Two microemulsion scheme with w/o system	–	Dong et al. (2013)

The microemulsion method has attained the considerable importance in the synthesis of nanomaterials due to several features such as the very low interfacial tension, thermodynamic stability, very large interfacial area and the great ability for two immiscible liquid to resolve into each other (Malik et al. 2012). The microemulsion technique is very useful for the preparation of the nanomaterials with required properties including the geometry of the particles, the surface area and most importantly the homogeneity of the obtained material. This method is comparatively simple and convenient and gives the controllable size distribution to NPs in contrast to co-precipitation and similar deposition methods. A large number of reports are available for synthesis of Cd-chalcogenide nanomaterials using the microemulsion method. The most important published scientific efforts are discussed in the following.

The formation of NPs using microemulsion method has been carried out along with Monte Carlo simulation to understand the growth process (Tojo et al. 1997). The parameters that play significant role in this method such as the flexibility of the surfactant, the numeral molecules of reagent per droplet, size of the droplet, autocatalysis by product effect, and the bulk fractional area formed by the droplets have been described. The mechanism of NPs formation under the microemulsion process was discussed in detail.

The provision of nanomaterials is a key requirement for development of novel functional materials through explicit chemical, physical, and electronic characteristics. CdS NPs have been obtained using ammonium perfluoropolyether stabilizer through microemulsion method (Holmes et al. 1999). The work demonstrated the control of size by varying the water to surfactant ratio. The observed band gap of 2.45 eV points to quantum confinement effect in the prepared nanomaterial. The formation of dispersed CdS NPs with cubic phase in polymer matrices have been reported (Li et al. 2004). CdS/PMMA nanocomposites have been prepared using the reverse microemulsion scheme. Higher pressure conditions appeared to affect the particle size. The result showed that CdS and polymethyl methacrylate (PMMA) interacted strongly. The reverse microemulsion technique has been mostly used to prepare the nanocrystals of Cd base materials. Conductive polyaniline (PANI)/CdS NCs have been synthesized using same method (Khiew et al. 2004). The NCs were coated with polyaniline having conducting property. The UV-absorption spectrum and the FTIR spectroscopy discussed the result of doping process, UV-absorption spectrum demonstrated the doping level in material and FTIR described the existing material was highly doped. These nanocomposites with average size of 17.8 nm showed better thermal response.

The formation of NRs, nanofibers and the nanostructured CdS thin film by means of microemulsion synthesis method have been reported (Zhang et al. 2005). The homogeneous NRs of CdS have been synthesized in microemulsion by means of nonionic surfactant TX-100 and the hexagonal co-surfactant. The reported NRs have been observed in the form of single crystal with wurtzite structure. The size of the NRs have been dependent on the concentration of the reagents used and defined the limit of concentration. Nucleation and synthesis process have been fully controlled to form good quality NRs. The effect of water content on the length and

diameter of these NRs has been observed. Different amount of water contents showed the identical NRs with length and diameters of 1.6 vol.% (200 and 20 nm), 2 vol.% (260 and 25 nm) and 2.4 vol.% (300 and 35 nm). In general, more water content provided the broad dispersion of NRs. It was described that the long and thick NRs will be obtained by higher amount of water in microemulsion process. CdS NPs have been prepared by using two different polymers (Lemke and Koetz 2012). The UV-visible and the fluorescence spectra have been used to study the effects of capping agents. In another study, the microemulsion method with water in olive oil without any surfactant have been applied to synthesis these CdS NPs having the average diameter of about 45 nm (EL-Hefnawy 2012). The aqueous and silica-encapsulated CdS QDs have been prepared by microemulsion method (Veeranarayanan et al. 2012). Bio-optical probes have been used for targeting purpose. CdS QDs have been found as a proficient cell label with fluorescence at the same level. The toxicity of pure QDs has been adequately reduced by encapsulating them in a biocompatible silica covering. Size of CdS QDs and silica-coated QDs have been found 4–5 nm and 35–40 nm, respectively. CdS QDs have been observed to be non-flourescent while silica-coated CdS QDs have shown florescence under UV illumination. The QDs prepared by this simple method do not require any intricate constraint and can be used in biomedical application for understanding human specific cell and for imaging of cells.

Core/shell structure of CdSe/CdS nanomaterials has been prepared using microemulsion method (Hao et al. 1999). These nanomaterials showed good photoluminescent QY. CdSe NPs with hexagonal structure have been prepared by microemulsion technique at temperature of about 100 °C (Xi and Lam 2007). In this scheme, hydrazine hydrate has been used as reducing and templating agent; it supports the rod-like structures of nanomaterial formation. Highly stable CdSe NPs have also been prepared in microemulsion showed intense PL spectral peaks at 500 and 580 nm (Guleria et al. 2012). CdSe QDs have been synthesized in reverse microemulsions using high-energy electron beam irradiation (Singh et al. 2013). These QDs have been obtained with the size within 3 nm and exhibited wide photoluminescence response in region 450–750 nm. These QDs have been obtained with ultra small size of less than 5 nm showing a QY of about 2.4%. The nanomaterials prepared using this easy and one-step process has the potential applications in white light-emitting devices.

Hollow-structured CdSe NPs have been prepared via microemulsion technique (Dong et al. 2013). A variety of hollow structures can be formed using microemulsion method. These NCs showed nanoball, nanotube, and bamboo-like nanotube as hollow structure with different conditions. The diameter of the obtained hollow NPs, NTs, and bomboo-like NTs were found 20–30 nm (with wall thickness of 5–10 nm), 30–35 nm (with wall thickness of 5–10 nm) and 10–20 nm (with wall thickness of 5–8 nm). Luminescent CdSe/CdS@SiO_2 NPs have also been synthesized through a water-in-oil microemulsion process (Aubert et al. 2014). The major plus point of these CdSe/CdS luminescent QDs is their high photoluminescent QY that stayed unaffected still placing in water for various months. The silica coating of these CdSe/CdS QDs provided a possibility for their application to cell labeling.

CdSe bluish-white light-emitting QDs have been prepared using electron beam irradiation system through one-step templated scheme in the reverse microemulsions (Guleria et al. 2015). These highly stable ultrasmall QDs showed the optical emission spectra ranging 450–750 nm.

Silica coating appeared to enhance the biological functionalization of these QDs for biological analysis. Water-soluble CdTe/CdS/SiO_2 core/multishell QDs have been synthesized with 3-mercaptopropionic acid as the stabilizers using the microemulsion technique (Song et al. 2013). These CdTe/CdS core/shell fluorescent complex NPs have been made using thiourea for sulfur source in aqueous solution. The resulting core/shell QDs (with diameter 64 nm) were found inert and chemically established even in insensitive environments as a consequence of the silica layer. CdTe NCs encapsulated in silica spheres (CdTe@SiO_2) as core–shell-structured spheres have been synthesized by hydrolysis and microemulsion (Yang and Gao 2005). Process of condensing the tetraethyl orthosilicate has been performed in reverse microemulsions. CdTe NCs have been obtained with size of 3.5 nm with a QY of about 7%. Results showed the importance of electrostatic interactions among CdTe NCs and silica to establish the morphology and structures of the product NPs. CdTe@SiO_2 NPs have been again prepared using same method. Incubation process for CdTe QDs with thioglycolic acid as stabilizer in ammoniacal solution enhances the fluorescence QY (Jing et al. 2009). Under optimized conditions, these highly fluorescent CdTe@SiO_2 NCs showed a QY of about 47%. In another study, (CdTe/CdS)@SiO_2 NPs with size of 50 nm have been prepared using a water-in-oil microemulsion method at ambient temperature (Wang et al. 2007). Hydrolysis of tetraethyl orthosilicate brought about the development of monodispersed silica nanospheres. CdTe NPs coated with CdS shell showed a red shift in optical spectra along with an increase in size distribution. CdTe/CdS particles coated by silica exhibited increased fluorescence intensity. The silica coating offered a special feasibility for the biological functionalization of the surface of luminescent QDs.

The QDs of CdTe prepared using reverse microemulsion and protected with polyelectrolyte are reported to possess strong fluorescence property (Tang et al. 2012). The spherical-shaped and homogeneously distributed NPs have been obtained with average size of 25 nm. The zeta potential demonstrated the large potential of about −35.07 mV which showed the excellent monodispersity of solution. The characterized material showed a wide range of applications in biological and cellular application. Water-soluble thioglycolic acid (TGA) stabilized CdTe QDs have been prepared using microemulsion technique (Wang et al. 2014). These QDs were coated with silica as inert materials to expand the chemical properties of the material. This surface adjustment decreased the toxicity of CdTe QDs. Silica-coated QDs with size 40 nm showed efficiency in the growth of rice seed.

Water-in-oil microemulsion has been applied for synthesis of an extensive diversity of morphology such as spherical and umbrella shaped CdO NPs. Antibacterial performance with diverse concentration of CdO nanoparticles has been studied (Shukla et al. 2012). CdO NPs showed great antibacterial performance and different concentration of CdO showed different effects on the growth of these

bacteria. These NPs revealed a decrease in the number of bacteria (optical density) in liquid culture. This method has been found very efficient in the preparation of the nanomaterials, as it provides good control over size and shape of the NPs. CdO NPs with size of 43 nm have been obtained through microemulsion–hydrothermal synthesis (Maryam and Hanish 2016). These NPs showed a blue shift of 1 eV in contrast to their bulk counterpart. ZnO–CdO nanocomposites with a surface area of 9.5 m^2/g have been prepared in water-in-oil system (Khalili and Hassanzadeh 2017). These nanostructures with a spherical shape showed an exceptional activity for quick elimination of methyl blue from the solution.

3.8 Polyol Synthesis

Polyols (such as ethylene glycol and 1,2-propanediol glycol) as medium allows the hydrolysis of precursors comprising of metallic salts at variety of conditions to prepare nanomaterials. This is a simple and powerful synthesis approach based upon poly (ethylene glycol)s as reaction medium (Palchik et al. 2001) due to it reducing power and high-boiling point (Wiley et al. 2005). It acts simultaneously as solvent, reducing agent, and complexing agent. Currently, it has been developed into an adaptable and competent method to reduce the metal salts and organo-metalic compounds to produce the efficient nanomaterials related to metals, metal oxides, metal chalcogenides, etc. Capping agent polyvinyl pyrrolidone (PVP) is utilized for stability of NPs and additionally, it may provide nucleation feasibility for nanoparticles growth (Zhong 2012). The concentration of starting agents and reaction time play important role in controlling the size and crystal structures of the nanomaterials. It should be noted that not only solvent concentration but also the polyol type affects the nucleation speed, morphology, and structure of the final products. The mechanism of polyol synthesis showing different stages of growth is sketched in Fig. 3.15a.

This is an easy method to create 1D, 2D, and 3D nanostructures with possibility of using simple metal salts as starting agents. As the particles are formed, surface efficiency and colloidal stability of particles are obtained giving low degree of agglomeration and homogeneous size distribution. In Fig. 3.15a, synthetic steps for NPs formation have been shown with PG and EG as typical examples of polyol solvents. Polyol adhere on the particles surface showing high viscosity especially in contrast to water. These are high-boiling point solvents allowing the growth process without involving high pressures. A list of commonly used polyols with boiling points is given in Table 3.6. This technique is extensively used to acquire nanomaterials with variety of structures, morphologies and diversity of applications. It offers a number of merits for technological and industrial use because of its mass production, cost-effectiveness, controllability, efficiency and green solvents. This method allows optimization of growth parameters to give control over many properties like size, morphology, and homogeneity. Unlike other techniques, this method has not yet gained the deserved attention for synthesis of nanomaterials.

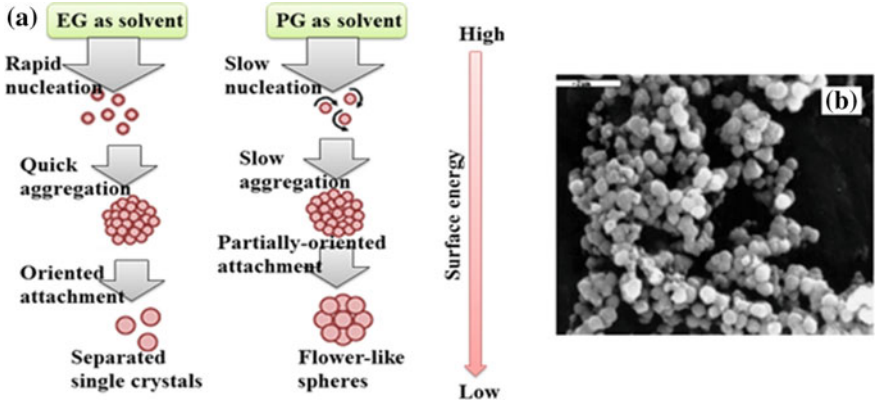

Fig. 3.15 **a** Synthetic diagram of Polyol synthesis (Cheng et al. 2011). **b** SEM image of hexagonal CdSe nanoballs prepared using microwave-assisted polyol method (Palchik et al. 2001). © 2001 Royal Society of Chemistry

CdS NPs having average diameter of 5–8 nm were prepared through the polyol technique (Ma et al. 2008). Spherical-shaped CdS NPs with high density and homogeneously have been coated on the surface of multiwalled carbon NTs (MWCNTs). These coated NTs showed extraordinary photocatalytic activity for degradation of azo dye, so an improvement of MWCNTs for photocatalytic behavior of CdS has been reported. Sphalerite-structured CdS NPs have also been prepared using polyol method (Feldmann and Metzmacher 2001). These non-agglomerated CdS NPs showed narrow size distribution with size ranging between 30 and 259 nm. Size can be adjusted with solubility under higher/lower solubility of the particles having larger/smaller diameter. The size of the NPs depends upon other conditions like precursor concentration, temperature and heating time.

CdS NPs have been prepared using propylene glycol in polyol synthesis method (Rathika Nath and Rajesh 2013). These nanostructures showed relatively narrow size distribution with hexagonal phase whereas the measured optical spectra exhibited blue shift as compared to bulk material. CdS–TiO_2 nanocomposite films have been synthesized using polyol method (Chaguetmi et al. 2013). Highly crystalline CdS QDs with WZ structure have been obtained without any structural defects. CdS sensitization in PEC devices showed an improvement in the photocurrent. CdS–TiO_2 nanocomposites have shown capability as photocatalytic materials for hydrogen production.

Cubic face centered and hexagonal structured CdS NPs have been prepared by a facile polyol method and their development over time has been studied in natural surroundings (Rocha et al. 2015). FCC structured CdS NPs showed agglomeration with size of particles larger than 500 nm. Hexagonal CdS particles have not been agglomerated and showed similar properties as that of precursors. PVP-capped CdS NPs have also been grown using simple polyol method with ethylene glycol

(Darwish et al. 2016). The size and structure of the particles were organized by the microwaves and calcination process. The grown NPs were hexagonal with typical size of 48 nm and exhibited 85% degradation of dye for UV (after 90 min) and visible light irradiation (after 9 h).

Hexagonal and cubic phased CdSe nanoballs have been prepared by microwave-assisted polyol method (Palchik et al. 2001). The prepared nanoballs having size of 346 nm were obtained in the form of NPs with diameter 6–7 nm and hexagonal structure (Fig. 3.15b). Ethylene glycol has been considered an appropriate material for microwave-assisted polyol synthesis route. Biocompatible, monodisperse and PAA capped CdSe QDs have been synthesized using one-pot polyol route (Zhai et al. 2011). CdSe/CdS core/shell QDs have been obtained by thin coating of CdS on CdSe QDs. PAA capping agent is selected to adjust the size, size distribution and crystallinity of QDs. The nanostructures showed an increase in size with increase in reaction time, exhibiting a red shift in optical spectra with reference to the bulk material. QY of 30% has been obtained with CdSe/CdS core/shell QDs. This one-pot method has been proved to be inexpensive and eco-friendly for growth of biocompatible CdSe and CdSe/CdS core/shell QDs.

CdO NPs have also been prepared using polyol method (Tabatabaee et al. 2013). PEG played an important role in synthesis of face centered cubes of CdO NPs with size of 151–25 nm.

3.9 Sol-Gel Synthesis

The sol-gel method is a popular chemical synthesis route for preparation of materials via polycondensation of molecular species from a solution. The "sol" consists of dispersed colloidal particles in a solvent whereas "gel" comprises of a rigid network. The preparation of ceramic materials takes place by means of sol-gelation of that sol and the removal of solvent. In this method, a liquid (sol) is chemically converted into gel state followed by condensation in the form of solid nanostructures. The materials via this method are classified into four groups; (i) well-organized lamellar constructions, (ii) covalent polymeric systems, (iii) polymer complexes created by aggregation process, (iv) specific disorder structures (Hench and West 1990). Generally, there are two sol-gel routes; particulate or colloidal route and the polymeric route. In the first route, *sols* are scattering of colloidal and non-polymeric particles in a liquid have radius of 0.5–50 nm. When the gel is formed the colloidal particles are connected through each other with van-der walls forces. The second route of the process involves the solution of polymeric molecules with diameter size less than 1 nm. In this case, the gel is formed due to covalent forces between the molecules.

In this process, frequently utilized precursor materials are metal chlorides, metal nitrates, and alkoxides. There are several hydrolysis and polycondensation reactions of the precursors which makes the development of sol-gel is a bit difficult process

(Zhong 2012). Gel is liquid, but its cross-linked network gives it a solid-like nature. The liquid held in the network of gel influence the pH value of liquid phase after aging and thermal process. Hydrolysis process decides about the capability of the process to obtain the required sol-gel. Thus, water or aqueous solutions are important gelating agents making this synthesis process environment-friendly. The sol is an important parameter to form thin films by spreading it onto a substance through dip coating or spin coating. The quality and morphology of the films can be controlled by adjusting the concentration of sol, spin speed in spin coating, pH value, post-thermal process and capping agents. The aging process is very effective to eliminate the organic solvents and support the synthesis of monophasic structures. A sufficient time is needed for aging process which directs the pH values to be changed affecting the gelation procedure, thus affecting the particle size and crystal structure.

Sol-gel is a wet chemical synthesis method which provides the feasibility to control the composition of nano materials. A flowchart diagram explaining the sol-gel synthesis is shown in Fig. 3.16. The sol-gel technique involves the two main steps: the first step comprises of hydrolysis and polymerization of alkoxides to prepare the gels, whereas the second step is sintering of amorphous colloidal into compact powder. After the hydrolysis process, suspension of very fine non-polymeric particles is formed in the solution which becomes a suspension of fine particles. These colloidal particles are linked to each other through van-der-walls forces. If hydrolysis and condensation processes occur to form gel then a solution of polymer molecules is formed, which are connected to each other through covalent bonding. In this method, when the particles achieve a significant size, the growth process is stopped and particles start to agglomerate with other NPs. During the pyrolysis process, the particles are formed by heating them with optimum temperature of 600 °C (Karami et al. 2010). Controlling the constraints for reaction gives the capability to manage the structure of created NPs. Therefore, adjustments in the reaction mechanism could considerably influence the structure of products. The synthesis of Cd-based nanomaterials with sol-gel method applying different experimental conditions is reviewed in Table 3.7.

The sol-gel technique is extensively used to synthesize the NPs, NRs etc. and also it provides the excellent means of coating to prepare the thin films. It is very easy to produce large area of coatings using this technique and it also provides low temperature synthesis of nanomaterials. From the past few years, this technique has

Table 3.6 Overview of mostly used polyols for Cd-based nanomaterials (Dong et al. 2015)

Polyol	Formula	Acronym	Boilling point (°C)
Ethylene glycol	HO–CH_2–OH	EG	197
Diethylene glycol	HO–CH_2–CH_2–O–CH_2–CH_2–OH	DEG	244
Triethylene glycol	HO–(CH_2–CH_2–O)$_2$–CH_2–CH_2–OH	TrEG	291
Tetraethylene glycol	HO–(CH_2–CH_2–O)$_3$–CH_2–CH_2–OH	TEG	314
Polyethylene glycol	HO–(CH_2–CH_2–O)$_n$–CH_2–CH_2–OH	PEG	>350

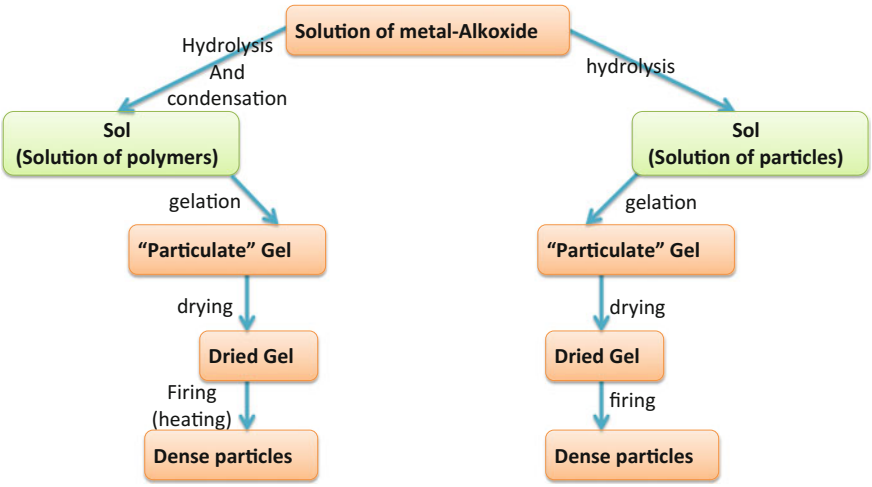

Fig. 3.16 Synthetic route of sol-gel mechanism

Table 3.7 Cd containing II–VI semiconductor nanomaterials prepared through sol-gel method using different synthesis conditions

Material	Solvent	Precursors	Drying temperature	Calcinations temperature	References
CdO–ZnO nanocomposites	Ethanol-water	Zinc nitrate, cadmium nitrate	80/4 h	600 °C	Karami et al. (2010)
CdO NPs	Distilled water	Cadmium nitrate tetra hydrate (Cd $(NO_3)_2 \cdot 4H_2O$) and aqueous ammonium hydroxide (NH_4OH)	50/4 h	600 °C	Vadgama et al. (2017)
CdO NPs	Starch and distilled water	Cadmium acetate equimolar ammonia	80/ overnight	600 °C	Kondawar et al. (2011)
CdO NPs	Double distilled (DD) water	Cadmium nitrate oxalic acid	70/18 h	400 °C/3 h	El Sayed et al. (2014)
CdS NPs embedded on SiO_2	Ethanol and double distilled water	TEOS ($Si(OC_2H_5)_4$) cadmium acetate and sodium sulfide (Na_2S) HCl as catalyst	–	RT/25 days	Hullavarad and Hullavarad (2007)
Ti-doped CdTe	Water	$Si(OC_2H_5)_4$, Cd $(CH_3COO)_2 . 2H_2O$, $Ti(CH_3COO)$	–	–	Li et al. (2004)

been utilized to synthesize the Cd–chalcogenides nanomaterials. It is a low temperature method providing smaller particle size, straightforward chemical reactions, morphological handling and improved uniformity. It presents high homogeneity along with tunable layer composition of the nanoscale materials. In this technique, the toxic materials are used for solvent systems and it is very responsive for hazardous atmospheric conditions.

CdO–ZnO nanocomposites have been prepared using sol-gel process; with control of morphology and size from gel system (Karami et al. 2010). This method is based on the polymeric network of polyvinyl alcohol (PVA) and forms the homogeneous nanocomposites. The chemical reaction of the process is given below:

$$Cd(NO_3)_2 \cdot Zn(NO_3)_2 \xrightarrow{heat} CdO \cdot ZnO + 4NO_2$$

The heat applied below 550 °C has not shown any considerable effects. On the other hand, at temperature above 600 °C larger particles were formed due to agglomeration. The finest sample showed a wonderful consistency in a linear cluster shape made up from numerous homogeneous spherical grains with size in range 70–90 nm (Fig. 3.17a). CdO has formed the core coated by ZnO layer. These nanocomposites showed great potential for detection of CO. In another study, CdO NPs synthesized using same method at ambient temperature has been carried out (Kondawar et al. 2011). After polymerization process, polyaniline (PANI) CdO nanocomposites have been obtained with cubic structure and size of 56 nm. The increased conductivity of these nanocomposites provided the benefits of low dimension and inorganic conduction for applications in nanoelectronics.

CdO nanomaterials have been prepared by sol-gel route and combined with PVC (El Sayed et al. 2014). The average size of these CdO NPs has been found about 70 nm. A high-quality dispersion of CdO NPs has been observed on the surface of

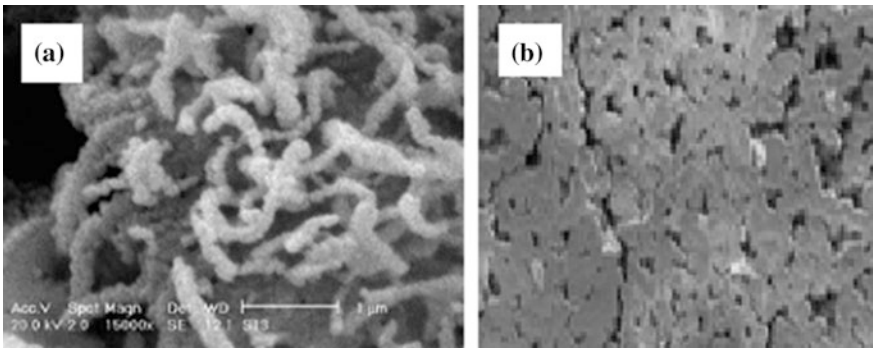

Fig. 3.17 **a** SEM image of CdO–ZnO nanocomposites prepared through sol-gel method under optimal conditions (Karami et al. 2010). © 2010 Springer Publishing. **b** FESEM images of nanostructured CdS thin films (Rathinamala et al. 2014). © 2014 Open Access

the PVC films. Dielectric and optical properties have been observed to increase by incorporation of CdO NPs into PVC matrix. These nanocomposites showed a red shift from 5.08 to 4.88 eV and can be applied in optical and electronic devices. In another study, CdO NPs prepared through sol-gel method have been characterized in detail (Vadgama et al. 2017). These spherical and thermally stable nanocrystalline have been found with cubic crystal structure and size ranging from 50 to 100 nm.

The crystals of CdTe doped with the silica glasses have been prepared with the help of so-gel method (Nogami et al. 1992). The gels have been prepared by the hydrolysis process of the complex compounds as $Si(OC_2H_5)_4$, $Cd(CH_3COO)_2 \cdot 2H_2O$. The cubic NCs of CdTe have been formed by heating the tellurium in hydrogen-nitrogen atmosphere from 350 to 600 °C. The characterization of the materials revealed the temperature dependence of the diameter of the crystals which increased from 4 to 9 nm by increasing the temperature. As a result, the absorption edge moved to the higher energy side by decreasing the size of the crystals. Glass-doped QDs have been prepared under the sol-gel process (Chia et al. 1997). The glasses of sodium borosilicate have been doped into CdTe QDs having size in the range of about 2.4–8.5 nm. Two methods have been established for the preparation of doped QDs. The first method involves usage of CdO-doped gel in methanol solution heated at 540 °C for 1–4 days or heating of the material at 570 °C for 6–12 h in inert atmosphere. The second method includes the direct formation at different temperatures under reducing environment. The result indicated the clear blue shift because of the quantum confinement which depends on the initial salt concentration and heating condition.

Chemically protected NPs of CdS have been synthesized via hydrolysis and polycondensation route of sol-gel method and then embedded in SiO_2 gel matrix (Hullavarad and Hullavarad 2007). The NPs incorporated into SiO_2 have been spin coated on substrate. The materials were obtained in the form of nanosheets and can be used as luminescent displays. This synthesis technique can be used to prepare the biocompatible materials with smaller size. In another study, NCs of CdS have been synthesized via sol-gel method (Skobeeva et al. 2008). The basic study of the reported work is the investigation of different technological factors such as the concentration of reagent and gelation effect on size distribution and crystal growth process. The obtained NCs have been found with a size ranging from 1.9 to 2.4 nm depending on the reagent concentration; increase in reagent concentration, decrease in particles size. The correlation was established between the photoluminescence and the dispersion in size. Nanocrystalline thin films of CdS have been fabricated by spin coating under sol-gel technique (Thambidurai et al. 2009). The annealing temperature produced the grain having size from 5 to 8.2 nm. The presence of quantum confinement due to small size of the particles has been observed and photoluminescence spectrum showed the yellow and green emission band.

The NPs of CdS semiconductor having the stability in silica matrix have been prepared via sol-gel process at room temperature (Anitha 2012). The prepared NPs were of 4 nm average size and exhibited blue shift in band gap. Sol-gel method has been used to synthesize the nanostructures of CdS, using cadmium nitrate and

thiourea as precursors (Rathinamala et al. 2014). CdS thin films have been deposited on the glass substrate and its structural, morphological and optical properties have been characterized using different techniques. The product material showed the noticeable size effects with aging of CdS sol whereas an increase in anealing temperature caused reduction of band gap. A homogeneous distribution of spherical-shaped NPs over the whole substrate was found (Fig. 3.17b). This study suggested the importance of aging time of starting solution to get the better structural properties in sol-gel method. In another study, CdS NPs prepared by sol-gel method showed a polycrystalline nature (Mahdi et al. 2017). CdS and Ag-doped CdS (Ag/CdS) NPs have been prepared through ultrasonic-assisted sol-gel method (Fard et al. 2016). The band gap of CdS was calculated 2.62 eV and Ag-doped CdS showed a reduction in band gap value by 0.16 eV.

Sol-gel method provides the convenient way to synthesis pure and doped NCs. The sol-gel technique has been used for addition of NCs of CdTe in the glass matrix to enhance luminescence properties of the material (Li and Murase 2004). The QY of 41% was observed and the obtained glass emitted various colors. A straight sol-gel route has been followed to form an extremely photoluminescent gel inserted with CdTe (Bu et al. 2015). Aminopropyltrimethoxysilane and citric acid (CA) have been used to prepare an inorganic–organic hybrid gel matrix by incorporating CdTe in it. The prepared sample showed exceptional transparency by inserting water-soluble CdTe QDs in gel and showed better photoluminescence efficiency (40%) by emitting light with a variety of colors.

References

Ahmadzadeh, S., Karimi, F., Atar, N., Sartori, E. R., Faghih-Mirzaei, E., & Afsharmanesh, E. (2017). Synthesis of CdO NPs using direct chemical precipitation method: Fabrication of novel voltammetric sensor for square wave voltammetry determination of chlorpromazine in pharmaceutical samples. *Inorganic and Nano-Metal Chemistry, 47*(3), 347–353.

Ahmed, H. H. (2017). Variation of the structural, optical and electrical properties of CBD CdO with processing temperature. *Materials Science in Semiconductor Processing, 66,* 215–222.

Al-Hussam, A. M., & Jassim, S. A. J. (2012). Synthesis, structure, and optical properties of CdS thin films NPs prepared by chemical bath technique. *Journal of the Association of Arab Universities for Basic and Applied Sciences, 11*(1), 27–31. doi:10.1016/j.jaubas.2011.10.001.

Aliofkhazraei, M. (2016). *Handbook of NPs*. Springer International Publishing: Imprint: Springer.

Anderson, M. A., Gorer, S., & Penner, R. M. (1997). A hybrid electrochemical/chemical synthesis of supported, luminescent cadmium sulfide NCs. *The Journal of Physical Chemistry B, 101* (31), 5895–5899.

Anitha, A. (2012). Surface sol-gel synthesis of cadmium sulfide fine particles in silica matrix. *Journal of Research in Nanobiotechnology, 1,* 14–18.

Arbuj, S. S., Bhalerao, S. R., Rane, S. B., Mulik, U. P., & Amalnerkar, D. P. (2013). Solvothermal synthesis of one dimensional copper doped cadmium sulphide NRs and their photocatalytic performance. *Journal of Nanoengineering and Nanomanufacturing, 3*(2), 107–113.

Arellano, I. H. J., Mangadlao, J., Ramiro, I. B., & Suazo, K. F. (2010). 3-component low temperature solvothermal synthesis of colloidal cadmium sulfide QDs. *Materials Letters, 64* (6), 785–788.

Arnepalli, R., & Dutta, V. (2005). Synthesis of mercury cadmium telluride NPs by solvothermal method. *MRS Online Proceedings Library Archive*, 878.

Ashith, V. K., & Rao, K. G. (2016). A study of microstructural properties and quantum size effect in SILAR deposited nano-crystalline CdS thin films. *Thin Solid Films, 616,* 197–203.

Asmial, R. A., Al-Samarai, A. M. E., Mohmed, S. J., & Ahmed, H. H. (2012). Characteristics of nanostructured CdO Films Prepared by chemical bath deposition technique. *International Journal of Modern Physics B, 26*(24), 1250135.

Aubert, T., Soenen, S. J., Wassmuth, D., Cirillo, M., Van Deun, R., Braeckmans, K., et al. (2014). Bright and stable CdSe/CdS@ SiO_2 NPs suitable for long-term cell labeling. *ACS Applied Materials & Interfaces, 6*(14), 11714–11723.

Balachandran, S., Praveen, S. G., Velmurugan, R., & Swaminathan, M. (2014). Facile fabrication of highly efficient, reusable heterostructured Ag–ZnO–CdO and its twin applications of dye degradation under natural sunlight and self-cleaning. *RSC Advances, 4*(9), 4353–4362.

Barve, A. K., Gadegone, S. M., Lanjewar, M. R., & Lanjewar, R. B. (2014). Synthesis and characterization of CdO nanomaterial and their photocatalyticactivity. *International Journal on Recent and Innovation Trends in Computing and Communication, 2,* 2806–2810.

Bensebaa F (2012) *Nanoparticle technologies: From lab to market* (Vol. 19). London: Academic Press.

Borse, V., Sadawana, M., & Srivastava, R. (2016, April). CdTe QDs: Aqueous phase synthesis, stability studies and protein conjugation for development of biosensors. In *SPIE Photonics Europe* (pp. 988423–988423). International Society for Optics and Photonics.

Bu, H. B., Watanabe, T., Hizume, M., Takagi, T., Sobue, S., Kawai, S., … & Kim, D. (2015). Preparation of highly luminescent hybrid gel incorporating NAC-capped CdTe QDs through sol–gel processing. *Materials Research Express*, *2*(3), 036202.

Byrappa, K., & Yoshimura, M. (2012). *Handbook of hydrothermal technology*. Norwich: William Andrew.

Cardoso, J., GomezDaza, O., Ixtlilco, L., Nair, M. T. S., & Nair, P. K. (2001). Conductive copper sulfide thin films on polyimide foils. *Semiconductor Science and Technology, 16*(2), 123.

Chaguetmi, S., Mammeri, F., Pasut, M., Nowak, S., Lecoq, H., Decorse, P., … & Ammar, S. (2013). Synergetic effect of CdS QDs and TiO_2 nanofibers for photoelectrochemical hydrogen generation. *Journal of Nanoparticle Research*, *15*(12), 2140. doi:10.1007/s11051-013-2140-1.

Chalapathi, G. V., Thaidun, M., Subramanyam, D., Rao, B. S., Balanarayana, C., & Kumar, B. R. (2015). Synthesis and characterization of fe doped Cdse NPs for spintronic devices. *Chalcogenide Letters, 12*(4), 181–190.

Chandra, P. P., Mukherjee, A., & Mitra, P. (2014). Synthesis of nanocrystalline CdS by SILAR and their characterization. *Journal of Materials*, 138163.

Chaudhari, K. B., Gosavi, N. M., Deshpande, N. G., & Gosavi, S. R. (2016). Chemical synthesis and characterization of CdSe thin films deposited by SILAR technique for optoelectronic applications. *Journal of Science: Advanced Materials and Devices, 1*(4), 476–481.

Cheng, C., Xu, F., & Gu, H. (2011). Facile synthesis and morphology evolution of magnetic iron oxide NPs in different polyol processes. *New Journal of Chemistry, 35*(5), 1072–1079. doi:10.1039/C0NJ00986E.

Chen, W., Grouquist, D., & Roark, J. (2002). Voltage tunable electroluminescence of CdTe nanoparticle light-emitting diodes. *Journal of Nanoscience and Nanotechnology, 2*(1), 47–53.

Chia, C., Kao, Y. H., Xu, Y., & Mackenzie, J. D. (1997, October). Cadmium telluride quantum dot-doped glass by the sol-gel technique. In *Proceedind SPIE—The International Society* for *Optical Engineering* (Vol. 3136, pp. 337–347).

Chinnu, M. K., Saravanan, L., Jayavel, R., Raghavan, C. M., Anand, K. V., Kumar, R. M., et al. (2011). Synthesis and characterization of hexamethylene tetramine (HMTA) capped CdS NPs by hydrothermal method. *International Journal of Nanoscience, 10*(03), 441–445.

Choi, Y., Seol, M., Kim, W., & Yong, K. (2014). Chemical bath deposition of stoichiometric CdSe QDs for efficient quantum-dot-sensitized solar cell application. *The Journal of Physical Chemistry C, 118*(11), 5664–5670.

Chopra, K. L., Kainthla, R. C., Pandya, D. K., & Thakoor, A. P. (1982). Chemical solution deposition of inorganic films. *Physics of Thin Films, 12,* 167–235.

Dangi, D., & Dhar, R. (2016). Study of non linear optical properties of Fe doped CdSe NPs. *Journal of Integrated Science and Technology, 4*(1), 25–28.

Dariani, R. S., & Emami, Z. (2015). Structural and optical studies of CdS and CdS: Ag nano needles prepared by a SILAR method. *Ceramics International, 41*(7), 8820–8827.

Dariani, R. S., & Salehi, F. (2016). Fabrication of CdS NWs with increasing anionic precursor by SILAR method. *Materials Research Express, 3*(5), 055018.

Darwish, M., Mohammadi, A., & Assi, N. (2016). Microwave-assisted polyol synthesis and characterization of pvp-capped cds NPs for the photocatalytic degradation of tartrazine. *Materials Research Bulletin, 74,* 387–396.

Datta, A., Kar, S., Ghatak, J., & Chaudhuri, S. (2007). Solvothermal synthesis of CdS NRs: Role of basic experimental parameters. *Journal of Nanoscience and Nanotechnology, 7*(2), 677–688.

Demazeau, G. (2008). Solvothermal reactions: An original route for the synthesis of novel materials. *Journal of Materials Science, 43*(7), 2104–2114.

Devi, R. A., Latha, M., Velumani, S., Oza, G., Reyes-Figueroa, P., Rohini, M.,… & Yi, J. (2015). Synthesis and characterization of cadmium sulfide NPs by chemical precipitation method. *Journal of nanoscience and nanotechnology*, *15*(11), 8434–8439.

Dhand, C., Dwivedi, N., Loh, X. J., Ying, A. N. J., Verma, N. K., Beuerman, R. W., … & Ramakrishna, S. (2015). Methods and strategies for the synthesis of diverse NPs and their applications: a comprehensive overview. *RSC Advances*, *5*(127), 105003–105037.

Dhawale, D. S., More, A. M., Latthe, S. S., Rajpure, K. Y., & Lokhande, C. D. (2008). Room temperature synthesis and characterization of CdO NWs by chemical bath deposition (CBD) method. *Applied Surface Science, 254*(11), 3269–3273.

Dong, C. Z., Zhang, L. F., Chen, S., Zhang, M. X., Feng, L., Cui, Z. M., & Zhang, Q. J. (2013). Hollow structure of CdSe by W/O microemulsion method. In *Advanced Materials Research* (Vol. 652, pp. 215–218). Zürich: Trans Tech Publications.

Dong, H., Chen, Y. C., & Feldmann, C. (2015). Polyol synthesis of NPs: Status and options regarding metals, oxides, chalcogenides, and non-metal elements. *Green Chemistry, 17*(8), 4107–4132.

Dumbrava, A., Badea, C., Prodan, G., & Ciupina, V. (2010). Synthesis and characterization of cadmium sulfide obtained at room temperature. *Chalcogenide Lett, 7*(2), 111–118.

Elavarthi, P., Kumar, A. A., Murali, G., Reddy, D. A., & Gunasekhar, K. R. (2016). Room temperature ferromagnetism and white light emissive CdS: Cr NPs synthesized by chemical co-precipitation method. *Journal of Alloys and Compounds, 656,* 510–517.

EL-Hefnawy, M. E. (2012). Water in olive oil surfactantless microemulsions as medium for CdS NPs synthesis. *Modern Applied Science, 6*(4), 101.

El Sayed, A. M., El-Sayed, S., Morsi, W. M., Mahrous, S., & Hassen, A. (2014). Synthesis, characterization, optical, and dielectric properties of polyvinyl chloride/cadmium oxide nanocomposite films. *Polymer Composites, 35*(9), 1842–1851. doi:10.1002/pc.22839.

Erenturk, B., Gurbuz, S., Corbett, R. E., Claiborne, S. A. M., Krizan, J., Venkataraman, D., et al. (2011). Formation of crystalline cadmium selenide NWs. *Chemistry of Materials, 23*(14), 3371–3376.

Ertis, I. F., & Boz, I. (2016). Synthesis and characterization of metal-doped (Ni Co, Ce, Sb) CdS catalysts and their use in methylene blue degradation under visible light irradiation. *Modern Research in Catalysis, 6*(01), 1.

Fard, N. E., Fazaeli, R., & Ghiasi, R. (2016). Band gap energies and photocatalytic properties of CdS and Ag/CdS NPs for azo dye degradation. *Chemical Engineering and Technology, 39*(1), 149–157. doi:10.1002/ceat.201500116.

Feldmann, C., & Metzmacher, C. (2001). Polyol mediated synthesis of nanoscale MS particles (M=Zn, Cd, Hg). *Journal of Materials Chemistry, 11*(10), 2603–2606. doi:10.1039/B103167H
.

Feng, Z., Zhang, Q., Lin, L., Guo, H., Zhou, J., & Lin, Z. (2010). ⟨0001⟩-Preferential growth of CdSe NWs on conducting glass: Template-free electrodeposition and application in photovoltaics. *Chemistry of Materials, 22*(9), 2705–2710.

Fomanyuk, S. S., Asaula, V. N., Kolbasov, G. Y., & Mirnaya, T. A. (2016). Electrochemical synthesis and optical properties of ultra-fine CdSe NPs. *Journal of Nanostructure in Chemistry, 6*(4), 289.

Gabriel, T., Nandhakumar, I. S., & Attard, G. S. (2002). Electrochemical synthesis of nanostructured tellurium films. *Electrochemistry Communications, 4*(8), 610–612.

Ganjiani, Z., Jamali-Sheini, F., & Yousefi, R. (2016). Electrochemical synthesis and physical properties of Sn-doped CdO nanostructures. *Superlattices and Microstructures, 100,* 988–996.

Gao, G., Xi, Q., Zhou, H., Zhao, Y., Wu, C., Wang, L., … & Xu, J. (2017). Selectivity of quantum dot sensitized ZnO nanotube arrays for improved photocatalytic activity. *Physical Chemistry Chemical Physics*, *19*(18), 11366–11372. doi:10.1039/C7CP01383C.

Ghoshal, T., Biswas, S., Nambissan, P. M. G., Majumdar, G., & De, S. K. (2009). Cadmium oxide octahedrons and NWs on the micro-octahedrons: a simple solvothermal synthesis. *Crystal Growth & Design, 9*(3), 1287–1292.

Gorer, S., & Hodes, G. (1994). Quantum size effects in the study of chemical solution deposition mechanisms of semiconductor films. *The Journal of Physical Chemistry, 98*(20), 5338–5346.

Grozdanov, I., Barlingay, C. K., Dey, S. K., Ristov, M., & Najdoski, M. (1994). Experimental study of the copper thiosulfate system with respect to thin-film deposition. *Thin Solid Films, 250*(1–2), 67–71.

Gubur, H. M., Septekin, F., & Alpdogan, S. (2015). CdSe NWs grown by using chemical bath deposition. *Journal of the Korean Physical Society, 67*(7), 1222–1227. doi:10.3938/jkps.67.1222.

Guleria, A., Singh, A. K., Rath, M. C., & Adhikari, S. (2015). Electron beam induced and microemulsion templated synthesis of CdSe QDs: Tunable broadband emission and charge carrier recombination dynamics. *Materials Research Express, 2*(4), 045006.

Guleria, A., Singh, S., Rath, M. C., Singh, A. K., Adhikari, S., & Sarkar, S. K. (2012). Tuning of photoluminescence in cadmium selenide NPs grown in CTAB based quaternary water-in-oil microemulsions. *Journal of Luminescence, 132*(3), 652–658.

Guo, Y., Wang, J., Yang, L., Zhang, J., Jiang, K., Li, W., … & Jiang, L. (2011). Facile additive-free solvothermal synthesis of cadmium sulfide flower-like three dimensional assemblies with unique optical properties and photocatalytic activity. *CrystEngComm*, *13*(16), 5045–5048.

Gupta, A. K., & Kripal, R. (2012). EPR and photoluminescence properties of Mn^{2+} doped CdS NPs synthesized via co-precipitation method. *Spectrochimica Acta Part A: Molecular and Biomolecular Spectroscopy, 96,* 626–631.

Hao, E., Sun, H., Zhou, Z., Liu, J., Yang, B., & Shen, J. (1999). Synthesis and optical properties of CdSe and CdSe/CdS NPs. *Chemistry of Materials, 11*(11), 3096–3102.

Hayashi, H., & Hakuta, Y. (2010). Hydrothermal synthesis of metal oxide NPs in supercritical water. *Materials, 3*(7), 3794–3817.

Haydous, F., & Halaoui, L. (2014). Quantum-confined CdTe films deposited by SILAR and their photoelectrochemical stability in the presence of Se_2–as a hole scavenger. *The Journal of Physical Chemistry C, 118*(32), 18334–18342.

Hench, L. L., & West, J. K. (1990). The sol-gel process. *Chemical Reviews, 90*(1), 33–72.

Hiie, J., Dedova, T., Valdna, V., & Muska, K. (2006). Comparative study of nano-structured CdS thin films prepared by CBD and spray pyrolysis: annealing effect. *Thin Solid Films, 511,* 443–447. doi:10.1016/j.tsf.2005.11.070.

Hirai, T., Sato, H., & Komasawa, I. (1994). Mechanism of formation of CdS and ZnS ultrafine particles in reverse micelles. *Industrial and Engineering Chemistry Research, 33*(12), 3262–3266.

Hodes, G. (2002). *Chemical solution deposition of semiconductor films*. Boca Raton: CRC Press.

Holmes, J. D., Bhargava, P. A., Korgel, B. A., & Johnston, K. P. (1999). Synthesis of cadmium sulfide Q particles in water-in-CO_2 microemulsions. *Langmuir, 15*(20), 6613–6615.

Hone, F. G., Ampong, F. K., Abza, T., Nkrumah, I., Nkum, R. K., & Boakye, F. (2015). Synthesis and characterization of CdSe nanocrystalline thin film by chemical bath deposition technique. *International Journal of Thin Films Science and Technology, 4*(2), 69–74.

Hou, T. C., Yang, Y., Lin, Z. H., Ding, Y., Park, C., Pradel, K. C., … & Wang, Z. L. (2013). Nanogenerator based on zinc blende CdTe micro/NWs. *Nano Energy*, *2*(3), 387–393.

Hu, H., & Nair, P. K. (1996). Electrical and optical properties of poly (methyl methacrylate) sheets coated with chemically deposited CuS thin films. *Surface and Coatings Technology, 81*(2–3), 183–189.

Hullavarad, N. V., & Hullavarad, S. S. (2007). Synthesis and characterization of monodispersed CdS NPs in SiO_2 fibers by sol–gel method. *Photonics and Nanostructures-Fundamentals and Applications*, *5*(4), 156–163.

Ismail, R. A., Ahmed, H. H., Al-Samarai, A. M. E., & Mohmed, S. J. (2014). Effect of pH on the structural and optical properties of nanostructured CdO films grown by chemical bath deposition technique. *Micro & Nano Letters, 9*(12), 935–939.

Jain, K., Srivastava, V., & Chouksey, A. (2009). Synthesis and optical properties of CdTe NCs with improved optical properties. *Indian Journal of Engineering & Materials Sciences,* 16, 188–192

Jia, Z., Tang, Y., Luo, L., & Li, B. (2008). Shape-controlled synthesis of single-crystalline $CdCO_3$ and corresponding porous CdO nanostructures. *Crystal Growth and Design, 8*(7), 2116–2120.

Jiang, L., & Zhu, Y. J. (2010). A general solvothermal route to the synthesis of CoTe, Ag_2Te/Ag, and CdTe nanostructures with varied morphologies. *European Journal of Inorganic Chemistry, 2010*(8), 1238–1243.

Jiang, L., Zhu, Y. J., & Cui, J. B. (2010). Nanostructures of metal tellurides (PbTe, CdTe, $CoTe_2$, $Bi2Te_3$, and Cu_7Te_4) with various morphologies: A general solvothermal synthesis and optical properties. *European Journal of Inorganic Chemistry, 2010*(19), 3005–3011.

Jing, L., Yang, C., Qiao, R., Niu, M., Du, M., Wang, D., et al. (2009). Highly fluorescent CdTe@ SiO_2 particles prepared via reverse microemulsion method. *Chemistry of Materials, 22*(2), 420–427.

Jothi, N. N., Gunaseelan, R., Raj, T. M., & Sagayaraj, P. (2012). Investigation on mild condition preparation and structural, optical and thermal properties of PVP capped CdS NPs. *Archives of Applied Science Research, 4,* 1723–1730.

Kale, R. B., Sartale, S. D., Chougule, B. K., & Lokhande, C. D. (2004). Growth and characterization of nanocrystalline CdSe thin films deposited by the successive ionic layer adsorption and reaction method. *Semiconductor Science and Technology, 19*(8), 980.

Kalhori, H., Irajizad, A., Azarian, A., & Ashiri, R. (2015). Synthesis and characterization of electrochemically grown CdSe NWs with enhanced photoconductivity. *Journal of Materials Science: Materials in Electronics, 26*(3), 1395–1402.

Kalska-Szostko, B. (2012). Electrochemical Methods in nanomaterials preparation. In *Recent Trend in Electrochemical Science and Technology*. InTech.

Kang, M. (2003). Synthesis of Fe/TiO_2 photocatalyst with nanometer size by solvothermal method and the effect of H_2O addition on structural stability and photodecomposition of methanol. *Journal of Molecular Catalysis A: Chemical, 197*(1), 173–183.

Karami, H., & Kaboli, A. (2010). Pulsed current electrochemical synthesis of cadmium sulfide nanofibers. *International Journal of Electrochemical Science, 5,* 706–719.

Karami, H., Aminifar, A., Tavallali, H., & Namdar, Z. A. (2010). PVA-based sol–gel synthesis and characterization of CdO–ZnO nanocomposite. *Journal of Cluster Science, 21*(1), 1–9.

Kawar, S. S. (2012). Development of nanostructured Cadmium Oxide (CdO) thin films. *International Journal of Chemical and Physical Sciences, 1*(1), 11–14.

Khalili, E., & Hassanzadeh-Tabrizi, S. A. (2017). ZnO–CdO nanocomposite: Microemulsion synthesis and dye removal ability. *Journal of Sol-Gel Science and Technology*, *81*(2), 475–482. doi:10.1007/s10971-016-4211-0.

Khatei, J., & Koteswara Rao, K. S. R. (2012, July). Temperature dependent photoluminescence studies in Hg 0.2 Cd 0.8 Te NRs synthesized by solvothermal method. In *AIP Conference Proceedings* (Vol. 1461, No. 1, pp. 349–352). AIP.

Khiew, P. S., Huang, N. M., Radiman, S., & Ahmad, M. S. (2004). Synthesis and characterization of conducting polyaniline-coated cadmium sulphide nanocomposites in reverse microemulsion. *Materials Letters, 58*(3), 516–521.

Kim, W., Baek, M., & Yong, K. (2016). Fabrication of ZnO/CdS, ZnO/CdO core/shell nanorod arrays and investigation of their ethanol gas sensing properties. *Sensors and Actuators B: Chemical, 223,* 599–605.

Kondawar, S., Mahore, R., Dahegaonkar, A., & Agrawal, S. (2011). Electrical conductivity of cadmium oxide NPs embedded polyaniline nanocomposites. *Advances in Applied Science Research, 2*(4), 401–406.

Kumar, A. A., Kumar, A., Quamara, J. K., & Priya, S. (2014). Fe (III) Induced structural, optical, magnetic and electrical behavior of hydrothermally synthesized polyvinyl pyrrolidone capped CdS NPS. *Chalcogenide Letters, 11*(8), 381–388

Kumar, R., Sharma, A., Parmar, R., Dahiya, S., & Kishor, N. (2016, May). To study the effect of doping concentration of silver on structural and optical properties of cadmium oxide (CdO) nanostructure. In *AIP Conference Proceedings* (Vol. 1728, No. 1, p. 020321). AIP Publishing, Melville.

Kumar, S., & Sharma, J. K. (2016). Stable phase CdS NPs for optoelectronics: a study on surface morphology, structural and optical characterization. *Materials Science-Poland, 34*(2), 368–373.

Kumar, V. N., Suryakarthick, R., Karuppusamy, S., Gupta, M., Hayakawa, Y., & Gopalakrishnan, R. (2015). Effect of precursor concentration on the properties and tuning of conductivity between p-type and n-type $Cu_{1-X}Cd_XS_2$ thin films deposited by a single step solution process as a novel material for photovoltaic applications. *RSC Advances, 5*(29), 23015–23021.

Kunita, M. H., Girotto, E. M., Radovanovic, E., Gonçalves, M. C., Ferreira, O. P., Muniz, E. C., et al. (2002). Deposition of copper sulfide on modified low-density polyethylene surface: Morphology and electrical characterization. *Applied Surface Science, 202*(3), 223–231.

Lemke, K., & Koetz, J. (2012). Polycation-capped CdS QDs synthesized in reverse microemulsions. *Journal of Nanomaterials, 2012,* 16.

Li, C., & Murase, N. (2004). Synthesis of highly luminescent glasses incorporating CdTe NCs through Sol–Gel processing. *Langmuir, 20*(1), 1–4. doi:10.1021/la035546o.

Li, J., Yang, T., Chan, W. H., Choi, M. M., & Zhao, D. (2013). Synthesis of high-quality N-Acetyl-L-Cysteine-capped CdTe QDs by hydrothermal route and the characterization through MALDI-TOF mass spectrometry. *The Journal of Physical Chemistry C, 117*(37), 19175–19181.

Li, J. J., Wang, Y. A., Guo, W., Keay, J. C., Mishima, T. D., Johnson, M. B., et al. (2003). Large-scale synthesis of nearly monodisperse CdSe/CdS core/shell NCs using air-stable reagents via successive ion layer adsorption and reaction. *Journal of the American Chemical Society, 125*(41), 12567–12575.

Li, Y., Hu, Y., Peng, S., Lu, G., & Li, S. (2009). Synthesis of CdS NRs by an ethylenediamine assisted hydrothermal method for photocatalytic hydrogen evolution. *The Journal of Physical Chemistry C, 113*(21), 9352–9358.

Li, Y., Huang, F., Zhang, Q., & Gu, Z. (2000). Solvothermal synthesis of nanocrystalline cadmium sulfide. *Journal of Materials Science, 35*(23), 5933–5937.

Li, Z., Zhang, J., Du, J., Mu, T., Liu, Z., Chen, J., et al. (2004). Preparation of cadmium sulfide/poly (methyl methacrylate) composites by precipitation with compressed CO_2. *Journal of Applied Polymer Science, 94*(4), 1643–1648.

Liang, Y. C., & Lung, T. W. (2016). Growth of hydrothermally derived CdS-based nanostructures with various crystal features and photoactivated properties. *Nanoscale Research Letters, 11*(1), 264.

Liu, J., & Li, X. (2014). Hydrothermal synthesis of CdTe QDs–TiO 2–graphene hybrid. *Physics Letters A, 378*(4), 405–407.

Liu, Z. Q., Guo, R., Li, G. R., Bu, Q., Zhao, W. X., & Tong, Y. X. (2012). Facile electrodeposition of large-area CdO and $Cd_{1-x}Co_xO$ curved NWs. *Electrochimica Acta, 59,* 449–454.

Liyanage, W. P., & Nath, M. (2016). CdS–CdTe heterojunction nanotube arrays for efficient solar energy conversion. *Journal of Materials Chemistry A, 4*(38), 14637–14648. doi:10.1039/C6TA03572H.

Ma, L. L., Sun, H. Z., Zhang, Y. G., Lin, Y. L., Li, J. L., Wang, E. K., … & Wang, J. B. (2008). Preparation, characterization and photocatalytic properties of CdS NPs dotted on the surface of carbon NTs. *Nanotechnology*, *19*(11), 115709.

Mahdi, H. S., Parveen, A., Agrawal, S., & Azam, A. (2017, May). Microstructural and optical properties of sol gel synthesized CdS nano particles using CTAB as a surfactant. In *AIP Conference Proceedings* (Vol. 1832, No. 1, p. 050012). AIP Publishing, Melville.

Mahdi, M. A., Hassan, J. J., Ng, S. S., & Hassan, Z. (2013). High-quality ZnCdS nanosheets prepared using solvothermal synthesis. *Journal of Nanoscience*, *2013*(897638), 1–6

Majid, A., Arshad, H., & Murtaza, S. (2015). Synthesis and characterization of Cr doped CdSe NPs. *Superlattices and Microstructures, 85,* 620–623.

Majid, A., Tanveer, M., Rana, U. A., Khan, S. U. D., & Kousar, S. (2016). Facile synthesis of Mn-doped CdTe NPs: Structural and magnetic properties. *Journal of Superconductivity and Novel Magnetism, 10*(29), 2615–2619.

Malik, M. A., Wani, M. Y., & Hashim, M. A. (2012). Microemulsion method: A novel route to synthesize organic and inorganic nanomaterials: 1st Nano Update. *Arabian journal of Chemistry, 5*(4), 397–417.

Mammadov, M. N., Aliyev, A. S., & Elrouby, M. (2012). Electrodeposition of cadmium sulfide. *International Journal of Thin Films Science and Technology, 1*(2), 43–53.

Manikandan, K., Dilip, C. S., Mani, P., & Prince, J. J. (2015). Deposition and characterization of CdS nano thin film with complexing agent triethanolamine. *American Journal of Engineering and Applied Sciences, 8*(3), 318.

Maryam, M., & Hanish, H. (2016). Synthesis and growth mechanism of CdO NPs prepared from thermal decomposition of $CdSO_3$ NRs. *Journal of Materials Science: Materials in Electronics, 27,* 6480–6487.

Miles, M. H., & McEwan, W. S. (1972). Electrochemical preparation of cadmium and mercury tellurides. *Journal of the Electrochemical Society, 119*(9), 1188–1190.

Montes, L., Muller, F., Gaspard, F., & Hérino, R. (1997). Investigation on the electrochemical deposition of cadmium telluride in porous silicon. *Thin Solid Films, 297*(1), 35–38.

Mugle, D., & Jadhav, G. (2016, May). Short review on chemical bath deposition of thin film and characterization. In *AIP Conference Proceedings* (Vol. 1728, No. 1, p. 020597). AIP Publishing, Melville.

Muruganandam, S., Anbalagan, G., & Murugadoss, G. (2017). Structural, electrochemical and magnetic properties of codoped (Cu, Mn) CdS NPs with surfactant PVP. *Optik-International Journal for Light and Electron Optics, 131,* 826–837.

Mustafa, M. K., Iqbal, Y., Majeed, U., & Sahdan, M. Z. (2017, January). Effect of precursor's concentration on structure and morphology of ZnO NRs synthesized through hydrothermal method on gold surface. In *AIP Conference Proceedings* (Vol. 1788, No. 1, p. 030120). AIP Publishing, Melville.

Nair, P. K., Cardoso, J., Daza, O. G., & Nair, M. T. S. (2001). Polyethersulfone foils as stable transparent substrates for conductive copper sulfide thin film coatings. *Thin Solid Films, 401* (1), 243–250.

Němec, P., Šimurda, M., Němec, I., Formanek, P., Němcová, Y., Sprinzl, D., … & Malý, P. (2008). Chemical bath deposition of CdSe and CdS nanocrystalline films: tailoring of morphology, optical properties and carrier dynamics. *physica status solidi (a)*, *205*(10), 2324–2329. doi:10.1002/pssa.200779414.

Nicolau, Y. F., & Menard, J. C. (1988). Solution growth of ZnS, CdS and $Zn_{1-x}Cd_xS$ thin films by the successive ionic-layer adsorption and reaction process; growth mechanism. *Journal of Crystal Growth, 92*(1–2), 128–142.

Nogami, M., Nagasaka, K., & Suzuki, T. (1992). Sol-gel synthesis of cadmium telluride-microcrystal-doped silica glasses. *Journal of the American Ceramic Society, 75*(1), 220–223.

Nwanya, A. C., Chigbo, C., Ezugwu, S. C., Osuji, R. U., Malik, M., & Ezema, F. I. (2016). Transformation of cadmium hydroxide to cadmium oxide thin films synthesized by SILAR deposition process: Role of varying deposition cycles. *Journal of the Association of Arab Universities for Basic and Applied Sciences, 20,* 49–54.

Nwanya, A. C., Deshmukh, P. R., Osuji, R. U., Maaza, M., Lokhande, C. D., & Ezema, F. I. (2015). Synthesis, characterization and gas-sensing properties of SILAR deposited ZnO–CdO nano-composite thin film. *Sensors and Actuators B: Chemical, 206,* 671–678.

Olmos, J. G., Hernández, A. G. R., Cruz, A. L. L., Droog, T. M. P., Mendoza, C. V. V., Marquina, A. V., … & Fuentes, R. G. (2015). CBD Synthesis and characterization of CdSe nanostructured thin films. *ECS Transactions*, *64*(44), 29–33. doi:10.1149/06444.0029ecst.

Palchik, O., Kerner, R., Gedanken, A., Weiss, A. M., Slifkin, M. A., & Palchik, V. (2001). Microwave-assisted polyol method for the preparationof CdSe "nanoballs". *Journal of Materials Chemistry, 11*(3), 874–878.

Peng, X. S., Zhang, J., Wang, X. F., Wang, Y. W., Zhao, L. X., Meng, G. W., et al. (2001). Synthesis of highly ordered CdSe nanowire arrays embedded in anodic alumina membrane by electrodeposition in ammonia alkaline solution. *Chemical Physics Letters, 343*(5), 470–474.

Phuruangrat, A., Thongtem, T., & Thongtem, S. (2012). Solvothermal synthesis and optical properties of wurtzite-type Cds NRs. *Chalcogenide Letters, 9*(7), 315–319.

Raj, F. M., & Rajendran, A. J. (2015). Synthesis and characterization of cadmium sulfide NPs for the applications of dye sensitized solar cell. *International Journal of Innovative Research in Science, Engineering and Technology, 4*(1), 56–60.

Ramalingam, G., Melikechi, N., Christy, P. D., Selvakumar, S., & Sagayaraj, P. (2009). Structural and optical property studies of CdSe crystalline NRs synthesized by a solvothermal method. *Journal of Crystal Growth, 311*(11), 3138–3142.

Ramimoghadam, D., Bagheri, S., & Hamid, S. B. A. (2014). Progress in electrochemical synthesis of magnetic iron oxide NPs. *Journal of Magnetism and Magnetic Materials, 368,* 207–229.

Rao, B. S., Kumar, B. R., Reddy, V. R., Rao, T. S., & Chalapathi, G. V. (2011). Preparation and characterization of CdS NPs by chemical co-precipitation technique. *Chalcogenide Lett, 8*(3), 177–185.

Rathika Nath, G., & Rajesh, K. (2013). Synthesis an d study of cadmium sulphide NPs from thiocomplexes. *Annalen der Chemischen Forschung, 1*(3), 10–14.

Rathinamala, I., Pandiarajan, J., Jeyakumaran, N., & Prithivikumaran, N. (2014). Synthesis and physical properties of nanocrystalline CdS thin films-influence of sol aging time & annealing temperature. *International Journal of Thin Films Science and Technology, 3*(3), 113–120.

Ravichandran, A. T., Xavier, A. R., Pushpanathan, K., Nagabhushana, B. M., & Chandramohan, R. (2016). Structural and optical properties of Zn doped CdO NPs synthesized by chemical precipitation method. *Journal of Materials Science: Materials in Electronics, 27*(3), 2693.

Reddy, C. V., Vattikuti, S. P., & Shim, J. (2016). Synthesis, structural and optical properties of CdS NPs with enhanced photocatalytic activities by photodegradation of organic dye molecules. *Journal of Materials Science: Materials in Electronics, 27*(8), 7799–7808.

Ribeiro, R. T., Dias, J. M., Pereira, G. A., Freitas, D. V., Monteiro, M., Cabral Filho, P. E., … & Santos, B. S. (2013). Electrochemical synthetic route for preparation of CdTe QDs stabilized by positively or negatively charged ligands. *Green Chemistry*, *15*(4), 1061–1066.

Rocha, A. D., Sivry, Y., Gelabert, A., Beji, Z., Benedetti, M. F., Menguy, N., et al. (2015). The fate of polyol-made ZnO and CdS NPs in Seine River Water (Paris, France). *Journal of Nanoscience and Nanotechnology, 15*(5), 3900–3908.

Sahin, B., Bayansal, F., & Yüksel, M. (2014). Influence of manganese concentration and annealing temperatures on the physical properties of CdO films grown by the SILAR method. *Philosophical Magazine, 94*(9), 956–963.

Sahin, B., Bayansal, F., & Yüksel, M. (2015). A novel approach to enhancement of surface properties of CdO films by using surfactant: Dextrin. *Philosophical Magazine, 95*(34), 3888–3895.

Saikia, D., Gogoi, P. K., & Saikia, P. K. (2010). Structural and optical properties of nanostructured CdS thin films deposited at different preparative conditions. *Chalcogenide letters, 7*(5), 317–324.

Salavati-Niasari, M. (2011). *Synthesis of cadmium sulfide nanostructures by novel precursor* (Doctoral dissertation, Видавництво СумДУ).

Salavati-Niasari, M., Davar, F., & Loghman-Estarki, M. R. (2009). Long chain polymer assisted synthesis of flower-like cadmium sulfide NRs via hydrothermal process. *Journal of Alloys and Compounds, 481*(1), 776–780.

Salavati-Niasari, M., Esmaeili, E., & Davar, F. (2013). Synthesis and characterization of cadmium sulfide nanostructures by novel precursor via hydrothermal method. *Combinatorial Chemistry & High Throughput Screening, 16*(1), 47–56.

Salazar, R., Delamoreanu, A., Saidi, B., Lévy-Clément, C., & Ivanova, V. (2014). CdTe deposition by successive ionic layer adsorption and reaction (SILAR) technique onto ZnO NWs. *Physica Status Solidi (A), 211*(9), 2115–2120.

Sankapal, B. R., Mane, R. S., & Lokhande, C. D. (2000). Successive ionic layer adsorption and reaction (SILAR) method for the deposition of large area (~ 10 cm^2) tin disulfide (SnS_2) thin films. *Materials Research Bulletin, 35*(12), 2027–2035.

Saravanan, L., Pandurangan, A., & Jayavel, R. (2012). Synthesis and luminescence enhancement of cerium doped CdS NPs. *Materials Letters, 66*(1), 343–345.

Selvakumar, D., Tripathi, S. K., Singh, R., & Nasim, M. (2007). Solvo-thermal preparation of cadmium telluride NPs from a novel single source molecular precursor. *Chemistry Letters, 37*(1), 34–35.

Shahi, A. K., Pandey, B. K., Singh, B. P., & Gopal, R. (2016). Structural and optical properties of solvothermal synthesized nearly monodispersed CdSe NCs. *Advances in Natural Sciences: Nanoscience and Nanotechnology, 7*(3), 035010.

Shameem, A., Devendran, P., Siva, V., Raja, M., Bahadur, S. A., & Manikandan, A. (2017). Preparation and characterization studies of nanostructured CdO thin films by SILAR method for photocatalytic applications. *Journal of Inorganic and Organometallic Polymers and Materials, 27*(3), 692–699.

Shpaisman, N., Givan, U., & Patolsky, F. (2010). Electrochemical synthesis of morphology-controlled segmented CdSe NWs. *ACS Nano, 4*(4), 1901–1906.

Shuang, S., Xie, Z., & Zhang, Z. (2017). Enhanced photocatalytic properties of CdS NPs decorated α-Fe_2O_3 nanopillar arrays under visible light. *Journal of Colloid and Interface Science, 494,* 107–113.

Shukla, M., Kumari, S., Shukla, S., & Shukla, R. K. (2012). Potent antibacterial activity of nano CdO synthesized via microemulsion scheme. *Journal of Materials and Environmental Science, 3*(4), 678–685.

Singh, R. S., Bhushan, S., Singh, A. K., & Deo, S. R. (2011a). Characterization and optical properties of CdSe nano-crystalline thin films. *Digest Journal of Nanomaterials and Biostructures, 6*(2), 403.

Singh, S., Guleria, A., Singh, A. K., Rath, M. C., Adhikari, S., & Sarkar, S. K. (2013). Radiolytic synthesis and spectroscopic investigations of Cadmium Selenide QDs grown in cationic surfactant based quaternary water-in-oil microemulsions. *Journal of Colloid and Interface Science, 398,* 112–119.

Singh, T., Pandya, D. K., & Singh, R. (2011b). Electrochemical deposition and characterization of elongated CdO nanostructures. *Materials Science and Engineering B, 176*(12), 945–949.

Skobeeva, V. M., Smyntyna, V. A., Sviridova, O. I., Struts, D. A., & Tyurin, A. V. (2008). Optical properties of cadmium sulfide NCs obtained by the sol-gel method in gelatin. *Journal of Applied Spectroscopy, 75*(4), 576–582.

Song, J., Dai, Z., Guo, W., Li, Y., Wang, W., Li, N., et al. (2013). Preparation of CdTe/CdS/SiO_2 core/multishell structured composite NPs. *Journal of Nanoscience and Nanotechnology, 13* (10), 6924–6927.

Sun, J., Gao, M., & Feldmann, J. (2001). Electric field directed layer-by-layer assembly of highly fluorescent CdTe NPs. *Journal of Nanoscience and Nanotechnology, 1*(2), 133–136.

Tabatabaee, M., Mozafari, A. A., Ghassemzadeh, M., Nateghi, M. R., & Abedini, I. (2013). A simple method for synthesis of cadmium oxide NPs using polyethylene glycol. *Bulgarian Chemical Communications, 45,* 90–92.

Tadjarodi, A., Imani, M., Kerdari, H., Bijanzad, K., Khaledi, D., & Rad, M. (2014). Preparation of CdO rhombus-like nanostructure and its photocatalytic degradation of azo dyes from aqueous solution. *Nanomaterials and Nanotechnology, 4,* 16.

Tang, J. H., Xie, L., Zhang, B., Qiu, T., Qi, B., & Xie, H. P. (2012). Preparation of strongly fluorescent silica NPs of polyelectrolyte-protected cadmium telluride QDs and their application to cell toxicity and imaging. *Analytica Chimica Acta, 720,* 112–117.

Thambidurai, M., Murugan, N., Muthukumarasamy, N., Vasantha, S., Balasundaraprabhu, R., & Agilan, S. (2009). Preparation and characterization of nanocrystalline CdS thin films. *Chalcogenide Letters, 6*(4), 171–179.

Tian, Y., Zhang, Y., Lin, Y., Gao, K., Zhang, Y., Liu, K.,… & Xia, Y. (2013). Solution-processed efficient CdTe nanocrystal/CBD-CdS hetero-junction solar cells with ZnO interlayer. *Journal of nanoparticle research*, *15*(11), 2053. doi:10.1007/s11051-013-2053-z.

Tiwari, A. K., Verma, V. K., Jain, T. A., & Bajpai, P. K. (2013). Conclusive growth of CdTe NRs by solvothermal decomposition using single source precursors. *Soft Nanoscience Letters, 3* (03), 52.

Tojo, C., Blanco, M. C., & Lopez-Quintela, M. A. (1997). Preparation of NPs in microemulsions: A Monte Carlo study of the influence of the synthesis variables. *Langmuir, 13*(17), 4527–4534.

Vadgama, V. S., Vyas, R. P., Jogiya, B. V., & Joshi, M. J. (2017, May). Synthesis and characterization of CdO nano particles by the sol-gel method. In *AIP Conference Proceedings* (Vol. 1837, No. 1, p. 040016). AIP Publishing, Melville.

VanderHyde, C. A., Sartale, S. D., Patil, J. M., Ghoderao, K. P., Sawant, J. P., & Kale, R. B. (2015). Room temperature chemical bath deposition of cadmium selenide, cadmium sulfide and cadmium sulfoselenide thin films with novel nanostructures. *Solid State Sciences, 48,* 186–192. doi:10.1016/j.solidstatesciences.2015.08.007.

Veeranarayanan, S., Poulose, A. C., Mohamed, M. S., Nagaoka, Y., Iwai, S., Nakagame, Y., … & Kumar, D. S. (2012). Synthesis and application of luminescent single CdS quantum dot encapsulated silica NPs directed for precision optical bioimaging. *International journal of nanomedicine*, *7*, 3769.

Waghulade, R. B., Patil, P. P., & Pasricha, R. (2007). Synthesis and LPG sensing properties of nano-sized cadmium oxide. *Talanta, 72*(2), 594–599.

Wang, A., Zheng, Y., & Peng, F. (2014). Thickness-controllable silica coating of CdTe QDs by reverse microemulsion method for the application in the growth of rice. *Journal of Spectroscopy*, *2014*.

Wang, H., Guo, Z., & Du, F. (2006a). Solvothermal synthesis of CdSe NRs via DEA solution. *Materials Chemistry and Physics, 98*(2), 422–424.

Wang, H., Xi, Y. Y., Zhou, J. Z., & Lin, Z. H. (2012). Electrochemical synthesis of CdS NCs on a gold electrode modified with a p-Aminothiophenol Self-assembled monolayer. *Acta Physico-Chimica Sinica, 28*(6), 1398–1404.

Wang, Q., Pan, D., Jiang, S., Ji, X., An, L., & Jiang, B. (2006b). A solvothermal route to size-and shape-controlled CdSe and CdTe NCs. *Journal of Crystal Growth, 286*(1), 83–90.

Wang, T., Wang, J., Zhu, Y., Xue, F., Cao, J., & Qian, Y. (2010). Solvothermal synthesis and characterization of CdSe NCs with controllable phase and morphology. *Journal of Physics and Chemistry of Solids, 71*(7), 940–945.

Wang, X. F., Xu, J. J., & Chen, H. Y. (2008). Dendritic CdO nanomaterials prepared by electrochemical deposition and their electrogenerated chemiluminescence behaviors in aqueous systems. *The Journal of Physical Chemistry C, 112*(18), 7151–7157.

Wang, Y., Niu, S. H., Zhang, Z. J., Wang, H. T., Yuan, C. W., & Fu, D. G. (2007). Silica coating of water-soluble cdte/cds core-shell NCs by microemulsion method. *Chinese Journal of Chemical Physics, 20*(6), 685.

Wiley, B., Sun, Y., Mayers, B., & Xia, Y. (2005). Shape-controlled synthesis of metal nanostructures: The case of silver. *Chemistry-A European Journal, 11*(2), 454–463. doi:10.1002/chem.200400927.

Xi, L. F., & Lam, Y. M. (2007). Synthesis and characterization of CdSe NRs using a novel microemulsion method at moderate temperature. *Journal of Colloid and Interface Science, 316*(2), 771–778.

Xie, Z., Liu, X., Wang, W., Liu, C., Li, Z., & Zhang, Z. (2014). Enhanced photoelectrochemical properties of TiO_2 nanorod arrays decorated with CdS NPs. *Science and Technology of Advanced Materials, 15*(5), 055006.

Xu, D., Shi, X., Guo, G., Gui, L., & Tang, Y. (2000). Electrochemical preparation of CdSe nanowire arrays. *The Journal of Physical Chemistry B, 104*(21), 5061–5063.

Xu, R., Wang, Y., Jia, G., Xu, W., & Yin, D. (2007). Synthesis of zinc blende CdS nanocrystallites using 3-Mercaptopropionic acid as precursor by hydrothermal method. *Chemical Journal Of Chinese Universities-Chinese Edition, 28*(2), 217.

Yamamoto, T., Tanaka, K., Kubota, E., & Osakada, K. (1993). Deposition of copper sulfide on the surface of poly (ethylene terephthalate) and poly (vinyl alcohol) films in aqueous solution to give electrically conductive films. *Chemistry of Materials, 5*(9), 1352–1357.

Yang, J., Zang, C., Wang, G., Xu, G., & Cheng, X. (2010). Synthesis of CdSe microspheres via solvothermal process in a mixed solution. *Journal of Alloys and Compounds, 495*(1), 158–161.

Yang, R., Yan, Y., Mu, Y., Ji, W., Li, X., Zou, M., … & Jin, Q. (2006a). A rapid and facile method for hydrothermal synthesis of CdTe NCs under mild conditions. *Journal of nanoscience and nanotechnology*, *6*(1), 215–220.

Yang, Y. J., He, L. Y., & Xiang, H. (2006b). Electrochemical synthesis of free-standing CdS NPs in ethylene glycol. *Russian Journal of Electrochemistry, 42*(9), 954–958.

Yang, Y., & Gao, M. Y. (2005). Preparation of fluorescent SiO2 particles with single CdTe nanocrystal cores by the reverse microemulsion method. *Advanced Materials, 17*(19), 2354–2357.

Yin, S., Fujishiro, Y., Wu, J., Aki, M., & Sato, T. (2003). Synthesis and photocatalytic properties of fibrous titania by solvothermal reactions. *Journal of Materials Processing Technology, 137*(1), 45–48.

Yin, X. L., Li, L. L., Jiang, W. J., Zhang, Y., Zhang, X., Wan, L. J., et al. (2016). MoS_2/CdS nanosheets-on-nanorod heterostructure for highly efficient photocatalytic H_2 generation under visible light irradiation. *ACS Applied Materials & Interfaces, 8*(24), 15258–15266.

Yong, S. M., Muralidharan, P., Jo, S. H., & Kim, D. K. (2010). One-step hydrothermal synthesis of CdTe NWs with amorphous carbon sheaths. *Materials Letters, 64*(14), 1551–1554.

Yuan, D., Jing, L., Yao, W., & Li-Xing, L. (2012). Sacrifice-template synthesis of CdTe nanorod arrays in glycol via a solvothermal process. *Chinese Physics Letters, 29*(8), 086801.

Zang, J., Zhao, G., & Han, G. (2007). Preparation of CdS NPs by hydrothermal method in microemulsion. *Frontiers of Chemistry in China, 2*(1), 98–101.

Zhai, C., Zhang, H., Du, N., Chen, B., Huang, H., Wu, Y., et al. (2011). One-pot synthesis of biocompatible CdSe/CdS QDs and their applications as fluorescent biological labels. *Nanoscale Research Letters, 6*(1), 31. doi:10.1007/s11671-010-9774-z.

Zhang, H., Wang, L., Xiong, H., Hu, L., Yang, B., & Li, W. (2003). Hydrothermal synthesis for high-quality CdTe NCs. *Advanced Materials, 15*(20), 1712–1715.

Zhang, Q., Huang, F., & Li, Y. (2005). Cadmium sulfide NRs formed in microemulsions. *Colloids and Surfaces A: Physicochemical and Engineering Aspects, 257,* 497–501.

Zhao, A. W., Meng, G. W., Zhang, L. D., Gao, T., Sun, S. H., & Pang, Y. T. (2003). Electrochemical synthesis of ordered CdTe nanowire arrays. *Applied Physics A: Materials Science & Processing, 76*(4), 537–539.

Zhao, D., He, Z., Chan, W. H., & Choi, M. M. (2008). Synthesis and characterization of high-quality water-soluble near-infrared-emitting CdTe/CdS QDs capped by N-acetyl-L-cysteine via hydrothermal method. *The Journal of Physical Chemistry C, 113*(4), 1293–1300.

Zhong, W. H. (2012). *Nanoscience and nanomaterials: synthesis, manufacturing and industry impacts*. Lancaster: DEStech Publications, Inc.

Zhou, R., Niu, H., Zhang, Q., Uchaker, E., Guo, Z., Wan, L., … & Cao, G. (2015). Influence of deposition strategies on CdSe quantum dot-sensitized solar cells: A comparison between successive ionic layer adsorption and reaction and chemical bath deposition. *Journal of Materials Chemistry A*, *3*(23), 12539–12549.

Zhou, X., Li, Z., Li, Z., & Xu, S. (2008). Preparation and formation mechanism of CdS nano-films via chemical bath deposition. *Frontiers of Chemistry in China, 3*(1), 18–22.

Zhu, J., Si, S., Zuo, R., Duan, W., & Jiang, Y. (2010). A new two-step route to CdTe micrometer-scaled spindles and NRs. *Journal of Nanoscience and Nanotechnology, 10*(5), 3109–3111.

Zhu, Y., Mei, T., Wang, Y., & Qian, Y. (2011). Formation and morphology control of NPs via solution routes in an autoclave. *Journal of Materials Chemistry, 21*(31), 11457–11463.

Zia, R., Riaz, M., & Anjum, S. (2016). Study the effect of thiourea concentration on optical and structural properties of CdS-nanocrystalline thin films prepared by CBD technique. *Optik-International Journal for Light and Electron Optics, 127*(13), 5407–5412. doi:10.1016/j.ijleo.2016.02.081.

Zuala, L., & Agarwal, P. (2016). Thermal and structural studies of CdSe NRs synthesized by solvothermal process. *Physica Status Solidi (A)*, *213*(7), 1885–1893.

Chapter 4
Vapor Deposition Synthesis

Vapor deposition synthesis is a family of coating techniques which is utilized to fabricate thin films of a wide range of materials on any substrate. The vapor phase methods involve different strategies and working mechanisms on the basis of which two categories are made, physical vapor deposition (PVD) and chemical vapor deposition (CVD). In PVD, a pure material is evaporated by physical processes after which vapors condense on substrate without involving any chemical process. However, in CVD process, some unstable starting agent is used to chemically deposite the vapors of relevant material on substrat.

4.1 Thermal Evaporation Method

Thermal evaporation is a PVD technique which has been traditionally used to synthesize a large variety of thin films. Though with technological emergence of several other resourceful techniques, a part of research and industrial attention has been diverted away from thermal evaporation (TED) deposition but still it is a popular technique due to its simple approach.

The TED is carried out in vacuum where a solid is heated to such a high temperature (above its melting point) that it is evaporated and the stream of vapors hits the substrate available inside the chamber and condenses there in the form of thin film. The target solid is usually placed in the crucible situated at the bottom whereas the substrate holder is located inverted at the interior top of the chamber. The basic principle of TED mentioned above is technologically implemented to ensure control over desired parameters of the deposited films which include thickness, uniformity, adhesion, composition, crystal quality, grain size, morphology, etc.

There are two basic technological requirements to operate TED; production of sufficient vacuum in the chamber and provision of source of heating. Vacuum is

Abdul Majid and Maryam Bibi, *Cadmium based II-VI Semiconducting Nanomaterials*, Topics in Mining, Metallurgy and Materials Engineering,
https://doi.org/10.1007/978-3-319-68753-7_4

offered to facilitate the vapors to move towards the substrate without facing any collision in the way. For this purpose, air is evacuated using a vacuum pump (diffusion, cryo, or turbo) to reduce the pressure to a point such that mean free path exceeds the source–substrate separation. The heating source usually works on principle of Joule heating in the form of electrical resistive heating where a high resistance and high temperature heating element or filament made of refractory material (tungsten or molybdenum for example) is employed. When a significantly high current is passed through the heating element, electrical energy is dissipated to generate enormous amount of heat to melt and evaporate the source material placed in the crucible. The provision of continuous current is needed to keep the deposition process; therefore, rate of deposition is essentially current dependent. A typical diagram of vacuum thermal evaporation is sketched in Fig. 4.1.

An extension to TED is vacuum flash evaporation or discrete evaporation which offers evaporation of compounds or alloys whose components have different vapor pressures. In VFE, the particles of the multicomponent material randomly arrive into a preheated flash exchanger which provides an averaged and approximately same flux to all constituents for simultaneous deposition to produce stoichiometric films (Gevorgyan et al. 2016).

Owing to simple approach and production of good crystal quality films, thermal evaporation is commonly used for production of Cd containing II–VI semiconducting nanostructures. In order to grow single crystalline CdS NBs at different temperatures, thermal evaporation technique has been used (Wang et al. 2005). It was brought into notice that the uniformity, surface morphology, and luminescence properties of the samples depend on growth temperature (Fig. 4.2a, b). In another effort, CdS NBs were deposited using hydrogen-assisted TEV technique (Wang and Fei 2009). The films owing to excellent optical properties were reported suitable for photonic devices. To explore the effects of growth parameters, nanomaterials of CdS have been deposited on different substrates under different growth conditions using thermal evaporation technique. The deposition of nanocrystalline CdS on glass substrate covered with ITO using thermal vacuum evaporation has been

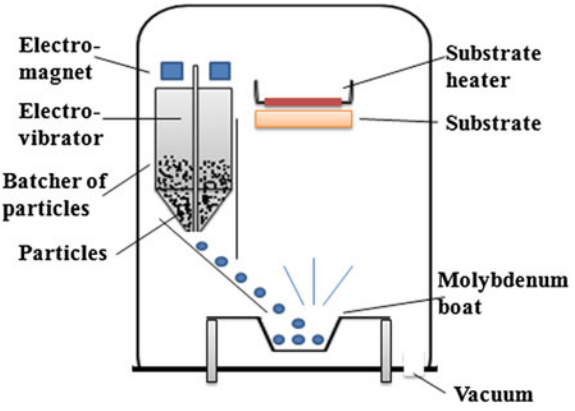

Fig. 4.1 Schematic of evaporation equipped with a vacuum pump (Gevorgyan et al. 2016)

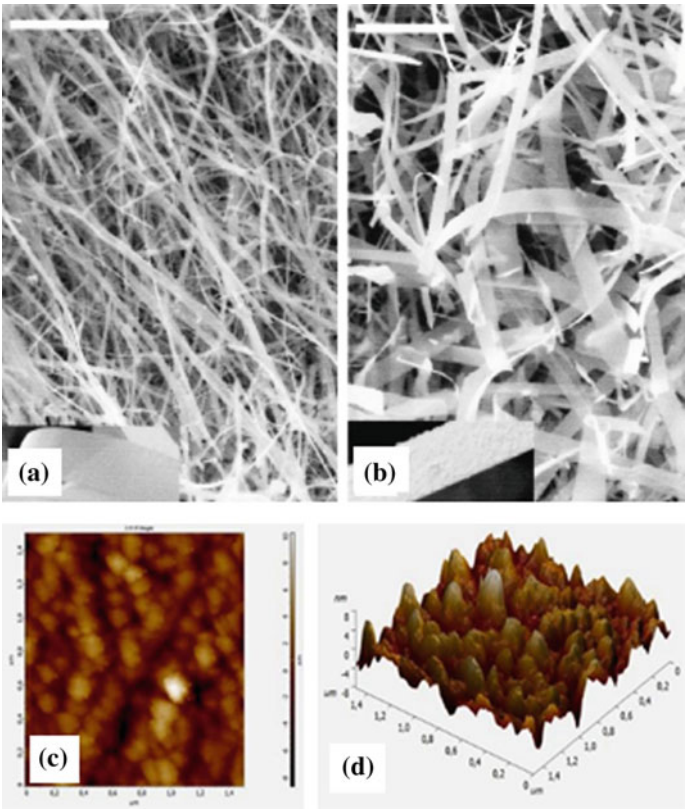

Fig. 4.2 SEM images of CdS with nanowire-like and NBs like structures prepared by TED at **a** 1000 °C and **b** 1200 °C (Wang et al. 2005). © 2005 American Institute of Physics **c** and **d** AFM images of CdS nanofilm deposited on a glass substrate at temperature of 100 °C (Gevorgyan et al. 2016). © 2016 Open Access

reported (Toma et al. 2011). The morphology and optical properties of the films were studied to monitor the thickness, surface roughness, and refractive index.

Upon modifications in conventional thermal evaporation strategies, several groups have obtained high-quality single-crystal nanostructures. The hierarchical single crystalline nanostructure of CdS in the form of nanocombs has been reported to be obtained by thermal evaporation of mixture of graphite and CdS powders (Yang et al. 2011). The authors investigated the structural and optical properties of the materials in detail and described the growth mechanism of the obtained structures. It was revealed that luminescence signatures of CdS will be different if it is grown in the form of nanocombs and NBs.

The process of thermal evaporation is usually carried out at low temperature. However, some studies have been devoted to investigate the effects of substrate temperature on different properties of the grown films. CdS nanomaterials have

been grown on glass substrates having different temperatures by using thermal evaporation (Singh 2015). The structural characterization of the deposited films indicated that the films grown at 300 K were amorphous whereas the films deposited at 473 and 573 K were crystalline which indicates strong dependence of crystallinity on the substrate temperatures. The optical measurements revealed that the value band gap decreases with increase in substrate temperature. Gevorgyan et al. have also conducted similar study when they deposited nanostructured CdS thin films using vacuum flash evaporation (VFE) at different temperatures of 100, 200, and 300 °C of substrate (Gevorgyan et al. 2016). The grain size, surface roughness, and morphology of the deposited films exhibited weak dependence on substrate temperature during deposition. AFM images of CdS nanofilms have been shown in Fig. 4.2c, d. The transmission measurements of the films were made which revealed that value of band gap depends upon temperature of the substrate.

Besides the growth of pure CdS nanomaterials, the thermal evaporation deposition of doped CdS has been carried out for different purposes. Pure CdS- and Mn-doped CdS NCs in the form of ternary alloy $Cd_{1-x}Mn_xS$ have been deposited on glass and silicon substrates using thermal evaporation method (Iacomi et al. 2006). The measurement of optical properties indicated the band gap dependence on doping concentration and grain size which was interpreted in terms of successful substitution of Mn into cationic sublattice of CdS.

In order to check the prospects of CdS NWs in devices, doping of Ga has been carried out in n-type CdS NWs using thermal evaporation route (Cai et al. 2011). Doping-dependent tuning of NWs have also been studied which showed an increase in their cunductivity.The doped NWs were used to fabricate field effect transistor which exhibited improved performance when compared with back gate FET. Furthermore, a light-emitting diode exhibiting bright yellow emission was also fabricated using a hybrid structure based on Ga-doped n-type NWs on p-silicon substrate. In another study, pure and tin-doped CdS nanocrystalline structures were prepared by thermal evaporation method and the effects of doping on structure and photo-responsivity of the materials were thoroughly investigated (Zhou et al. 2014). The nanostructures were found feasible for photodetectors on the basis of detailed photoconductivity measurements. The doped NWs exhibited broader spectral response, improved optical properties, and enhanced photoconductivity as compared to that of undoped CdS NWs. The effects of Zn doping on structural and optical properties of CdS NPs deposited on Si and SiO_2 substrates using thermal evaporation method have been performed (Baghchesara et al. 2016). It was brought into notice that CdS was shaped as nanobelts and nanorods which turned into purely NRs after Zn doping. It was claimed that dopants have been successfully incorporated and band gap of CdS increases after doping with Zn. The materials were further studied for photodetection and it was reported that the doped nanostructures are better photodetectors as compared to undoped ones.

Several groups have tested thermal evaporation growth of Cd-related nanostructures in the presence of carrier gases. Li et al. reported the deposition of NBs and NWs of CdS by employing hydrogen-assisted thermal evaporation technique

(Li et al. 2006). They revealed the influence of deposition parameters and hydrogen as carrier gas on the quality of products and the growth process. The hydrogen-assisted thermal evaporation synthesis of high quality CdSe NWs suitable for photonic devices has also been reported (Wang and Fei 2009). Another effort to grow CdS using hydrogen-assisted thermal evaporation technique resulted in fabrication of nanostructures of CdS on gold and silicon substrates (Peng and Zou 2012). The deposition temperature was found to strongly influence the morphology which was observed in the form of sward- and saw-like nanostructures. The optical properties of the materials were carefully investigated and waveguide properties of the films were observed. Keeping in view that conventional thermal evaporation process generates films having deficiency of metallic ions, Fan et al. proposed a way to increase the Cd content and improve the stoichiometry of CdS films (Fan et al. 2015). They prepared the precursor materials by co-precipitation process and then carried out deposition of the CdS QDs on ITO-coated glass substrate. The deposited films exhibiting nanorod structures were analyzed in detail and found suitable as photoanode for photo-electro-chemical applications.

Thermal evaporation has been a resourceful technique for the production of device grade nanomaterials. In an effort to prepare self-assembled structures, thermal evaporation strategy has been adopted to prepare CdS NBs and CdS/SiO_2 NWs by using mixed power of CdS and CdO along with simultaneous etching of silicon (Yu et al. 2006). The mechanism was carefully monitored and it was found that growth of CdS structure strongly influences the product CdS/SiO_2 arrays. The hetero-structures comprising of CdS/silicon coaxial nanocables have been prepared using thermal evaporation in which silicon sheath and CdS core were reported to have amorphous and hexagonal structures, respectively (Fu et al. 2005). This method can be utilized to synthesize several hetero-structures based on Cd containing semiconducting nanomaterials.

Similarly, several efforts have been reported to deposit CdSe nanomaterials of different morphologies using this technique. In order to find a correlation between structural and optical properties, CdSe NCs have been prepared in SiO_x matrix by using thermal vacuum evaporation (Nesheva and Levi 1997). The deposited materials were reported to have a consistent variation in band gap with size of NCs which pointed towards tuning of the optical properties for applications in devices. The variable thickness layers of NPs of CdS inserted between amorphous chalcogenide films have been prepared using vacuum thermal evaporation (Nesheva 2001). On the basis of observation of layer thickness, shapes, and spatial distribution of NPs, the growth mechanism of the materials as well as carrier transport in the films has been described.

An effort to deposit single crystal CdSe nanoribbons in wurtzite phase using thermal evaporation has been reported (Ma et al. 2004). The workers noticed growth of saw-like nanostructures during asymmetric growth process which may have caused by c-plane polarization. Using thermal evaporation method, quasi-spherical NCs of CdSe on glass substrate has been obtained (Pal et al. 2008). It was revealed that the shape of grains changed into oval upon changing the film thickness on the basis of which a model to describe the morphological changes was

presented. In the same films, quantum confinement effect was also observed. Another effort to achieve single crystal material of CdSe in the form of nanoribbons using thermal evaporation has been reported (Hou et al. 2008). The authors used modified thermal evaporation in the form of two-step process and recommended their method to obtain large-scale NCs of CdSe having regular shapes. The effects of laser irradiation on nanocrystalline CdSe deposited on glass deposited by thermal evaporation method have been investigated (Khudiar et al. 2009). It was observed that grain size increases whereas optical band gap decreases with laser irradiation.

The prospects of thermal evaporation deposited CdSe nanostructures for different applications and devices have also been investigated. The NWs of CdSe/SiO_x in the form of core/shell structure have been deposited on silicon substrate using thermal evaporation method (Dai et al. 2010). The core consisted of single crystal CdSe whereas shell comprised of amorphous zone of SiO_x. The usage of substrate in the form of equilateral triangle designed template was found responsible to produce core/shell structures. The formation of core/shell structures was also confirmed from photoluminescence measurements. Another effort to synthesize core/shall structures for solar energy harvesting comprises of growth of CdSe/ZnTe using combined thermal evaporation of CdSe has been reported (Wang et al. 2014). The deposited core CdSe was in form of NWs which have good structural quality and morphology as well as epitaxially oriented with ZnTe.

A number of reports on doping of CdSe nanostructures via thermal evaporation technique are also found in literature. The thermal evaporation preparation of Sn-doped CdSe whiskers and pure CdSe NPs has been reported (Zhou and Tang 2013). While measuring the excitation power dependent optical properties, a red shift in band edge emission of doped CdSe was found whereas emission in case of pure material exhibited no such with increase in excitation power. In order to tune the properties of CdSe nanostructures for device grade applications, Ga-doped CdSe NWs have been prepared by thermal evaporation method (Hu et al. 2011). The doping was observed to notably change the structural and electronic properties. The wurtzite phase of pure CdSe NWs was changed into cubic zinc blende with increase in doping concentration. The measurement of electrical transport properties revealed the possibility to tune the conductivity by changing the doping level. The doped NWs were successfully tested in field effect transistor, photodetectors, and light-emitting diodes were expected to be potential material for future nano-opto-electronic applications.

The preparation of chlorine-doped NBs of single-crystal CdSe in wurtzite phase by using thermal evaporation has been reported (Du and Lei 2013). The doped material was found as n-type on the basis of single nanobelt as field effect transistor. The material was further tested as Schottky diode having excellent rectification ratio and small ideality factor. On the basis of observed characteristics, the doped NBs of CdSe were found suitable for use as photodetectors and other electronic/optoelectronic devices.

Thermal evaporation technique has been successfully used to deposit nanocrystalline CdTe films as well. Al-Ghamdi et al. deposited nanocrystalline CdTe thin films of 40, 60, and 100 nm thickness on silicon by using thermal

evaporation technique (Al-Ghamdi et al. 2012). The current–voltage and capacitance–voltage measurements on the films were carried out which revealed the thickness-dependent electrical properties. It was pointed out that the current obeys diode equation at low voltages and thermionic emission is dominant mechanism. The single crystalline NWs of zinc blende CdTe were synthesized using thermal evaporation (Li et al. 2013). The NWs were used to fabricate field effect transistor whose characterization indicated excellent p-type conductivity of the material which pointed towards its potential for nanoelectronic devices. The CdTe films have been prepared by thermal evaporation and then thermally annealed at different temperatures to determine the effects of annealing on structural and optical properties (Dongol et al. 2015). The upgradation in value of band gap and other optical properties of the films were attributed to nanostructural properties and suppression of defects.

4.2 Electron Beam Evaporation

Electron beam or E-beam evaporation (EBE) being a member of physical vapor deposition, referred as electron beam physical vapor deposition, is a popular technique for deposition of thin films on substrates. Its basic principle of working is similar to that of thermal evaporation deposition with the difference of heating source which comprises basically of an electron gun in EBE. An energetic beam of electrons generated from a filament strikes the target material in vacuum chamber and, as a result of direct energy transfer mechanism, the source material is heated and the atoms from its surface acquire sufficient energy to evaporate. The evaporated atoms then rushed away from the surface of the target and condense in the form of a coating on the substrate (Fig. 4.3).

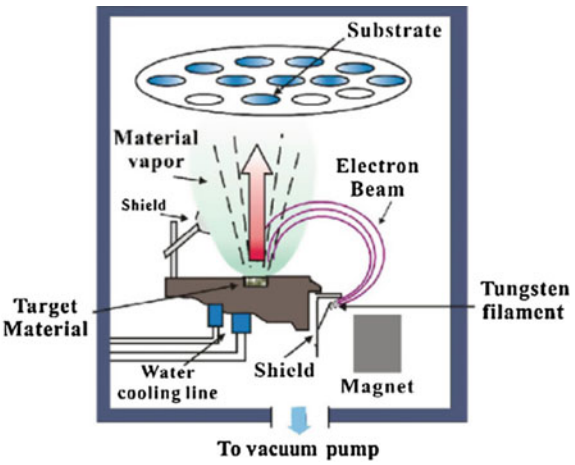

Fig. 4.3 Schematic diagram explaining the working principle of EBE (Xie et al. 2014). © 2014 Elsevier Publishing

The EBE emerged basically to cope with the existing problems related to available techniques and thus offers several advantages. It offers high material utilization, structural, and compositional control, strong adhesion, low contamination, high deposition rate, and controlled morphology of the deposited films. Moreover, usage of multiple target materials for deposition of compounds as well as doping and uniformity over large areas are also merits of this technique. Sometimes, in order to clean the substrate's surface before coating, an ion source is also attached inside the chamber.

The preparation of EBE deposited polycrystalline CdS/glass thin films comprising of nanocone arrays has been reported (Eshraghi and Naderi 2016). The deposition was carried out at different evaporation rates to investigate the effects of the rate on structure, morphology, and optical properties of the films. A decrease in surface roughness and an increase in optical band gap with increase in the rate were observed. The changes in band gap were described on the basis of change in Cd/S ratio to reveal stoichiometric profile of the films. Furthermore, changes substrate temperatures were also monitored to study the modifications in crystal quality and film thickness.

EBE has been employed to deposit nanocrystalline CdSe films on glass substrate maintained at different temperatures 100, 200, 300 °C, and room temperature (Kissinger et al. 2002). The films were hexagonal irrespective of substrate temperature but a consistent increase in crystallite size and decrease in strain with the temperature were observed. The optical band gap measured from transmission spectra was found increased with increase in substrate temperature and the films were found spectrally suitable for photovoltaic applications. Zn-doped CdSe films containing nanosized grains deposited via EBE on glass have been reported (Suthagar et al. 2010). The band gap of the doped material was observed to increase from 2.08 to 2.64 eV upon increase in Zn content from 0.2 to 0.8. Owing to doping-dependent tunable properties of the films, the material was recommended as a potential candidate for photovoltaic applications.

In order to check the effects of substrate temperature on properties of CdTe, its nanocrystalline films were deposited on glass using EBE technique (Begam et al. 2013). While deposited, the temperature of the substrate was maintained at different values 423, 573, 623, and 673 K to grow the respective thin films. It was observed that crystalline size increased from 35 to 116 nm whereas optical band gap of the material decreased from 2.87 to 2.05 eV with increase in substrate temperature. CdTe/Co nanomaterials in the form of staking layers have been deposited on glass substrate by using EBE (Mohamed et al. 2014). In order to explore the effects of Co diffusion and its concentration in the films, detailed structural and magnetic characterizations were carried out. The material was found with zinc blende structure and an increase in lattice parameter was observed with increase in Co content. The films exhibited well-defined magnetic hysteresis at room temperature with a Co-layer-thickness-dependent increase in saturation magnetization. The materials were found to be ferromagnetic with electronic exchange interactions between localized Co-3d carriers and free carriers in the material. The staked layers structure containing Co is a potential diluted magnetic semiconductor for applications in

spintronic devices. CdS layer on the CdTe core using 8 meV electron beam irradiation. They studied the results obtained during the irradiation on thioglycolic acid (TGA)-capped CdTe QDs (Pai et al. 2013). The characterization techniques XRD, XPS, TEM, and UV–Vis spectroscopy were used to investigate the material. The photoemission frequency, strength, and duration were observed to change with electron dosage. Their work showed that electron beam assisted method provided a potential epitaxial growth of water soluble CdTe/CdS core–shell composites to be applied in biomedical category.

4.3 Pulsed Laser Ablation Synthesis

Pulsed laser ablation is one of thin film deposition strategies among the family of physical vapor deposition processes due to which it is known as pulsed laser ablation physical vapor deposition (PLD). The basic principle of this technique comprises of laser–matter interaction as a result of which a plum (atoms, molecules, clusters, particles, etc.) of material is expelled out of the surface of target. The ejected vapors are then deposited onto substrate placed in line of its sight in an evacuated chamber. The PLD is vastly adopted due to its simplicity and provision of options to control the process to manipulate the deposition of a wide class of materials. This technique offers such a clean process of deposition of materials on substrates without contamination which gives it a priority over other techniques. It can be used to grow virtually any material at high deposition rate with broad window of tunable parameters related to laser and the entire experimental setup. Furthermore, it is a low cost process which offers controlled morphology and composition, good uniformity, high stoichiometry, and strong adhesion of the deposit without involving solvents.

A PLD process involves several stages which include laser–target interaction, ablation of material, and condensation of ablated vapors on substrate surface and growth of the films (Soonmin 2016). The process is carried out in a chamber as shown in Fig. 4.4. In order to carry out this process to achieve high quality thin films as per requirement, several scientific and technological strategies are adopted. The deposition of nanomaterials using PLD is mainly found in last decade. Owing to technological improvement in field of lasers, vacuum production and engineering related to experimental techniques, the PLD technique has lot of prospects over sister deposition methods. This method carried out in liquids has several benefits including controlled environment, ambient conditions, formation of nanomaterials without loss of materials at low temperatures, etc. (Yang 2007).

Keeping in view the potential and simplicity of PLD technique, a number of reports are available in literature on deposition of CdS nanostructures using this strategy. In a work, CdS NCs have been deposited on silicon substrate using femtosecond laser (Sanz et al. 2010). Ti:Sapphire laser source producing 60 f-sec

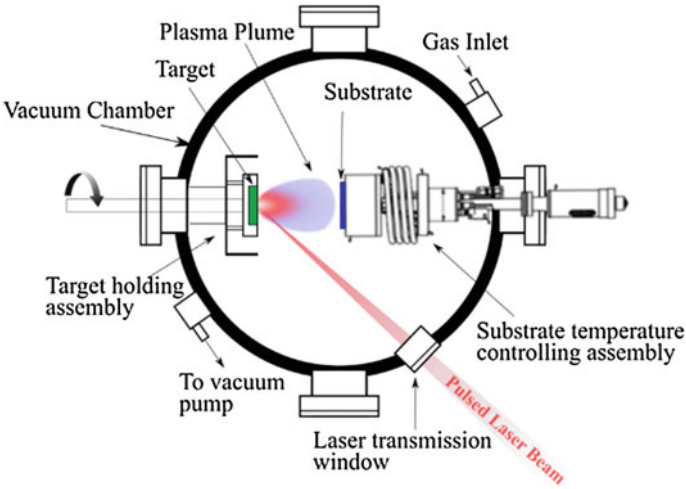

Fig. 4.4 Schematic diagram showing PLD process in a chamber (Chaudhary et al. 2016). © 2016 Open Source

pulses at different wavelengths (266, 400, and 800 nm) with different fluences (1.5 and 3.5 times of the threshold) was used to irradiate the substrate maintained at different temperatures (from 25 to 450 °C) to investigate the effects of growth conditions on the quality of the materials prepared by using this technique. It was concluded that the crystallite orientation can be changed by adjusting the fluence and wavelength of laser. It has been observed that uniformity of the films and density of NPs is directly proportional to lasing wavelength. The observed trends shed light on the efficiency of this technique to tune the properties of the deposited material. As another effort to investigate the effects of laser wavelengths on structure and morphology, Sanz et al. prepared thin films of CdS nanomaterials on silicon substrate by using PLD technique (Sanz et al. 2011). The detailed investigations pointed out dependency of crystalline quality, dimensions, and morphology of nanomaterials on temperature of substrate and wavelength of laser. PLD has been used to deposit NPs of CdS on quartz substrate in argon atmosphere (Khan and Bibi 2014). The deposited NPs showed zinc blende crystal structure with size in range 5–10 nm and contained dense spatial distribution as per SEM and Raman measurements. The absence of defect-related emission in luminescence spectra was taken as suitability of this technique for production of high quality and pure CdS nanomaterials.

In order to investigate the role of substrate, PLD technique has been employed to deposit CdS nanoneedles on Ni-coated silicon substrate maintained at different temperatures (Chen et al. 2012). The outcomes of this study pointed out that the morphology and size of the NCs can be tailored by selecting the temperature and

pre-deposition conditions of the substrate. The same group reported another effort to study the effects of growth parameters on quality of CdS nanoneedles deposited on Ni-coated silicon substrates by PLD-PVD (Li et al. 2014). The monitoring of growth at different substrate temperatures pointed out that pre-deposited Ni acts as catalyst and appears in the form of molten spheres to provide nucleation base to CdS nanoneedles. It was further observed that energy of laser pulses also influences growth of the needles. On the basis of their detailed investigations, the authors explained PLD growth mechanism of CdS nanoneedles by considering vapor (V), liquid (L), and solid (S) phases of the materials at different stages of the process. The substrate temperature is not very high during V–S growth mode due to which Ni grains are stable and CdS nanoneedles nucleate and deposit directly on these grains. On the other hand in case of V–L–S growth, Ni grains are not stable when substrate temperature is high due to which nanoneedles start nucleating at the bottom of the grains. The growing nanoneedles push the catalyst upwards and Ni-tipped CdS nanoneedles are obtained as shown in Fig. 4.5 a, b.

The NCs of CdS-doped glass has been deposited on silicon substrate and annealed in-situ using this technique (Wang et al. 2001). The photoluminescence measurements of the grown films pointed out formation of new phase CdO whose luminescence was found dependent on deposition time but independent on the annealing. The size and orientation of the crystallites however depends upon annealing treatment of the films. This technique has also been used for preparation of films for applications in devices. The PLD preparation of heterojunction of vertically aligned CdS/g–C_3N_4 has been reported (Xu et al. 2016). The films grown on silicon substrate comprise of nanocone structure were characterized in detail for optical absorption using time-resolved photoluminescence measurements. The heterojunctions were found suitable for photocatalytic applications.

The Se-rich CdSe NPs of CdSe have been prepared via laser ablation carried out in methanol (Semaltianos et al. 2008). The NPs exhibited narrow and green luminescence. Research attention has also been paid to fabricate quantum dot sensitized solar cells. Laser ablation has been carried out in water to prepare CdSe QDs (Horoz et al. 2012). The QDs were ligand free and could be used for applications in quantum sensitized solar cells. The same group has reported PLD synthesis of solar cells based on CdSe QDs on NWs of Zn_2SnO_4 without involving

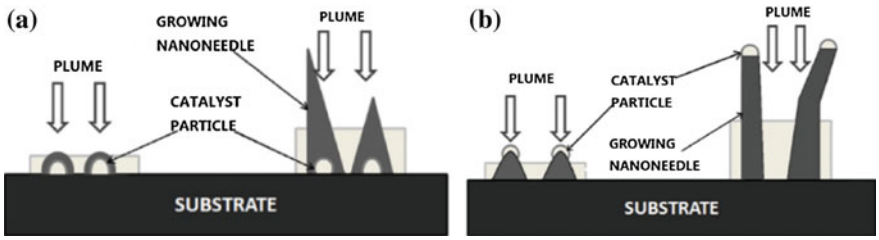

Fig. 4.5 Growth models for CdS nanoneedles **a** VS and **b** VLS modes (Li et al. 2014). © 2014 Open Access

ligands (Dai et al. 2012). The growth conditions including substrate temperature, laser parameter and time of deposition along with environment were expected to play role to improve the efficiency of solar cells.

There has been wide research interest to study doping-induced modifications and preparation of CdSe nanomaterials for applications in devices. Dia et al. have reported PLD preparation of QDs of pure and Mn-doped CdSe on Zn_2SnO_4 photoanodes (Dai et al. 2014). The deposited materials were characterized for applications as quantum dot sensitized solar cells. The doping appeared to modify the band structure of host material in such a way that band gap was reduced and a threefold increase in quantum efficiency was observed. The PLD technique has been employed to incorporate core/shell structured colloidal CdSe/CdS QDs in amorphous matrix of Y_2O_3 (Aubret et al. 2016). The method was claimed to be equally beneficial for other nanoemitters and matrices to realize device grade nanomaterials.

A number of reports on PLD preparation of CdTe nanomaterials are also available in literature. Using sequential deposition from separate sources in a PLD process, the nanostructures of CdTe have been deposited on mica, InSb, and KBr substrates (Yeremyan et al. 2008). The growth of NCs at about 150 °C pointed out significance of this technique as a low temperature growth when compared with other technologies as MBE and MOCVD. The layers grown on InSb and KBr were zinc blende whereas those deposited on mica substrate were wurtzite in structure. Keeping in view the applications window of CdTe nanostructures, the laser ablation mechanism needs to be understood. The optical emission study of laser ablated CdTe has been carried out to investigate the mechanism of etching by using KrF excimer laser (Abe et al. 2005). The compositional changes were monitored during different stages of etching with the help of optical emission measurements. It was observed that rate of etching depends upon energy density of the laser but for energy density higher than 0.4 J/cm^2 etching rate was reduced due to shielding of laser beam by plasma plume. The findings of this study can help understanding the deposition of CdTe nanomaterials by using PLD technique. In another reported attempt, CdTe NPs were deposited on silicon by using this technique to prepare cluster assembled thin films (Neretina et al. 2006). The films were in the form of mix of wurtzite and zinc blende phases but upon rising the substrate temperature, wurtzite component was observed to increase. The observation of metastable phase formed at the employed synthesis conditions and transformation of zinc blende to wurtzite structure are salient feature of this work.

Unlike other Cd containing II–VI nanomaterials, comparatively less is reported on PLD prepared CdO NPs. CdO nanocrystalline thin films have been deposited on glass by using PLD technique (Pan et al. 2014). It was observed that grain size is directly proportional whereas defect density and strain are inversely proportional to energy density of the laser. The film containing smallest grains was found having oxygen vacancies whereas electrical and optical properties of the films were found grain size dependent. In another reported work, PLD technique has been used to synthesize CdO NPs in solution of polyvinylpyrrolidone (Ibrahim et al. 2016). The analysis of morphology revealed the grains of the films in the form of packed

nanospheres shaped of size around 50 nm. The optical band gap of the material was measured as 2.8 nm.

This survey indicates availability of reported literature on CdS, CdSe, CdTe, and CdO but the work on these nanomaterials is still limited despite the simplicity and worth of PLD technique. Although, preparation of nanomaterials using this technique faces some problems including reproducibility, stoichiometry, large area uniform growth and interfacial issues during growth of multilayered heterojunctions but still PLD deserves more attention for deposition of nanocrystalline thin films of interest.

4.4 Chemical Vapor Deposition

Chemical vapor deposition (CVD) is a famous thin film deposition technique in which vapors condense into solid phase onto the surface of a substrate as a result of chemical reaction. The conventional CVD is also known as thermal CVD in which the deposition is carried out in a furnace usually at high temperature to vaporize the precursor material and promote the chemical reaction. A typical CVD process involves several steps. The precursors placed in the reaction chamber/furnace are evaporated and the reactant vapors are transported towards the substrate with the gas flow. The reactants are adsorbed on the surface of the substrate followed by diffusion, nucleation, and chemical reaction which leads to formation of deposition of material of interest in the form of thin film. In parallel to this, the precursor vapors can also go through gas phase reaction to produce products and by-products in gaseous phase. These products can adsorb on the substrate surface or ejected out of the furnace with gas flow (Mahajan 1996).

A conventional CVD reactor consists of several components which basically include (i) reactor chamber or furnace (ii) substrate holder (iii) carrier gas as H, N, Ar, or mixture of these gases (iv) heating source (v) boats to load precursors in the chamber (vi) exhaust system (vii) vacuum system. The schematic diagram of a conventional CVD reactor is given in Fig. 4.6.

The conventional CVD process involving vapor–solid mechanism is not efficient for deposition of nanomaterials (e.g., NWs) because direct adsorption of vapors on solid is a slow process. The synthesis stages include: (i) loading of the precursor reactants and inert gases into the chamber, (ii) shifting of vapor species to substrate

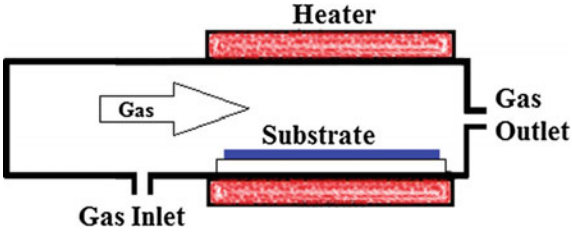

Fig. 4.6 Schematic diagram of a conventional CVD reactor (Park and Sudarshan 2001)

surface (iii) adsorption of reactants on surface sites (iv) chemical reaction and nucleation (v) formation of nanostructured thin film (vi) gaseous reaction products are emptied out of the chamber. In order to speed up the process and increase the deposition rate of nanomaterials, an intervention is applied thereby using a catalyst in liquid phase (Rashid et al. 2015). The modified process then involves vapor–liquid–solid or VLS mechanism which comprises of different stages. The layer of catalyst (usually Au, Bi, etc.) is grown on the surface of substrate prior to loading into CVD chamber. While the deposition process is carried out, catalyst melts and the reactant vapors diffuse towards the catalyst droplet. Under the continuous supply of vapors, the supersaturation takes place which leads to nucleation at liquid–solid interface and hence the nanomaterials are deposited on the substrate surface.

The growth rate and quality of deposited film depend upon number of factors including nature of precursors, nature of substrate, nature of catalyst, temperature, pressure, gas flow rate, etc.

Chemical vapor deposition is resourceful technique which can be applied to prepare the thin films comprising of nanomaterials of any metal, ceramic, semiconductor or insulator. In addition to growth of elements, this technique can be efficiently used to deposit alloys, intermetallic compounds including carbides, nitrides, oxides, sulfides, etc. This method is one of the effective techniques used to deposit heterojunctions, QDs, core/shell structures, and a variety of semiconductor devices on a substrate in more efficient way. The advantages of deposition using this technique include fast deposition rate, purity of deposits, adhesion, and possibility of optimization of deposition to achieve controlled crystal structure, shape, and morphology of nanomaterials (Hampden-Smith and Kodas 1995).

Owing to improved understanding in coating technologies and available possibilities to engineer the CVD process, the CVD has been modified in a number of ways to improve the deposition due to which it has become a family of deposition technique. It can be classified on the basis of precursors, operating pressure, vapor characteristics, temperature, geometry, plasma utilization, light and laser irradiation.

The CVD process has been utilized by industry as well as a number of research groups over the years for growth of Cd containing nanomaterials. The growth of arrays, NWs, and nanocombs of CdS has been carried out by employing VLS mechanism implemented in CVD process (Ge and Li 2004). The work was carried out to grow the nanomaterials under different growth conditions including temperature, gas flow, and deposition location to control the morphology, structure, and properties of the deposit. It was found that, higher temperature facilitates the growth of NWs along (100) direction whereas lower temperature caused the growth in (002) direction. On the basis of photoluminescence measurements, the grown material was recommended for use in lasers and optical nanodevices. The growth of nanocrystalline CdS thin films deposited on SiO_2 substrate has been deposited (Barreca et al. 2004). The deposition of the films was carried out at different temperatures from 473 to 723°C which resulted in growth rates of 4.0×10^3–3.5×10^3 nm/sec, respectively. The XRD analysis indicated the presence of cubic as well as hexagonal phases in the films whereas no variations in peak position and

intensity with change in deposition temperature were observed. The measurement of optical properties revealed that the value of optical band gap of the films was 2.5 ± 0.2 eV.

An effort to produce n-type conductivity in CdS NBs was carried out by doping with indium in a CVD furnace (Ma et al. 2006). The NBs were single crystalline with wurtzite structure and observed grown in [1000] direction. Though CdS is an unintentionally n-doped material but the authors observed a dramatic increase in electron concentration upon doping with indium which acted as a shallow donor. In order to check the potential of the material, FET was fabricated by shifting the NBs to p-Si which acted as gate whereas UV lithography was employed to make the source and drain of the device. The characterization of the prepared FET revealed excellent device performance thereby exhibiting very high on-off ratio and a small subthreshold swing. Furthermore, the NBs were also tested as light-emitting diodes which demonstrated green emission when forward biased. It is worth mentioning that LED prepared with undoped CdS NBs did not show any emission.

The preparation of CdS NCs in tetrahedral structure using CVD setup has been reported (Zheng et al. 2008). The deposition temperature is an important CVD parameter which determines quality of deposits as well as its properties. The NCs in this study were prepared at low temperature which resulted into preparation of tetrahedral structure after going through structural evolution and metastable phases.

The CVD growth, under vapor–liquid–solid mechanism, of high purity, high yield, and controlled nanocrystalline CdS films have been reported (Green et al. 2008). The gold-coated quartz was placed as substrates in different compartments made of ceramics in CVD furnace for deposition of films. Gold played role of catalyst and its thickness was found strongly related with morphology and yield of nanostructures. Moreover, the arrangement of the compartments also influenced the growth process and yield. The grown films were found dependent upon deposition temperature and comprised of nanosized grains in the form of rods, wires, and belts. Another effort to grow CdS NBs via VLS mechanism implemented as CVD process and utilize them to fabricate Schottky junctions for photovoltaics has also been reported (Wu et al. 2009). The NBs were single crystalline in wurtzite structure with 0.206 nm spacing between lattice planes along growth direction. The grown single nanobelt acting as gate was transferred to p^+-Si substrate having SiO_2 epilayer and UV lithography was then employed to build ohmic contacts to fabricate metal–insulator–semiconductor FET. A layer of dielectric material HfO_2 was deposited followed by creating an electrode of Au gate between source and drain. The detailed study of the device revealed its excellent performance based on measurements of on/off ratio, threshold voltage, transconductance, and transfer characteristics. In another study, these CdS NBs were utilized to fabricate Schottky junctions for photovoltaics (Ye et al. 2009). Au and In/Au were used as Schottky and Ohmic contacts, respectively. The junctions exhibited notable rectification as per I–V characteristics measured in dark. Similarly, the junction based on single nanobelt presented clear photovoltaic response when measured under illumination. The multiplication of output power upon connecting a number of such devices in series or parallel is also possible.

Another effort to grow CdS nanostructures having different morphologies prepared via CVD under vapor–liquid–solid mechanism has been reported (Geburt et al. 2012). They observed formation of nanostructures of different shapes upon using different deposition temperatures. The growth did not happen below 600 °C and above 720 °C. At higher temperatures (above 680 °C), the growth in the form of nanobands was observed. The growth of VLS nature was fast along axis of the bands and was comparatively slower on lateral axis. On the other hand, growth of bands at low temperatures was observed only when Ar gas pressure was kept low. The observation of growth profile of the nanostructures as variable deposition temperature and gas pressure could help to establish growth phase diagram. The excitation power dependent luminescence of the NCs was also carried out which revealed the potential of the grown nanomaterials for application in lasers.

CVD has been applied to prepare nanostructures of different morphologies, shapes, and geometries to explore their innovative applications. The nanosheets of CdS have been prepared by CVD technique in Cd rich environment (Ye et al. 2012). The prepared nanosheets were tested to fabricate a nanotransistor which exhibited the best performance. Moreover, these nanosheets were employed to fabricate light-emitting diode comprising of large active region and offer high injection current for applications in light emitters. The CVD strategy along with self-assembly mechanism has been adopted to prepare CdS nanostructures which appeared in the form of highly ordered comb-like morphology (Liu et al. 2013). The comb-like structures contain branched teeth of nanosize whereas backbone in micro-size whose architecture, size, and density could be tuned by monitoring the growth conditions. The optical properties of the components were separately investigated by micro-photoluminescence which revealed excellent waveguide properties of branches in visible region. The optical characterization of the trunk exhibited its monolithic structure whose strong coupling points make the structure to be utilized for applications in trunk-branch type waveguides cavities.

CVD can be efficiently used for doping into nanostructures. The deposition of Ni-doped CdS nanoribbons on gold-coated silicon substrate using this technique has been reported (Kamran et al. 2013). The dopant atoms of Ni were observed homogeneously distributed in the matrix whose tip sides were wurtzite in structure. The photoluminescence measurements revealed red shift of band edge emission after doping which was interpreted in terms of appearance of magnetic polarons in the samples. On the basis of temperature dependent photoluminescence measurements, the band found at 1.61 eV was attributed to emission related to Ni 3d states in the nanoribbons. The Ni 3d states hybridized with Sp states which points to enhanced interactions and thus covalency of Ni–S bond. Another effort to dope CdS which resulted in growth of trunk-branch network in the form of CdS comb-like nanomaterials by using CVD has been reported (Song et al. 2015). In order to modify the properties, the nanomaterials were also doped with Sn whose incorporation slightly changed the lattice constant. The results pointed out less concentration of Sn dopant in trunk as compared to that of branch and junctions of the network. The microscopy of the samples revealed wurtzite structure of comb-like branches of CdS NCs. The electron–phonon coupling strength, as per Raman

investigations, increased with increase in Sn concentration in the doped nanostructures. The optical properties of the grown materials were studied in detail to explore their optoelectronic response for applications in nanodevices.

Keeping into account the importance of geometry of nanostructures for applications, CVD being highly resourceful technique is commonly utilized for growth of nanomaterials of different shapes. Recently, single crystalline NRs of CdS have been deposited on SiO_2/Si using this technique (Zhao et al. 2017). The grown NRs were transferred to the substrate after which photolithography and e-beam evaporation were employed to fabricate photodetector device based on single nanorod of CdS. The grown NRs were characterized using photoluminescence spectroscopy for application as photodetector. The device exhibited excellent photo-responsivity in UV–visible region even at low illumination intensity.

Besides CVD synthesis of CdS nanomaterials, a number of appreciable efforts to prepare nanocrystalline CdSe have also been reported. The growth of n-type CdSe NBs comprised of different electronic concentrations have been grown via CVD technique (Liu et al. 2009). The unintentionally grown CdSe nanomaterials have high resistivity which disqualifies them for application in FETs. It opens ways to increase the electron carrier concentration by doping or other methods. Keeping in view the poor crystalline quality of n-type CdSe nanomaterials when prepared via commonly employed strategy of doping with indium, the authors of this work tested utilization of Cd enriched ambient during CVD process. In order to carry out the deposition process in a Cd-enriched environment, Cd particles were also placed in addition to CdS precursor powder in the furnace. They could vary the electron concentration by changing the temperature of Cd particles during deposition process. It was found that electron concentration and hence conductance in the NBs increased upon increasing the Cd vapor pressure and temperature. The grown NBs exhibited electron mobility of about 800 cm^2/V.s and were tested for application in devices. The field effect transistors fabricated using single CdSe nanobelt exhibited excellent performance on the basis of measured parameters including on/off ratio, threshold voltage, and transconductance. The light-emitting diode prepared using CdSe NBs was also tested which shows intense band edge emission peak at 708 nm.

The growth of NWs and nanoribbons of CdSe by employing hydrogen-assisted CVD process has been reported (Wu et al. 2012). In the presence of gold catalyst, the grown NWs and NRs of CdSe were single crystalline wurtzite structured having [010] growth direction. On the other hand, in absence of gold catalyst, CdSe nanopods and nanocones were obtained. During growth under gold catalyst, the NPs of gold produced dislocations as well as nucleation centers which facilitated growth of CdSe NWs at low supersaturation level.

Besides these devices, CdSe nanomaterials have also been utilized for application in lasers. The CVD preparation of core/shell structures of CdSe/SiO_2 in the form of nanocables exhibiting room temperature lasing has been reported (Ye et al. 2011). Nanocable with a core of 220 nm in diameter and a sheath of 70 nm in thickness has been found. The core structured NWs were wurtzite having [0001] growth direction whereas shells were amorphous. The tips of the nanocables were

free from metal particles and growth of SiO_2 shells have emerged from oxidation reaction occurred on the silicon surface. In order to observe lasing from the nanocables, evanescent coupling method was employed to observe the emission of light from facet end. The measurement of PL spectra of the nanocables recorded at variable excitation power revealed prospects of lasing features. The observation of broad and featureless luminescence features at low excitation power pointed out possibility of spontaneous emission whereas appearance of period and sharp emission lines at higher excitation power revealed possibility of amplified spontaneous emission process.

An effort to grow CdSe nanostructures whose shape and structure can be controlled by Bi doping by using CVD has been reported (Heo et al. 2016). The doping with Bi appeared to play important role in the growth process. The substrate was found slightly covered by a rough CdSe film in the absence of Bi powder in precursor. However, addition of Bi appeared to significantly influence the growth process due to which well-defined and high aspect ratio nanostructures of uniform density and large in number were obtained. Moreover, the synthesis process was found strongly affected by growth conditions. The grown material in the presence of Bi doping was observed to be in the form of NCs, bumpy film, and NBs at growth temperatures of 700, 750, and 850 °C, respectively. The device grade potential of the grown materials was also investigated by fabricating photodetector and field effect transistor by utilizing CdSe NWs. The devices exhibited good performance, therefore; the reported intervention in CVD growth of CdSe nanostructures can be applied to prepare functional nanodevices. A work carried out to deposit CdSe and CdTe NWs on plastic by using Bi-assisted CVD process has been reported (Lee et al. 2009). There has been great research interest in growth of functional materials on flexible substrates for applications in conformal solar cells and display devices. This study was carried out to deposit CdSe and CdTe NWs (Fig. 4.7b) on flexible polyimide plastic which is thermally and chemically stable at the selected growth temperature. These NWs were deposited at minimum temperature of 300 °C and maximum temperature of 430 °C after which substrate became brittle. In this study, Bi-coated substrates were used to promote the growth

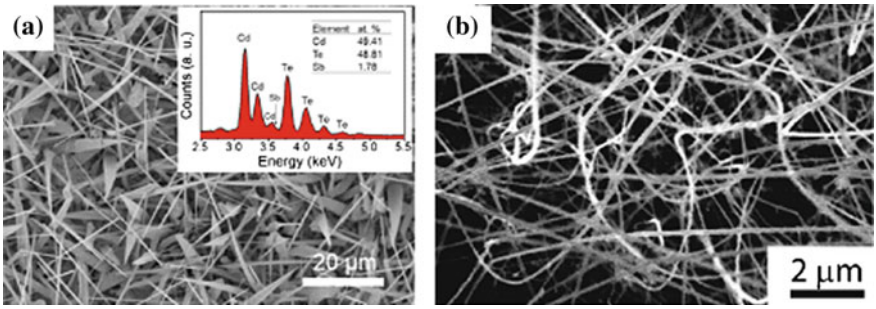

Fig. 4.7 SEM images of **a** Sb:CdTe NBs (Huang et al. 2015). © 2015 American Chemical Society, **b** CdTe NWs (Lee et al. 2009). © 2009 American Chemical Society

of NWs. Bi acted as catalyst and the growth process was optimized by selecting different Bi thickness to improve the growth process.

Some more work has been reported on CVD growth of CdTe nanomaterials. An effort to grow CdTe NWs using CVD process for applications in photodetection devices has been reported (Ye et al. 2010). The grown NWs were of high crystalline quality, smooth surface, cubic in structure, and stoichiometric. The photoluminescence measurements exhibited sharp emission related to band edge at 824 nm pointing towards absence of any defect related luminescence. Besides the growth of straight NWs, the simultaneous production of kinked CdTe NWs was also noticed. The photodetectors based on the straight and the kinked NWs were fabricated. The characterization of the detector prepared using straight CdTe NWs exhibited very fast response time, high photocurrent decay ratio, and responsivity. On the other hand, photocurrent of the detector based on kinked NWs was lower but its decay ratio and responsivity were still high. The outcomes of this work pointed out worth of CdTe nanomaterials for applications in electronic and photonic nanodevices. In an effort to grow nanocrystalline CdTe using this technique high density, stoichiometric and vertically aligned NRs in cubic structure have been deposited on graphene (Hou et al. 2011). Since, temperature is a critical growth factor in CVD, different stages of Bi-assisted growth process were found strongly influenced by temperature. At a low temperature of 271 °C, bismuth powder evaporated and started flowing towards low temperature region of the furnace with flow of carrier gas. At higher temperature of 570 °C, decomposition of CdTe powder took place. The further increase in temperature to 800 °C caused the production of Cd and Te_2 vapors which made downstream flow with Ar towards the low temperature region and reacted to start nucleation process over the substrate surface.

The ambient and gas flow rate is an important growth parameter in CVD process. In order to explain the mechanism of hydrogen-assisted vapor–solid–solid growth of nanostructures, CdTe NWs were grown in a CVD furnace under H_2 gas flow (Huang et al. 2014). The single crystalline stoichiometric CdTe NWs having zinc blende crystal structures were grown whose tips were decorated with polygonal NPs. The authors suggested vapor–solid–solid type growth due to presence of Au–Cd alloy in solid form at low temperatures as per relevant phase diagram. The existence of inhomogeneous strain was observed in the NWs which strongly influence the electronic structure of the material and hence affect the performance of resulting device.

The nanoflakes of CdTe have been deposited on FTO substrate via tellurization-assisted CVD process (Zhu et al. 2014). The authors of this work developed a procedure to synthesize the nanoflake arrays by using a CVD furnace. In the first step, they deposited Cd nanoflakes on FTO substrate by using CdS powder in the furnace heated up to 710 °C under 300 sccm gas flow. In the second step, the as-prepared Cd nanoflakes were rinsed to remove the adsorbed molecules followed by put-in-heating (PIH) process of the precursors (Cd nanoflakes and Te powder) taken place at 420 °C. The PIH is rapid heating process to carry out tellurization of pre-deposited Cd nanoflakes without disturbing the morphology and

by avoiding oxidation. The prepared CdTe nanoflake arrays were regular in shape, high in purity and exhibited excellent photo-response properties.

The addition of Bi powder to use it as a catalyst has been found advantageous for deposition of CdTe nanostructures by several groups. The Bi-assisted controlled growth of CdTe NWs and fabrication of hierarchical CdSe/CdS nanostructures in CVD furnace has been carried out (Heo et al. 2015). The NWs grown with only Au catalyst or Bi catalyst were observed short and having low aspect ratio. The Bi-assisted growth in the presence of Au was found highly useful as it has strongly influenced the morphology, uniformity, and aspect ratio of the NWs. Moreover, the temperature of 460 °C was found suitable to produce high aspect ratio NWs of CdTe. These observations pointed out possibility of controlling the dimensions and morphology of CdTe NWs upon optimizing the catalyst and deposition temperature. After production of thin films of CdSe NWs, the coating of CdS NWs on the film was carried out to fabricate hierarchical nanostructure for use as photodetector. The structure CdTe/CdS was obtained in such a way that n-type CdS NWs were in the form of backbone on which p-type CdTe NWs were randomly oriented as branches. The device characterization to measure photodetection performance indicated that photo-responsivity of CdTe/CdS nanostructures was 100 times higher than that of individual CdTe NWs.

The production NBs of CdTe-doped with Sb has been reported (Huang et al. 2015). The grown NBs were nearly stoichiometric, single crystalline oriented in [200] axis, homogeneously doped and zinc blend in structure. These NBs have been found with length 10–30 μm and width of 100 nm–1 μm (Fig. 4.7a). The electrical characterization of the doped NWs carried out in FET configuration revealed p-type character of the material. On the basis of low temperature photoluminescence measurements of the doped NWs, the emission found at 1.59 eV was identified as free exciton transition. The persistent photoconductivity and temperature cycle measurements were carried out which points to the presence of lattice relaxation related AX deep level center in the NWs. The compensation effects in CdTe NBs caused by Sb doping have been described in detail.

The synthesis of CdO nanostructures by utilizing CVD process has also been reported by several groups. The needle-like nanomaterials of CdO produced by CVD have been reported (Liu et al. 2003b). The authors explained the deposition of the material in terms of VLS mechanism. The substrate is heated at 850–900 °C to trigger the catalytic process of gold followed by heating of Cd source at 350 °C to generate Cd vapors. In this way due to reaction of Cd vapors and Au particles, the undersaturated alloy in the form of Au–Cd liquid droplets is formed. However, due to available supply of Cd vapors in the furnace, a stage comes when quantity of Cd in alloy droplets supersaturates that result into nucleation of Cd. At this stage, Cd reacts with oxygen to produce CdS NWs. Besides this VLS mechanism, the direct reaction of Cd vapors and oxygen also takes place to add into yield of the nanostructures. The grown materials were characterized for optical and electrical properties on the basis of which CdO nanoneedles were found suitable for IR detectors. Furthermore, CdO nanoneedles were found sensitive for gas sensing and demonstrated good performance for detection of NO_2. Another effort has been

Table 4.1 Growth parameters used for growth of Cd containing nanomaterials by employing VLS mechanism in CVD process

Material deposited	Substrate	Precursors	Deposition temperature °C	Ambient	Reference
CdS NCs	SiO_2	$CdCl_2$ $K(S_2COCH(CH_3)_2$	473–723	N_2 at 150 sccm	Barreca et al. (2004)
CdS NWs and nanocombs	Silicon	$CdCl_2$ and S powder	650	Ar at 100–150 mL/min	Ge et al. (2004)
In:CdS nano	Au-coated Silicon	CdS powder	800	Ar at 200 sccm	Ma et al. (2006)
CdS NCs	Silicon	$CdCl_2$ Polysulfide	400	N2 flux was kept at 200 sccm	Zheng et al. (2008)
CdS NCs as rods, wires and belts	Au-coated Quartz	CdS powder	501–630	Ar at 90 sccm	Green et al. (2008)
CdS NBs	Au-coated Silicon	CdS powders	850	Ar gas at 200 sccm	Wu et al. (2009)
CdS nanobands and NWs	Au-coated Silicon	CdS powder	600–720	Ar gas	Geburt et al. (2012)
CdS NCs	Silicon	CdS powder	1000	Ar (90%) and H2 (10%) at 10 sccm	Liu et al. (2013)
CdS nanosheets	Silicon	CdS powder	850	Ar at 150 sccm	Ye et al. (2012)
Ni:CdS nanoribbons	Au-coated Silicon	CdS and Ni $(OH)_2$ Powder	820	Ar (90%) and H_2 (10%) at 50-60 sccm	Kamran et al. (2013)
CdS nanostructures	fluorine-doped tin oxide (FTO)	CdS powder	715	N_2 at 200 sccm	Yi et al (2014)
Sn:CdS comb-like nanostructures	Au-coated Silicon	CdS and SnO_2 powders	1000	Ar (90%) and H_2 (10%) at 10 sccm	Song et al. (2015)
CdS NRs	Si/SiO_2	Sulfur and cadmium powders	700	Ar at 30 sccm	Zhao et al. (2017)
CdSe NBs	Au-coated Silicon	CdSe powder	700	Ar at 100 sccm	Liu et al. (2009)
$CdSe/SiO_2$ nanocables	Au-coated Silicon	CdSe powder	900	Ar at 150 sccm	Ye et al. (2011)

(continued)

Table 4.1 (continued)

Material deposited	Substrate	Precursors	Deposition temperature °C	Ambient	Reference
CdSe NWs and NRs	Silicon/SiO_2	$CdCl_2$ and Se powders	600	H_2 at 25 sccm	Wu et al. (2012)
CdSe NBs and NWs	Au-coated SiO_2	CdSe and Bi powders	650	Ar gas	Heo (2016)
CdSe and CdTe NWs	Polyimide, glass, ITO and Teflon	$CdMe_2$, $(TMS)_2Se$, $(TMS)_2Te$, Bismuth pellets, indium wire	400	N_2 at 200 cc/min	Lee et al. (2009)
CdTe NWs	Au-coated Silicon	Te powder and Cd shots	600	Ar at 150 sccm	Ye et al. (2010)
CdTe NWs and NRs	graphite	CdTe and Bi powders	800	Ar at 50 sccm	Hou et al. (2011)
CdTe NWs	Au-coated Silicon	CdTe powder	465	H_2 at 10 sccm	Huang et al. (2014)
CdTe nanoflakes	FTO	CdS and Te powder	710	99% Ar and 1% O_2 at 300 sccm	Zhu et al. (2014)
CdTe NWs and CdTe/CdS nanostructures	Au- or Bi-coated SiO_2	CdTe and Bi powders	650	Ar at 300 sccm	Heo et al. (2015)
Sb:CdTe NBs	Au-coated Silicon	CdTe and Sb powders	470	H_2 at 10 sccm	Huang et al. (2015)
CdO nanostructures	Au-coated Si/SiO_2	Cd powder	350	Ar and O_2	Liu et al. (2003b)

carried out to grow CdO nanoneedles using CVD technique for detection of toxic gases (Liu et al. 2003a). The device prepared using single nanoneedle exhibited high conductance and carrier concentration. Moreover, the device showed good performance as IR detector and sensor of diluted NO_2 gas.

Owing to simplicity and availability of several options to optimize the growth parameters, CVD is one of the popular techniques used for growth of thin films. The growth parameters used for growth of Cd containing nanomaterials by employing VLS mechanism in CVD process are listed in Table 4.1. The survey of literature pointed out the presence of sufficient literature on CVD growth of CdS, CdSe, CdTe, and CdO nanomaterials. The dimensions, shape, morphology, film thickness, stoichiometry, and crystalline quality of the CVD grown nanomaterials are found strongly dependent on precursor materials, substrate, deposition temperature, ambient used, catalyst, geometrical arrangements within furnace, etc.

4.5 Magnetron Sputtering

One of the very popular and resourceful physical vapor deposition techniques is referred as magnetron sputtering which is known to offer high uniformity, control over composition and thickness, less radiation damage, deposition of virtually any material, and strong adhesion of the film to the substrate. Its technology has reasonably developed over the years and currently, it has been preferentially employed for high quality industrial applications including wear-resistant, surface hardening, low friction, decorative and corrosion-resistant coating as well as deposition of films for academic and research purposes (Constantin et al. 2011).

The process of sputtering involves basically removal of atoms, clusters or molecules from suitable solids upon bombardment of energetic ions, particles or radiations. The steps of the process include plasma production, acceleration of ions, sputtering and adsorption of atoms on the substrate to finally produce the resulting film. In the technological development of sputtering deposition, several types of systems evolved which include diode sputtering, ion beam sputtering, hybrid sputtering, and magnetron (RF and DC) sputtering.

The deposition mainly involves creation the plasma and acceleration of ions towards target substrate. In order to improve the process, magnetron sputtering is employed where magnetic field is used and deposition is carried out in high vacuum (Kelly and Arnell 2000). An RF sputtering system has resemblance with capacitor having an inert gas as dielectric. The substrate onto which film needs to be deposited is made negative to act as cathode whereas the Ar atoms are introduced into the chamber which has a target containing source material as cathode whereas substrate is made anode. In the process of creating the plasma, accelerated free electrons collide with neutral Ar atoms and convert them into Ar+ ions. The ions accelerate towards cathode and strike the surface of target to release the neutral particles of source material during an energy transfer mechanism. Upon ejection, these particles rush in straight line towards anode and deposit on the substrate to produce the required coating (Fig. 4.8).

An extension to magnetron sputtering is high power pulsed magnetron sputtering in which power is given to the cathode target in pulses (Sarakinos et al. 2010). It results in production of highly dense plasma and efficient ionization as well as sputtering which leads to upgraded migration of sputtered particles to provide smooth, dense, and high grade coating of substrate. In addition to these sputtering strategies, some further interventions including reactive sputtering, ion poisoning, and closed field unbalanced magnetron sputtering have also been utilized (Kelly and Arnell 2000).

The operation of power source in RF and DC magnetron sputtering needs to be understood when efficiency of coating is considered. As the Ar+ ion hits the source material on cathode, an electron is ejected to neutralize the ion. As a result, the surface becomes positively charged due to which no further ions are attracted towards it and the available plasma quenches to shut down the sputtering process.

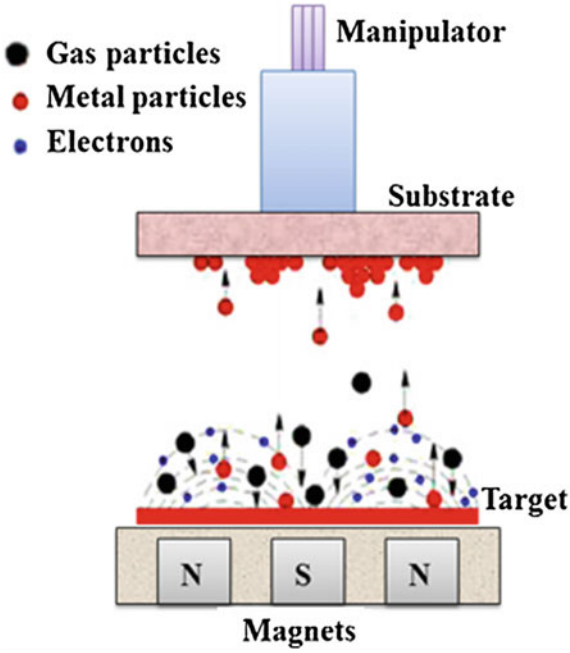

Fig. 4.8 **a** Schematic diagram showing dc magnetron sputtering mechanism (Castro et al. 2010)

Therefore, an AC or pulsed power source is required to remove the positive charge build up on the surface of insulating targets in order to keep attracting the Ar+ ions and continue the sputtering. Due to this reason, the efficiency of sputtering is comparatively smaller in case of DC power supply.

Keeping in view the advantages of coating via RF magnetron sputtering, the deposition of Cd containing nanomaterials is common for research and industrial purposes. The deposition of thin films containing CdS nanocrystallites of 2–5.36 nm average size was carried out using RF magnetron sputtering (Ghosh et al. 2007). The deposited films were transparent and it was observed that crystal quality as well as direct band gap of the films increases with increase in deposition time. The thin films comprising of CdS and CdS–ZnO NCs exhibiting noticeable photoconductivity, photostability and very fast photo-response have been deposited using high pressure RF magnetron sputtering (Vasa et al. 2001). The same two-component semiconducting NCs having 2–3 nm grain size have also been deposited on silicon substrate using high pressure magnetron sputtering (Ayyub et al. 2005). These nanocomposites exhibited very high photoluminescence and faster relaxation dynamics when compared with component NCs of CdS and ZnO.

The growing interest in nanotechnology during last couple of decades owes to potential applications of nanomaterials in electronic and optoelectronic devices. When a material is downscaled to nanometer range, the electrons are confined to cause the quantization. This structural size dependence of discreteness of energy levels is known as quantum confinement and is a major tool to investigate the

properties of nanomaterials. In order to study the quantum confinement effects in CdTe crystals, the nanocrystallites of 4.6-15.8 nm average size were deposited on glass using sequential RF magnetron sputtering (Potter and Simmons 1990). The deposited films having thickness up to 4.5 μm were tested for applications in planer waveguiding and exhibited superior excitonic properties when compared with bulk counterpart.

Quantum size and semiconductor volume fraction effects on the intensity, line width, and position of photoluminescence (PL) peaks from CdTe nanocrystallites have been measured. CdTe-glass composite thin films were grown by using a sequential RF magnetron sputtering process. Post-deposition heat treatments were used to produce average crystallite sizes between 1.2 and 16 nm. The PL spectra consist of single, broad peaks that undergo larger blue shifts with decreasing crystallite sizes. The PL signals degrade with increasing the nanocrystallite size and are quenched at the higher semiconductor volume fractions. The spectral characteristics of the clusters are discussed in terms of the electron–hole pair and the effect of surface states (Ochoa et al. 1996). The quantum confinement effects were also investigated on CdTe NCs passivated by TiO_2 passivated NCs prepared using composite TiO_2:CdTe target via RF magnetron sputtering (Rastogi et al. 2000). The strong dependence of optical band gap on crystallite size was explained on the basis of nucleation-dependent growth of CdTe NCs and passivation by TiO_2 NCs. A strong quantum confinement in RF magnetron sputtering grown films comprising of CdTe:TiO_2 having high volume fraction of CdTe NCs has also been studied (Sharma et al. 2005). The measured values of absorption edge were slightly different than the predicted values, explained in terms of presence of oxygen and inhomogeneity of size of NCs in the film.

Unlike other CdS, CdSe, and CdTe which are preferably deposited using RF magnetron sputtering, the nanostructures of CdO are usually grown on glass using a single target Cd in DC reactive magnetron sputtering system in oxygen environment (Dhivya et al. 2014). After growth of such films, the shape of grains of the material was observed to change from spherical to elliptical shape with increase in thickness of the film. The band gap of the films was observed consistently decreased with increase in film thickness and the films were tested for ammonia sensing. The same group has prepared these materials for methane sensing and demonstrated dependence of sputtering power on variation in crystallographic orientation of the deposited films (Dhivya et al. 2015). Several efforts have also been reported to modify the properties of CdO nanostructures after doping. The nanostructures of CdO-doped with Cr have been deposited on glass substrate using DC reactive magnetron sputtering technique (Hymavathi et al. 2014). The optical transmission and band gap of the films are reported to increase with increase in substrate temperature which has been assigned to increase in crystal quality of the material. The same group further deposited these films using their system under variable oxygen flow rate and observed growth of columnar structures whose width decreases with rise in oxygen flow rate (Hymavathi et al. 2015).

4.6 Reactive Sputtering Deposition

Reactive sputtering is a modified strategy to deposit thin films by employing magnetron sputtering deposition system. The major difference is availability of gases in the chamber instead of vacuum to assist the process of deposition as a result of chemical reaction. The target is sputtered in presence of mixture of gases in the form of Ar (main carrier gas) and oxygen (reactive gas) usually when deposition of oxides (e.g., CdO) is required. This technique has become popular for industrial coating of variety of films and is renowned to produce high quality deposits with excellent finish. However, unlike other techniques, not a reasonable number of research reports are available on reactive sputtering deposition of Cd containing semiconducting nanomaterials.

A comparative study of CBD and RF magnetron sputtering synthesis of CdS NCs has been conducted (Liang and Wang 2012). The characterization results pointed out superior structural and morphological properties of the films grown using RF sputtering. The deposition of Cr-doped nanocrystalline CdO films has been deposited on glass using DC reactive magnetron sputtering technique (Hymavathi et al. 2014). The deposition carried out at different substrate temperatures revealed that the grain size, optical transmission, and band gap increase with increase in the temperature. Moreover, as per electrical characterization, electrical resistivity of the films decreases with increase in substrate temperature. The same group repeated the study to investigate the effects of variable oxygen flow rates on physical properties of Cr-doped CdO NCs by employing DC reactive magnetron sputtering (Hymavathi et al. 2015). The authors observed a decrease in crystallite size and increase in strain as well as dislocation density with increase in oxygen flow rate while deposition of the films. The electrical resistivity and optical band gap of the material were observed consistently increased with increase in oxygen flow rate of the deposits.

Oxygen incorporated nanocrystalline CdS thin films have been prepared using RF sputtering technique at different RF powers (Islam et al. 2015). The experiment was performed at different values of RF power which revealed an increased incorporation of oxygen with decrease in RF power. With increase in oxygen content in the film, crystalline quality was reduced but band gap increased. The authors mentioned substitutional incorporation of oxygen atoms on S sites to reveal donor type behavior upon the observed increase in carrier concentration in the films.

4.7 Glancing Angle Deposition

The glancing angle deposition (GLAD) or oblique angle deposition (OAD) or ballistic deposition is a physical vapor deposition (PVD) in which source is inclined at an angle with the substrate (Barranco et al. 2016). Though, GLAD is being used for

more than a century but due to recent technological implementation and computer controlled orientation of substrate, it has emerged as reliable deposition strategy during last two decades. The majority of scientific material related to GLAD which includes theory, apparatus, historical developments, applications, comparison with other techniques and challenges has been comprehensively reviewed in literature (Taschuk et al. 2010; Hawkeye et al. 2014; Barranco et al. 2016). GLAD due to its promising features is highly resourceful deposition technique and offers numerous degrees of freedom in fabrication of nanostructures. The salient features of this technique include growth of nanocolumnar structures of controlled geometry, morphology, porosity etc. During the process of deposition, columnar structures are obtained whose shape is controlled by rotation of the substrate. A distinction of deposition using GLAD is availability of lateral growth rate which offers self-alignment and lateral sculpturing effects to give additional control over morphology of the grains of the films. The glancing angle gives control over shape of the columns whereas the pitch of deposition (ratio of deposition rate to substrate rotational rate) determines the vertical morphology of columns (Zhao et al. 2003). Owing to high quality of GLAD outcomes, the deposited thin films have been utilized in variety of devices including electronics, optoelectronics, sensing, catalysis, data storage, charge storage, electrochemical, and energy applications.

The initial stages of this technique are based on OAD in which incidence of source beam is set at an angle with the normal to the surface of the substrate. As the deposition starts, the initially striking atoms start formation of nucleation islands on the surface of the substrate. After this, for the next coming atoms, these islands become shadowing centers due to which taller islands receive more atoms and their growth turns into columnar structures on the substrate. Though thin films with nanocolumnar structures of porous nature are obtained but tilting angle of the columns causes anisotropy in the deposited layers which has issues with control, orientation, and reproducibility. The intervention made in order to handle this issue involves rotation of the substrate which transforms the OAD into GLAD. The rotation of the substrate is controlled by two stepper motors to monitor the azimuthal angle and incidence angle (Fig. 4.9). The computer control of these two orientations, speed of rotation and deposition rate provide degrees of freedom whose proper selection results into a variety of shapes including C, S, and zigzag along with different morphologies like matchstick, helical, and twisted columns (Zhao et al. 2003).

Owing to variety of technological applications of nanocolumnar structures, several groups have deposited nanocolumnar thin films but similar work on GLAD deposition of Cd containing nanomaterials is very limited. Recently, CdS nanocrystallites deposited on glass and ITO-coated glass substrates using GLAD have been reported (Daza et al. 2017). The samples were synthesized at different incidence angles by keeping both source and substrate rotating which resulted in production of dense nanocolumns of hexagonal structure.

The work on GLAD deposition of pure and composite nanocolumnar structures based on CdS, CdSe, CdTe, and CdO is yet to be carried out. The materials will be of potential use for electrochemical, optoelectronic, and energy applications.

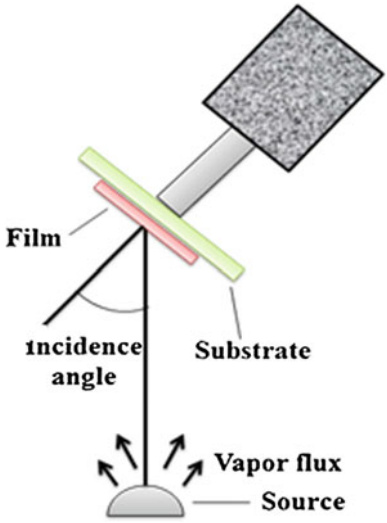

Fig. 4.9 Schematic diagram showing principle of GLAD (Borhani-Haghighi et al. 2016)

4.8 Spark Discharge Generation

Spark discharge generation (SDG, also known as spark ablation) is an energy proficient synthesis technique in which plasma channel is applied between two conducting electrodes. This method has a very straightforward design in a chamber with electrode pairs positioned parallel, a DC power supply (a basic resistance, capacitance, and inductance RCL circuit) to produce repeated sparks. The electric spark is used to evaporate the electrode material and then it is moved from the heated gap area through carrier gas. Use of electric arcs to provide the high temperature gives the reduction in total gas throughput. The energy of the spark is roughly proportional to the capacitance and square of discharge voltage. Plasma channel is formed between the electrodes with every spark and the spark recurrence frequency is proportional to the charging current (Tabrizi et al. 2009; Hontañón et al. 2013).

Due to high temperature of plasma, ions from cathode, anode, and carrier gas are bombarded on electrodes removing the electrode material (Wagner et al. 2016). When these vapors are cooled and combined with carrier gas, then nanoclusters formation takes place. These clusters then agglomerate to form the compact particles and agglomeration can be avoided by controlling the carrier gas flow. There are some other factors that can affect the particle formation process like electrode material, discharge frequency, electrode distance, and geometry of chamber, kind of carrier gas, and pressure of gas.

This technique has many advantages because of proficiently adaptation of electrodes into the NPs and reprocessing of non-heated carrier gas as high quality products (Heurlin et al. 2012), environment friendly (Slotte et al. 2015) and cost-efficient manufacturing process. The avoidance of chemicals (because of using inert gas) is one of the key benefits of SDG. This method is eco-friendly, as no

chemical starting agents, no chemical waste, and neither requirement to handle it. The material used in electrode is transformed into NPs during the process and small amount of unprocessed material and unused carrier gas can be recycled. NPs with high quality, high purity, and well-defined size can be achieved due to direct check throughout the particles formation process. NPs particularly having size less than 10 nm are formed with high energy efficiency. No expensive precursors are required, only with efficient conversion of electrode material into NPs, so this is an eco-friendly technique. SDG positioned parallel gives a higher output over a lower cost formation process for nanoparticles synthesis. The final benefit is the fully enclosed arrangement for processing that prevents health risks with a very low chance of unnecessary particles production.

A pure nanostructured cadmium sulfide has been synthesized with a temperature of 150 °C (Karami and Kaboli 2010). Size of cadmium sulfide particles and their morphology has also been studied by scanning and transmission electron microscopes as well by X-ray diffractometer. Cadmium sulfide NPs formed indeed showed excellent nanofibers having uniformity. SEM imaging showed that less concentration increases uniformity whereas particle growth and agglomeration rates were reduced. XRD of cadmium sulfide NPs indicates that at higher pH values, synthesized samples have cadmium hydroxide.

4.9 Spray Pyrolysis Deposition

The spray pyrolysis deposition (SPD) is a simple and cost-effective deposition technique based on chemical synthesis method in which layer of thin film is deposited on the surface of substrate by spraying the solution. This technique is used for deposition of mono or multilayer thin films having high density, controlled thickness, and usually porous structure. A speciality of this technique is the preparation of the product material in the form of porous or dense powder comprising of ultrafine grains. This capability of spray pyrolysis makes it a suitable technique for synthesis of nanomaterials.

The processing via this technique basically consists of spraying the precursor solution onto the surface of heated substrate. For controlled deposition of the desired products, the growth process is carried out in thermally insulated chamber equipped with necessary components. In this technique, the initial solution is prepared by melting the metal salt into a solvent. The small droplets of solution are then atomized into the furnace where the velocity and concentration of these droplets establish the morphology and size of the grown NPs. In this method, the characteristic solvent evaporation time and characteristic solute diffusion time are important and define the deposition rate and quality of grown layers. The product composition can be controlled by composition of reactants in precursor solution, growth parameters, and dynamics of the chemical reaction. The product particle will be a porous material or a hollow particle, the morphology of the particles is decided by the characteristic times. Temperature plays an important role in

determining the density of the nanomaterial, higher density gives the further spherical shape of the particles. The influence of growth parameters on the properties of the product in the form of thin films or powder can be found in literature (Perednis and Gauckler 2005). Spray pyrolysis is comparatively low-cost, eco-friendly, scalable and can be appropriate for a variety of substrate.

The apparatus required for SPD comprises of precursor in solution form, substrate holder, electrical heaters, temperature controller, cooling system, filters, spray nozzle or atomizer, and thermally insulated chamber (Kozhukharov and Tchaoushev 2013). The option to adjust the opening of nozzle tip offers the control on particle size of the product which points to suitability of this technique for growth of NPs. The deposition rate and quality of the product strongly depend upon the processes, equipment, and growth parameters. Though, several atomizers have been tested but air blast, ultrasonic, and electrostatic type atomizers have been commonly utilized. The schematic diagram showing spray pyrolysis process is sketched in Fig. 4.10.

SPD is a solution-based chemical technique but the films deposited using this technique should be different in properties when prepared using other similar chemical synthesis techniques. In order to investigate this assertion, Hiie et al. carried out a comparative study to deposit thin films of CdS nanostructures on glass using SPD and CBD techniques (Hiie et al. 2006). The electrical characterization

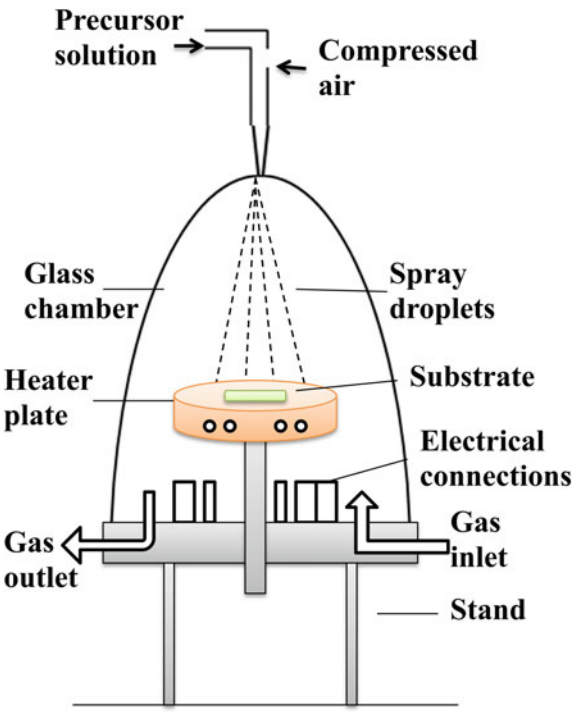

Fig. 4.10 Schematic diagram for spray pyrolysis system (Gunjal et al. 2014)

was carried out which revealed smaller value of dark resistivity of CdS/ITO films prepared using CBD in comparison to that of SPD technique. The thermal annealing treatment appeared to reduce the electrical resistivity of SPD prepared CdS/glass film. The films deposited using both techniques exhibited same band gap per photoluminescence measurements but the PL band of SPD prepared films was broader in width. The width of PL band in case of SP prepared film reduced after annealing pointing towards crystalline improvement. Another comparative effort has been reported when Marathe et al. prepared CdS nanocrystalline films using two chemical synthesis routes of sol-gel and SPD (Marathe and Shrivastava 2011). The band gap of the films was 3.25 and 2.87 eV when deposited using sol-gel and SPD, respectively. The photocatalytic and photodegradation investigations were carried out on the deposited films. The rate of degradation studied for different Cr concentrations revealed higher photo-decomposition efficiency of films prepared using sol-gel as compared to that of SPD.

The thin films of nanocrystalline CdS have been prepared by SPD technique on FTO-coated glass substrate (Yadav et al. 2010a). The films were grown at different temperatures 275, 300, 325, and 350 °C in order to study the effects of substrate temperature on quality of films. The grown films were stoichiometric, polycrystalline in nature, having hexagonal structure and contain uniformly distributed, and uneven spherical grains of size about 120 nm. The films deposited at 300 °C were n-type semiconducting with direct band gap of 2.44 eV and have minimum resistivity. The grown materials were found suitable for applications in optoelectronic devices. Thin films of pure CdS- and Al-doped CdS NCs have been deposited on glass via SPD technique (Rubel and Podder 2011). There were no considerable changes in morphology of CdS thin films after doping with Al. It was observed that doping increases carrier concentration and reduces electrical conductivity. The variations in grain size, electrical conductivity, carrier mobility and carrier concentration with increase in Al doping concentration were described.

Thin films of nanocrystalline CdS were synthesized by Yadav et al. through SPD technique by using combination of solutions of CH_4N_2S and $CdCl_2$ on preheated FTO covered substrates of glass (Yadav and Masumdar 2011). An increase in crystal quality was observed when substrate temperature was raised to 300 °C. The fabricated n-CdS films were utilized as photoanode along with counter electrode of graphite and a reference electrode of calomel to prepare photo-electro-chemical cell. The study of photovoltaic characteristics indicated an increase in short circuit current density and open circuit voltage when measured for films grown at increasing temperature up to 300 °C. The value of flat band potential was also observed with change in substrate temperature and this variation was interpreted in terms of decrease in electron affinity and increase in surface adsorption. Hasnat et al. carried out a study to investigate the effects of annealing on properties of nanocrystalline CdS thin films grown via SPD technique (Hasnat and Podder 2012). Thermal annealing of the films strongly influenced the properties of as-grown films. The as-deposited films were uniform but the annealing has increased the surface roughness of the films. Moreover, lattice constant and grain size increased consistently with increase in annealing temperature of the films. On the other hand,

optical transmission measurements revealed decrease in band gap of the material with increase in annealing temperature of the films.

In order to study Pb doping dependent modifications in properties of nanocrystalline CdS, the pure and Pb-doped films were prepared using SPD technique (Anbarasi et al. 2016). The XRD analysis of the films indicated that the crystalline quality of the material degraded with increase in concentration of Pb doping in CdS NCs. Moreover, a linear decrease in crystallite size with doping concentration was noticed. Despite the observed crystalline degradation, the doping did not cause any change in basic crystalline structure of the host material. The lattice constant of host material was observed to increase after Pb doping which is assigned to strain induced due to substitution of larger sized dopant Pb^{2+} in place of host cation Cd^{2+}. The analysis of morphology pointed out transformation of irregularly shaped nanosized grains of pure CdS into nanoneedles after doping with Pd. The optical transmission studies showed the variations in band gap of the material after doping. The band gap was reduced for doping concentrations of 2 and 4wt% but its value was observed to increase for films containing doping concentration of 6 and 8wt%.

Another effort reporting the effects of doping on properties of CdS NCs is found in literature. SPD preparation of Cu-doped CdS nanocrystalline films has been reported for photocatalytic applications (Su et al. 2016). It was found that the grain size of the films depends upon metal nitride concentration in the precursor solution. It was observed that crystallite size consistently decreases with increase in Cu doping concentration. The band gap of Cd was observed to increase after Cu doping which was assigned to filling of intrinsic vacancies pointing towards crystalline improvement. SEM images of pure CdS- and Cu-doped CdS NPs have been shown in Fig. 4.11. The PL spectrum pointed out decrease in excitonic emission as well as appearance of new emission band after doping. The new peak was assigned to Cu acceptor level appearing from triplet charge state of the dopant. The deposited materials were photocatalytically characterized for hydrogen evolution and it was found that Cu doping has enhanced the efficiency of hydrogen production of CdS films. The findings of this study revealed suitability of SPD technique for large-scale preparation of CdS nanomaterials for use in photocatalytic applications.

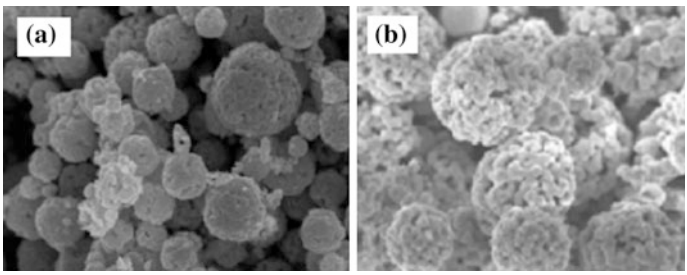

Fig. 4.11 SEM images of **a** CdS and **b** Cu-doped CdS NPs prepared through SPD (Su et al. 2016).

Since SPD is a solution-based chemical deposition method, the nature of solution plays major role in determining the quality of grown materials. Recently, Kerimova et al. deposited CdS nanocrystalline films at different pH values of the solution using SPD technique (Kerimova et al. 2017). The films grown at pH values of 6.7 and 9.5 were of wurtzite crystal structure whereas the film grown at pH value of 10.2 was nearly amorphous. On the basis of structural and optical characterizations, it was concluded that crystallinity and grain size of SP deposited films decrease with increase in pH value of the solution used.

Recently, another study has been carried out to prepare CdS NCs using SPD technique at variable substrate temperatures (Diwate et al. 2017). The deposition rate was found strongly dependent upon substrate temperature. It was observed that the thickness of grown films consistently decreases with increase in temperature of the substrate. This finding was interpreted by taking the size of droplet into account when it reaches the surface of substrate. The size of droplet reaching the substrate is inversely proportional to the substrate temperature. Moreover, the crystallite size was found directly proportional to substrate temperature due to temperature dependence of formation of nucleation centers in the growth process. At higher substrate temperatures, the grains of the films converted into very dense clusters of clear grain boundaries. The measurement of optical properties revealed an increase in band gap with increase in substrate temperature. The effects of deposition parameters on quality of CdSe films grown by PSD have also been studied. Yadav et al. have deposited CdSe films comprising of nanograins by using PSD technique at different temperatures (Yadav et al. 2010b). It was observed that crystallinity of grown films decreased with increase in temperature up to 300 °C. The deposited films were having dense and uniform coverage of nanograins throughout without cracks. The optical and electrical properties of the films were found dependent of substrate temperature.

SPD technique has been applied to deposit $Cd_{0.5}Fe_{0.5}Se$ NCs on glass (Ibrahim and Ubale 2014). The grown films were found porous, hexagonal in structure and contain grains in form of uniformly and densely distributed NTs and nanodiscs. The properties of the deposited films were found dependent on quantity of solution used for spray. The grains in the form of nanoneedles were obtained for 15 mL solution whereas the shape of the grains was transformed to nanodiscs with increase in quantity of solution. Film thickness and band gap decreased whereas the crystallite size of the films increased with increase in the quantity of solution.

This technique has also been utilized for the deposition of CdTe nanocrystalline thin films for different purposes. The SPD preparation of p-CdTe films comprising of nanocrystalline grains for photo-electro-chemical applications has been reported (Nikale et al. 2011). The films have been deposited on FTO-coated glass under different synthesis conditions including substrate temperature as well as pH, concentration and quantity of the solution. The crystalline quality of the films was found to increase with increase in solution concentration which reveals the dependence of growth rate on the concentration. The crystallite size increased with solution centration until the value of 10 mL after which the size was reduced. Furthermore, the crystallite size shows dependence on substrate temperature and the

lowest size was obtained at the temperature of 250 °C was observed. In order to investigate photo-electro-chemical (PEC) performance, PEC cell was fabricated using the grown p-CdTe thereby creating electrodes. It was observed that the values of short circuit current and open circuit voltage of PEC cell increase with pH of the solution until pH = 10.5 after which these values decrease. The CdTe nanocrystalline films were deposited on glass using SPD technique using nitrogen as carrier gas (Gunjal et al. 2014). The average crystalline size of the films was 32 nm having crystalline orientation of [3 1 1] and [5 1 1]. The band gap measured for the films was 1.44 eV with direct nature whereas the maximum value of absorbance was 0.94. The nature of grown films was p-type semiconductor having resistivity about 2.228×10^{1} Ωcm. The authors found SPD method a simple and low-cost route for deposition of cadmium telluride films.

CdO nanocrystalline film has been deposited on glass via SPD and characterized for optical measurements (Naje 2013). The grown films were polycrystalline having average grain size of 24.4 nm and direct band gap of 3.46 eV. In another effort, nanocrystalline CdO films have also been prepared using SPD technique. Bari et al.

Table 4.2 Growth parameters used for growth of Cd containing nanomaterials by employing SPD process

Material Deposited	Substrate	Substrate temperature °C	Precursors	Spray rate ml/min	Reference
CdS NCs	ITO-coated glass	400	$CdCl_2I2.5H_2O$, $(NH2)_2CS$	2.5	Hiie et al. (2006)
CdS NCs	FTO-coated glass	275, 300, 325 and 350	$CdCl_2 \cdot H_2O$ H_2NCSNH_2	3	Yadav et al. (2010a)
CdS and Al: CdS NCs	Glass	300	$Cd(COOCH_3)_2$, (NH_2CSNH_2) and (Al $(CH_3COO)_3 \cdot 2H_2O$)	–	Rubel et al. (2011)
CdS NCs	Glass	250	$CdCl_2$ and Thiourea	3	Marathe (2011)
CdS and Pb: CdS NCs	Glass	400	$(CdCl_2)$, $(SC(NH)_2$, Pb (NO_3)	–	Anbarasi et al. (2016)
CdS NCs	Glass	400	$CdAc_2$, $(NH_2)_2CS$, (NH_4) Ac	–	Kerimova et al. (2017)
CdSe nanograins	Glass	275, 300, 325 and 350	$CdCl_2 \cdot H_2O$, H_2NC (Se)NH_2	3	Yadav et al. (2010b)
$Cd_{0.5}Fe_{0.5}Se$ nanoneedles and nanodiscs	Glass	573	Ferric chloride, $CdCl_2$, SeO_2	6	Ibrahim and Ubale (2014)
p-CdTe NCs	Glass	225–300	$CdCl_2$ TeO_2	1.5	Nikale et al. (2011)
p-CdTe NCs	Glass	350	$CdCl_2 \cdot H_2O$ TeO_2	5	Gunjal (2014)
CdO NCs	Glass	300	$(CH_3COO)_2Cd \cdot 2H_2O$	7	Bari and Patil (2014)
Zn:CdO nanostructures	Glass	300	Cd acetate dehydrates, Zinc acetate dihydrate	7	Bari et al. (2016)

have studied the effects of spray deposition time on quality of SPD grown CdO NCs deposited on glass substrate (Bari and Patil 2014). The authors observed an increase in crystallite size and film thickness with increase in spray deposition time during the growth process. It points that crystalline quality of the grown films is proportional to the spray time. The deposited films were also tested for electrical properties and sensing of several gases. The gas sensing response in case of LPG and CO_2 gases was found higher than other gases including H_2, NH_3, Cl_2, NO, and H_2S. The same group has reported another effort to use SPD technique for deposition of Zn-doped CdO nanostructures to prepare sensor for LPG gas (Bari et al. 2016). The deposited films contained mixed grains of spherical and cubical shapes whose size increased with increase in concentration of Zn doping. The value of optical band gap of the doped films exhibited a consistent trend of doping concentration dependent increase in band gap. On the basis of gas sensing response measurements, the authors reported Zn:CdO nanomaterial with 5% doping concentration as best sensor for LPG gas.

SPD is such a simple technique which is capable of producing films suitable for devices and several applications, but literature survey does not point out significant number of research reports on preparation of Cd containing nanomaterials using this technique. The growth parameters related to deposition of CdS, CdSe, CdTe, and CdO nanomaterials used by different workers are given in Table 4.2.

References

Abe, K., Eryu, O., Nakashima, S., Terai, M., Kubo, M., Niraula, M., et al. (2005). Optical emission characteristics of ablation plasma plumes during the laser-etching process of CdTe. *Journal of Electronic Materials, 34*(11), 1428–1431.

Al-Ghamdi, A. A., El-sadek, M. A., Nagat, A. T., & El-Tantawy, F. (2012). Synthesis, electrical properties and transport mechanisms of thermally vacuum evaporated CdTe nano-crystalline thin films. *Solid State Communications, 152*(17), 1644–1649.

Anbarasi, M., Nagarethinam, V. S., Baskaran, R., & Narasimman, V. (2016). Studies on the structural, morphological and optoelectrical properties of spray deposited CdS: Pb thin films. *Pacific Science Review A: Natural Science and Engineering, 18*(1), 72–77.

Aubret, A., Houel, J., Pereira, A., Baronnier, J., Lhuillier, E., Dubertret, B., …, & Pillonnet, A. (2016). Nondestructive Encapsulation of CdSe/CdS QDs in an Inorganic Matrix by Pulsed Laser Deposition. *ACS applied materials & interfaces, 8*(34), 22361–22368.

Ayyub, P., Vasa, P., Taneja, P., Banerjee, R., & Singh, B. P. (2005). Photoluminescence enhancement in nanocomposite thin films of CdS–ZnO. *Journal of Applied Physics, 97*(10), 104310.

Baghchesara, M. A., Yousefi, R., Cheraghizade, M., Jamali-Sheini, F., & Saáedi, A. (2016). Photocurrent application of Zn-doped CdS nanostructures grown by thermal evaporation method. *Ceramics International, 42*(1), 1891–1896.

Bari, R. H., & Patil, S. B. (2014). *Nanostructured CdO thin films for LPG and CO_2 gas sensor prepared by spray pyrolisis technique* (p. 18). Physics and Astronomy: International Letters of Chemistry.

Bari, R. H., Patil, S. B., & Deshmukh, S. B. (2016). Nanostructured spray Pyrolysis Zinc doped CdO thin films for LPG gas sensor. *Journal of Nanoscience and Technology, 2*(3), 181–185.

Barranco, A., Borras, A., Gonzalez-Elipe, A. R., & Palmero, A. (2016). Perspectives on oblique angle deposition of thin films: From fundamentals to devices. *Progress in Materials Science, 76,* 59–153.

Barreca, D., Gasparotto, A., Maragno, C., & Tondello, E. (2004). CVD of nanosized ZnS and CdS thin films from single-source precursors. *Journal of the Electrochemical Society, 151*(6), G428–G435.

Begam, M. R., Rao, N. M., Kaleemulla, S., Shobana, M., Krishna, N. S., & Kuppan, M. (2013). Effect of substrate temperature on structural and optical properties of nano-crystalline CdTe thin films deposited by electron beam evaporation. *Journal of Nano-and Electronic Physics, 5* (3), 3019.

Borhani-Haghighi, S., Khare, C., Trócoli, R., Dushina, A., Kieschnick, M., LaMantia, F., et al. (2016). Synthesis of nanostructured $LiMn_2O_4$ thin films by glancing angle deposition for Li-ion battery applications. *Nanotechnology, 27*(45), 455402.

Cai, J., Jie, J., Jiang, P., Wu, D., Xie, C., Wu, C., …, & Peng, Q. (2011). Tuning the electrical transport properties of n-type CdS NWs via Ga doping and their nano-optoelectronic applications. *Physical Chemistry Chemical Physics, 13*(32), 14663–14667.

Castro, C., Sanjines, R., Pulgarin, C., Osorio, P., Giraldo, S. A., & Kiwi, J. (2010). Structure–reactivity relations for DC-magnetron sputtered Cu-layers during E. coli inactivation in the dark and under light. *Journal of Photochemistry and Photobiology A: Chemistry, 216*(2), 295–302.

Chaudhary, K., Rizvi, S. Z. H., & Ali, J. (2016). Laser-induced plasma and its applications. In *Plasma science and technology-progress in physical states and chemical reactions*. InTech.

Chen, L., Fu, X., Lai, J., Sun, J., Ying, Z., Wu, J., et al. (2012). Growth of CdS nanoneedles by pulsed laser deposition. *Journal of Electronic Materials, 41*(7), 1941–1947.

Constantin, D. G., Apreutesei, M., Arvinte, R., Marin, A., Andrei, O. C., & Munteanu, D. (2011). Magnetron sputtering technique used for coatings deposition; technologies and applications. In *7th International Conference on Materials Science and Engineering* (*BRAMAT 2011*), Brasov, Romania, February (pp. 24–26).

Dai, G., Yang, S., Yan, M., Wan, Q., Zhang, Q., Pan, A., et al. (2010). Simple synthesis and growth mechanism of core/shell cdse/SiO_x NWs. *Journal of Nano-materials, 2010,* 5.

Dai, Q., Chen, J., Lu, L., Tang, J., & Wang, W. (2012). Pulsed laser deposition of CdSe QDs on Zn_2SnO_4 NWs and their photovoltaic applications. *Nano Letters, 12*(8), 4187–4193.

Dai, Q., Sabio, E. M., Wang, W., & Tang, J. (2014). Pulsed laser deposition of Mn doped CdSe QDs for improved solar cell performance. *Applied Physics Letters, 104*(18), 183901.

Daza, L. G., Castro-Rodríguez, R., Cirerol-Carrillo, M., Martín-Tovar, E. A., Méndez-Gamboa, J., Medina-Esquivel, R., …, & Iribarren, A. (2017). Nanocolumnar CdS thin films grown by glancing angle deposition from a sublimate vapor effusion source. *Journal of Applied Research and Technology*. doi:10.1016/j.jart.2017.02.003.

Dhivya, P., Prasad, A. K., & Sridharan, M. (2014). Magnetron sputtered nanostructured cadmium oxide films for ammonia sensing. *Journal of Solid State Chemistry, 214,* 24–29.

Dhivya, P., Prasad, A. K., & Sridharan, M. (2015). Effect of sputtering power on the methane sensing properties of nanostructured cadmium oxide films. *Journal of Alloys and Compounds, 620,* 109–115.

Diwate, K., Pawbake, A., Rondiya, S., Kulkarni, R., Waykar, R., Jadhavar, A., …, & Pathan, H. (2017). Substrate temperature dependent studies on properties of chemical spray pyrolysis deposited CdS thin films for solar cell applications. *Journal of Semiconductors, 38*(2), 023001.

Dongol, M., El-Denglawey, A., El Sadek, M. A., & Yahia, I. S. (2015). Thermal annealing effect on the structural and the optical properties of Nano CdTe films. *Optik-International Journal for Light and Electron Optics, 126*(14), 1352–1357.

Du, L., & Lei, Y. (2013). Synthesis of high-quality Cl-doped CdSe nanobelts and their application in nanodevices. Materials Letters, *106*, 100–103.

Eshraghi, M. J., & Naderi, N. (2016). Band-Gap tuning of electron beam evaporated Cds thin films. *Journal of Advanced Materials and Processing, 4*(7), 68–76.

Fan, L., Wang, P., Guo, Q., Lei, Y., Li, M., Han, & Yang, J. (2015). Improved stoichiometry and photoanode efficiency of thermally evaporated CdS film with QDs as precursor. *Nanotechnology, 26*(33), 335606.

Fu, X. L., Ma, Y. J., Li, P. G., Chen, L. M., Tang, W. H., Wang, X., et al. (2005). Fabrication of CdS/Si nanocable heterostructures by one-step thermal evaporation. *Applied Physics Letters, 86*(14), 143102.

Ge, J., & Li, Y. (2004). Selective atmospheric pressure chemical vapor deposition route to CdS arrays, nano-wires, and nanocombs. *Advanced Functional Materials, 14*(2), 157–162.

Geburt, S., Thielmann, A., Röder, R., Borschel, C., McDonnell, A., Kozlik, M., & Ronning, C. (2012). Low threshold room-temperature lasing of CdS NWs. *Nanotechnology, 23*(36), 365204.

Gevorgyan, V. A., Hakhoyan, L. A., Mangasaryan, N. R., & Gladyshev, P. P. (2016). Substrate temperature and annealing effects on the structural and optical properties of nano-CdS films deposited by vacuum flash evaporation technique. *Chalcogenide Letters, 13*(8), 331–338.

Ghosh, P. K., Ahmed, S. F., Saha, B., & Chattopadhyay, K. K. (2007, December). Effect of deposition time on optical properties of nano-crystalline CdS thin films synthesized via rf-sputtering technique. In *Physics of Semiconductor Devices, 2007. IWPSD 2007. International Workshop on* (pp. 410–412). IEEE.

Green, J. M., Lawrance, J., & Jiao, J. (2008). Controlled fabrication of high-yield CdS nanostructures by compartment arrangement. *Journal of Nano-materials, 2008,* 8.

Gunjal, S. D., Khollam, Y. B., Jadkar, S. R., Shripathi, T., Sathe, V. G., Shelke, P. N., …, & Mohite, K. C. (2014). Spray pyrolysis deposition of p-CdTe films: Structural, optical and electrical properties. *Solar Energy, 106*, 56–62.

Hampden-Smith, M. J., & Kodas, T. T. (1995). Chemical vapor deposition of metals: Part 1. An overview of CVD processes. *Chemical Vapor Deposition, 1*(1), 8–23.

Hasnat, A., & Podder, J. (2012). Effect of annealing temperature on structural, optical and electrical properties of pure CdS thin films deposited by spray pyrolysis technique. *Advances in Materials Physics and Chemistry, 2*(04), 226.

Hawkeye, M. M., Taschuk, M. T., & Brett, M. J. (2014). Introduction: Glancing angle deposition technology. *Glancing Angle Deposition of Thin Films: Engineering the Nanoscale,* 1–30.

Heo, K., Lee, H., Jian, J., Lee, D. J., Park, Y., Lee, C., …, & Hong, S. (2015). Bi-Assisted CdTe/CdS hierarchical nanostructure growth for photoconductive applications. *Nanoscale research letters, 10*(1), 331.

Heo, K., Lee, H., Kim, T., & Lee, B. Y. (2016). Structural control of photoconductive CdSe nanostructures through a Bi-assisted VLS process. *Materials Letters, 182,* 129–133.

Heurlin, M., Magnusson, M. H., Lindgren, D., Ek, M., Wallenberg, L. R., Deppert, K., et al. (2012). Continuous gas-phase synthesis of NWs with tunable properties. *Nature, 492*(7427), 90.

Hiie, J., Dedova, T., Valdna, V., & Muska, K. (2006). Comparative study of nano-structured CdS thin films prepared by CBD and spray pyrolysis: annealing effect. *Thin Solid Films, 511,* 443–447.

Hontañón, E., Palomares, J. M., Stein, M., Guo, X., Engeln, R., Nirschl, H., et al. (2013). The transition from spark to arc discharge and its implications with respect to nanoparticle production. *Journal of Nanoparticle Research, 15*(9), 1957.

Horoz, S., Lu, L., Dai, Q., Chen, J., Yakami, B., Pikal, J. M., …, & Tang, J. (2012). CdSe QDs synthesized by laser ablation in water and their photovoltaic applications. *Applied Physics Letters, 101*(22), 223902.

Hou, D. D., Liu, Y. K., Zapien, J. A., Shan, Y. Y., & Lee, S. T. (2008). High-quality single-crystal CdSe nanoribbons and their optical properties. *Optoelectronics Letters, 4*(3), 161–164.

Hou, J., Yang, X., Lv, X., Peng, D., Huang, M., & Wang, Q. (2011). One-step synthesis of CdTe branched NWs and nano-rod arrays. *Applied Surface Science, 257*(17), 7684–7688.

Hu, Z., Zhang, X., Xie, C., Wu, C., Zhang, X., Bian, L., …, & Jie, J. (2011). Doping dependent crystal structures and optoelectronic properties of n-type CdSe: Ga nanowries. *Nanoscale, 3*(11), 4798–4803.

Huang, L., Lin, C. C., Riediger, M., Röder, R., Tse, P. L., Ronning, C., et al. (2015). Nature of AX centers in antimony-doped Cadmium Telluride NBs. *Nano Letters, 15*(2), 974–980.

Huang, L., Lu, S., Chang, P., Banerjee, K., Hellwarth, R., & Lu, J. G. (2014). Structural and optical verification of residual strain effect in single crystalline CdTe NWs. *Nano Research, 7* (2), 228.

Hymavathi, B., Kumar, B. R., & Rao, T. S. (2014). Temperature dependent structural and optical properties of nanostructured Cr doped CdO thin films prepared by DC reactive magnetron sputtering. *Procedia Materials Science, 6,* 1668–1673.

Hymavathi, B., Kumar, B. R., & Rao, T. S. (2015). Investigations on physical properties of nanostructured Cr doped CdO thin films for optoelectronic applications. *Procedia Materials Science, 10,* 285–291.

Iacomi, F., Salaoru, I., Apetroaei, N., Vasile, A., Teodorescu, C. M., & Macovei, D. (2006). Physical characterization of CdMnS nanocrystalline thin films grown by vacuum thermal evaporation. *Journal of Optoelectronics and Advanced Materials, 8*(1), 266.

Ibrahim, R. A., Ahmed, N. A., & Mohammed, O. D. (2016). Preparation and study of colloidal CdO NPs by laser ablation in polyvinylpyrrolidone. *International Journal of Engineering and Technologies, 6,* 1–7.

Ibrahim, S. G., & Ubale, A. U. (2014). Size dependent physical properties of spray deposited nano-crystalline $Cd_{0.5}Fe_{0.5}Se$ thin films. *International Journal of Materials and Chemistry, 4* (1), 1–8.

Islam, M. A., Rahman, K. S., Haque, F., Rashid, M. J., Akhtaruzzaman, M., Sopian, K., …, & Amin, N. (2015, May). Nanostructured and wide bandgap CdS: O thin films grown by reactive RF sputtering. In *AIP Conference Proceedings* (Vol. 1660, No. 1, p. 070048). AIP Publishing.

Kamran, M. A., Liu, R., Shi, L. J., Zou, B., & Zhang, Q. (2013). Near infrared emission band and origin in Ni(II)-doped CdS nanoribbons by CVD technique. *The Journal of Physical Chemistry C, 117*(34), 17777–17785.

Karami, H., & Kaboli, A. (2010). Pulsed current electrochemical synthesis of cadmium sulfide nanofibers. *International Journal of Electrochemical Science, 5,* 706–719.

Kelly, P. J., & Arnell, R. D. (2000). Magnetron sputtering: A review of recent developments and applications. *Vacuum, 56*(3), 159–172.

Kerimova, A., Bagiyev, E., Aliyeva, E., & Bayramov, A. (2017). Nanostructured CdS thin films deposited by spray pyrolysis method. *physica status solidi* (*c*).

Khan, T., & BiBi, T. (2014). Application of NS pulsed laser ablation for dense CdS NPs deposition in argon atmosphere. *Sop Trans Appl Phys, 1*(2), 48.

Khudiar, A. I., Zulfequar, M., & Khan, Z. H. (2009). Laser radiation effects on optical and structural properties of nanostructure CdSe thin film. *Radiation Effects and Defects in Solids, 164*(9), 551–560.

Kissinger, N. J., Suthagar, J., Balasubramaniam, T., & Perumal, K. (2002). Effect of substrate temperature on the structural and optical properties of nano-crystalline cadmium selenide thin films prepared by electron beam evaporation technique. *Solid State Sci. and Technol, 17*(2), 208–219.

Kozhukharov, S., & Tchaoushev, S. (2013). Spray pyrolysis equipment for various applications. *Journal of Chemical Technology and Metallurgy, 48*(1), 111–118.

Lee, S. K., Yu, Y., Perez, O., Puscas, S., Kosel, T. H., & Kuno, M. (2009). Bismuth-assisted CdSe and CdTe nano-wire growth on plastics. *Chemistry of Materials, 22*(1), 77–84.

Li, C., Liu, Z., & Yang, Y. (2006). The selective synthesis of single-crystalline CdS NBs and NWs by thermal evaporation at lower temperature. *Nanotechnology, 17*(8), 1851.

Li, H., Chen, L., Zhao, Y., Liu, X., Guan, L., Sun, & Xu, N. (2014). Effects of experimental conditions on the morphologies, structures and growth modes of pulsed laser-deposited CdS nanoneedles. *Nanoscale research letters, 9*(1), 91.

Li, S., Li, X., & Zhao, H. (2013). Synthesis and electrical properties of p-type CdTe NWs. *Micro & Nano Letters, 8*(6), 308–310.

Liang, C. J., & Wang, Z. Z. (2012). Comparative study on thin films of cadmium sulfide prepared by chemical bath deposition and radio frequency magnetron sputtering. *Spectroscopy and Spectral Analysis, 32*(4), 1094–1097.

Liu, C., Wu, P., Sun, T., Dai, L., Ye, Y., Ma, R., et al. (2009). Synthesis of high quality n-type CdSe NBs and their applications in nanodevices. *The Journal of Physical Chemistry C, 113* (32), 14478–14481.

Liu, R., Li, Z. A., Zhang, C., Wang, X., Kamran, M. A., Farle, M., et al. (2013). Single-step synthesis of monolithic comb-like CdS nanostructures with tunable waveguide properties. *Nano Letters, 13*(6), 2997–3001.

Liu, X., Li, C., Han, S., & Zhou, C. (2003a). Synthesis of CdO nanoneedles for photonic and sensing applications. *MRS Online Proceedings Library Archive,* 776.

Liu, X., Li, C., Han, S., Han, J., & Zhou, C. (2003b). Synthesis and electronic transport studies of CdO nanoneedles. *Applied Physics Letters, 82*(12), 1950–1952.

Ma, C., Ding, Y., Moore, D., Wang, X., & Wang, Z. L. (2004). Single-crystal CdSe nanosaws. *Journal of the American Chemical Society, 126*(3), 708–709.

Ma, R. M., Dai, L., Huo, H. B., Yang, W. Q., Qin, G. G., Tan, P. H., …, & Zheng, J. (2006). Synthesis of high quality n-type CdS NBs and their applications in nanodevices. *Applied physics letters, 89*(20), 203120.

Mahajan, R. L. (1996). Transport phenomena in chemical vapor-deposition systems. *Advances in Heat Transfer, 28,* 339–425.

Marathe, Y. V., & Shrivastava, V. S. (2011). Synthesis and Application of CdS nano-crystaline thin films. *Advances in Applied Science Research, 2*(3), 295–301.

Mohamed, R. B., Nasina, M. R., Shaik, K., Narayananellore, S. K., & Kuppan, M. (2014). Structural and magnetic properties of Co diffused CdTe nano-crystalline thin films deposited by electron beam evaporation. *Journal of Superconductivity and Novel Magnetism, 27*(9), 2147–2152.

Naje, A. N. (2013). Optical characteristics of CdO nanostructure. *Physical Review & Research International, 3*(4), 372–478.

Neretina, S., Mascher, P., Hughes, R. A., Braidy, N., Gong, W. H., Britten, J. F., …, & Dippo, P. (2006). Evolution of wurtzite CdTe through the formation of cluster assembled films. *Applied physics letters, 89*(13), 133101.

Nesheva, D. (2001). Nano-particle layers of CdSe in various multilayer structures. *Journal of optoelectronics and advanced materials, 3*(4), 885–896.

Nesheva, D., & Levi, Z. (1997). NCs of CdSe in thin film matrix. *Semiconductor Science and Technology, 12*(10), 1319.

Nikale, V. M., Shinde, S. S., Bhosale, C. H., & Rajpure, K. Y. (2011). Physical properties of spray deposited CdTe thin films: PEC performance. *Journal of Semiconductors, 32*(3), 033001.

Ochoa, O. R., Colajacomo, C., Witkowski, E. J., Simmons, J. H., & Potter, B. G. (1996). Quantum confinement effects on the photoluminescence spectra of CdTe nano-crystallites. *Solid State Communications, 98*(8), 717–721.

Pai, S. C., Joshi, M. P., Mohan, S. R., Deshpande, U. P., Dhami, T. S., Khatei, & Sanjeev, G. (2013). Electron irradiation effects on TGA-capped CdTe QDs. *Journal of Physics D: Applied Physics, 46*(17), 175304.

Pal, U., Zaldivar, M. H., Sathyamoorthy, R., Manjuladevi, V., Sudhagar, P., Mohan, S. C., et al. (2008). Nano-crystalline CdSe thin films of different morphologies in thermal evaporation process. *Journal of Nanoscience and Nanotechnology, 8*(12), 6474–6480.

Pan, L. L., Li, G. Y., Xiao, S. S., Zhao, L., & Lian, J. S. (2014). Bandgap variation in grain size controlled nanostructured CdO thin films deposited by pulsed-laser method. *Journal of Materials Science: Materials in Electronics, 25*(2), 1003–1012.

Park, J. H., & Sudarshan, T. S. (Eds.). (2001). *Chemical vapor deposition* (Vol. 2). ASM international.

Peng, Z. W., & Zou, B. S. (2012). Optical properties of CdS NBs and nanosaws synthesized by thermal evaporation method. *Chinese Journal of Chemical Physics, 25*(2), 226.

Perednis, D., & Gauckler, L. J. (2005). Thin film deposition using spray pyrolysis. *Journal of Electroceramics, 14*(2), 103–111.

Potter, B. G., Jr., & Simmons, J. H. (1990). Quantum-confinement effects in CdTe-glass composite thin films produced using RF magnetron sputtering. *Journal of Applied Physics, 68*(3), 1218–1224.

Rashid, H. U., Yu, K., Umar, M. N., Anjum, M. N., Khan, K., Ahmad, N., et al. (2015). Catalyst role in chemical vapor deposition (CVD) process: A review. *Review on Advanced Materials Science, 40*(3), 235–248.

Rastogi, A. C., Sharma, S. N., & Kohli, S. (2000). Size-dependent optical edge shifts and electrical conduction behaviour of RF magnetron sputtered CdTe NCs: TiO_2 composite thin films. *Semiconductor Science and Technology, 15*(11), 1011.

Rubel, A. H., & Podder, J. (2011). Structural and electrical transport properties of CdS and Al-doped CdS thin films deposited by spray pyrolysis. *Journal of Scientific Research, 4*(1), 11.

Sanz, M., López-Arias, M., Rebollar, E., De Nalda, R., & Castillejo, M. (2011). Laser ablation and deposition of wide bandgap semiconductors: Plasma and nanostructure of deposits diagnosis. *Journal of Nano-particle Research, 13*(12), 6621–6631.

Sanz, M., Nalda, R. D., Marco, J. F., Izquierdo, J. G., Banares, L., & Castillejo, M. (2010). Femtosecond pulsed laser deposition of nanostructured CdS films. *The Journal of Physical Chemistry C, 114*(11), 4864–4868.

Sarakinos, K., Alami, J., & Konstantinidis, S. (2010). High power pulsed magnetron sputtering: A review on scientific and engineering state of the art. *Surface & Coatings Technology, 204*(11), 1661–1684.

Semaltianos, N. G., Logothetidis, S., Perrie, W., Romani, S., Potter, R. J., Sharp, M., …, & Watkins, K. G. (2008). CdSe NPs synthesized by laser ablation. *EPL* (*Europhysics Letters*), *84* (4), 47001.

Sharma, S. N., Kohli, S., & Rastogi, A. C. (2005). Quantum confinement effects of CdTe NCs sequestered in TiO_2 matrix: effect of oxygen incorporation. *Physica E: Low-dimensional Systems and Nanostructures, 25*(4), 554–561.

Singh, R. S. (2015). Studies on some chemically deposited cd (se-s) nano-crystalline thin films. *International Journal of Advanced Engineering Research and Studies*/IV/II/Jan–March, 275, 277.

Slotte, M., Metha, G., & Zevenhoven, R. (2015). Life cycle indicator comparison of copper, silver, zinc and aluminum nanoparticle production through electric arc evaporation or chemical reduction. *International Journal of Energy and Environmental Engineering, 6*(3), 233–243.

Song, G. L., Guo, S., Wang, X. X., Li, Z. S., Zou, B. S., Fan, H. M., et al. (2015). Temperature dependent raman and photoluminescence of an individual Sn-doped CdS branched nanostructure. *New Journal of Physics, 17*(6), 063024.

Soonmin, H. (2016). A brief review of the growth of pulsed laser deposited thin films. *British Journal of Applied Science & Technology, 14*(6), 1.

Su, J., Zhang, T., Li, Y., Chen, Y., & Liu, M. (2016). Photocatalytic activities of copper doped cadmium sulfide microspheres prepared by a facile ultrasonic spray-pyrolysis method. *Molecules, 21*(6), 735.

Suthagar, J., Rajesh, S., Perumal, K., Balasubramaniam, T., & Suthan Kissinger, N. J. (2010). Growth and characterization of wide-gap $Cd_{1-x}Zn_xSe$ ternary alloys by using electron beam evaporation technique. *Acta Physica Polonica-Series A General Physics, 117*(3), 506.

Tabrizi, N. S., Ullmann, M., Vons, V. A., Lafont, U., & Schmidt-Ott, A. (2009). Generation of NPs by spark discharge. *Journal of Nanoparticle Research, 11*(2), 315.

Taschuk, M. T., Hawkeye, M. M., & Brett, M. J. (2010). Glancing angle deposition. *Handbook of Deposition Technologies for Films and Coatings,* 621–678.

Toma, O., Pascu, R., Dinescu, M., Besleaga, C., Mitran, T. L., Scarisoreanu, N., et al. (2011). Growth and characterization of nanocrystalline CdS thin films. *Chalcogenide Letters, 8*(9), 541–548.

Vasa, P., Taneja, P., Ayyub, P., Singh, B. P., & Banerjee, R. (2001). Photoconductivity in sputter-deposited CdS and CdS-ZnO nanocomposite thin films. *Journal of Physics: Condensed Matter, 14*(2), 281.

Wagner, M., Kohut, A., Geretovszky, Z., Seipenbusch, M., & Galbács, G. (2016). Observation of fine-ordered patterns on electrode surfaces subjected to extensive erosion in a spark discharge. *Journal of Aerosol Science, 93,* 16–20.

Wang, C., Ip, K. M., Hark, S. K., & Li, Q. (2005). Structure control of CdS NBs and their luminescence properties. *Journal of Applied Physics, 97*(5), 054303.

Wang, H., Zhu, Y., & Ong, P. P. (2001). Structural properties of CdS-doped glass nano-crystallites grown by pulsed laser deposition in high vacuum. *Journal of Vacuum Science & Technology A: Vacuum, Surfaces, and Films, 19*(1), 306–310.

Wang, K., Rai, S. C., Marmon, J., Chen, J., Yao, K., Wozny, & Zhou, W. (2014). Nearly lattice matched all wurtzite CdSe/ZnTe type II core–shell NWs with epitaxial interfaces for photovoltaics. *Nanoscale, 6*(7), 3679–3685.

Wang, M., & Fei, G. T. (2009). Synthesis of tapered CdS NBs and CdSe NWs with good optical property by hydrogen-assisted thermal evaporation. *Nanoscale Research Letters, 4*(10), 1166.

Wu, H., Meng, F., Li, L., Jin, S., & Zheng, G. (2012). Dislocation-driven CdS and CdSe nano-wire growth. *ACS Nano, 6*(5), 4461–4468.

Wu, P. C., Ma, R. M., Liu, C., Sun, T., Ye, Y., & Dai, L. (2009). High-performance CdS nano-belt field-effect transistors with high-κ HfO_2 top-gate dielectrics. *Journal of Materials Chemistry, 19*(15), 2125–2130.

Xie, W., Yang, M., Cheng, Y., Li, D., Zhang, Y., & Zhuang, Z. (2014). Optical fiber relative-humidity sensor with evaporated dielectric coatings on fiber end-face. *Optical Fiber Technology, 20*(4), 314–319.

Xu, Z., Li, H., Wu, Z., Sun, J., Ying, Z., Wu, J., et al. (2016). Enhanced charge separation of vertically aligned CdS/g-C_3N_4 heterojunction nano-cone arrays and corresponding mechanisms. *Journal of Materials Chemistry C, 4*(31), 7501–7507.

Yadav, A. A., & Masumdar, E. U. (2011). Photoelectrochemical investigations of cadmium sulphide (CdS) thin film electrodes prepared by spray pyrolysis. *Journal of Alloys and Compounds, 509*(17), 5394–5399.

Yadav, A. A., Barote, M. A., & Masumdar, E. U. (2010a). Studies on nano-crystalline cadmium sulphide (CdS) thin films deposited by spray pyrolysis. *Solid State Sciences, 12*(7), 1173–1177.

Yadav, A. A., Barote, M. A., & Masumdar, E. U. (2010b). Studies on cadmium selenide (CdSe) thin films deposited by spray pyrolysis. *Materials Chemistry and Physics, 121*(1), 53–57.

Yang, G. W. (2007). Laser ablation in liquids: Applications in the synthesis of NCs. *Progress in Materials Science, 52*(4), 648–698.

Yang, Z. X., Zhong, W., Deng, Y., Au, C. T., & Du, Y. W. (2011). Design and synthesis of novel single-crystalline hierarchical CdS nanostructures generated by thermal evaporation processes. *Crystal Growth & Design, 11*(6), 2172–2176.

Ye, Y., Dai, L., Sun, T., You, L. P., Zhu, R., Gao, J. Y., & Qin, G. G. (2010). High-quality CdTe NWs: Synthesis, characterization, and application in photoresponse devices. *Journal of Applied Physics, 108*(4), 044301.

Ye, Y., Dai, L., Wu, P. C., Liu, C., Sun, T., Ma, R. M., et al. (2009). Schottky junction photovoltaic devices based on CdS single NBs. *Nanotechnology, 20*(37), 375202.

Ye, Y., Ma, Y., Yue, S., Dai, L., Meng, H., Li, & Qin, G. (2011). Lasing of CdSe/SiO_2 nanocables synthesized by the facile chemical vapor deposition method. *Nanoscale, 3*(8), 3072–3075.

Ye, Y., Yu, B., Gao, Z., Meng, H., Zhang, H., Dai, L., et al. (2012). Two-dimensional CdS nanosheet-based TFT and LED nanodevices. *Nanotechnology, 23*(19), 194004.

Yeremyan, A., Avetisyan, H., Avjyan, K., Vardanyan, G., & Khachatryan, A. (2008, March). Pulsed laser deposition of layers and nanostructures based on cadmium telluride and bismuth. In *Micro-and Nanoelectronics 2007* (pp. 70250R-70250R). International Society for Optics and Photonics.

Yi Ren Lu, T. Ling, X.W. Du, P.F. Yin, H. Zhang, & X.Y. Chen, (2014) One Step growth of semiconductor cds uniform branched nanowire on FTO. *Applied Mechanics and Materials 472*:744–749.

Yu, L. M., Zhu, C. C., Fan, X. H., Qi, L. J., & Yan, W. (2006). CdS/SiO_2 nanowire arrays and CdS nanobelt synthesized by thermal evaporation. *Journal of Zhejiang University-SCIENCE A, 7* (11), 1956–1960.

Zhao, W., Liu, L., Xu, M., Wang, X., Zhang, T., Wang, Y., Liu, Z. (2017). Single CdS nano-rod for high responsivity UV–visible photo-detector. *Advanced Optical Materials*.

Zhao, Y., Ye, D., Wang, G. C., & Lu, T. M. (2003, October). Designing nanostructures by glancing angle deposition. In *Optical Science and Technology, SPIE's 48th Annual Meeting* (pp. 59–73). International Society for Optics and Photonics.

Zheng, J., Song, X., Chen, N., & Li, X. (2008). Highly symmetrical CdS tetrahedral NCs prepared by low-temperature chemical vapor deposition using polysulfide as the sulfur source. *Crystal Growth & Design, 8*(5), 1760–1765.

Zhou, W., & Tang, D. (2013). Structure and Optical waveguide property of Sn doped CdSe whiskers. *Science of Advanced Materials, 5*(6), 612–616.

Zhou, W., Peng, Y., Yin, Y., Zhou, Y., Zhang, Y., & Tang, D. (2014). Broad spectral response photodetector based on individual tin-doped CdS nanowire. *AIP Advances, 4*(12), 123005.

Zhu, Z. L., Cui, L., Ling, T., Qiao, S. Z., & Du, X. W. (2014). CdTe nanoflake arrays on a conductive substrate: Template synthesis and photoresponse property. *Journal of Materials Chemistry A, 2*(4), 957–961.

Chapter 5
Mechanical, Radiation-Assisted, Plasma, and Green Synthesis

The majority of synthesis routes to produce cadmium-containing nanomaterials have been given in chapters. However, in order to conclude the ongoing discussions, the description of some additional techniques which have been utilized to prepare these materials is still due. Keeping this in view, the preparation of cadmium-based nanomaterials using mechanical, radiation-based, and biological synthesis is given in this chapter. The discussion on biological methods mentions, how enzymes and bacteria are helpful in the synthesis of Cd-based nanomaterials. The synthesis strategy and principles of photochemical method are also described herein. The role of microwave irradiation process used to initiate chemical reactions for the preparation of the inorganic nanomaterials is also discussed. Gamma irradiation synthesis technique has also been found to enhance the growth mechanism of the nanomaterials. The fabrication and characterization of nanomaterials prepared using sonochemical, plasma and mechanochemical methods have also been given in detail.

5.1 Biological Synthesis/Green Synthesis

Recently, the combination of nanotechnology and biotechnology has formed an advance field for the synthesis of nanomaterials. This is a bottom-up approach and it uses various biological units like algae, bacteria, fungus, plants, viruses, yeast, etc. for synthesis process. The biosynthesis method for preparing the NPs proved to be a hazardless and a striking method as compared to all other (physical and chemical) methods. The biosynthesis method is a low-cost method and mostly scientist used the microorganism and the extraction of plants to find out route to synthesize the required particles. This technique includes various pathways to prepare the materials having dimensions from micro- to nano scale and the several issues are still unexplored in this field. The synthesis of NPs from microbial is explained by green chemistry (a bridge of nano- and biotechnology) which utilizes

Abdul Majid and Maryam Bibi, *Cadmium based II-VI Semiconducting Nanomaterials*, Topics in Mining, Metallurgy and Materials Engineering,
https://doi.org/10.1007/978-3-319-68753-7_5

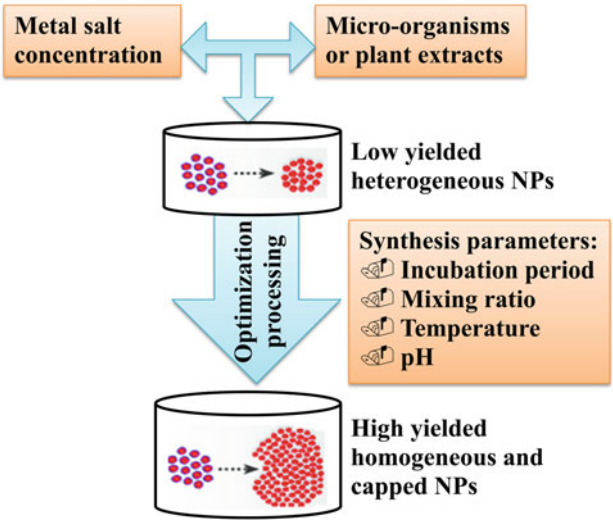

Fig. 5.1 Mechanism of biological synthesis (Singh et al. 2016b)

unicellular, multicellular units like plants and microorganisms. A schematic illustration of this technique is shown in Fig. 5.1.

In microorganism approach, microorganisms like bacteria (Singh et al. 2011), fungi (Castro-Longoria et al. 2011), and yeast (Apte et al. 2013) are cultured for the most favorable time period and conditions (light, nutrients, pH, temperature, medium components, mixing speed, and buffer strength). Optimization of all these culturing conditions can considerably enhance the enzyme activities. In this process, biomass can be separated using centrifugation process and washed through sterilized water. Then a metal salt solution is included in the obtained material and incubated. Nanomaterial synthesis is observed by visual investigation of variations in the color of the culture medium. A short review for biosynthesis with different conditions is provided in Table 5.1. After incubation, there are two types of synthesis strategies involved: intracellular and extracellular synthesis processes. In extracellular synthesis, centrifugation at diverse speeds and washing process are used to get rid of biomass. In intracellular process, the medium constituents and large particles are separated through repetitive cycles of ultrasonic, washing, and centrifugation. Mostly, extracellular process is favored above intracellular due to its possibility for easy downstream processing as well its efficiency for a low-cost process in industrial applications (Karimi and Mohsenzadeh 2012). Finally, after washing through water/solvent (ethanol/methanol), the particles are obtained in the form of bottom pellet.

Plant components, i.e., leaves (Jemal et al. 2017), fruits (Edison and Sethuraman 2012), flowers (Mittal et al. 2012), seeds (Tho et al. 2013), roots (Singh et al. 2016a),

and peel (Sasidharan et al. 2014), are extracted with cleansing process through filtration and centrifugation. Suitable amount of water, metal solution, and diverse fractions of plant extracts are utilized for the synthesis process. During the incubation process, metal salts are decreased and the process is observed for a variation in color, and then NPs are assembled similar to the microorganism-mediated synthesis. In biosynthesis with plants approach, there are no requirements of a well-conditioned culture formation, costly isolation methods, or any special, complex and mutistep processes.

Microorganisms and plant extracts have the capacity to attract, interact, and build up the available metallic salt concentration. These biological units have the capability to utilize their intrinsic biochemical procedures to convert inorganic metallic salts into required NPs (Baker et al. 2013). In both of the synthesis approaches, a narrow size distribution of NPs can be obtained via managing the significant factors as described in Fig. 5.1. There is still a considerable level of research needed to completely understand the size and morphology of different nanomaterials utilizing the same microorganism. In the case of plants extracts, more research investment is required to realize the genuine plant mechanism from a variety of plant species. Therefore, it is an unexplored field and a considerable level of research is required to completely employ the green synthesis approach through biological units.

This section provides some basic discussion on microorganism route in case of biologically synthesized nanomaterials. The peptide-capped intracellular CdS NPs in yeasts Candida glabrata and Schizosaccharomyces pombe have been prepared. These particles were then cultured in the presence of Cd salts and after this process the NPs with 1 nm size have been obtained (Dameron et al. 1989). CdS NPs showed better uniformity in size distribution than prepared by other chemical methods. CdS NPs have also been prepared using intracellular microorganism approach in Schizosaccharomyces pombe. NPs were observed with wurtzite-type hexagonal lattice structure and showed an absorbance maximum at 305 nm (Kowshik et al. 2002). CdS NPs were found with size range of 1–1.5 nm and showed perfect properties for a diode. Mao et al. reported a genetically organized biological synthesis method to prepare the heterostructures of ZnS NCs and CdS NWs with a dual-peptide virus in a similar virus capsid (Mao et al. 2003). The NCs of CdS have been synthesized by an efficient and low-cost biological synthesis process. Escherichia coli (E. coli) have been processed with $CdCl_2$ and Na_2S for the fabrication of intracellular CdS NCs (Sweeney et al. 2004). The reported work indicated the enhancement of the NCs formation by drawing attention toward the change in genetic and physiological parameters within bacterial cell.

The biosynthesis method lies among bottom-up approaches, and the oxidation and reduction reactions are most commonly employed methods in the production process. QDs play the significant rule in biological applications such as the imaging of cell and as biosensing materials (Drbohlavova et al. 2009). CdS NCs with size 2–5 nm have been prepared using extracellular biosynthesis method (Kang et al. 2008a, b). This synthesis process has been found as phyto-chelatins-mediated intracellular process. The NPs of CdS with size-controlled property have been

synthesized by means of immobilized rhodobacter sphaeroides with about 85% yield (Bai et al. 2009). The incubation process was done at 30 °C in dark and aerobic environment and then cadmium ions were transferred into living cell from solution. The culture time was the basic parameter for immobilized rhodobacter sphaeroides to enable the significant control on the size of NPs. The material was characterized by the TEM which demonstrated the average size of the particles ranging 2.3 ± 0.15, 6.8 ± 0.22, and 36.8 ± 0.25 nm obtained with the culture time as 36, 42, and 48 h, respectively. Protein-capped CdTe QDs have been prepared through easy and efficient biosynthesis route (Bao et al. 2010). Cubic zinc blende structured CdTe QDs have been found with size 2–3.6 nm and showed good biocompatibility for bio-imaging and bio-labeling applications. These nanostructures showed high QY of about 33% because of their good crystallinity. It has been found that different incubation time periods have diverse effects on size- and size-dependent properties of product materials.

CdS QDs have been prepared via biological method in genetically engineered Escherichia coli (E. coli). These QDs were made by encoding their required peptide through foreign genes and cleansed by anion-exchange resin (Mi et al. 2011). CdS QDs were taken apart from the bacteria using the techniques of lysis and freezing–thawing of cells. Biologically prepared CdS QDs were anticipated to show additional biocompatible properties in bio-labeling and imaging. Biologically synthesized CdS QDs have been prepared using surfactin and studied the use of surfactin taken out from a new surfactant making bacterial strain Bacillus amyloliquefaciens KSU-109 (Singh et al. 2011). Surfactin, in this process, separated from rhizosphere of Phoenix dactylifera was found as an important, efficient, and low-cost stabilizer and capping agent for growth of stable CdS NPs. Fluorescent CdS nanoparticles with size 10–30 nm have been prepared using biosynthesis technique (Pandian et al. 2011). Brevibacterium casei SPKP2 has been applied with $CdCl_2$ and Na_2S for green synthesis. These NPs showed their potential to be utilized for imaging and diagnostic in biomedical field.

The inorganic NPs have been synthesized by using chitosan and acyl-modified chitosan to form the novel carbohydrate which is based on nanobioconjugates in order to cure the diseases and the health disorders (Santos et al. 2013). Extracellular microbial synthesis of CdS QDs has been done in the solution of cadmium nitrate tetrahydrate with synthesis mechanism shown in Fig. 5.2a (Chen et al. 2014). FCC-structured CdS nanostructures have been obtained with good crystallinity and homogeneous size of 2.56 nm. A blueshift in photoluminescence absorption spectra has been observed with decrease in pH value. In this study, the microbial synthesis method for these protein-capped CdS QDs has been described; Equation $Cd^{2+} + HR - R - COOH \rightarrow Cd - S - RCOOH + H^+$ shows Cd-binding particles on cell wall, $CH_3CSNH_2 + 3OH^- \leftrightarrow CH_3OH^- + NH_3 + S^{2-} + H_2O$ process of releasing the S ions due to TTA hydrolysis, $Cd^{2+} + S^{2-} \rightarrow CdS$ combination of Cd and S ions, $CdS + Cd - S - RCOOH \rightarrow CdSCd - S - RCOOH$ covalent bonding between Cd–S–R complexes and finally carboxylic acid accumulated on the surface of CdS NCs $CdSCd - S - RCOOH + NH_2CH(R)COOH \rightarrow$

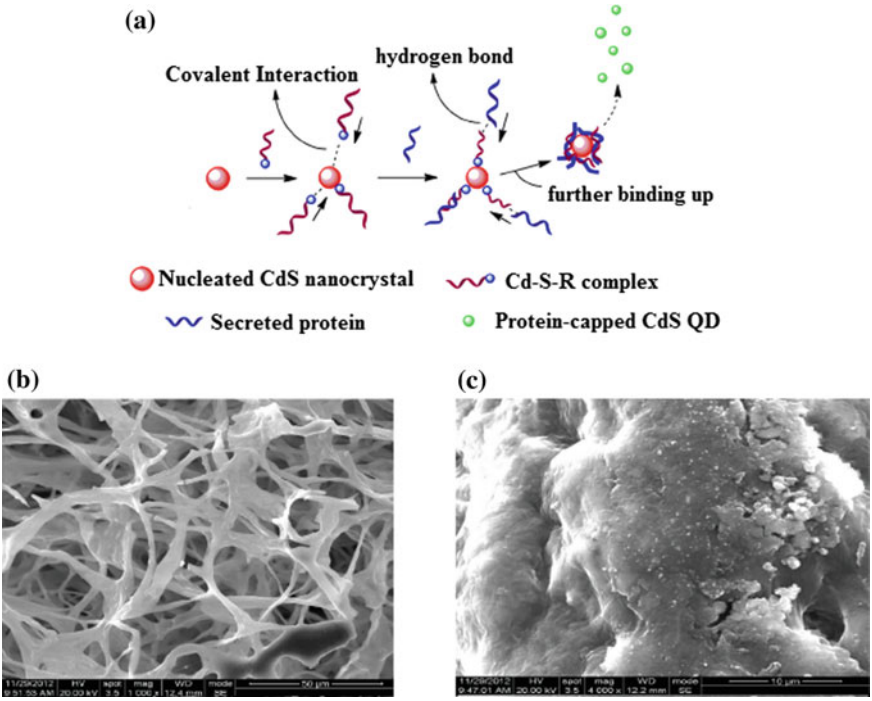

Fig. 5.2 **a** Schematic diagram of microbial synthesis of protein-capped CdS QDs, **b** Smooth and clear surface of native P. chrysosporium fungus, **c** Cd ions adsorbed on the surface of the fungus (Chen et al. 2014). © 2014 Elsevier Publishing

$CdSCd - S - RCOOH \ldots\ldots NH_2CH(R)COOH$ forming the protein-capped CdS nanostructures. The excellent optical behavior and low toxicity of these biologically synthesized protein-capped CdS nanostructures have proved them highly practical in bio-labeling and bio-imaging applications. The SEM images of native and Cd-ion-treated fungi are shown in Fig. 5.2b, c, respectively.

The progress in bio-mediated synthesis of CdS NPs is one of the important areas in NPs research. CdS NPs have been prepared by employing the environmental friendly biosynthesis using yeast, Trichosporon jirovecii with an average Cd:S molar ratio of 1.0:0.98 (El-Baz et al. 2016). The growth of these NPs was verified by UV–vis spectra and the product nanomaterials were characterized by different techniques. Generally, the characterization results showed the size of spherical-shaped particles as 6–15 nm and their stability has been checked for the cadmium toxicity to convert it into CdS NPs on the medium holding cysteine. CdS and CdTe QDs have also been prepared using biological synthesis technique and studied the variations in their fluorescence emission spectra (Plaza et al. 2016).

The use of plant extracts for the synthesis process is discussed here. Plant synthesis of stable CdO NPs by using flower broth of Achillea wilhelmsii plants has been utilized to compose the aqueous extract (Karimi and Mohsenzadeh 2012). During the photosynthesis process under ambient conditions, a reaction occurs

Table 5.1 Cd containing II–VI semiconductor nanomaterials prepared through biological method using different synthesis conditions

Material	Reagents	Biological entity	pH	Intracellular/ Extracellular	Incubation time	References
CdS NPs	$CdCl_2$ and Na_2S	Brevibaterium casei SPKP2	9	Extracellular	12 h	Pandian et al. (2011)
CdS NPs	–	Escherichia coli (E. coli)	–	Intracellular	3 h	Kang et al. (2008b)
CdTe QDs	$CdCl_2{\cdot}2.5H_2O$, $NaNO_3$, $C_6H_6O_7Na_3{\cdot}2H_2O$, KCl, Na_2TeO_3, K_2HPO_4, $MgSO_4{\cdot}7H_2O$ and MSA	Yeast	–	Extracellular	35 °C/2 days	Bao et al. (2010)
Protein-capped CdS QDs	Cadmium nitrate tetrahydrate, Thioacetamide (TAA Mercaptoacetic acid (TGA)	White rot fungus *Phanerochaete chrysosporium*	–	Extracellular	37 °C/12 h	Chen et al. (2014)
CdSe QDs	$CdCl_2$ and $SeCl_4$ $NaNO_2$	Fungus, *Fusarium oxysporum*	–	Extracellular	RT/9 h	Kumar et al. (2007)
CdS NPs	$Cd(NO_3)_2$ and Na_2S	Bacteria from roots of *P. dactylifera*	–	–	30 °C/24 h	Singh et al. (2011)
CdO NPs	Cadmium chloride ($CdCl_2$)	Extract of Achillea wilhelmsii	–	Extracellular	RT	Karimi and Mohsenzadeh (2012)

between the aqueous solution of cadmium chloride ($CdCl_2$) and flower extracts. The flower extracts were then reduced to Cd ions and consequently extracellular CdO NPs were formed. CdS QDs have been successfully prepared with this capable and eco-friendly technique utilizing the hairy root culture of Linaria maroccana L (Borovaya et al. 2014). Cadmium sulfate and sodium sulfide were incubated with this plant extract for synthesis process. The prepared NPs of size 5–7 nm with spherical shape showed the absorption peaks at 362, 398, and 464 nm, and luminescent peaks at 425, 462, and 500 nm. CdO NPs have also been prepared by using the Parkia speciosa Hassk (PSH) plant seeds as basic source and stabilizing agent (Permana and Yulizar 2017). The functional group of compound PSH showed its significance for the synthesis of cubic CdO NPs with size ranging between 28.9 and 44.9 nm. CdS NPs with size of 1.48 nm have been prepared utilizing the banana peel extract as a suitable, harmless, environment-friendly capping agent (Zhou et al. 2014). Reaction situations like quantity of banana peel extract, pH, concentration, and temperature played significant role in NPs formation. Extremely luminescent CdSe QDs have been prepared by the fungus, Fusarium oxysporum (Kumar et al. 2007). These QDs were incubated with $CdCl_2$ and $SeCl_4$ at room temperature.

Biosynthesis is a low-cost and quick technique used for the nanoparticle growth. It is environment-friendly technique and provides an extensive variety of environmentally suitable synthesis process. It is completely free of the poisonous chemical agents and high energy requirement as in physiochemical methods. In contrast to microorganism, plants approach provides more benefits because it is faster, more cost-effective, and straightforward (Shah et al. 2015). This technique provides advanced resources for the production of innovative nanomaterials that are stable, harmless, eco-friendly, and prepared by green chemistry methods. This method is more supportive for the synthesis of metal chalcogenide especially metal oxide NPs. It is needed to improve the control over size, shape, and complete monodispersivity of the nanostructures. In future, a more accurate mechanism of biosynthesis is required for manufacturing of nanomaterials for technological applications (Table 5.1).

5.2 Microwave Combustion Synthesis

The microwaves having the frequency range from 300 MHz to 300 GHz can also be utilized for the synthesis of nanomaterials (Gerbec et al. 2005). Inorganic composites synthesized using microwave technique has been studied for last three decades. As a heating process, microwave irradiation is used to initiate chemical reactions to prepare the inorganic nanomaterials and has many applications in field of nanotechnology. Microwave heating is an amazing heating source to assist chemical reactions and the frequencies utilized for microwave combustion synthesis are 918 MHz and 2.45 GHz. The NPs produced via this technique are smaller in size and have narrow size distribution. This technique offers short reaction time because of quick and uniform heating mechanism as a result of which the particles are quickly created at the same time.

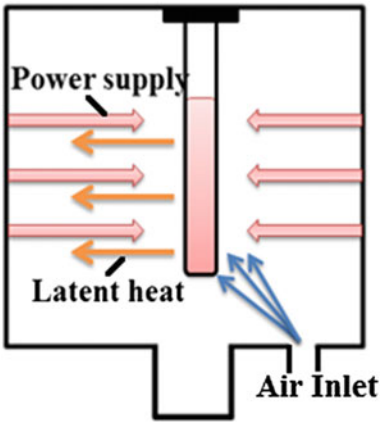

Fig. 5.3 Schematic diagram showing microwave combustion synthesis process (Gerbec et al. 2005)

Dielectric heating provided by microwave irradiation has been efficiently utilized for the growth mechanism of metal chalcogenides. In this synthesis method, a definite quantity of precursors mixed solution enclosed in a special vessel and heated up in a microwave absorption oven by means of microwave irradiation (Fig. 5.3). Microwave irradiation generates friction and collision of molecules at high temperature to synthesize the nanomaterials from chemicals. After completion of reaction, the solution is cooled down to room temperature. The value of pH of the solution is also an important parameter to be considered; the optimal value of pH for this method is 9–10 (Li et al. 2015). It is a valuable synthesis route in aqueous phase and works with a microwave absorption/extraction arrangement supplying with some exclusive Teflon inner vessels.

The consequences of microwave irradiation on synthesis process have not been yet recognized. Quick changes due to electric and magnetic forces directions, friction, and collisions of molecules are observed (Li et al. 2015). Thermal effects of microwave irradiations include consistent heating and superheating, while non-thermal effects have not been properly understood. It is considered that microwave irradiation reduces the activation energy of the materials and consequently provides a quick growth mechanism.

The benefits of microwave synthesis include the following: (i) no thermal gradient is observed in process; (ii) it gives the high yield as compared to the conventional heating method that leads to the great importance from the industrial point of view; (iii) high-quality nanoscale products are obtained; (iv) it has enhanced rate of formation; and (v) it has enhanced crystal quality and distribution of size. Furthermore, short reaction time, efficient heat transfer, and eco-friendly nature are added advantages of this method. There are many other benefits of this method to prepare the Cd-based particles like high-energy competence, very short reaction time, narrow size distribution, and high purity. Solvents put high influencing consequence on the size, shape, and morphology of the product particles. Microwave-assisted synthesis can be useful in mild chemical growth of cadmium containing nanomaterials. A glimpse of the work carried out for the synthesis of

Table 5.2 Cd containing II–VI semiconductor nanomaterials prepared through microwave method using different synthesis conditions

Material	Power/ frequency	Precursors	Irradiation temp./time	pH	References
CdSe–CdS QDs	0–1000 W/ 2450 MHz	$CdCl_2$, NaHSe 3-mercaptopropionic acid (MPA)	140/5–60 min	9	Qian et al. (2005)
CdTe/CdS core–shell nanostructures	0–300 W/ 2450 MHz	$CdCl_2$, Na_2S, NaHTe, MPA	–	8.4	He et al. (2006)
CdSe–CdS QDs	0–1000 W/ 2450 MHz	$CdCl_2$, NaHSe 3-mercaptopropionic acid (MPA)	130/30 min	9	Zhan et al. (2014)
CdSe NCs	900 W/ 2.43 GHz	$CdSO_4$, potassium nitriloacetate, Na_2SeSO_3	–/30–60 min	–	Zhu et al. (2000)
CdTe QDs	400 W/ 2450 MHz	$CdCl_2$, Na_2TeO_3, $NaBH_4$, MPA	80–140/10–40 min	–	Duan et al. (2009)
CdO nanocubes	900 W/ 2.4 GHz	–	1200/60 s	–	Rashidzadeh (2014)
CdO NWs	1 kW/ 2.45 GHz	Cadmium nitrate *n*-heptane, Urea	–/13 min	–	Sathya Raj et al. (2013)
CdO and CdO–NiO nanocomposites	800 W/ 2.45 GHz	$Cd(CH_3COO)_2{\cdot}4H_2O$ NaOH	Annealing temp/time 673/4 h Irradiation time 10 min	–	Karthik and Dhanuskodi (2016)
CdO nanostructures	800 W/ 2.45 GHz	NaOH and $CdCl_2$ polyvinyl alcohol	–/10 min	–	Lagashetty (2016)
CdO NPs	2.45 GHz	$CdCl_2$ Camellia sinensis	–/5 min	–	Mohanraj et al. (2017)
(PVP)-capped CdS NPs	1000 W/ 2450 MHz	$Cd(Ac)_2$ and thiourea in *N*,*N*-dimethylformamide (DMF)	30 s with cycles, on for 9 s, and off for 21 s	–	He et al. (2003)
CdS NTs	10 W/ 2450 MHz	Na_2S and $CdSO_4$	–	–	Shao et al. (2002)
CdS NPs	1300 W/ 2.4 GHz	Thioacetamide (CH_3CSNH_2) and of $CdCl_2$	–/60 s	8	Serranoa et al. (2009)
CdS and Cu: CdS NPs	720 W/ 2.45 GHz	$CdCl_2{\cdot}2.5H_2O$, CH_2CSNH_2 $Cu(CH_3COO)_2{\cdot}H_2O$	–/1–15 min	–	Saraji et al. (2012)

Cd-based materials with different experimental conditions of this method has been given in Table 5.2.

The preparation of NPs of CdS under the different suitable parameters has been reported by several groups. The synthesis of CdS NTs has been reported by following the TM_{01}-type microwave irradiation method in aqueous media at room temperature (Shao et al. 2002). CdS NTs with external diameter 50–140 with wall thickness of 5–15 nm appeared straight with well-defined boundary as shown in Fig. 5.4a. This procedure has been found favorable for the synthesis of a variety of

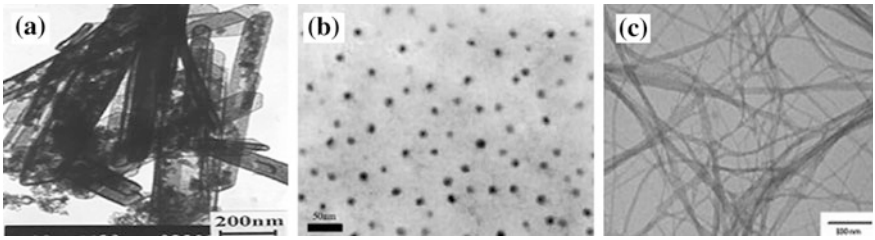

Fig. 5.4 **a** TEM images of CdS NTs (Shao et al. 2002). © 2005 Royal Society of Chemistry **b** TEM image of alloyed CdSe–CdS QDs (Qian et al. 2005). © 2005 Elsevier Publishing, **c** CdO NWs synthesized by microwave technique (Sathya Raj et al. 2013). © 2005 Elsevier Publishing

NTs. The as-prepared nanomaterials showed cubic face-centered structure. PVP-capped CdS monodispersed NPs have also been synthesized using microwave method (He et al. 2003). CdS NPs possessing high photocatalytic and luminescence properties have been prepared via microwave process (Yang et al. 2005). The prepared CdS NPs showed strong luminescence peak at 602 nm. The photodegradation of methyl orange in CdS suspension has been observed to be increased at low values of pH and temperature of solution. Microwave irradiation is verified as suitable, well-organized, and eco-friendly one-step method to manufacture the NPs. CdS NPs without the use of capping agent have been prepared by using the microwave initiated combustion and sonochemical method (Arora and Manoharan 2007). The powder synthesized by sonochemical method has been found more amorphous than that of microwave method. The synthesized nanoparticles were having a size of 5–12 nm. The PL spectra for NPs with sizes <10 and >15 nm showed a blueshift with FWHM $\sim$100 nm and blue to green emission with FWHM $\sim$60 nm, respectively. The CdS NPs have been synthesized in sodium citrate with the help of microwave irradiations (Serrano et al. 2009). These light-sensitive NPs with cubic zinc blende structure showed a QY of about 70%. The size of the particles was found less than 20 nm and their PL peaks were observed in UV and visible range. The preparation of CdS NPs using the microwave-assisted polyol method has also been reported (Soltani et al. 2013). Cadmium chloride and thioacetamide were used as the source salts for cadmium and sulfur, respectively. The control of the size was carried out by controlling the irradiation time of the microwaves as well as cadmium and sulfide molar ratio. The results indicated that the product attained the hexagonal structure without any impurity and showed a spectral blueshift. Doped CdS NPs have also been prepared with the help of microwave synthesis method (Saraji et al. 2012). The size of NPs was obtained between 15–20 nm and Cu doping in CdS caused a doping-dependent redshift in the PL spectra.

Microwave synthesis is a resourceful and time-saving route for growth of nanomaterials. NPs of CdSe along with other II–VI binary chalcogenides have been synthesized using microwave irradiation (Zhu et al. 2000). The results indicated small dimensions and high monodispersivity of CdSe NPs. The prepared CdSe NPs having a size of 4–5 nm with band gap value of about 1.70 eV. Irradiation time

affects the morphology of the nanomaterials in such a way that the irradiation of 10 and 30 min produced CdSe cubic (sphalerite) phase and cadmoselite phase, respectively. This method was found as influential to optimize the growth rates to control the properties of different nanostructures.

A lot of work has been done on the preparation of QDs by considering the microwave synthesis method. The microwave-assisted method has been utilized to prepare highly luminescent CdTe QDs (Duan et al. 2009). The QDs have been obtained with a size of 3 nm and high monodispersity. By increasing the particle diameter, an increase in photoluminescence QY was observed. The synthesis of CdTe QDs through microwave irradiation process can be explained via the following chemical reactions:

$$4\mathrm{TeO}_3^{2-} + 3\mathrm{BH}_4^- \rightarrow 4\mathrm{Te}^{2-} + 3\mathrm{B}O_2^- + 6\mathrm{H}_2\mathrm{O}$$

$$\mathrm{CdCl}_2 + \mathrm{Te}^{2-} + \mathrm{MPA} \rightarrow \mathrm{Cd} - (\mathrm{MPA})_x\mathrm{Te}_y + 2\mathrm{Cl}^-$$

$$\mathrm{Cd} - (\mathrm{MPA})_x\mathrm{Te}_y \longrightarrow \mathrm{CdTe}.$$

As a result of above reduction reactions under microwave irradiation, CdTe QDs have been obtained. The effects of temperature, time, and pH value on the deposition process have been discussed in detail. In order to obtain high-quality CdTe NCs at fast rates, a facile method assisted by the microwave irradiation has been applied (He et al. 2007). This water-dispersed NC showed the elevated value of QY and with very narrow size distribution. It is observed that taking the great advantage of powerful microwaves synthesis, the NPs of different materials can be synthesized. Microwave-assisted route has also been followed for the preparation of CdTe NCs capped by thiol group (El-Sadek et al. 2009). The obtained CdTe NCs had the cubic zinc blende structure. The reported work has described the synthesis of a series of CdTe samples by varying the pH values and caped with mercaptoacetic acid. Cubic ZB-structured CdTe nanostructures have been obtained with low density of deep traps states and size of 10, 15, 17, and 20 nm. The QDs of CdTe have been prepared by establishing the easiest and rapid method (He et al. 2012). The effects of various controlling parameters such as pH values, temperature, and time of reactions and reagents molar ratio on quality of the products were discussed in detail. The analysis of the QDs described the average size of 3.5 nm and QY of 75%. From the analysis of fluorescence probes, the obtained QDs have been found suitable for imaging purpose especially for live Madin-Darby canine kidney (MDCK) cells.

High-quality alloyed CdSe–CdS QDs have been prepared in aqueous phase by using microwave irradiation (Qian et al. 2005). These alloyed QDs have been quickly formed with microwave irradiation in a furnace. The QDs showed better optical properties with QY up to 25%. FWHM of peak of emission spectrum has been observed about 28 nm which points to narrow size distribution. CdSe–CdS QDs having size of about 12 nm prepared on Cu lattice using microwave method showed fine monodispersity (Fig. 5.4b). High concentrations of precursors offered a

quick synthesis rate and well-organized coatings of thicker shell on core of QDs. The growth of high-quality CdTe/CdS core/shell NCs has been done in aqueous medium under the microwave-assisted method (He et al. 2006). The reported work described the microwave irradiation possessing the special characteristics, extremely valuable for the quick epitaxial growth of NCs. CdTe has been first prepared and used as core to synthesize the CdTe/CdS core/shell structures.

CdSeS QDs have been synthesized by a simplistic aqueous phase method using microwave irradiation process (Zhan et al. 2014). These quasi-core–shell CdSeS QDs showed XRD peak at approximately similar positions to that of bulk cubic CdS crystal structures. Thick CdS shell on CdSe core has been found in these CdSeS QDs having distinct spherical shape and comparatively narrow size distribution. These quasi-core–shell QDs have been found stable in an oxidative atmosphere and showed high tolerance for H_2O_2 which is clearly better than usually fabricated CdTe QDs and core–shell CdTe/CdS QDs. It was due to their exclusive quasi-core–shell CdSeS crystal structure and little lattice difference between CdSe and CdS. Extremely luminescent, photostable CdTe/CdS/ZnS core/multishell QDs for biological applications were prepared using microwave irradiations (He et al. 2014). The effects of molecular structures of ligands (as well as L-cysteine, L-cysteine hydrochloride, *N*-acetyl-L-cysteine (NAC), glutathione, and 3-mercaptopropionic acid) on CdTe/CdS/ZnS have been studied. Cell culturing showed the low cytotoxicity of CdTe/CdS/ZnS QDs as contrast to CdTe and CdTe/CdS QDs, recommending the superior capability for applications in biomedical imaging and diagnostics.

Metal chalcogenides and metal oxides can easily be synthesized by chemical reactions and microwave irradiations. CdO NWs have been prepared using an inexpensive and time-saving microwave combustion method (Sathya Raj et al. 2013). These NWs (with diameter 25–30 nm) have been found crystalline in nature and the size of each crystallite of CdO nanoparticle was found in the range of 8–20 nm. Microwave method has been found supportive to prepare such type of oxide nanomaterials with a well-defined structure (Fig. 5.4c). Cadmium metal was used under oxidation process to prepare CdO nanomaterials under microwave irradiation process (Rashidzadeh 2014). The exposure time is less than 2 min to microwaves, evaporated Cd reacted with oxygen in air, and consequently CdO NPs have been obtained on the internal surface of glassy container. Antibacterial activity of CdO nanopowder has also been examined and it is found as efficient antibacterial material. In another study, microwave-irradiated CdO NPs have been obtained with band gap value 0.07 eV (Veeraputhiran et al. 2014). This straight and easy synthesis route can be applied for growth of CdO NPs within short time and simple setup.

Ethanol/PTES-treated CdO NPs have been synthesized by an innovative and inexpensive microwave evaporation technique within a commercial microwave oven (Rashidzadeh et al. 2016). The high purity Cd flakes have been evaporated in less than 2 min. The evaporated Cd produces CdO NPs upon reaction with ambient oxygen and deposited on a glass substrate. NPs surfaces have been processed by a solution having the ethanol and phenyltriethoxysilane (PTES), and the morphological and structural properties were characterized through XRD and SEM

techniques. Thus cubic-shaped CdO NPs prepared through this process exhibited the hydrophobicity characteristics to be applied in micro-fluidic devices and several other technological applications. CdO NPs have also been prepared using green tea extract with microwave irradiation technique (Mohanraj et al. 2017). These NPs were proved to be appropriate photocatalysts due to their good optical response. An excellent rectifying behavior along with good thermal conductance of the product was observed.

Hexagonal cubic CdO–ZnO nanocomposites have been synthesized through microwave-assisted technique with an estimated band gap as 2.92 eV (Karthik et al. 2015). These nanocomposites have been obtained with size of 27 nm and their band edge emission has been observed at 422 nm. In another study of Cd-based nanocomposites, CdO–NiO nanocomposites have been synthesized by microwave-assisted technique (Karthik and Dhanuskodi 2016). CdO NPs and CdO–NiO nanocomposites have been obtained with size of 45 and 30 nm, respectively. The characterization revealed average dislocation densities of 4.938×10^{14} lines/m^2 (CdO) and 11.11×10^{14} lines/m^2 (CdO–NiO) and band gap values of 2.35 eV (CdO) and 3.75 eV (CdO–NiO). These nanocomposites showed their applications in optoelectronics. Nanosized CdO and CdO–ZnO materials have been prepared by microwave route with an efficient fuel polyvinyl alcohol (Lagashetty 2016). CdO NPs showed agglomeration and majority of the obtained particles were irregularly shaped.

5.3 Photochemical Synthesis

Photochemical method involves promotion of chemical reactions and deposition of species onto conducting and insulating substrates under light illumination. It is extremely efficient solution-based chemical synthesis route to prepare the cadmium-based nanomaterials with a variety of morphologies. The apparatus is simple, inexpensive, and allows control over film thickness, composition, and morphology.

The commonly used deposition techniques based on chemical reaction are usually simple, economical, and direct but offer drawbacks. For example, in case of electrodeposition, the substrate attached to the cathode should be conductive due to which this technique disqualifies for deposition of compounds on insulating substrates. In case of chemical bath deposition (CBD) or SILAR, resistive substrates can be used but the rate of reaction cannot be controlled by current. An alternate solution-based chemical technique to avoid such drawbacks is photochemical deposition (PCD) in which reaction is carried out under light illumination. The wavelength, intensity, and duration of illumination provides freedom to control the ongoing reaction/deposition, and hence the film thickness. The setup showing the mechanism of photochemical deposition is sketched in Fig. 5.5.

The mechanism to explain synthesis of CdS films using PCD can be found in the literature (Goto et al. 1997). In order to deposit CdS films on glass substrate, the substrate was dipped into solution (aqueous solution of $CdSO_4$ and $Na_2S_2O_3$) and illuminated with UV light by mercury lamp. The irradiation causes photoexcitation of

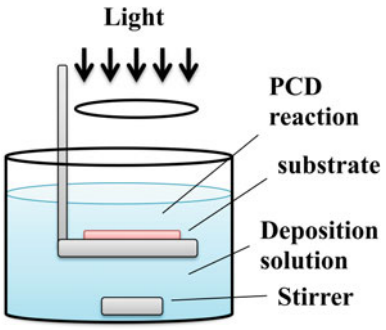

Fig. 5.5 Sketch showing principle of photochemical deposition method (Ichimura and Maeda et al. 2015)

molecular species (for example, Cd^{2+}, Na^{+}, $S_2O_3^{2-}$, and SO_4^{2-} in the present *case*). The recorded absorption spectrum indicated major UV absorption by $S_2O_3^{2-}$ as a result of which the ions are disassociated into S and SO_3^{2-}. After this step, two electrons are required for reduction of Cd^{2+} in order to produce CdS. The requisite electrons will be supplied by ions $S_2O_3^{2-}$ which are capable of transformation into $S_4O_6^{2-}$ upon losing two electrons when illuminated.

Kundu et al. synthesized the NWs of CdS on DNA scaffolds via photochemical route (Kundu and Liang 2008). The authors reported the capability of their deposition method to provide a shape control mechanism according to which DNA helped the preferential growth of CdS particles in specific crystallographic direction to yield the product in the form of NWs. The experiment to synthesize the NWs was carried out by varying the UV irradiation exposure time as well as the concentrations of Cd and S in the precursor solution. In the deposition process, initially Cd^{2+} ions condensed on DNA by forming a complex which is followed by reaction of Cd^{2+} and S^{2-} ions under irradiation of UV light to nucleate CdS and finally crystallize the product in the form of NWs. It points to the importance of decomposition of salts, formation of the complex, and chemical reaction in the growth of CdS NWs on DNA via photochemical route. The microscopy of the samples pointed out an increase in DNA diameter which reveals uniform coverage of DNA by CdS NWs.

Photocatlytic process was used for the synthesis of CdS NPs in the company of an optically transparent and semi-crystalline polyvinyl alcohol (PVA). The NPs were directly produced in polymer matrix by using cadmium dithiocarbamate precursors which were incorporated into a polymer substrate and irradiated with nanosecond laser to cause nucleation of cadmium sulfide NPs. The NPs were spherical whose size was found to be increased with increase in substrate temperature. However, band gap of NPs decreased with increase in substrate temperature. These NCs were then characterized by different techniques (Onwudiwe et al. 2014). The spectrum was obtained due to the absorption of UV–visible radiations, and a blueshift in the band gap was considered. They finally came into conclusion that the XRD technique exhibited a decrease in the crystallinity behavior of the polymer and this behavior is due to entrapped particles. These NCs revealed cubic and hexagonal phases.

In order to get rid of hazardous-free Cd ions and introduce Cd as cocatalyst for the synthesis of CdS under visible light, $Na_2S_2O_3{\cdot}5H_2O$ was used for photochemical synthesis of Cd/CdS nanocomposites (Wang et al. 2014). The metallic Cd used as a cocatalyst with CdS to split electrons and holes that effectively enhance the photocatalytic behavior of the grown nanocomposites for hydrogen production. The certain amounts of $Na_2S_2O_3{\cdot}5H_2O$ were added to CdSO4 in different molar ratios (of 5–10) to remove Cd ions and produce a series of Cd/CdS photocatalysts as a green synthesis strategy. As per XRD analysis, the content of metallic Cd in the products can be controlled by changing the amount of $Na_2S_2O_3{\cdot}5H_2O$. When the ratio of $Na_2S_2O_3{\cdot}5H_2O$ over cadmium salt was seven, the hydrogen production rate was highest with value 1753 μmol/h. The loading of CdS with metallic Cd was observed to enhance the photocatalytic activity of the photocatalyst due to interfacial effects and formation of Schottky barriers at the metal. The authors explained the mechanism of charge transfer and enhancement of activity of Cd/CdS on the basis of theoretical predictions and experimental findings.

Recently, photochemical method was used to deposit CdS NPs on the surface of MIL-125(Ti) to obtain nanocomposites for photocatalytic applications (Zhang et al. 2017). The nanocomposites were synthesized by chemical reaction of precursors cadmium chloride, MIL-125(Ti), and S_8 in the presence of UV light to prepare a series of samples by using different amounts of S_8. The characterization revealed the formation of CdS NPs and its uniform decoration on the surface of MIL-125 (Ti). The photocatalytic performance of the nanocomposites was investigated in the oxidation of benzyl alcohol using visible light. An increase in benzyl alcohol concentration was observed initially which was then decreased in case of nanocomposites prepared with increasing amount of S_8 until it went beyond 18 mg. It was explained in terms of reduction in light absorption capability of nanocomposites upon aggregation of CdS NPs and their diffuse reflectivity.

CdSe NPs have been prepared by photochemical synthesis by chemical reaction of $CdCl_2$ and Na_2SeSO_3 along with complexing agent nitrilotriacetic acid under 420–450 nm irradiation from indium lamp (Zhu et al. 2001). The chemical reaction yielded Se^{-2} ions which react with Cd^{2+} ions to produce CdSe NPs in powder form. The spherical CdSe NPs having cubic crystal structure with average size about 7 nm were obtained. The measured optical spectrum of the NPs revealed band gap of 1.82 eV which is blueshifted as compared to that of bulk CdSe (1.70 eV) pointing toward quantum size effects.

An effort to prepare CdSe NCs using photochemical route has been reported (Yan et al. 2003). The precursors comprise cadmium acetate, sodium sulfite, trisodium citrate, selenium powders, and cetyltrimethylammonium bromide (CTAB) as surfactant where chemical reaction was carried out under light from mercury lamp for 4 days. The NCs were prepared with and without CTAB to explore the effects of surfactant. It was observed that aggregation of NCs is linked to the presence/absence of CTAB which points to possibility of control on morphology of the product by utilizing surfactant. The results showed the formation of cubic phase CdSe grains with average size of 25 nm. The measured absorption spectrum showed a blueshifted band edge of CdSe NPs with reference to that of bulk

counterpart. This finding was interpreted in terms of quantum confinement effects related to grown NPs.

CdSe and lead selenide nanoparticles were successfully produced by photochemical method. The reaction was carried out in the presence of aqueous solution of $CdCl_2$ and Na_2SeSO_2 as well as complexing agent under UV irradiation for 1.5 h (Zhao et al. 2003). The intensity of light, pH value of the solution, and the complexing agents were found playing important role in photochemical synthesis of the NCs. The increase in irradiation intensity appeared to shorten the reaction time. The optimal value of pH for the synthesis of CdSe was reported to be in the range of 10–11. The photoluminescence spectrum indicated blueshifted band edge emission of the NWs when compared to that of bulk CdSe.

5.4 Gamma Irradiation Synthesis

Gamma irradiation synthesis is a powerful and efficient method to synthesize different nanomaterials like metals, oxides, and nanocomposites like metal/polymer and chalcogenide/polymer. The composites of organic/inorganic species are commonly used in the field of nanotechnology for the preparation of a variety of nanomaterials. The utilization of gamma irradiation has been found to enhance the growth mechanism of nanomaterials. This method is found to provide instantaneous polymerization and creation of monomers as well as inorganic NPs, respectively.

This method involves gamma irradiation of solution containing precursors and offers a synthesis of nanomaterials with control over size, shape, and morphology. The irradiation causes reduction of metallic ions and facilitates the nucleation process to grow nanomaterials. The synthesis using this method is carried out at room temperature under ambient conditions and provides control overgrowth as well as physicochemical mechanism by monitoring irradiation dose and chemical reaction dynamics (Jurkin et al. 2016). CdS NRs were prepared in tubules of polymer vinyl acetate monomer templates under gamma radiations assisted with chemical reaction of cadmium sulfide and thioacetamide (Zhao et al. 2009). The microscopy of the samples pointed out wrapping of some CdS NRs in the tubules. These NRs were cubic in structure and have diameter below 100 nm and length of 2–5 microns. The NRs presented the luminescence due to band edge at 448 and 527 nm, which point to size distribution of the grains. An effort to embed CdS NPs in polyvinyl alcohol films by using gamma irradiation procedure has been reported (Kharazmi et al. 2013). The NPs were found surrounded by OH bonds of polyvinyl chain. It was observed that distribution of prepared NPs was narrowed with increase in radiation dose. However, the size of the NPs was found unaffected with increase in the dose. Owing to the quantum confinement effects related to nanomaterials, the band edge-related emission of the NPs was found blue-shifted when compared to the bulk counterpart.

The production of nanocomposites comprising CdS and polyvinyl alcohol carried out by using gamma irradiation strategy has been reported (Ali et al. 2015). The

films were prepared at different concentrations of Cd by employing different radiation doses. The UV/Vis spectrum of the samples revealed that peak related to band edge shifts to low energy, whereas width of the peak increased with increase in irradiation dose. The dose-dependent redshift of absorption edge indicates a consistent increase in size of NPs. The prepared CdS NPs having low or high Cd ionic concentration were found in cubic or mixed cubic-hexagonal structures.

CdS NPs were prepared by Ni et al. using reaction of cadmium chloride and carbon disulfide via gamma irradiation method (Ni et al. 2001). In order to investigate the effects of gamma irradiation dose on size of the NPs, the absorption spectrums of precursor solutions before and after irradiation were recorded. On the basis of redshift of absorption edge, it was revealed that nanoparticle size grows with increase in irradiation dose. The mechanism of formation of the NPs and effects of irradiation of gamma rays has been investigated in detail. The CdS NCs have been prepared via gamma irradiation route and then dispersed in matrix of silica gel (Pan et al. 2004). The prepared CdS particles were spherical in shape and were found uniformly dispersed in the matrix. An increase in size of the particles was observed with increase in irradiation time. The photoluminescence measurements indicated a notable redshift as well as increase in intensity of band edge emission with increase in average size of the NPs. Moreover, an emission related to surface states disappeared for a prolonged irradiation exposure of the NCs.

Similarly, several efforts have been reported to prepare CdSe using this technique. Kang et al. reported the preparation of CdSe QDs coated with Chitosan in aqueous solution using polymer assisted gamma radiations technique (Kang et al. 2008a). These QDs were cubic in structure having average size of 4 nm and exhibited a narrow size distribution. The coating of CdSe QDs by silk fibroin protein performed using gamma irradiation technique has been reported (Chang et al. 2009). In order to prepare the QDs, the aqueous solution comprising $CdAc_2$ and SeO_2 along with silk fibroin was irradiated by gamma rays at room temperature. The mechanism of growth involved capturing of Cd^{2+} ions by silk fibroin, reaction of Cd^{2+} with Se^{2-}, and nucleation of CdSe QDs. The measurements of photobleaching revealed improved photostability of the QDs when coated with silk fibroin. Furthermore, as per measurement of cytotoxicity, the coated QDs appeared to exhibit lower cytotoxicity when compared with uncoated samples. These findings pointed out significance of coating to improve the biomaterial for several applications including treatment and imaging of tumors.

The effects of surfactant on the properties and growth mechanism of CdO QDs prepared by gamma irradiation technique have been studied (Mahfouz et al. 2016). The damage caused by irradiation with gamma rays appeared to enhance the nucleation process and play its role in defining the shape of the product. Two types of samples were prepared by thermal decomposition of gamma irradiation on cadmium acetate: one in the presence of anhydrous benzyl alcohol as surfactant and the other without this surfactant. The obtained material was found to contain NPs of CdO in the form of mesoporous structures in the absence of the surfactant. However, upon using the surfactant, the nanomaterial was formed as cauliflower-shaped mesoporous structures.

5.5 Sonochemical Technique

Sonochemistry provides a simple, novel, and resourceful method for the chemical preparation of nanomaterials. In this method, ultrasounds are used as energy source to create exclusively hot spots that provide intense conditions for synthesis. Due to some significant current characteristics of sonochemistry, this technique has been applied for the growth and adjustment of different organic and inorganic materials. There is an extensive variety of the chemical and physical results that can be produced using high-intensity ultrasound. There are three categories for the chemical effects of sonochemistry: (i) Homogeneous sonochemistry of liquids, (ii) Heterogeneous sonochemistry of liquid–liquid or liquid–solid system which includes the formation of amorphous metal and intercalation process, and (iii) Sonocatalysis, extending beyond the former two categories and such reactions are significant for both laboratory and industrial applications.

Throughout the ultrasonic process, high-intensity sound is irradiated and acoustic cavitations happen; the collisions between the particles have a great impact on the size, shape, composition, and reactivity. The equipment for sonochemical equipment contains a thermo-stated glass reactor cell along with gas inlets/outlets. In the glass cell, there is a high-intensity ultrasonic titanium horn, controlled by a piezoelectric transducer.

Typically, sonochemical synthesis involved very powerful ultrasound radiation with speed 1000–1500 m/s, wavelength approximately from 10 cm to 100 μm, and frequency ranging from 20 kHz to 15 MHz in order to improve the chemical reaction (Xu et al. 2013). The physical consequences of sonochemistry comprise the improved mass transport, thermal warming etc. at lower frequencies. There is no direct reaction between ultrasound and material on molecular level due to large wavelength of ultrasounds than the molecular dimensions. So, chemical reactions due to ultrasound arise from transient hot spots created throughout acoustic cavitations.

When the sound waves spread through a liquid, the density varies with successive compression and expansion of waves. Consequently, due to acoustic cavitations, small bubbles are produced which absorb the sound energy and vibrate with the irradiated ultrasounds. With the appropriate circumstances and utilizing the ultrasound energy, a bubble can overgrow, consequently without further absorption of sound energy it implodes. After such collapse, bubbles release the stored intense energy and create a situation for chemical reactions (Bang and Suslick 2010). A localize, short-lived hotspot is created, which is a source of homogeneous sonochemistry. Intense conditions during acoustic cavitations cause a physical phenomenon by emitting short bursts of light which is known as "sono-luminescence". This process quantifies the temperature of the high-energy species formed throughout the cavitations. Time, energy, and pressure conditions make the sonochemistry a distinct process as compared to other conventional methods. Ultrasonic spray pyrolysis is also another scheme to prepare nanomaterial by using ultrasounds (Suslick et al. 1999). The chemical reactions are thermally

stimulated in ultrasonic spray pyrolysis without direct interaction with ultrasounds. In this method, low-intensity ultrasound radiations with high frequency are employed; both USP and cavitation-induced sonochemistry are multiphase techniques. This is a low-cost synthesis technique and can be used to prepare the high-quality nanostructures. High-boiling-point solvents have been sprayed ultrasonically to synthesize continuously the fluorescent CdS, CdSe, and CdTe NPs (Didenko and Suslick 2005).

In liquid–solid homogeneous systems, the cavity collapse is very asymmetric and potential energy of the cavity is converted into kinetic energy of high-energy liquid jets. In such systems, there is a decrease in liquid tensile strength, and due to this effect, minor sound intensities can be applied. The physical consequences of sonochemistry comprise the emulsification, improved mass transport, thermal warming, and a diversity of consequences on materials. Sonochemical method is a capable, advanced, adaptable, inexpensive, and facile synthesis technique that allows managing the size, morphology, and tuning of photocatalytic behavior which is unapproachable by other conventional techniques (Colmenares et al. 2016).

Supramolecular compounds have been proved to be most suitable precursors for the preparation of metal oxide nanomaterials. Direct calcination of sonochemically prepared supramolecular is the best method for obtaining the CdO nanomaterials. Cd (II) supermolecular, $[Cd(L)_2(H_2O_2)_2]$, has been prepared through sonochemical method and then converted into CdO NPs after calcinations process (Safarifard and Morsali 2012). These NPs showed agglomerated structure (Fig. 5.6a). CdO NPs have been obtained through thermolysis of supramolecular NRs cadmium (II) fluorine-substituted β-diketonate prepared through sonochemical method (Hanifehpour et al. 2012). By direct calcination of $[Cd(2,2'\text{-bpy})(dfpb)_2]$ at 180 °C, CdO flower-like nanostructures have been formed with the size of 20 nm. Hanifehpour et al. synthesized CdO nanoparticles through same method with just calcination temperature changed from 180 to 400 °C with size of 25 nm. CdO NPs have been obtained through direct calcination of sonochemically prepared cadmium (II) compound $[CdL_{0.5}(NO_3)(H_2O)]$ (Ranjbar et al. 2014). These CdO NPs were found having a size range of 40–60 nm.

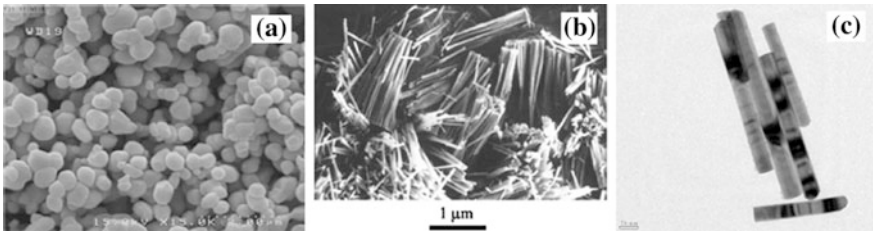

Fig. 5.6 Sonochemical synthesized **a** Agglomerated CdO NPs (Safarifard and Morsali 2012). © 2012 Elsevier Publishing **b** SEM image of CdS NRs (Zhou et al. 2003). © 2013 Elsevier Publishing **c** CdS nanorod synthesized through combined sonochemical–solvothermal methods (Bozkurt and Derkuş 2016). © 2016 Open Access

The sonochemical synthesis is appropriate and well-organized method for the preparation of Cd-based chalcogenide nanostructures and also during the acoustic cavitations. The NCs of CdS colloids have been synthesized using sonochemical technique and their spectroscopic results revealed quantum confinement effects (Sostaric et al. 1997). Coated on the submicron spherical silica, CdS NPs have been prepared by means of sonochemical method (Arul Dhas and Gedanken 1998). The comparison of the pure CdS and the coated CdS was described in detail. CdS NPs of 3 nm in diameter have been prepared utilizing the sonochemical reduction method in Ar atmosphere at room temperature (Wang et al. 2001). It was observed that increasing the sonication time increased the quantity of CdO NPs. Sonochemical route is a simple and efficient way to synthesize CdS NPs at room temperature. By adjusting the surfactants, carriers, and solvents, this method can be used to prepare the modern nanodevices for electronics and electro-optics.

CdS nanostructures have been prepared using sonochemical method with Cd (EDTA) and $Na_2S_2O_3$ in deionized water solution (Zhou et al. 2003). These large-scale single-crystal NRs showed identical structures with width of 80 nm and length of 1.3 μm (Fig. 5.6b). During the synthesis, it was observed that concentration of EDTA greatly affects the process. Concentration of EDTA below seven produced spherical-shaped CdS NPs, while with 8.5–10.5 concentration mostly CdS NRs were developed. Semiconductor CdS with nanoporous hollow structure has been prepared utilizing the sonochemical method with the help of Escherichia coli bacteria as template (Shen et al. 2010). The structure of CdS showed a change from cubic to hexagonal form. The hexagonal-structured CdS nanoporous hollow microrods showed the unique improvements in photoconversion performance with the highest photoelectrochemical cell of about 4.3% under the global AM illumination of 1.5. This method can be used for the synthesis of other sulfide nanomaterials.

CdS NRs and NPs through joint sonochemical–solvothermal technique and these NPs have been compared to the NPs synthesized by sonochemical method (Bozkurt and Derkuş 2016). CdS NPs made by sonochemical–solvothermal route showed better morphological homogeneity in contrast to the sonochemical method. The parameters influencing the development process were reaction time, different types and ratios of starting agents. CdS NRs have been observed about a radius of 25 nm and length of 200 nm (Fig. 5.6c). It has also been observed that the addition of ethylenediamine solutions is beneficial to avoid agglomeration in joint sonochemical–solvothermal technique. Tb doped CdS NPs have been prepared by sonochemical method (Hanifehpour et al. 2016). CdS NPs have been formed with well-defined and clear crystallinity and size of 40–60 nm. Sonication power has a great effect on particles performance, increasing power from 50 to 200 W/L showing an increase in discolourization effectiveness from 68 to 100%. Through different terbium contents, 8% of terbium-doped CdS exhibited the maximum sonocatalytic degradation of methylene blue.

Sound energy strongly affects the course of reaction; by using the sound energy, CdS and CdSe NPs have been prepared in aqueous solution (Kristl et al. 2010). The increase in the temperature has been observed due to irradiation of the sample to the

sound energy radiations. The method involved the direct immersion of ultrasound radiation by using Vibracell as a probe instrument, which operates at 20 kHz frequency. The obtained product is evaluated by thermal analysis involved in TGA, SDTA, X-ray powder diffraction, and with the transmission electron microscopy. The sizes of the obtained CdS and CdSe nanoparticles have been found as 4.5 and 9.7 nm, respectively. CdS NPs showed a uniform cubic structure, while CdSe NPs showed agglomerated spherical shape. CdSe NPs have been prepared using sonochemical method with cadmium acetate and sodium selenite as starting agents (Sharma et al. 2014). Hydrazine hydrate and ammonia have been employed to organize the size of particles and these NPs have been studied with crystalline size of 65 nm. Through Fourier transform infrared spectroscopy (FTIR), its absorbance spectra have been calculated showing a blueshift with reduction in size.

Highly luminescent CdTe QDs have been synthesized in a very short period of time with sonochemical method in an aqueous medium, where ultrasound radiations have been applied to accelerate the reduction process of the tellurium (Menezes et al. 2011). The characterization results demonstrate the only one fluorescence band and very strong quantum confinement effect. Uniformly shaped CdTe NPs with a size of 20 nm–30 μm have been prepared through sonochemical method (Hwang et al. 2011). Sonication and thermal heating can affect the size of cubic-phased CdTe (20 nm size) and showed a band gap of 1.53 eV. CdTe/TiO_2 NPs under the visible-light-induced photocatalysts have been synthesized by the multi-bubble sonoluminescence condition (Li et al. 2013). The photocatalyst behavior of the obtained material has been characterized by photocatalytic degradation of rhodamine B used as the reaction probe. The results of the techniques revealed that under multi-bubble sonoluminescence, the obtained material exhibited very high photocatalytic activities when compared with the nonirradiated material with multi-bubble sonoluminescence. CdTe NPs have been prepared using sonochemical method derived from the reactions between $Cd(OAC)_2$, $TeCl_4$, and KBH_4 in water and the presence of a variety of capping agents (Salavati-Niasari et al. 2015). The synthesis of these particles followed the precipitation and sonochemical method. Cubic-structured CdTe NPs with lattice constants a = b = c = 6.481 nm have been formed with average size of 45 nm. It has been found that morphology, particle size, and phase of the products could be significantly influenced by preparation parameters.

5.6 Mechanochemical Synthesis

Synthesis of nanomaterials is one of the largest parts of research and technology; it is a very dynamic field of material sciences. Solid-phase reactions are frequently triggered by high temperature action. Syntheses of various II–VI materials have been done using mechanochemical synthesis. Mechanochemical synthesis corresponds to a versatile way to produce innovative materials and can be applied to prepare NPs using both chemical and mechanical manufacturing (Avvakumov et al.

2001). The synthesis of nanomaterials using this method exhibited exceptional properties like narrow size distribution of particles and fine morphology.

5.6.1 Dry and Wet Grinding Systems

Grinding is one of the oldest methods used for the synthesis of fine particles from solid precursors. In this technique, mechanical energy is used to break the atomic bonds of the precursor and form new materials on the basis of mechanochemical process (Nogi et al. 2012). Though a variety of techniques based on CVD and PVD process are used to synthesize the NPs, several problems are linked with these routes. As the surface energy and size of the NPs have an inverse relation, grinding method applied to prepare diverse types of NPs has potential to enlarge the surface energy. The new surface encourages the solid-state reactions at atomic/molecular level to trigger the formation of particles on nanoscale. As the particles are strained in the grinding method, the structures of the products show some surface disorders. The mechanical grinding produces alloying of the precursors to produce NPs and their agglomerates based on the surface reactions. This difficulty is resolved by using a liquid in the system (wet grinding) which offers a noticeable improvement in managing the stability of product NPs.

5.6.2 Ball Milling

There is top-down physical technique for the preparation of NPs in which precursors are grinded via milling systems. The grinding mill systems comprise balls which are used as the agitation media to carry out mechanochemical processes for the synthesis of NPs (Fig. 5.7).

The bulk material is placed inside the milling jar and grinding balls are used in synthesis process of nanomaterials. During this high-energy ball milling process, there is a choice to add a surfactant. Without a surfactant, the aggregation process takes place because of high surface energy of the particles, which results in the formation of larger NPs during mechanical grinding. If the surfactant is added, then the surfactant molecules form an organic layer on the surface of particles. The adsorption of these molecules lowers the surface energy of particles, and consequently no agglomeration takes place and NPs are produced with smaller size range and desired surface properties.

The rotation speed of the balls collision determines the efficiency of the grinding mechanism. The grinding capability also depends upon the number of balls and ball diameter, as the ball diameter is inversely proportional to the frequency of the balls collisions. The structure, shape, and morphology of nanomaterials strongly depend upon parameters of bill milling strategy. The variety of milling parameters, growth

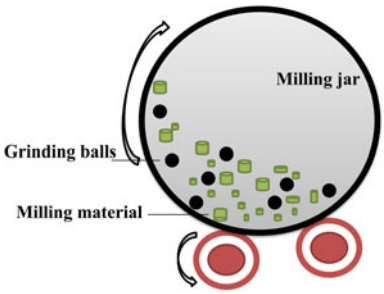

Fig. 5.7 Schematic diagram of high-energy ball milling system (Dhand et al. 2015)

conditions, and growth velocity directions produce nanomaterials in the form of diverse shapes like particles, rods, cubes, fibers, etc. In this method, it is very easy to introduce the impurities with less effort, high uniformity, and high yield (Kanatzia et al. 2013).

The top-down techniques are inexpensive, well-established, and traditional methods for the preparation of large-scale nanomaterials (Saravanan et al. 2008). However, the synthesized nanomaterials are often irregular in shapes and may have defects. The QDs of the cadmium sulfide were synthesized by Tsuzuki et al. via mechanochemical synthesis (Tsuzuki and McCormick 1997). The precursors comprising Na_2S, $CdCl_2$, and NaCl were milled to prepare CdS. The product was prepared in NaCl matrix to produce separate NPs where the NaCl:CdS ratio was 16:1. The NPs were prepared by using different sizes of milling balls from 4.8 to 12.6 mm to explore the effects of synthesis parameters on properties of the product. The XRD patrons pointed out the presence of mixed cubic and hexagonal phases in CdS NPs prepared by using balls of diameter 12.6 mm. However, upon decreasing the ball size to 4.8 mm, the samples were found completely in cubic crystal structure. Furthermore, it was found that particle size of the product decreased in direct proportion to the size of milling balls.

In order to compare the properties of chemically prepared CdS NPs, high-energy milling was employed by Dutkova et al. to prepare the same material (Dutková et al. 2009). The synthesis process of the NPs comprised several stages including milling, washing, and decantation and drying. The chemically prepared CdS NPs were found containing mixed cubic and hexagonal phases, whereas the milled samples contained cubic phases. The work explored the benefits of the mechanochemical synthesis by demonstrating the formation of uniform crystallites and the large surface area under the mechanochemical process. The mechanochemical approach was found superior to produce uniform particles in comparison to that of chemical route. The mechanochemical preparation of CdS nanomaterials has been reported (Baláž et al. 2003). The product was composed of mixed cubic and hexagonal crystal structures. On the basis of mixed phases and transformation of one phase into the other, this method appears to be an appropriate route for optimizing the composition of crystalline structure by suitable selection of milling conditions.

In order to prepare CdS NPs via mechanochemical route by employing industrial eccentric vibratory mill (Godočíková et al. 2006), during the grinding process, the impact and friction produced during movement of balls and the walls of the container caused the reaction of precursors. The obtained NPs were found in mixed hexagonal and cubic structures with average size of 9 nm. CdS NCs have been prepared by using a mechanical alloying to investigate the effects of milling time and capping agent (Tan et al. 2009). The capping of as-milled NPs was carried out with trioctylphosphine oxide/trioctylphosphine/nitric acid (TOPO/TOP/NA). The samples were withdrawn from the mill at different time intervals to investigate the structural evolution of the material. No peak related to CdS was detected in first 30 min milling time, whereas the milling of 10 h appeared to convert the elemental precursors completely into CdS NPs. A yellow dispersion solution was appeared, and the XRD and HRTEM results showed the wurtzite structure of the product nanocrystals with size varying from 1.6 to 6.2 nm. These mechanically synthesized CdS NCs revealed the same optical properties as created through the wet chemical process. The longer milling time caused blueshift of absorption peaks which points to the possibility of tuning the optical properties of NPs. The absorption intensity peaks for the capped CdS NCs were found in the range of 345–380 nm. In case of capped CdS NPs, the value of band gap was found blueshifted by an amount of 0.86 eV when compared to that of bulk CdS.

The billing milling strategy has been adopted to prepare CdS and other sulfide NPs by using precursors comprising of metal acetates and sodium sulfide (Tolia et al. 2012). The milled product was extracted after every 2 h during 2–10 h time and investigated using XRD technique. It was observed that phase transformation of CdS NPs takes place after 6 h milling time. The average size of NPs was decreased which was expected to increase in milling time to 8 h after which the size started increasing due to agglomeration. The variations in structural and optical properties of the NPs prepared at different milling times were discussed in this report.

Mechanical alloying carried out by ball milling has also been used for the preparation of CdSe NPs. Tan et al. reported the preparation of CdSe NCs by ball milling of elemental powders (Tan and Yu 2009). In order to study the structural evolution, XRD analysis of milled product was carried out at different intervals including 6, 14, 20, and 40 h. It was observed that milled product consisted of mixed phase of cubic and hexagonal crystal structures. The increase in milling time up to 40 h did not cause any structural change except broadening of XRD peaks pointing toward decrease in particle size. The milling time of 40 h exhibited formation of good crystal quality CdTe NPs with complete absence of impurities and elemental phases. The optical properties before and after capping of NCs with organic–inorganic composites were investigated in detail. As per optical excitation spectrum measurements, the peak recorded at 550 nm was assigned to zinc blende, whereas the peak found at 516 nm was attributed to wurtzite structure of CdTe NCs. The photoluminescence spectrum of CdSe NCs prepared at different milling times revealed shift in emission wavelength from 520 to 547 nm. The changes in

peak positions with milling duration pointed out the possibility of tuning of optical properties of the material.

The NCs of CdTe have also been prepared by using this method. The preparation of CdTe NPs prepared by using powdered precursors of Cd and Te in ball miller by varying the milling time has been reported (Tan et al. 2003). The milling of 30 min revealed the formation of cubic phase of CdTe in addition to the presence of elemental components. When milling time increased to 8 h, the evidence of elemental Cd and Te phases disappeared and the XRD patron showed the presence of cubic phase of CdTe. Furthermore, the consistent increase in broadening of XRD peaks was found to increase in milling time with points to decrease in particle size. The size of the NPs was decreased from 23 to 3.5 nm when milling time was increased from 4.5 to 50 h; their respective TEM images are shown in Fig. 5.8a, b. The optical characterization of capped and un-capped NPs was also carried out. It was observed that absorption peak shifted to lower wavelengths with an increase in milling time which was explained in terms of change in particle size. The optical properties of the NPs were notably changed after capping. The absorption peak of CdTe NPs was found redshifted upon capping which could be either due to small particle size before capping or absence of charge transfer between particle surface and capping material prior to capping.

The mechanochemical route is eco-friendly and is used to perform solid-state reaction without including any organic solvent; so this technique has got a wide-reaching attention in the preparation of CdO nanomaterials. The NPs of CdO have been obtained by ball milling of precursors cadmium nitrate tetrahydrate and acetamide followed by calcination at 450 °C in a furnace (Tadjarodi and Imani 2011). The obtained NPs were cubic in structure having good crystalline quality and average size of about 41 nm. The same group carried out another study to prepare CdO NPs using this technique (Tadjarodi et al. 2013). The precursor comprising cadmium acetate dihydrate and urea was milled and then calcinated at 500 °C for 2 h in a furnace which results in the production of spherical NPs of CdO. The prepared particles had fine crystalline structure and spherical shape with

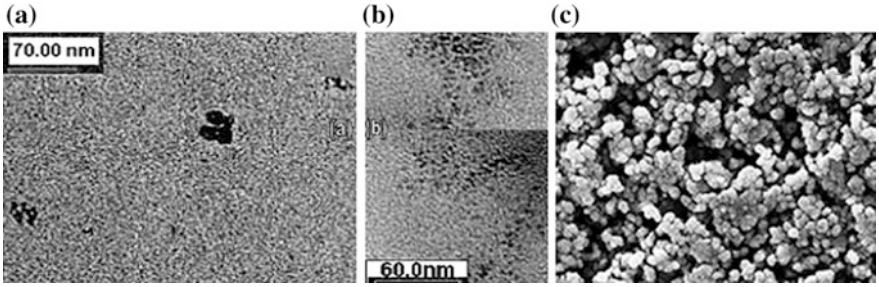

Fig. 5.8 TEM images of capped CdTe NCs dispersed in hexane; ball milling for **a** 4.5 h and **b** 5 h (Tan et al. 2003). © 2003 Elsevier Publishing **c** SEM image of spherical-shaped CdO NPs prepared through mechanical synthesis (Tadjarodi et al. 2013). © 2013 Springer Open Access

size range of 40–50 nm (Fig. 5.8c). A statistical method and image processing program was employed to study the particle size division, where as the band gap energy values provided the information about the optical properties of the NPs. Thermogravimetric investigations of the prepared material indicate weight loss of 13% at temperature range of 178–245 °C and 44% at 350–500 °C.

Cadmium chalcogenide NPs were prepared by M. Kristl using the mechanochemical method (Kristl et al. 2013). The milling of Cd and S in air after 60 min exhibited the presence of CdO and hexagonal CdS. Though milling of the same precursor by 120 min caused disappearance of peaks related to Cd and S, an increase in the concentration of phase CdO was found. CdS NPs with average size of 8 nm were found in hexagonal phase. The milling of Cd and S powders did not show any new phase after milling time up to 30 min but hexagonal phase of CdSe

Table 5.3 Cd containing II–VI semiconductor nanomaterials prepared using different mechanochemical synthesis conditions

Material deposited	Precursors	Loading conditions of mills	Bal-to-powder mass ratio	Milling rate	Atmosphere	References
CdS NPs	Cadmium acetates and sodium sulfide	50 balls of 10-mm diameter	–	500 rpm	Argon	Baláž et al. (2003)
CdS NPs	cadmium acetate and sodium sulfide	50 balls of 10 mm diameter	–	500 rpm	Argon	Dutková et al. (2009)
CdSe NCs	Cd and Se powders	2–12 mm	10:1	–	Inert gas	Tan & Yu (2009)
CdS NPs	Cadmium acetates and sodium sulfide	3 mm diameter	10:1	350 rpm	Air	Tolia (2012)
CdS NPs	Cd and S powders	2–12 mm	10:1	–	Inert gas	Tan et al. (2009)
CdTe NPs	Cadmium and tellurium powders	2–12 mm diameter	20:1	–	–	Tan et al. (2003)
CdO NPs	Cd $(NO_3)_2{\cdot}4H_2O$ and CH_3CONH_2	2 balls of 10 mm diameter	–	1800 rpm	Air	Tadjarodi and Imami (2011)
CdO NPs	cadmium acetate dihydrate and urea	2 balls of 10 mm diameter	8:1	1800 rpm	Air	Tadjarodi et al. (2013)
CdS, CdSe, CdTe NPs	Cd, S, Se, and Te powders	–	20:1	–	Air	Kristl et al. (2013)

NPs appeared after 45 min. The alloying of Cd and Te powders in air produces mixed phase of CdO and CdTe after milling at 30 min. The structural characterization of the samples revealed the formation of NCs having size of 8–19 nm at milling time of 15–120 min. The synthesis conditions used by different workers for mechanochemical synthesis of Cd containing II–VI semiconductors are summarized in Table 5.3.

5.7 Thermal Plasma Synthesis

The plasma state of matter exists ($T \geq 10^4 K$) in the form of an ionized gas including the constituents in the form of ions. This state has its exclusive characteristics in which free electrons (unbound to any atom or molecule) are present. Due to the existence of ions, it shows good conductive behavior. The plasma can be applied for the synthesis of NPs because it is responsive to electromagnetic field. Now-a-days, plasma deposition of nanofilms is a famous strategy in nanomaterial fabrication; it consists of plasma spraying and is available in the form of thermal plasma chemical vapor deposition (TPCVD) and thermal plasma physical vapor deposition (TPPVD). Thermal activation is required for the beginning of a chemical reaction.

Plasma spraying has been recognized for more than 50 years, but TPCVD is a relatively advanced technique with a potential for future applications. In TPCVD, the material is evaporated in the high-energy density plasma; these vapors are then connected with the cooled substrate. The high-energy vapor phase starting agents cross a nonequilibrium boundary layer for the nucleation process at the surface of substrate. The high-quality coatings can be attained with the great homogeneity of crystal direction in diverse grains. In contrast to traditional CVD or laser CVD method, TPCVD gives relatively higher deposition rates due to higher densities of precursors. In principle, similar equipment can be used for both the plasma spraying and TPCVD methods. The precursor residence time in thermal plasma is made longer to fully evaporate the NPs. In TPPVD, one or more gaseous reactants react with vapor formed from material. Plasma provides the heat necessary to evaporate the material and then it is deposited on the substrate.

The apparatus used for plasma synthesis consists of (i) A thermal plasma reactor, (ii) a water-cooled stainless-steel aerosol feeding probe, (iii) an ultrasonic nebulizer, and (iv) a helium-cooled substrate holder in the chamber. There are three different types of thermal plasma reactors that are utilized: (i) single DC (direct current) torch method in a Plasma technik A 300 S (Sulzer Metco Inc., Wohlen, Switzerland), (ii) triple DC customized torches AS-103L with jets 30 mm under the plane of torch exits (Tekna Plasma System Inc., Sherbrook, Canada), and (iii) HF (radio frequency) Plasma torch PL-35 (Tekna Plasma Systerm Inc., Sherbrook, Canada). Traditional single DC torch is employed in plasma spraying systems (also known as

Suspension Plasma Spray) through a radial plasma injection utilized at one position to prepare NPs around the size of 50 nm. Liquid atomization is used for thick coating nanostructures applications (Xiong et al. 2016).

DC torches with hot cathodes produces a flame with temperature from 8000 to 16000 K with velocities hundred to several thousand m/s (Fauchais and Vardelle 1997). In this process, a water-cooled insertion probe is used for supplying the starting agents into converging jets. The HF plasma torch is also known as induction plasma and produces flames with mild velocities equal to several tens m/s with temperature range of 5000–10000 K (Park and Hong 1997). It utilizes a water-cooled copper Mach 1 nozzle along with axial starting agent's insertion. As well as the DC torches, RF torches can also be used for the spray plasma coating process. Liquid starting agents are sprayed in plasma jet with a mixture of Ar, H_1, N_2, He, C_2H_2, and CH_4. These gases can be mixed to make more plasma gas combinations; these mixtures have a great control on the coating composition. The temperature of the system is maintained to stay constant during the synthesis process (Seo and Hong 2012).

In comparison to other synthesis methods, plasma synthesis has some advantages: (i) high temperature provides the melting and verification of the inorganic waste; (ii) high-energy density reduces the waste throughputs and consequently low costs and supports the manufacture of small portable units; (iii) the use of electric arc is another benefit in using the electric arc, as discussed in SDG section; (iv) smaller system size and high-energy density permit the quick start-up and shut-down times; and (v) ultraviolet radiations produced through plasma also take part in waste annihilation procedure. There is a great attention in research toward the advancements in use of thermal plasma for waste-processing technology.

5.8 Some Other Techniques

There are numerous techniques to control the size and shape of the NPs that have been suggested to synthesize using liquid precursors in the gas phase. In order to organize the size and shape of the nanoparticle, it is necessary to understand their synthesis mechanisms.

Seeded growth of CdS and CdSe nanocrystal was studied by Karthish M. et al. with quantum rods and tetrapods morphology (Manthiram et al. 2013). Their phase, morphology extinction coefficient, and quantum yield were studied using XRD, TEM, UV–vis spectra, and photoluminescence spectra. Vapor-phase transportation method is also used for the synthesis of NPs. L. Li et al. prepared the CdS NBs as optical sensor through this method and studied through TEM and XRD characterization methods (Li et al. 2014). These hexagonal wurtzite NBs showed the photosensitivity, dark current, and decay time as 4×10^4, 0.2 pA, and 31 ms, correspondingly.

Atomic layer deposition, also known as electrochemical atomic layer epitaxy (ECALE), is a gas-phase method and encapsulates the NPs on various types of

supporting materials. It is a recent method offering the possibility of atomically organized post-adaptation of the sustained catalyst. Underpotential deposition process is involved in this technique and nanostructures are developed layer by layer on a single-crystal substrate. CdS thin films with 1:1 ratio between the elements grown by ALD, are very structured and epitaxial (Carlà et al. 2014).

A straightforward and environmentally gracious synthesis method has been established to prepare the aqueous CdS QDs at room temperature (Li et al. 2007). The material was characterized by the X-ray diffraction and with transmission electron microscopy (TEM). The result demonstrated the very small size and the physical structure which was cubic zinc blende structure. By optimization of the various processing parameters, the photoluminescence properties of the aqueous cadmium sulfide could be adjusted. The stronger emission was obtained with very high pH value and ratio of MPA/Cd was 2. These aqueous cadmium sulfide QDs possessed very long lifetime by the UV–visible light and had the good stability in deionized water. This material provided the very simple processing and excellent photoluminescence properties which provide the practical application for single-target imaging. Wet chemical method has been applied to synthesize CdTe/CdS core–shell QDs with characteristic luminescence of 650–720 nm (Bakar et al. 2010). At the optimized temperature of 300 °C, the whole synthesis method involved two steps. First, the formation of core and then the synthesis of shells were made. The characterization of the QDs of photoluminescence demonstrated that these QDs emit the wavelength in the red region and possessed the quantum yield of about 37%. The above-demonstrated property has the application in LED, bio-labeling, and in solar cells.

Many scientists have done work on cadmium sulfide QDs under the aqueous synthesis method. From single precursor, the luminescence cadmium sulfide QDs have been prepared using the aqueous method (Zhang et al. 2004). The water-soluble cadmium sulfide QDs possessed the tunable sizes between 25 and 40 Å were established from the readily prepared [(2,2′ bipyridine) $Cd(SC\{O\}ph)_2$] complex by the refluxing of the aqueous solution. The size of the NPs could be tuned by simply varying the capping agent concentration. The optical band gap edge was obtained which demonstrated the particle aging kinetics. By changing the refluxing time, the QDs sized were changed. When the 10 mmol capping agent was used, extraordinary dimerization of the QDs upon the very long reflexive time caused the doubling of the nanocrystal size. The result described the redshift of the wavelength peaks. Very advanced technology has been used to synthesize cysteamine (CA)-CdTe QDs (QDs) in aqueous medium which is called as the one-step aqueous method (Wang et al. 2012). This reported work demonstrates the change in quantum yield which is obtained by changing the molar ratio and the pH value. The material obtained is characterized by TEM and X-ray diffraction for structural and shape analysis of the material. The photoluminescence gives the quantum yield which is 10.73% in case of green-orange emitting CdTe QDs.

CdTe NCs have been synthesized using Proline dithiocarbamic acid disodium salt (Yuwen et al. 2010). This method took the low temperature and rapid crystal growth process due to weak bonding between cadmium ions and proDTC which

show the advantage on TGA. This variation in the kinetic growth caused the major influence on the monomer. The quantum yield obtained by this method was very low as compared to the thiol-capped quantum yield which could be increased up to 50% by using the mercaptopropionic acid. Aqueous synthesis approach has been applied to synthesize the thiol-capped CdTe/CdS/ZnS QDs (Li et al. 2011). This synthesis involves several conditions, by following some optimization to control the size of CdTe QDs. This reported work involves more conditions like refluxing time, good photostability, and the chemical stability; products give the quantum yield of photoluminescence and have the good pH tolerance, the salt tolerance, and favorable biocompatibility. The characterization is made by X-ray powder diffraction method, HRTEM (high-resolution transmission electron microscopy), and fluorescence correlation spectroscopy which described the crystal structure and good monodispersity. The stabilized CdTe/CdS/ZnS established by the fluorescence lifetime spectra is used for the cell imaging. The method involved in this method is described as the reproducible, cost-effective, and very useful for the large-scale synthesis.

Manganese-doped cadmium sulpfide quantum-doped have been prepared by aqueous synthesis method where l-cysteine (2-amino 3-mercaptopropionic acid) used as the capping agent (Kumar et al. 2013). The material was characterized by various techniques including X-ray diffraction, Raman spectroscopy, Fourier transform infrared, UV–visible spectrum and energy-dispersive X-ray analysis. The X-ray diffraction demonstrated crystal structure. Fourier transform infrared and Raman confirmed the existence of carboxylic and amine functional groups. EDX showed the manganese doping in CdS structure. UV–visible spectrum demonstrates the redshift. The theoretical result showed the maximum band energy of 2.83 eV. The results exhibit many applications due to its multifunctional crystal property. These applications include the clinical analysis and disease diagnosis. This material characterization has the application in the magnetic resonance imaging for the best contrast. The aqueous synthesis method provides the convenient way to prepare the NCs of the specific materials (Choi et al. 2012). Cadmium telluride NCs have been prepared by using dithiol-functionalized ionic liquids. The quantum yield of dTFIL-capped CdTe QDs of photoluminescence approaches to $\sim$40% and this property of luminescence was maintained up to 8 weeks, which enhanced stability in the water phase.

References

Abd El-Sadek, M. S., Ram Kumar, J., & Moorthy Babu, S. (2009). Optical properties of thiol-stabilised CdTe nanoparticles. *International Journal of Nanoparticles*, *2*(1–6), 20–29.

Ali, Z. I., Ebraheem, O., Saleh, H. H., Salam, F. H. A., & Sokary, R. (2015). In situ preparation of CdS/PVA nanocomposites using gamma radiation. *Polymer Engineering & Science, 55*(11), 2583–2590.

Apte, M., Sambre, D., Gaikawad, S., Joshi, S., Bankar, A., Kumar, A. R., et al. (2013). Psychrotrophic yeast Yarrowia lipolytica NCYC 789 mediates the synthesis of antimicrobial silver NPs via cell-associated melanin. *AMB Express, 3*(1), 32.

Arora, S., & Manoharan, S. S. (2007). Size-dependent photoluminescent properties of uncapped CdS particles prepared by acoustic wave and microwave method. *Journal of Physics and Chemistry of Solids, 68*(10), 1897–1901.

Arul Dhas, N., & Gedanken, A. (1998). A sonochemical approach to the surface synthesis of cadmium sulfide NPs on submicron silica. *Applied Physics Letters, 72*(20), 2514–2516.

Avvakumov, E. G., Senna, M., & Kosova, N. V. (2001). *Soft mechanochemical synthesis: A basis for new chemical technologies*. Springer Science & Business Media.

Bai, H., Zhang, Z., Guo, Y., & Jia, W. (2009). Biological synthesis of size-controlled cadmium sulfide NPs using immobilized Rhodobacter sphaeroides. *Nanoscale Research Letters, 4*(7), 717.

Bakar, N. A., Umar, A. A., Salleh, M. M., & Yahaya, M. (2010). Synthesis of CdTe–CdSe core-shell QDs with luminescence in the red. *Sains Malaysiana, 39*(3), 473–477.

Baker, S., Harini, B. P., Rakshith, D., & Satish, S. (2013). Marine microbes: Invisible nanofactories. *Journal of Pharmacy Research, 6*(3), 383–388.

Baláž, P., Boldižárová, E., Godočí, E., & Briančin, J. (2003). Mechanochemical route for sulphide NPs preparation. *Materials Letters, 57*(9), 1585–1589.

Bang, J. H., & Suslick, K. S. (2010). Applications of ultrasound to the synthesis of nanostructured materials. *Advanced Materials, 22*(10), 1039–1059.

Bao, H., Hao, N., Yang, Y., & Zhao, D. (2010). Biosynthesis of biocompatible cadmium telluride QDs using yeast cells. *Nano Research, 3*(7), 481–489. doi:10.1007/s12274-010-0008-6.

Borovaya, M. N., Naumenko, A. P., Matvieieva, N. A., Blume, Y. B., & Yemets, A. I. (2014). Biosynthesis of luminescent CdS QDs using plant hairy root culture. *Nanoscale Research Letters, 9*(1), 686.

Bozkurt, P. A., & Derkuş, B. (2016). Synthesis and characterization of CdS NRs by combined sonochemical-solvothermal method. *Materials Science-Poland, 34*(3), 684–690. doi:10.1515/msp-2016-0089.

Carlà, F., Loglio, F., Resta, A., Felici, R., Lastraioli, E., Innocenti, M., et al. (2014). Electrochemical atomic layer deposition of CdS on Ag single crystals: Effects of substrate orientation on film structure. *The Journal of Physical Chemistry C, 118*(12), 6132–6139.

Castro-Longoria, E., Vilchis-Nestor, A. R., & Avalos-Borja, M. (2011). Biosynthesis of silver, gold and bimetallic NPs using the filamentous fungus Neurospora crassa. *Colloids and Surfaces B: Biointerfaces, 83*(1), 42–48.

Chang, S. Q., Dai, Y. D., Kang, B., Han, W., & Chen, D. (2009). γ-radiation synthesis of silk fibroin coated CdSe QDs and their biocompatibility and photostability in living cells. *Journal of Nanoscience and Nanotechnology, 9*(10), 5693–5700.

Chen, G., Yi, B., Zeng, G., Niu, Q., Yan, M., Chen, A., et al. (2014). Facile green extracellular biosynthesis of CdS QDs by white rot fungus Phanerochaete chrysosporium. *Colloids and Surfaces B: Biointerfaces, 117,* 199–205.

Choi, S. Y., Shim, J. P., Kim, D. S., Kim, T., & Suh, K. S. (2012). Aqueous synthesis of CdTe quantum dot using dithiol-functionalized ionic liquid. *Journal of Nanomaterials, 2012,* 10.

Colmenares, J. C., Kuna, E., & Lisowski, P. (2016). Synthesis of photoactive materials by sonication: Application in photocatalysis and solar cells. *Topics in Current Chemistry, 374*(5), 59.

Dameron, C. T., Reese, R. N., Mehra, R. K., Kortan, A. R., Carroll, P. J., Steigerwald, M. L., et al. (1989). Biosynthesis of cadmium sulphide quantum semiconductor crystallites. *Nature, 338* (6216), 596–597.

Dhand, C., Dwivedi, N., Loh, X. J., Ying, A. N. J., Verma, N. K., Beuerman, R. W., et al. (2015). Methods and strategies for the synthesis of diverse NPs and their applications: A comprehensive overview. *Rsc Advances, 5*(127), 105003–105037.

Didenko, Y. T., & Suslick, K. S. (2005). Chemical aerosol flow synthesis of semiconductor NPs. *Journal of the American Chemical Society, 127*(35), 12196–12197.

Drbohlavova, J., Adam, V., Kizek, R., & Hubalek, J. (2009). QDs—characterization, preparation and usage in biological systems. *International Journal of Molecular Sciences, 10*(2), 656–673.

Duan, J., Song, L., & Zhan, J. (2009). One-pot synthesis of highly luminescent CdTe QDs by microwave irradiation reduction and their Hg^{2+} -sensitive properties. *Nano Research, 2*(1), 61–68.

Dutková, E., Balaz, P., & Pourghahramani, P. (2009). CdS NPs mechanochemically synthesized in a high-energy mill. *Journal of optoelectronics and advanced materials, 11*(12), 2102–2107.

Edison, T. J. I., & Sethuraman, M. G. (2012). Instant green synthesis of silver NPs using Terminalia chebula fruit extract and evaluation of their catalytic activity on reduction of methylene blue. *Process Biochemistry, 47*(9), 1351–1357.

El-Baz, A. F., Sorour, N. M., & Shetaia, Y. M. (2016). Trichosporon jirovecii–mediated synthesis of cadmium sulfide NPs. *Journal of Basic Microbiology, 56*(5), 520–530.

Fauchais, P., & Vardelle, A. (1997). Thermal plasmas. *IEEE Transactions on Plasma Science, 25*(6), 1258–1280.

Gerbec, J. A., Magana, D., Washington, A., & Strouse, G. F. (2005). Microwave-enhanced reaction rates for nanoparticle synthesis. *Journal of the American Chemical Society, 127*(45), 15791–15800.

Godočíková, E., Baláž, P., Gock, E., Choi, W. S., & Kim, B. S. (2006). Mechanochemical synthesis of the nanocrystalline semiconductors in an industrial mill. *Powder Technology, 164*(3), 147–152.

Goto, F., Ichimura, M., & Arai, E. (1997). A new technique of compound semiconductor deposition from an aqueous solution by photochemical reactions. *Japanese Journal of Applied Physics, 36*(9A), L1146.

Hanifehpour, Y., Hamnabard, N., Mirtamizdoust, B., & Joo, S. W. (2016). Sonochemical synthesis, characterization and sonocatalytic performance of terbium-doped CdS NPs. *Journal of Inorganic and Organometallic Polymers and Materials, 3*(26), 623–631. doi:10.1007/s10904-016-0352-4.

Hanifehpour, Y., Mirtamizdoust, B., & Joo, S. W. (2012). Sonochemical synthesis and characterization of the first flower-like cadmium (II) coordination compound: New precursor to produce pure phase nano-sized Ccdmium (II) oxide. *Journal of Inorganic and Organometallic Polymers and Materials, 22*(2), 549–553.

He, H., Sun, X., Wang, X., & Xu, H. (2014). Synthesis of highly luminescent and biocompatible CdTe/CdS/ZnS QDs using microwave irradiation: A comparative study of different ligands. *Luminescence, 29*(7), 837–884.

He, R., Qian, X. F., Yin, J., Xi, H. A., Bian, L. J., & Zhu, Z. K. (2003). Formation of monodispersed PVP-capped ZnS and CdS NCs under microwave irradiation. *Colloids and Surfaces A: Physicochemical and Engineering Aspects, 220*(1), 151–157. doi:10.1016/S0927-7757(03)00072-4.

He, Y., Lu, H. T., Sai, L. M., Lai, W. Y., Fan, Q. L., Wang, L. H., et al. (2006). Microwave-assisted growth and characterization of water-dispersed CdTe/CdS core—shell NCs with high photoluminescence. *The Journal of Physical Chemistry B, 110*(27), 13370–13374.

He, Y., Sai, L. M., Lu, H. T., Hu, M., Lai, W. Y., Fan, Q. L., et al. (2007). Microwave-assisted synthesis of water-dispersed CdTe NCs with high luminescent efficiency and narrow size distribution. *Chemistry of Materials, 19*(3), 359–365.

He, Z., Zhu, H., & Zhou, P. (2012). Microwave-assisted aqueous synthesis of highly luminescent carboxymethyl chitosan-coated CdTe/CdS QDs as fluorescent probe for live cell imaging. *Journal of fluorescence, 22*(1), 193–199.

Hwang, C. H., Park, J. P., Song, M. Y., Lee, J. H., & Shim, I. W. (2011). Syntheses of CdTe QDs and NPs through simple sonochemical method under multibubble sonoluminescence conditions. *Bulletin of the Korean Chemical Society, 32*(7), 2207–2211.

Ichimura, M., & Maeda, Y. (2015). Conduction type of nonstoichiometric alloy semiconductor Cu x Zn y S deposited by the photochemical deposition method. *Thin Solid Films, 594,* 277–281.

Jemal, K., Sandeep, B. V., & Pola, S. (2017). Synthesis, characterization, and evaluation of the antibacterial activity of allophylus serratus leaf and leaf derived callus extracts mediated silver NPs. *Journal of Nanomaterials, 2017*.

Jurkin, T., Gotić, M., Štefanić, G., & Pucić, I. (2016). Gamma-irradiation synthesis of iron oxide NPs in the presence of PEO, PVP or CTAB. *Radiation Physics and Chemistry, 124,* 75–83.

Kanatzia, A., Papageorgiou, C. H., Lioutas, C. H., & Kyratsi, T. H. (2013). Design of ball-milling experiments on Bi_2Te_3 thermoelectric material. *Journal of Electronic Materials, 42*(7), 1652.

Kang, B., Chang, S. Q., Dai, Y. D., & Chen, D. (2008a). Synthesis of green CdSe/chitosan QDs using a polymer-assisted γ-radiation route. *Radiation Physics and Chemistry, 77*(7), 859–863.

Kang, S. H., Bozhilov, K. N., Myung, N. V., Mulchandani, A., & Chen, W. (2008b). Microbial synthesis of CdS NCs in genetically engineered *E. coli*. *Angewandte Chemie International Edition, 47*(28), 5186–5189. doi:10.1002/anie.200705806.

Karimi, J. A., & Mohsenzadeh, S. (2012). Phytosynthesis of cadmium oxide NPs from Achillea wilhelmsii flowers. *Journal of Chemistry*, *2013*.

Karthik, K., & Dhanuskodi, S. (2016, May). Structural and optical properties of microwave assisted CdO-NiO nanocomposite. In *AIP Conference Proceedings* (Vol. 1731, No. 1, p. 050021). New York: AIP Publishing.

Karthik, K., Dhanuskodi, S., Gobinath, C., & Sivaramakrishnan, S. (2015). Microwave-assisted synthesis of CdO–ZnO nanocomposite and its antibacterial activity against human pathogens. *Spectrochimica Acta Part A: Molecular and Biomolecular Spectroscopy, 139,* 7–12.

Kharazmi, A., Saion, E., Faraji, N., Soltani, N., & Dehzangi, A. (2013). Optical properties of CdS/PVA nanocomposite films synthesized using the gamma-irradiation-induced method. *Chinese Physics Letters, 30*(5), 05780.

Kowshik, M., Deshmukh, N., Vogel, W., Urban, J., Kulkarni, S. K., & Paknikar, K. M. (2002). Microbial synthesis of semiconductor CdS NPs, their characterization, and their use in the fabrication of an ideal diode. *Biotechnology and Bioengineering, 78*(5), 583–588.

Kristl, M., Ban, I., & Gyergyek, S. (2013). Preparation of nanosized copper and cadmium chalcogenides by mechanochemical synthesis. *Materials and Manufacturing Processes, 28*(9), 1009–1013.

Kristl, M., Ban, I., Danč, A., Danč, V., & Drofenik, M. (2010). A sonochemical method for the preparation of cadmium sulfide and cadmium selenide NPs in aqueous solutions. *Ultrasonics Sonochemistry, 17*(5), 916–922. doi:10.1016/j.ultsonch.2009.12.013.

Kumar, P., Kumar, P., Bharadwaj, L. M., Paul, A. K., Sharma, S. C., Kush, P., et al. (2013). Aqueous synthesis of l-cysteine stabilized water-dispersible CdS: Mn QDs for biosensing applications. *BioNanoScience, 3*(2), 95–101.

Kumar, S. A., Ansary, A. A., Ahmad, A., & Khan, M. I. (2007). Extracellular biosynthesis of CdSe QDs by the fungus, Fusarium oxysporum. *Journal of Biomedical Nanotechnology, 3*(2), 190–194.

Kundu, S., & Liang, H. (2008). Photochemical synthesis of electrically conductive CdS NWs on DNA scaffolds. *Advanced Materials, 20*(4), 826–831.

Lagashetty, A. (2016). Journal of Nanoscience and Technology. *Journal of Nanoscience and Technology, 2*(2), 97–99.

Li, H., Shih, W. Y., & Shih, W. H. (2007). Synthesis and characterization of aqueous carboxyl-capped CdS QDs for bioapplications. *Industrial and Engineering Chemistry Research, 46*(7), 2013–2019. doi:10.1021/ie060963s.

Li, D., Wang, S., Wang, J., Zhang, X., & Liu, S. (2013). Synthesis of CdTe/TiO 2 nanoparticles and their photocatalytic activity. *Materials Research Bulletin*, *48*(10), 4283–4286.

Li, H., Wang, C., Peng, Z., & Fu, X. (2015). A review on the synthesis methods of CdSeS-based nanostructures. *Journal of Nanomaterials, 2015,* 5.

Li, L., Yang, S., Han, F., Wang, L., Zhang, X., Jiang, Z., et al. (2014). Optical sensor based on a single CdS nano-belt. *Sensors, 14*(4), 7332–7341.

Li, Z., Dong, C., Tang, L., Zhu, X., Chen, H., & Ren, J. (2011). Aqueous synthesis of CdTe/CdS/ZnS QDs and their optical and chemical properties. *Luminescence, 26*(6), 439–448.

Mahfouz, R. M., Ahmed, G. A., & Al-Rashidi, T. (2016). Effect of surfactant-free addition and γ-irradiation on the synthesis of CdO QDs by thermal decomposition of γ-irradiated anhydrous cadmium acetate. *Cogent Chemistry, 2*(1), 1215233.

Manthiram, K., Beberwyck, B. J., Talapin, D. V., & Alivisatos, A. P. (2013). Seeded synthesis of CdSe/CdS rod and tetrapod NCs. *Journal of visualized experiments: JoVE,* (82).

Mao, C., Flynn, C. E., Hayhurst, A., Sweeney, R., Qi, J., Georgiou, G., et al. (2003). Viral assembly of oriented quantum dot NWs. *Proceedings of the National Academy of Sciences, 100*(12), 6946–6951.

Menezes, F. D., Galembeck, A., & Junior, S. A. (2011). New methodology for obtaining CdTe QDs by using ultrasound. *Ultrasonics Sonochemistry, 18*(5), 1008–1011. doi:10.1016/j.materresbull.2013.06.052.

Mi, C., Wang, Y., Zhang, J., Huang, H., Xu, L., Wang, S., et al. (2011). Biosynthesis and characterization of CdS QDs in genetically engineered Escherichia coli. *Journal of Biotechnology, 153*(3), 125–132.

Mittal, A. K., Kaler, A., & Banerjee, U. C. (2012). Free radical scavenging and antioxidant activity of silver NPs synthesized from flower extract of rhododendron dauricum. *Nano Biomedicine & Engineering, 4*(3).

Mohanraj, K., Balasubramanian, D., Jhansi, N., Bakkiyaraj, R., & Chandrasekaran, J. (2017). Structural, optical and electrical properties of green synthesis CdO NPs and its Ag/CdO/P—Si junction diode fabricated Via JNS pyrolysis technique. *International Journal of Thin Films Science and Technology, 6,* 87–91.

Ni, Y., Ge, X., Liu, H., Xu, X., & Zhang, Z. (2001). γ-Irradiation preparation of CdS NPs and their formation mechanism in non-water system. *Radiation Physics and Chemistry, 61*(1), 61–64.

Nogi, K., Hosokawa, M., Naito, M., & Yokoyama, T. (Eds.). (2012). *Nanoparticle technology handbook*. Oxford: Elsevier.

Onwudiwe, D. C., Krüger, T. P., Oluwatobi, O. S., & Strydom, C. A. (2014). Nanosecond laser irradiation synthesis of CdS NPs in a PVA system. *Applied Surface Science, 290,* 18–26.

Pan, A. L., Ma, J. G., Yan, X. Z., & Zou, B. S. (2004). The formation of CdS NCs in silica gels by gamma-irradiation and their optical properties. *Journal of Physics: Condensed Matter, 16*(18), 3229.

Pandian, S. R. K., Deepak, V., Kalishwaralal, K., & Gurunathan, S. (2011). Biologically synthesized fluorescent CdS NPs encapsulated by PHB. *Enzyme and Microbial Technology, 48* (4), 319–325. doi:10.1016/j.enzmictec.2011.01.005.

Park, J. H., & Hong, S. H. (1997). Optimization analysis of an inductively coupled plasma torch for material processing by using local thermal equilibrium numerical models. *Journal of the Korean Physical Society, 31*(5), 753–763.

Permana, Y. N., & Yulizar, Y. (2017, April). Potency of Parkia speciosa Hassk seed extract for green synthesis of CdO NPs and its characterization. In *IOP conference series: Materials science and engineering* (Vol. 188, No. 1, p. 012018). Bristol: IOP Publishing.

Plaza, D. O., Gallardo, C., Straub, Y. D., Bravo, D., & Pérez-Donoso, J. M. (2016). Biological synthesis of fluorescent NPs by cadmium and tellurite resistant Antarctic bacteria: Exploring novel natural nanofactories. *Microbial Cell Factories, 15*(1), 76.

Qian, H., Li, L., & Ren, J. (2005). One-step and rapid synthesis of high quality alloyed QDs (CdSe–CdS) in aqueous phase by microwave irradiation with controllable temperature. *Materials Research Bulletin, 40*(10), 1726–1736.

Ranjbar, Z. R., Sheikhshoaie, I., & Bagheri, Z. (2014). Solid state preparation of CdO NPs by thermolysis of a precursor as compacted nanosheet. *International Journal of Nano Dimension, 5*(4), 409.

Rashidzadeh, M. (2014). Antibacterial properties Of CdO nano-cubes synthesized via microwave method. In *Advanced materials research* (Vol. 829, pp. 294–298). Trans Tech Publications.

Rashidzadeh, M., Carbajal-Franco, G., & Tiburcio-Silver, A. (2016). Hydrophobic coatings composed by cubic-shaped CdO NPs grown by a novel and simple microwave method. *Journal of NPs*, *2016* doi:10.4028/www.scientific.net/AMR.829.294.

Safarifard, V., & Morsali, A. (2012). Sonochemical syntheses of a NPs cadmium (II) supramolecule as a precursor for the synthesis of cadmium (II) oxide NPs. *Ultrasonics Sonochemistry, 19*(6), 1227–1233.

Salavati-Niasari, M., Bazarganipour, M., & Ghasemi-Kooch, M. (2015). Facile sonochemical synthesis and characterization of CdTe NPs. *Synthesis and Reactivity in Inorganic, Metal-Organic, and Nano-Metal Chemistry, 45*(10), 1558–1564. doi:10.1080/15533174.2013.865218.

Santos, J. C., Mansur, A. A., & Mansur, H. S. (2013). One-step biofunctionalization of QDs with chitosan and N-palmitoyl chitosan for potential biomedical applications. *Molecules, 18*(6), 6550–6572.

Saraji, M., Dizajib, H. R., & Fallaha, M. (2012). An efficient method for synthesis and characterization of CdS and CdS: Cu NPs by microwave irradiation. Proceedings of the 4th International Conference on Nanostructures. 1495–1497.

Saravanan, P., Gopalan, R., & Chandrasekaran, V. (2008). Synthesis and characterisation of nanomaterials. *Defence Science Journal, 58*(4), 504.

Sasidharan, S., Sowmiya, R., & Balakrishnaraja, R. (2014). Biosynthesis of selenium NPs using citrus reticulata peel extract. *World Journal of Pharmaceutical Sciences, 4,* 1322–1330.

Sathya Raj, D., Jayaprakash, R., Prakash, T., Neri, G., & Krishnakumar, T. (2013). Impact of n-heptane as surfactant in the formation of CdO NWs through microwave combustion. *Applied Surface Science, 266,* 268–271. doi:10.1016/j.apsusc.2012.12.009.

Seo, J. H., & Hong, B. G. (2012). Thermal plasma synthesis of nano-sized powders. *Nuclear Engineering and Technology, 44*(1), 9–20.

Serrano, T., Gómez, I., Colás, R., & Cavazos, J. (2009). Synthesis of CdS NCs stabilized with sodium citrate. *Colloids and Surfaces A: Physicochemical and Engineering Aspects, 338*(1), 20–24.

Shah, M., Fawcett, D., Sharma, S., Tripathy, S. K., & Poinern, G. E. J. (2015). Green synthesis of metallic NPs via biological entities. *Materials, 8*(11), 7278–7308.

Shao, M., Xu, F., Peng, Y., Wu, J., Li, Q., Zhang, S., et al. (2002). Microwave-templated synthesis of CdS NTs in aqueous solution at room temperature. *New Journal of Chemistry, 26*(10), 1440–1442.

Sharma, K., et al. (2014). Synthesis and characterization of pure and Zn doped CdSe NPs by ultrasonication technique. *American International Journal of Research in Science, Technology, Engineering & Mathematics, 8,* 75–79.

Shen, L., Bao, N., Prevelige, P. E., & Gupta, A. (2010). Escherichia coli bacteria-templated synthesis of nanoporous cadmium sulfide hollow microrods for efficient photocatalytic hydrogen production. *The Journal of Physical Chemistry C, 114*(6), 2551–2559. doi:10.1021/jp910842f.

Singh, B. R., Dwivedi, S., Al-Khedhairy, A. A., & Musarrat, J. (2011). Synthesis of stable cadmium sulfide NPs using surfactin produced by Bacillus amyloliquifaciens strain KSU-109. *Colloids and Surfaces B: Biointerfaces, 85*(2), 207–213.

Singh, P., Kim, Y. J., Wang, C., Mathiyalagan, R., El-Agamy Farh, M., & Yang, D. C. (2016a). Biogenic silver and gold NPs synthesized using red ginseng root extract, and their applications. *Artificial Cells, Nanomedicine, and Biotechnology, 44*(3), 811–816.

Singh, P., Kim, Y. J., Zhang, D., & Yang, D. C. (2016b). Biological synthesis of NPs from plants and microorganisms. *Trends in Biotechnology, 34*(7), 588–599.

Soltani, N., Saion, E., Hussein, M. Z., Yunus, R. B., & Navaseri, M. (2013). Characterization of CdS NPs synthesized using microwave-assisted polyol method. In *Advanced Materials Research* (Vol. 667, pp. 122–127). Trans Tech Publications.

Sostaric, J. Z., Caruso-Hobson, R. A., Mulvaney, P., & Grieser, F. (1997). Ultrasound-induced formation and dissolution of colloidal CdS. *Journal of the Chemical Society, Faraday Transactions, 93*(9), 1791–1795.

Suslick, K. S., Fang, M. M., Hyeon, T., & Mdleleni, M. M. (1999). Applications of sonochemistry to materials synthesis. In *Sonochemistry and sonoluminescence* (pp. 291–320). Springer Netherlands.

Sweeney, R. Y., Mao, C., Gao, X., Burt, J. L., Belcher, A. M., Georgiou, G., et al. (2004). Bacterial biosynthesis of cadmium sulfide NCs. *Chemistry & Biology, 11*(11), 1553–1559.

Tadjarodi, A., & Imani, M. (2011). Synthesis and characterization of CdO nanocrystalline structure by mechanochemical method. *Materials Letters, 65*(6), 1025–1027.

Tadjarodi, A., Imani, M., & Kerdari, H. (2013). Application of a facile solid-state process to synthesize the CdO spherical NPs. *International Nano Letters, 3*(1), 43.

Tan, G. L., Hömmerich, U., Temple, D., Wu, N. Q., Zheng, J. G., & Loutts, G. (2003). Synthesis and optical characterization of CdTe NCs prepared by ball milling process. *Scripta Materialia, 48*(10), 1469–1474.

Tan, G. L., & Yu, X. F. (2009). Capping the ball-milled CdSe nanocrystals for light excitation. *The Journal of Physical Chemistry C*, *113*(20), 8724–8729.

Tan, G. L., Zhang, L., & Yu, X. F. (2009). Preparation and optical properties of CdS NCs prepared by a mechanical alloying process. *The Journal of Physical Chemistry C, 114*(1), 290–293.

Tho, N. T. M., An, T. N. M., Tri, M. D., Sreekanth, T. V. M., Lee, J. S., Nagajyothi, P. C., et al. (2013). Green synthesis of silver NPs using Nelumbo nucifera seed extract and its antibacterial activity. *Acta Chimica Slovenica, 60*(3), 673–678.

Tolia, J. V., Chakraborty, M., & Murthy, Z. V. P. (2012). Mechanochemical synthesis and characterization of Group II-VI semiconductor NPs. *Particulate Science and Technology, 30* (6), 533–542.

Tsuzuki, T., & McCormick, P. G. (1997). Synthesis of CdS QDs by mechanochemical reaction. *Applied Physics A: Materials Science & Processing, 65*(6), 607–609.

Veeraputhiran, V., Gomathinayagam, V., Udhaya, A., Francy, K., & Kathrunnisa, B. (2014). Microwave mediated synthesis and characterizations of CdO NPs. *Journal of Advanced Chemical Sciences*, 17–19.

Wang, G. Z., Chen, W., Liang, C. H., Wang, Y. W., Meng, G. W., & Zhang, L. D. (2001). Preparation and characterization of CdS nanoparticles by ultrasonic irradiation. *Inorganic chemistry communications*, *4*(4), 208–210.

Wang, Q., Li, J., Bai, Y., Lian, J., Huang, H., Li, Z., et al. (2014). Photochemical preparation of Cd/CdS photocatalysts and their efficient photocatalytic hydrogen production under visible light irradiation. *Green Chemistry, 16*(5), 2728–2735.

Wang, Y., Feng, Q., Zhou, L., Gong, F., & Lan, Y. (2012). Synthesis and characterization of cysteamine-CdTe QDs via one-step aqueous method. *Materials Letters, 66*(1), 261–263.

Xiong, H. B., Zhang, C. Y., Zhang, K., & Shao, X. M. (2016). Effects of atomization injection on nano-particle processing in suspension plasma spray. *Nano-materials, 6*(5), 94.

Xu, H., Zeiger, B. W., & Suslick, K. S. (2013). Sonochemical synthesis of nanomaterials. *Chemical Society Reviews, 42*(7), 2555–2567.

Yan, Y. L., Li, Y., Qian, X. F., Yin, J., & Zhu, Z. K. (2003). Preparation and characterization of CdSe NCs via Na_2 SO_3-assisted photochemical route. *Materials Science and Engineering B, 103*(2), 202–206.

Yang, H., Huang, C., Li, X., Shi, R., & Zhang, K. (2005). Luminescent and photocatalytic properties of cadmium sulfide NPs synthesized via microwave irradiation. *Materials Chemistry and Physics, 90*(1), 155–158.

Yuwen, L., Lu, H., He, Y., Chen, L., Hu, M., Bao, B., et al. (2010). A facile low temperature growth of cdte NCs using novel dithiocarbamate ligands in aqueous solution. *Journal of Materials Chemistry, 20*(14), 2788–2793.

Zhan, H. J., Zhou, P. J., Ma, R., Liu, X. J., He, Y. N., & Zhou, C. Y. (2014). Enhanced oxidation stability of quasi core-shell alloyed CdSeS QDs prepared through aqueous microwave synthesis technique. *Journal of Fluorescence, 24*(1), 57–65.

Zhang, R., Li, G., & Zhang, Y. (2017). Photochemical synthesis of CdS-MIL-125 (Ti) with enhanced visible light photocatalytic performance for the selective oxidation of benzyl alcohol to benzaldehyde. *Photochemical & Photobiological Sciences, 16*(6), 996–1002.

Zhang, Z. H., Chin, W. S., & Vittal, J. J. (2004). Water-soluble CdS QDs prepared from a refluxing single precursor in aqueous solution. *The Journal of Physical Chemistry B, 108*(48), 18569–18574.

Zhao, B., Wang, Y., Zhang, H., Jiao, Z., Wang, H., Ding, G., et al. (2009). Synthesis of CdS NRs in soft template under γ-irradiation. *Journal of Nanoscience and Nanotechnology, 9*(2), 1312–1315.

Zhao, W. B., Zhu, J. J., & Chen, H. Y. (2003). Photochemical preparation of rectangular PbSe and CdSe NPs. *Journal of Crystal Growth, 252*(4), 587–592.

Zhou, G. J., Li, S. H., Zhang, Y. C., & Fu, Y. Z. (2014). Biosynthesis of CdS NPs in banana peel extract. *Journal of Nanoscience and Nanotechnology, 14*(6), 4437–4442.

Zhou, S. M., Feng, Y. S., & Zhang, L. D. (2003). Sonochemical synthesis of large-scale single crystal CdS NRs. *Materials Letters, 57*(19), 2936–2939.

Zhu, J., Liao, X., Zhao, X., & Wang, J. (2001). Photochemical synthesis and characterization of CdSe NPs. *Materials Letters, 47*(6), 339–343.

Zhu, J., Palchik, O., Chen, S., & Gedanken, A. (2000). Microwave assisted preparation of CdSe, PbSe, and Cu2-x Se NPs. *The Journal of Physical Chemistry B, 104*(31), 7344–7347.